Synapsis of *res* sites by Tn*3* resolvase

A thesis submitted for the Degree of
Doctor of Philosophy at the
University of Glasgow

by

Mark Albert Watson

Institute of Genetics
Church Street
Glasgow

January 1994

The research reported in this thesis is my own and original work except where otherwise stated and has not been submitted for any other degree.

Dedicated to my parents,
James and Madeleine, for
everything...

Who'd have thought?

Contents.

Abbreviations.

Ap	ampicillin
ATP	adenosine 5'-triphosphate
bp	base pairs
BSA	bovine serum albumin
Chloroquine	7-chloro-4-[4-diethylamino-1-methyl-butylamino]-quinoline (diphosphate salt)
CIP	calf intestine phosphatase
DMS	dimethyl sulphate
DMSO	dimethyl sulphoxide
DNA	deoxyribonucleic acid
DNase I	bovine pancreatic deoxyribonuclease I
dNTP	2'-deoxyribonucleoside 5'-triphosphate
DSP	dithio*bis*(succinimidylpropionate)
DTT	dithiothreitol
EDC	1-ethyl-3-(3-dimethylaminopropyl)carbodiimide hydrochloride
EDTA	ethylenediaminetetra-acetic acid
EGS	ethylene glycol*bis*(succinimidylsuccinate)
Iodogen	1,3,4,6-tetrachloro-3α, 6α-diphenylglycouril
IPTG	isopropyl-β-D-thiogalactopyranoside
kDa	kilodaltons
$Lk - Lk_0$	linking number difference
MOPS	3-(*N*-morpholino)propanesulphonic acid
NHS	*N*-hydroxysuccinimide
PAGE	polyacrylamide gel electrophoresis
PMSF	phenylmethyl sulphonyl fluoride
SDS	sodium dodecyl sulphate
Spermidine .3 HCl	*N*-[3-Aminopropyl]-1,4-butanediamine trihydrochloride
TAE	tris-acetate-EDTA (electrophoresis buffer)
TBE	tris-borate-EDTA (electrophoresis buffer)
Tc	tetracycline
TCA	trichloroacetic acid
TE	Tris-EDTA buffer (10 mM Tris-HCl (pH 8.0), 1 mM EDTA)
TEMED	*N,N,N',N'*-tetramethyl-ethylenediamine
Tris	tris(hydroxymethyl)aminomethane
UV	ultraviolet

Acknowledgements.

In chronological order, thanks to my sister, Patricia, for her love and support from day one. Thanks to staff at Medical and Biological Sciences, Leicester University who started all this with their enthusiastic lectures for the Adult Education Department. Many thanks to Brian Wilkins, also at Leicester, for his encouragement. And, not forgetting the other 'mature' undergraduates: Rita, Anne, and David.

Moving to Glasgow, special thanks to Marshall Stark, my supervisor, for taking me on, for his finely-judged guidance throughout, and for critical (long-distance) reading of this thesis. Thanks also to Dave Sherratt for his help and encouragement.

A special mention for two people. Martin Boocock for his widespread knowledge, the generous giving of his time, and for showing me how to make resolvase. Mary Burke for making lab.63, and the whole sixth floor, a great place to work, for her technical advice, encouragement, and for gradually taking over more and more of my communal chores as darkroom monitor (and for being closer to the telephone than me!)

That leaves the prep. room ladies, whose provision of sterile labware and culture media was essential and who were generous in their assistance on numerous occasions despite a very heavy workload, as were the secretarial staff. Finally, thanks to the other occupants of the sixth and seventh floors, past and present, for their friendship and advice throughout (Amir, Amy, Angela, David, Elizabeth, Garry, Gerhard, Jennifer, Karen, Lidia, Liz, Michael, Nick, Richard, Sally, Sean, Shahnaz, Stephen, Sue) and to other members of the department whose paths I crossed while riding that central artery, the paternoster.

My studies were financed by the Wellcome Trust which, through its Prize Studentship scheme, provides a level of assistance that should be (though regrettably is not) enjoyed by all graduate research students.

Summary.

Protein-DNA complexes formed by synapsis of *res* sites by Tn*3* resolvase were isolated by agarose gel electrophoresis. Prior treatment with a protein crosslinking reagent was required in order to isolate synaptic complexes with a characteristic gel mobility following restriction endonuclease cleavage within one or both domains of a negatively supercoiled plasmid DNA substrate containing direct repeats of the Tn*3* *res* site.

An intramolecular synaptic complex was observed, following treatment with various protein crosslinking reagents, in a yield that represented between 20 and 50% of the input substrate DNA when Mg^{2+} was omitted from the reaction. The gel mobility of this species was shown to vary in a predictable manner when the site of restriction endonuclease cleavage was altered. There was no evidence of an equivalent synaptic complex when a negatively supercoiled plasmid containing a single Tn*3* *res* site and a single Tn*21* *res* site in direct repeat orientation was assayed in the presence of both resolvase proteins. Despite the apparent stability of the crosslinked Tn*3* resolvase synaptic complex during agarose gel electrophoresis, attempts to recover it intact following elution from the gel were unsuccessful.

The gel mobility assay also indicated that a synaptic interaction, stabilised by protein crosslinking, occurred between two *res* sites present in inverted repeat orientation on a negatively supercoiled plasmid DNA molecule. Similarly, intramolecular synapsis between two copies of the isolated accessory subsites (subsites II and III) of *res* was demonstrated. Although intramolecular synapsis was observed between an isolated copy of subsite I and an intact *res* site, there was no evidence of synapsis between two copies of the isolated subsite I of *res* oriented as direct repeats on a negatively supercoiled plasmid.

Intramolecular synapsis of two copies of the intact *res* site present in direct repeat orientation on either nicked or linearised plasmid substrate was observed. In addition, intermolecular synapsis was seen; interactions between plasmids containing two *res* sites (involving two, three, and four *res* sites on two DNA molecules) were characterised. The two-plasmid four-site intermolecular synaptic complex was seen in by far the highest yield when two intact *res* sites were in direct repeat orientation on a

supercoiled DNA molecule. Surprisingly, the two-*res*-site intermolecular synaptic complex, clearly in evidence when the plasmid substrate assayed contained two *res* sites (whether supercoiled, nicked, or linearised) was barely detectable when interacting supercoiled DNA molecules contained only a single *res* site.

In the presence of Mg^{2+}, a protein-DNA complex representing synapsis of the *res* sites in the (–2) catenane product of the resolution reaction was isolated following treatment with a protein crosslinking reagent and restriction endonuclease cleavage. It is not known whether this species represented an intermediate in the resolution reaction, trapped prior to dissociation of the synapse, or whether it was due to re-synapsis of catenane product. Although re-synapsis of catenane was demonstrated, it appeared too inefficient to account for the yield of the product synaptic complex typically seen in the 'forward reaction.'

Assays of the rate of synapsis indicated rapid formation of the intramolecular synaptic complex. The ensuing gradual decline in the amount of this substrate synaptic complex was concomitant with an increase in the amount of the product synaptic complex. Preincubation of plasmid substrate with resolvase in the absence of Mg^{2+} was followed by a burst of recombination occurring within 30 seconds of the addition of Mg^{2+}, suggesting accumulation of a productive intermediate.

An assay of synapsis involving a determination of the linking number difference seen after ligation of nicked plasmid substrate in the presence and absence of resolvase was developed.

A pre-existing method for purification of Tn*3* resolvase was modified in order to increase the yield of protein. Attempts to determine the multimeric state of crosslinked resolvase in the intramolecular synaptic complex were inconclusive; no crosslinked resolvase multimers larger than dimer were detected in the yield predicted. A tendency for resolvase to fail to appear in the gel when SDS-polyacrylamide gel electrophoresis was preceded by treatment with a relatively low concentration of a protein crosslinking reagent was attributed to aggregation of the protein, followed by crosslinking to form an insoluble precipitate.

Treatment of synapsis reactions with restriction endonucleases that cleave within the *res* site revealed that protection due to resolvase was predominantly confined to the crosslinked synaptic complex. Methylation protection and DNase I protection footprinting of the crosslinked synapse indicated that the subsites of *res* were occupied by resolvase in both the substrate and product synaptic complexes, with no evidence of any non-specific resolvase-DNA interactions. The DNase I and methylation protection footprints obtained were broadly similar to previously published footprints of resolvase bound to linear DNA fragments containing the *res* site, with some evidence of a increased accessibility to footprinting reagents at subsite I in the crosslinked synaptic complex.

Chapter 1

Introduction

General remarks.

Conservative site-specific recombination occurs by a precise breakage and rejoining of participating DNA segments at specific sites. No DNA synthesis or degradation accompanies the strand exchange. The single reciprocal crossover occurs within a short region of sequence homology shared by the two participating sites (Craig, 1988). These features distinguish conservative site-specific recombination from other means of bringing about rearrangements in DNA. Thus, the high degree of specificity for both partners is not seen in homologous recombination; exchange can occur at any point within an extensive region of homology shared by the participating DNA segments, although recombination frequency can be influenced by DNA sequence (West, 1992). In transposition, there is no homology between the transposon ends and the site of insertion, and strand exchange includes DNA synthesis (Mizuuchi, 1992).

During the site-specific recombination reaction, the two sites are brought together by specific protein-DNA and protein-protein interactions – this is the phenomenon of synapsis.

The site-specific recombination reaction can be intermolecular (when the recombining sites are located on different DNA molecules) or intramolecular (when the sites are on the same DNA molecule). Furthermore, the inherent asymmetry of the recombination site means that the outcome of an intramolecular reaction depends on the relative orientation of the two sites. In the reaction between two identical sites, it is characteristic for the left side of one site to become linked to the right side of the other site, and *vice versa*. Thus, recombination of sites oriented as direct repeats results in excision of the intervening DNA (or resolution of a single circular DNA molecule into two circles), while recombination of sites oriented as inverted repeats leads to inversion of the intervening DNA. Examples of these different outcomes of conservative site-specific recombination, brought about by the appropriate initial configuration of sites, are seen in a number of naturally occurring processes (Sadowski, 1986).

In this introductory chapter, a brief outline of the best characterised site-specific recombination systems is followed by a detailed look at what is known about the reaction catalysed by Tn*3* resolvase, the system

investigated in this thesis. Finally, I focus on synapsis. Details of other systems are included where they contribute to understanding of resolvase-mediated synapsis.

Tn*3* resolution and bacteriophage lambda integration are the archetypes of two groups into which all site-specific recombination systems are divided on the basis of comparison of reaction mechanisms, recombination sites, and recombinases (Stark *et al.*, 1992). Tn*3* resolvase-mediated site-specific recombination will be described in detail below. The site specific recombination events that mediate bacteriophage lambda integration and excision occur at four *att* DNA sites (Landy, 1989). *att*P and *att*B are the phage and chromosomal sites, respectively, which recombine to integrate the phage genome. Recombination at *att*L and *att*R, the sites created by integration, results in excision of the phage DNA.

Other members of the integrase family include phage P1 Cre which circularises the infecting phage DNA and breaks down multimers of P1 when it is in the plasmid state (Hamilton and Abremski, 1984), and the *Saccharomyces cerevisiae* 2 μm plasmid-encoded FLP recombinase which, by inverting a segment of DNA, converts between bi-directional replication and a 'double rolling circle' form that results in multiple copies of the plasmid from a single initiation event (Cox, 1989). *Escherichia coli* XerC and XerD act together to monomerise the bacterial chromosome, ensuring normal segregation at cell division (Blakely *et al.*, 1991).

In addition to Tn*3* resolvase, the resolvase family comprises other transposon-encoded resolvases such as those of γδ (Tn*1000*) and Tn*21*, and the DNA invertases (Hatfull and Grindley, 1988). Examples of the latter group are the bacteriophage Mu-encoded Gin and the Hin invertase of *Salmonella typhimurium*, which switch between the expression of alternative forms of a tail fibre protein (thereby affecting host-range) and alternative antigenically distinct flagellar filament proteins (thereby allowing evasion of host immune response), respectively (Glasgow *et al.*, 1989).

Site-specific DNA rearrangements are involved in the generation of diversity in the vertebrate immune system, where different members from the pools of V, D, and J coding regions come together to form single immunoglobulin or T cell receptor genes (Gellert, 1992). Periodic change

in the variant cell-surface glycoprotein (VSG) coat of trypanosomes, allowing evasion of the host immune response, also results from site-specific DNA rearrangement (van der Ploeg *et al.*, 1992).

Protein-mediated interaction of distant DNA sites, with looping of the intervening DNA, is also a common feature of the regulation of gene expression (Matthews, 1992; Schleif, 1992). One advantage of analysing such interactions in a site-specific recombination system is the fact that the topology of DNA reaction products can provide considerable information on the structure of the synaptic intermediate.

Site-specific recombination by Tn*3* resolvase.

Transposition of the bacterial transposon Tn*3* is replicative; a circular cointegrate made up of donor and target replicons separated by two directly repeated copies of Tn*3* is formed initially. This intermediate in the transposition process is produced by the action of the Tn*3*-encoded *tnpA* gene product (the transposase) and the DNA replication machinery of the host bacterium. The cointegrate is resolved by conservative site-specific recombination between the two copies of the transposon. This generates the end products of replicative transposition: the two replicons, each containing a single copy of Tn*3* (Figure 1.1).

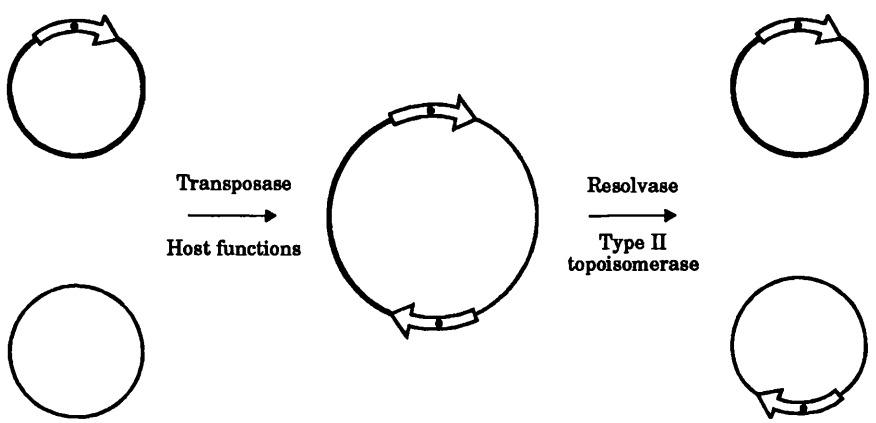

Figure 1.1 Replicative transposition of Tn*3*. An intermediate circular cointegrate, in which the donor and target replicons (here represented by different line thicknesses) are separated by two directly repeated copies of Tn*3* (represented by arrows), is resolved by site-specific recombination between the two copies of the transposon at *res* (solid black circles).

Site-specific recombination to resolve the cointegrate is catalysed by the transposon-encoded protein resolvase (the product of the *tnpR* gene), acting at the DNA site termed *res* (Figure 1.2), (reviewed in: Sherratt, 1989; Stark *et al.*, 1989a). The site-specific recombination systems of Tn*3* and γδ are very similar and the components are functionally interchangeable (Hatfull *et al.*, 1988). Thus, information obtained from study of either system is generally applicable to both.

The recombination site, *res*, is a region of DNA about 115 base pairs (bp) in size, containing three subsites that bind resolvase, each made up of inverted repeats of an imperfectly conserved 9 bp sequence (consensus: T G T C Py Pu T T A), (Hatfull and Grindley, 1988; Sherratt, 1989 are reviews containing the primary references), (see Figure 6.1). The subsites are not evenly spaced, and their lengths differ because the spacing between the inverted repeats in each subsite is not identical (Figure 1.2).

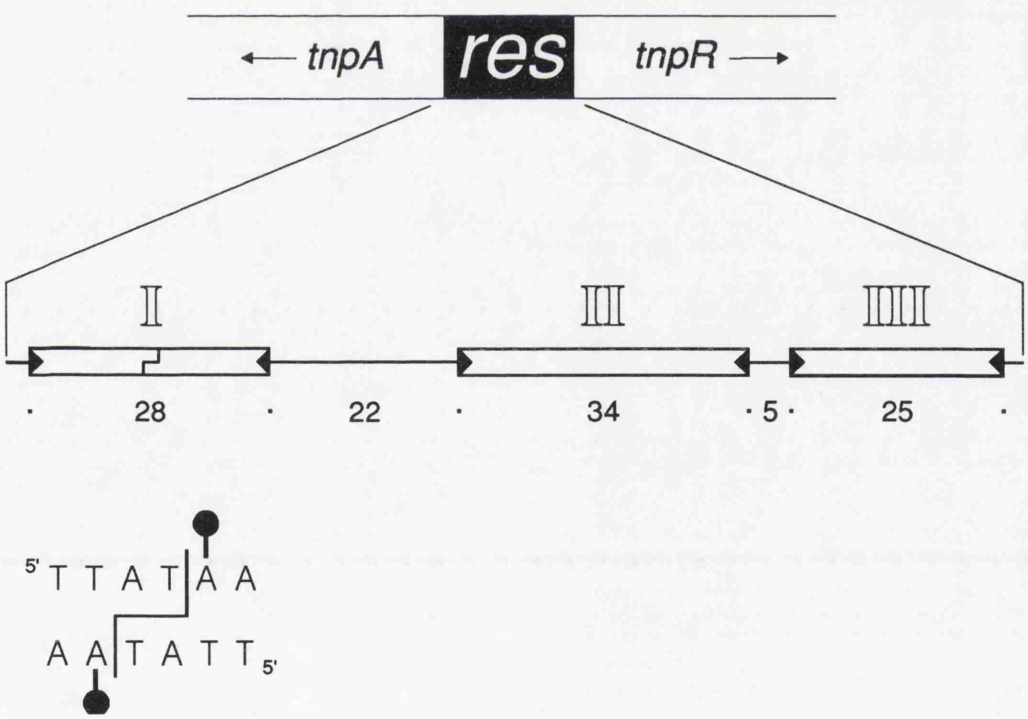

Figure 1.2 The Tn*3* recombination site, *res*. Subsites (resolvase binding sites) are represented as boxes, with arrowheads indicating the imperfect inverted repeat sequences at the outer arms of each subsite. Lengths (in bp) of the different elements forming the *res* site are given. The sequence at the point of crossover in the centre of subsite I is shown, as is the staggered cleavage and the positions at which resolvase becomes covalently attached to the DNA.

During the site-specific recombination reaction, resolvase cuts and religates the DNA within a region of perfect dyad symmetry at the centre of *res* subsite I (Reed and Grindley, 1981). Subsites II and III are known as the accessory subsites. In the case of γδ and Tn*3*, the *res* site is located between the divergently transcribed *tnpA* and *tnpR* genes (Figure 1.2), and the promoters for these genes are situated within *res* (Wells and Grindley, 1984). In addition to its role in recombination, resolvase acts as a repressor of its own synthesis, and that of the transposase, at the level of transcription (Reed *et al.*, 1982).

In contrast to *res*, the recombination site of the Gin and Hin invertase systems is simply a single two-fold symmetric 26 bp sequence with a central 2 bp 'core' where DNA strand exchange occurs, although an enhancer sequence bound by the host factor FIS (Factor for Inversion Stimulation) is required for efficient recombination (Johnson, 1991; van de Putte and Goosen, 1992).

The recombinase, resolvase, a protein with a molecular weight of about 20.5 kilodaltons (kDa), is cleaved by limited proteolysis into two fragments thought to represent distinct functional domains (Abdel-Meguid *et al.*, 1984). The 5 kDa carboxy-terminal fragment binds specifically to the conserved sequences present in inverted repeat configuration at the outer ends of each *res* subsite. This C-terminal domain contains a region with amino acid sequence homology to the helix-turn-helix structural element present in a number of sequence-specific DNA-binding proteins (Harrison and Aggarwal, 1990). Results from footprinting and DNA mutagenesis studies are consistent with resolvase binding via the helix-turn-helix motif interacting primarily with the consensus sequence in the major groove, together with some contacts in the adjacent minor groove (Rimphanitchayakit *et al.*, 1989; Rimphanitchayakit and Grindley, 1990; Graham and Dervan, 1990). Each subsite of *res* binds a dimer of resolvase (Blake, 1993).

The 15.5 kDa amino-terminal fragment of resolvase generated by mild proteolysis is thought to mediate protein-protein interactions, in addition to forming the catalytic site of the enzyme (Abdel-Meguid *et al.*, 1984; Hughes *et al.*, 1990). The crystal structure of the N-terminal domain of γδ resolvase has been determined (Sanderson *et al.*, 1990). The first 120 amino acid residues form a five-stranded β-pleated sheet core surrounded by five α-helices (see Figure 5.3). In a crystal structure of intact

resolvase, the C-terminal domain was disordered, possibly a reflection of flexibility between the two domains (Rice and Steitz, 1994). The presence of a flexible hinge region connecting the two domains of resolvase has been proposed to account for the observation that binding to all three subsites of *res* was comparable in efficiency despite the differences in intra-subsite spacing (Hatfull *et al.*, 1988). A series of mutants of γδ resolvase provided additional evidence that the two domains of the protein fulfil distinct roles (Newman and Grindley, 1984; Hatfull *et al.*, 1988). Footprinting using EDTA·Fe coupled to various amino acid residues to cleave a bound linear subsite I fragment placed the N-terminal domains of the resolvase dimer on the opposite side of the DNA helix from the C-terminal DNA-binding domains (Mazzarelli *et al.*, 1993).

Viewed by electron microscopy, **the complex formed by resolvase and a single *res* site** (termed the resolvosome by some authors) was a compact object (Hatfull *et al.*, 1988), and analysis of the topological effects of resolvase binding suggested that approximately half a negative superhelical turn was trapped (Benjamin and Cozzarelli, 1988). Gel retardation studies showed resolvase-induced bending of the DNA at each subsite of *res* (Salvo and Grindley, 1988). Correct phasing between subsites I and II was required for formation of the compact resolvase-single *res* site complex and for efficient recombination, and DNase I cleavage indicated that the DNA between subsites I and II was in the form of a loop (Salvo and Grindley, 1988), (see the introduction to Chapter 6). This looping of DNA, proposed to arise through an interaction of bound resolvase dimers, was only seen in the presence of subsite III, and when there was correct phasing between subsites I and II. The interaction could be between resolvase dimers bound at subsites I and III, between dimers bound at all three subsites, or between dimers at subsites I and II, but in a subsite III-dependent manner (perhaps reflecting a stabilising or a modifying function for the occupied subsite III). Recombination-defective resolvase mutants unable to form this loop between subsites I and II of *res* (as detected following DNase I treatment) had single amino acid substitutions in a region of the N-terminal domain crystal structure proposed to mediate interactions between resolvase dimers (Hughes *et al.*, 1990; Sanderson *et al.*, 1990).

Footprinting studies suggested that the resolvase-induced bend within subsite I was qualitatively different from those within subsites II and III. Apparently, a structural distortion of the DNA at the centre of subsite I,

the crossover site, was required for recombination (Hatfull *et al.*, 1987). When the DNA was modelled with a helical repeat of 10.5 bp/turn, the direction of this subsite I bend opposed the subsite II and inter-subsite bends discussed above. Models of the path of the DNA and the protein-protein interactions in the complex formed by resolvase and a single *res* site have been proposed on the basis of these experimental observations (Salvo and Grindley, 1988; Hughes *et al.*, 1990).

Mutants of the Gin invertase that catalyse recombination in the absence of the enhancer sequence and FIS appear to induce unwinding of the DNA at the crossover site when bound (Klippel *et al.*, 1993). This distortion of the DNA, equivalent to an unwound region of 5 bp, is not produced by binding of wild-type Gin, but is proposed to arise when the FIS-bound enhancer interacts with the paired recombination sites in a synaptic complex (see Figure 1.7). Localised unwinding of the DNA could aid strand exchange by disrupting base-pairing interactions at the crossover site.

The relationship between the complex formed by resolvase and a single *res* site (the resolvosome) and the synaptic complex formed when resolvase interacts with two *res* sites (termed a synaptosome by some authors) is unclear. Prior to the observations described in this thesis (Chapter 3), the resolvase-single *res* site complexes analysed were all formed on linear DNA, with the exception of the determination of the linkage change trapped by resolvase binding (Benjamin and Cozzarelli, 1988). A comparison of models of the structure of each complex (Salvo and Grindley, 1988; Boocock *et al.*, 1986) suggests that interactions in the resolvase-single *res* complex must be broken before two *res* sites can form a synaptic complex. However, the fact that the resolvase mutants unable to form a normal resolvase-single *res* site complex also fail to catalyse recombination suggests that the same protein-protein interactions may be important in both complexes. The relative simplicity of the invertase recombination sites apparently precludes the formation of a wrapped single-site complex, but such a complex is formed by lambda integrase at *att*P, one of the partners in integrative recombination (Nash, 1990), and at *att*L and *att*R, the partners in excisive recombination (Kim *et al.*, 1990; Kim and Landy, 1992).

Much of our current understanding of the Tn*3* *res*-resolvase system has come from study of **the *in vitro* site-specific recombination reaction.**

The requirements for efficient *in vitro* recombination are: purified resolvase, the DNA substrate - negatively supercoiled plasmid DNA carrying two *res* sites in direct repeat orientation, and simple buffering conditions (Reed, 1981). Virtually all of the reaction product is in the form of a specific supercoiled singly interlinked catenane, with two negative nodes[1] (Figure 1.3), (Krasnow and Cozzarelli, 1983; Wasserman and Cozzarelli, 1985).

Two important points emerge from basic observations of *in vitro* Tn*3* resolvase-catalysed recombination:

i) As mentioned above, nearly all of the product is a specific simple catenane.
ii) There is a strong bias against recombination between *res* sites in inverted repeat orientation, or between *res* sites on different DNA molecules (Krasnow and Cozzarelli, 1983).

Taken together, these observations suggest that the synapsis of *res* sites, and the ensuing strand exchange, is topologically constrained. The DNA substrate for resolvase-catalysed recombination can be divided into two domains defined by the two crossover sites (Figure 1.3). Nodes in the negatively supercoiled substrate DNA can therefore be intradomainal (when the duplexes that cross are part of the same domain), or interdomainal (when the duplexes that cross are from different domains). Only interdomainal nodes trapped between the crossover sites in the productive synapse can contribute to product topology by forming knot and/or catenane nodes following recombination (Benjamin and Cozzarelli, 1986). Synapsis by random collision of *res* sites in three-dimensional space would trap a variable number of interdomainal nodes, giving a mixture of products. Such multiply-linked catenanes are seen in lambda integrase-catalysed recombination (Landy, 1989), highlighting fundamental differences in the action of Tn*3* resolvase and lambda integrase. It is generally true that members of the integrase family will execute inter- and intramolecular recombination of sites in either direct or inverted orientation, in contrast to the more stringent requirements of the resolvase family of recombinases.

---

[1] The sign convention for nodes – crossings of DNA duplex when the DNA is represented in plane projection – can be summarised as follows: the DNA is assigned an arbitrary direction along its axis and the topmost duplex is rotated by not more than 180° so that it is aligned in the same direction as the underlying duplex. If clockwise rotation of the topmost duplex is required, then the node is negative; if counter-clockwise rotation is necessary, then the node is positive (Cozzarelli *et al.*, 1990).

However, although virtually all of the product resulting from the *in vitro* recombination reaction catalysed by Tn*3* resolvase is in the form of a (-2) catenane, small amounts (1-3%) of more complex catenanes and knotted circles are produced (Figure 1.3), (Wasserman and Cozzarelli, 1985). Assuming that these minor products are formed by iteration of the strand exchange mechanism without dissociation of the synaptic complex, the topology of the resolution reaction can be deduced (Wasserman and Cozzarelli, 1985; Wasserman *et al.*, 1985).

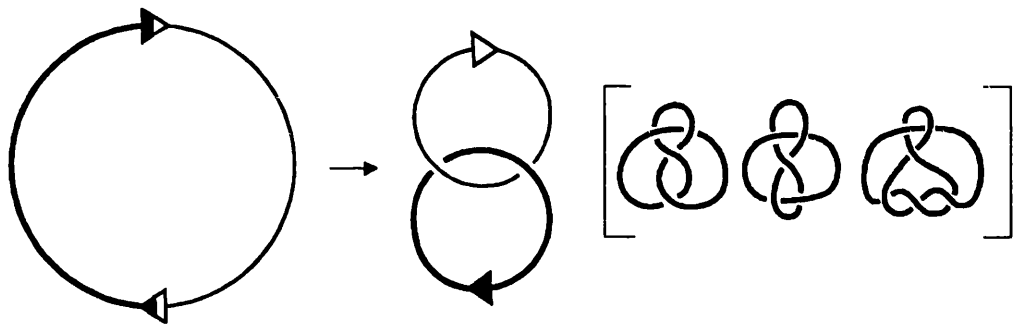

Figure 1.3 *In vitro* site-specific recombination by Tn*3* resolvase. The major product is a specific (-2) catenane. The two domains of the plasmid DNA substrate, delimited by the points of crossover within each *res* subsite I, are represented by different line thickness. The more complex minor products of the reaction are shown bracketed.

It was proposed that three negative interdomainal nodes were trapped between the parallel-aligned crossover sites in the synaptic complex. If the strand exchange mechanism then introduced one positive node by rotating the cleaved DNA strands 180° in a right-handed sense (i.e. clockwise looking from the synapsed subsite I's towards the accessory subsites of *res*) prior to religation, the observed simple catenane was produced (Figure 1.4). The minor products were then readily explained by the continued rotation of the cleaved strands without dissociation of the synapse. Thus, products formed by an odd number of rounds of 180° rotation prior to religation of the DNA strands will be catenanes, while an even number of rounds gives products identical to the substrate in primary sequence. The complexity of these minor products is due to the introduction of an additional positive node with each iteration of the strand exchange mechanism. The products of recombination *in vivo* were essentially the same as those generated *in vitro*. *In vivo*, the component

circles of the catenane were efficiently separated by the action of DNA gyrase (Bliska *et al.*, 1991).

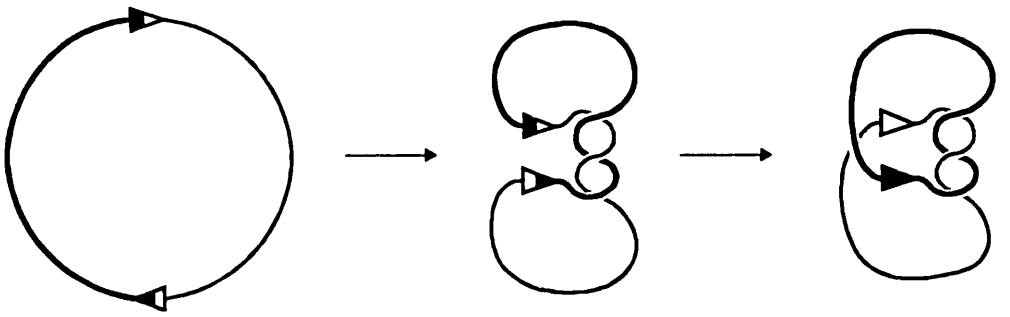

Figure 1.4 Proposed topology of the cointegrate resolution reaction catalysed by Tn*3* resolvase. Three negative interdomainal nodes are trapped between the *res* crossover sites at synapsis. Strand exchange has a right-handed sense, generating a positive node. This gives the observed major product, the (-2) catenane.

When an *in vitro* recombination reaction catalysed by γδ resolvase was performed in the absence of Mg^{2+}, a presumptive intermediate accumulated. This intermediate had 2 bp staggered double-strand breaks at the centre of *res* subsite I, and resolvase was covalently linked to the 5' position of the recessed A nucleotide via a phosphoserine bond (Reed and Grindley, 1981; Reed and Moser, 1984), (see Figure 1.2). A similar phosphoserine linkage was demonstrated for the Gin invertase (Klippel *et al.*, 1988). The amino acid residue implicated in the covalent attachment of resolvase to the DNA at the crossover site was serine-10 (Hatfull and Grindley, 1986). This is reminiscent of the reaction mechanisms of topoisomerases in which the energy of the phosphodiester bond is conserved in a protein-DNA linkage so that religation does not require a 'high-energy' cofactor (Maxwell and Gellert, 1986). There is no ATP requirement in the resolvase catalysed reaction. Indeed, in addition to its recombinase activity, resolvase also has a site-specific type I topoisomerase activity with the same substrate requirements (Krasnow and Cozzarelli, 1983).

Lambda integrase is also a type I topoisomerase. However, although the type I topoisomerase activity of resolvase is suggestive of an integrase-type recombination mechanism that involves single strand exchanges

(Krasnow and Cozzarelli, 1983), it has been proposed instead to be an undesirable side-reaction brought about by premature destabilisation of the recombinational synapse (Falvey *et al.*, 1988). The use of a conserved serine to form a covalent intermediate with DNA is a distinguishing feature of the resolvase family of site-specific recombinases (Stark *et al.*, 1992). The integrase family recombinases also form a 'high-energy' intermediate, but it is a tyrosine residue that is covalently linked to DNA. Recent studies of γδ resolvase structure by X-ray crystallography indicated that the conserved tyrosine at position 6 in the resolvase sequence was more exposed than initially thought, suggesting that a role in catalysis cannot be completely discounted at this time (Grindley, 1994).

The evidence obtained to date suggests that resolvase cleaves all four strands of DNA at the point of crossover in the centre of *res* subsite I before any of the strands are religated. No Holliday intermediates (molecules in which only one pair of strands have been cleaved and exchanged) have been detected (Sherratt, 1989). This represents another difference between the resolvase and integrase families, since the latter do form such an intermediate (Landy, 1989).

Resolvase-mediated synapsis.

Various models have been proposed, detailing the way in which two copies of the *res* site come together in the presence of resolvase, the structure of the resulting synaptic complex, and the ensuing strand exchange step. Two proposals for the kinetic mechanism of synapsis attempt to explain the topological selectivity and the selectivity for direct repeats of the *res* site by constraining the ways that the two sites can come together initially.

A tracking mechanism in which resolvase, bound to one *res* site, diffuses along the adjacent DNA until it encounters a second *res* site (Kitts *et al.*, 1983; Krasnow and Cozzarelli, 1983), although attractive as an explanation for the bias against intermolecular recombination and recombination of inverted *res* sites, was refuted (Benjamin *et al.*, 1985; Brown, 1986). In fact, the orientation specificity and intramolecular preference of the *res*-resolvase system disappear when linear or relaxed circular DNA substrates are used under appropriate conditions *in vitro* (Boocock *et al.*, 1986).

Slithering, a dimensionally constrained diffusion proposed to occur in plectonemically wound supercoiled DNA, has been suggested as a process that could bring together *res* sites in a defined synapse (Benjamin and Cozzarelli, 1986). Although there is good evidence that negatively supercoiled DNA in solution is plectonemically wound (Boles *et al.*, 1990; Adrian *et al.*, 1990), continual conveyor belt-like motion to juxtapose segments of DNA that may be distant in the primary structure has not been shown to occur. If such a process were to play a major role in defining the *res*-resolvase synaptic complex, then the recombination seen to occur with non-supercoiled substrates (Boocock *et al.*, 1986) would have to take place via a reaction mechanism very different from that involved in the recombination of supercoiled DNA substrates.

In contrast, **the two-step synapsis model** (Boocock *et al.*, 1986; Boocock *et al.*, 1987) proposes that selection of a unique synapse topology occurs after the initial encounter of *res* sites: a random collision of two *res* sites with resolvase bound goes on to form a stable productive synapse only when three negative interdomainal nodes are trapped between the crossover sites. It is suggested that this occurs most readily following an initial antiparallel alignment of subsites II and III of the two *res* sites with no trapped interdomainal nodes. The paired accessory subsites of *res* interact via the bound dimers of resolvase which come together to form tetramers. The three negative interdomainal nodes are trapped by right-handed plectonemic wrapping of the antiparallel duplexes around the tetramers (Figure 1.5), (Stark *et al.*, 1989b; Benjamin and Cozzarelli, 1990). This interwrapping of the accessory subsites could be in part stabilised by the relief of superhelical tension in a negatively supercoiled DNA substrate.

Antiparallel alignment and wrapping of the accessory subsites is step one of the two-step model for resolvase-mediated synapsis. This allows a parallel alignment of the two *res* subsite I's, paired by the interaction of the bound resolvase dimers to form a catalytic tetramer – step two (Figure 1.5). It has been shown that the accessory subsites of *res* are important for correct subsite I alignment (Bednarz *et al.*, 1990), (see the later discussion on the role of subsites II and III in synapsis of *res* sites).

An analysis of the *res* site DNA sequence using known sequence preferences for DNA 'bendability' was consistent with the path of the DNA in the original model of the synapse (Boocock *et al.*, 1986). The

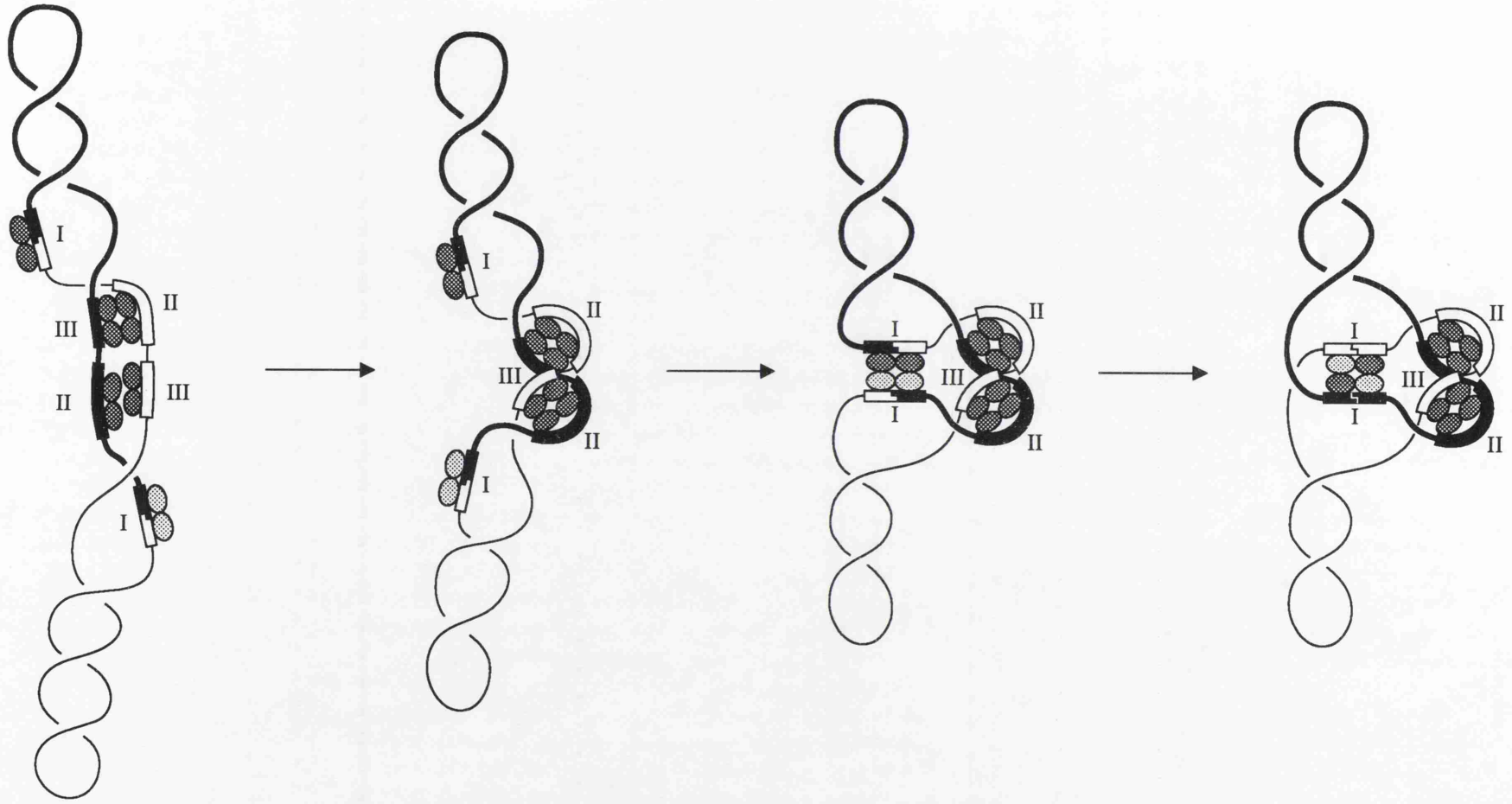

Figure 1.5 The two-step synapsis model for resolvase-catalysed recombination (Boocock *et al.*, 1986; Boocock *et al.*, 1987). The two domains of the negatively supercoiled substrate DNA (shown plectonemically wound) are represented by different line thickness. Interacting resolvase monomers, bound to the *res* subsites, are shown as ellipses. Strand exchange is depicted as a simple rotation of subunits within the catalytic tetramer at the synapsed subsite I. See the text for further details.

figures used in the analysis were those for variation in occurrence of the ten dinucleotides with respect to whether the minor grooves faced in toward the protein or outward in 177 different DNA molecules from nucleosome core particles (Satchwell *et al.*, 1986). These sequence preferences on the nucleosome have been shown to apply well to other complexes where the path of the DNA around the protein is known. A more detailed model of the path of the DNA in the Tn*3* resolvase-*res* synaptic complex produced using these data is shown in Figure 1.6 (J.L. Brown, M.R. Boocock, and D.J. Sherratt, unpublished). Important features of this model are:

- The major groove faces inward at the centre of subsite I.
- There is tight bending of the DNA helix at subsite II.
- The minor groove faces inward at the centre of the subsite II-III spacer.
- There are 6.5 turns of the helix (local frame) between the crossover site and the centre of the subsite II-III spacer (72.5 bp). Thus, the DNA in the synapse is undertwisted, particularly in the subsite I-II spacer region.

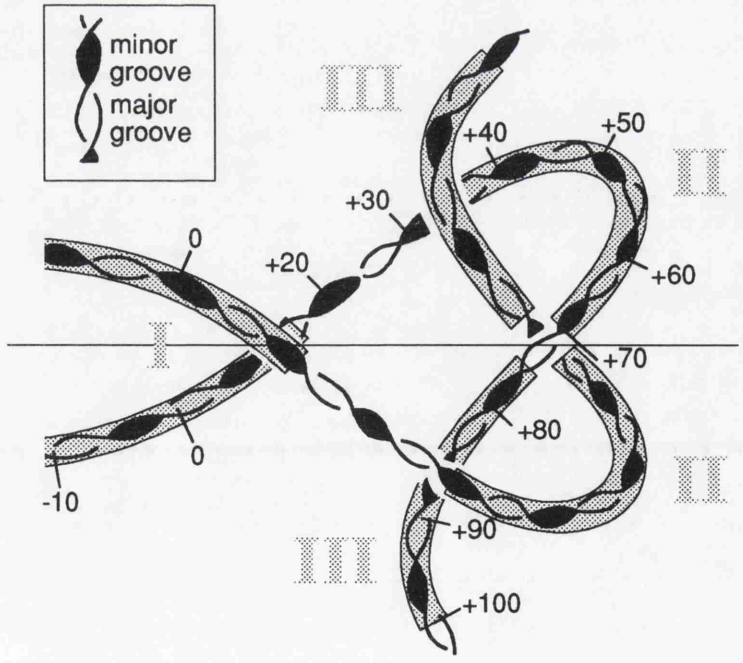

Figure 1.6 A model for the path of the DNA in the synapse formed by Tn*3* resolvase with two copies of the *res* site in direct repeat orientation (J.L. Brown, M.R. Boocock, and D.J. Sherratt, unpublished). The DNA sequence is numbered relative to the centre of the crossover site (designated zero). DNA major and minor grooves are differentiated, with the latter shown in black. See the text for further details.

- At subsite I, the N-terminal catalytic domain of resolvase is positioned on the same side of the helix as the C-terminal DNA-binding domain.

In the two-step synapsis model, the requirement for a synapse structure in which three negative interdomainal nodes are trapped between the crossover sites acts as a topological filter, only letting through the initial *res* site collisions that can go on to form a stable productive synapse (Boocock *et al.*, 1987). Thus, more complex initial collisions of direct repeats of *res*, and all interactions of inverted repeats and sites on different DNA molecules, are proposed to result in a 'tangled' synapse conformation that is energetically unfavourable in a negatively supercoiled substrate. Such unproductive synapses readily dissociate, so that a productive synapse can form rapidly by trial and error.

It is tempting to equate the proposed role of the enhancer site in the inversion reaction with that of the accessory subsites of *res* in resolvase-catalysed recombination. A model suggested for the synaptic complex formed during the DNA inversion reaction catalysed by Gin or Hin incorporates the enhancer site in a tripartite complex with the recombination sites (Johnson, 1991; van de Putte and Goosen, 1992). The recombination sites interact with the enhancer in a branched plectonemically supercoiled structure and strand exchange occurs via a single 180^{o} clockwise rotation (Figure 1.7). A recent hypothesis for enhancer action proposed that Gin was unable to catalyse strand cleavage until the FIS-bound enhancer joined the synaptic complex and induced a conformational change resulting in partial unwinding of the DNA at the recombination site (Klippel *et al.*, 1993).

Strand exchange in the resolvase system could occur by a 180^{o} rotation of one half of the catalytic tetramer with respect to the other half after all four DNA strands have been cleaved at the crossover site and each resolvase monomer has become covalently linked to a 5' end (Figure 1.5), (Stark *et al.*, 1989b). This 'simple rotation' model for strand exchange is consistent with evidence that the catalytic domain of the resolvase monomer acts on the *res* site to which it is bound (Dröge *et al.*, 1990; Mazzarelli *et al.*, 1993; Grindley, 1994). However, it is not known whether a resolvase subunit becomes covalently linked to the DNA half-site to which it is bound, or whether it becomes linked to its partner's half-site.

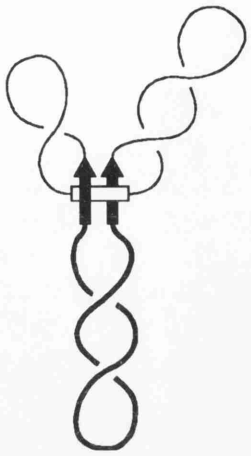

Figure 1.7 A proposed structure for the invertasome complex formed by interaction of the paired recombination sites (bound by the invertase; represented by black arrows) and the FIS-bound enhancer (open box) in bacterial DNA inversion systems. See the text for further details. Figure adapted from Johnson (1991).

The values for linkage change determined for the forward resolution reaction (+4), the reverse catenane fusion reaction (-4; occurring only at low superhelical densities), and the formation of four-noded non-recombinant knot (+4) are all consistent with the simple rotation model (Stark *et al.*, 1989b; Stark and Boocock, 1994). Note that in this model it is not the resolvase dimers originally bound to the unpaired *res* subsite I's that rotate with respect to one another, but rather a new combination of monomers. This suggests that major changes in interactions between resolvase monomers must occur on synapse formation. The problem of maintaining sufficient subunit contact throughout the rotation step in order to prevent dissociation of the four cleaved DNA ends with attached resolvase monomers is not inconsiderable.

Data from X-ray crystallography have provided little information on the structure of the synaptic complex, but suggest subunit interactions that may be involved in synapsis. Of the three dimeric pairs found in the crystal structure of the N-terminal domain of γδ resolvase (Sanderson *et al.*, 1990), the 1,2 dimer represents the solution and DNA-binding dimer (Hughes *et al.*, 1993). However, the 1,2 dimer appears unsatisfactory when considering a role in synapsis and strand exchange. Although a tetramer having the expected 222 symmetry is present in the crystal, the 1,2 dimer is not part of it, and the active site serine residues in the 1,2

dimer are considered too far apart to interact with the DNA at the centre of the crossover site. Of course, it may be that the 1,2 dimer and a subsite of *res* distort considerably when they interact, in which case it is perhaps not surprising that a synaptic tetramer is not represented in a crystal structure of the protein component alone. The implications of recent evidence that the 1,2 dimer is involved in catalysis of strand exchange at subsite I of *res* are considered in the introduction to Chapter 5 (Grindley, 1993).

A model for the synaptic complex suggested by the packing of γδ resolvase subunits in the crystal has recently been proposed (Rice and Steitz, 1994). It differs considerably from the model of Boocock *et al.* (1986) in that the two copies of *res* subsite I are in close proximity in the centre of a catalytic complex with subsite I-bound resolvase dimers on the outside (Figure 1.8). After resolvase-induced unwinding of the crossover site DNA, strand exchange is proposed to occur via movement only of the free 3'-hydroxyls generated by cleavage, rather than by subunit exchange. In this model, the resolvase dimers at subsite I interact with a octamer formed by synapsis of the resolvase-bound accessory subsites (see Figure 5.1b). However, it remains the case that the *res* site DNA cannot be modelled accurately as interacting with any of the multimeric forms of resolvase present in the crystal without significant distortion of both the DNA and the protein, and there is insufficient structural information on the nature of this distortion.

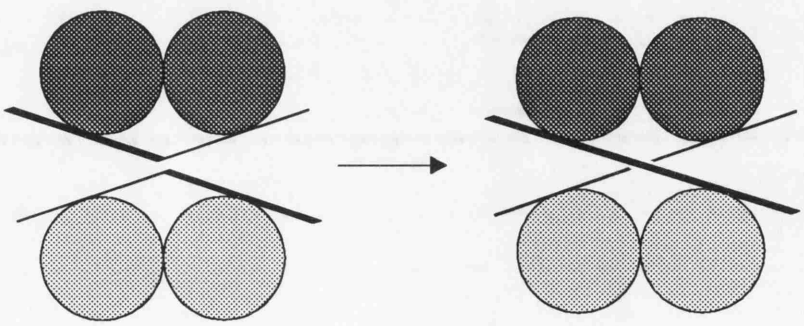

Figure 1.8 A proposal for resolvase-catalysed DNA strand exchange occurring without subunit exchange (Rice and Steitz, 1994). In this model, the two copies of subsite I of *res*, with the 1,2 dimer form of resolvase bound, synapse such that the DNA strands are in close proximity in the centre of the complex. Strand exchange is accomplished via movement of the free 3'-hydroxyls, without dissociation of bound resolvase. See the text for further details.

The resolution characteristics of multiple *res* site plasmids provide information relevant to synapsis (Brown, 1986). Implicit in the two-step model is the notion that synapsis is reversible – an unstable pairing of recombination sites will rapidly fall apart, thus allowing a more stable, productive, pairing. Observations are consistent with an unstable pairing of non-adjacent sites in a substrate carrying four *res* sites in direct repeat orientation; one non-adjacent pair can form a productive synapse (and produce recombinant as efficiently as the adjacent pairs) if the destabilising interaction of the other non-adjacent pair is prevented. Having three of the four sites close together in the substrate achieved this, possibly by trapping one member of a non-adjacent pair on an inflexible small loop formed when the other non-adjacent pair of sites were synapsed. Inhibition of recombination between non-adjacent pairs of *res* sites in a plasmid containing four sites in direct repeat orientation was also seen when one of the sites had subsite I deleted (R. McCulloch, unpublished). This suggests that an intact *res* site can pair with a copy of subsites II and III, an observation consistent with the proposed importance of accessory subsite interactions during step one of the two-step model for resolvase-mediated synapsis (Boocock *et al.*, 1986; Boocock *et al.*, 1987).

Additional information on **the role of subsites II and III in synapsis of *res* sites** can be gleaned from the results of various experiments. Subsite I of *res* was replaced by the recombination site from the Gin DNA inversion system, maintaining the spacing between recombination site and subsite II found in the wild-type *res* site. When a supercoiled plasmid, containing two copies of this hybrid site in direct repeat orientation, was incubated with both the Gin invertase and Tn*3* resolvase, the predominant product was (–2) catenane (M.R. Boocock, personal communication). In contrast, reaction with the Gin invertase alone produced the non-recombinant trefoil and 6-node knots characteristic of the reaction of the Gin invertase and direct repeats of its recombination site (Kanaar *et al.*, 1990). Incubation of the hybrid site substrate with resolvase alone gave no product. Thus, the accessory subsites of *res* can define the topology of the product of Gin-mediated recombination, a finding that indicates both a major role in synapsis of wild-type *res* sites and a degree of independence from synapsis of the two copies of subsite I, as predicted by the two-step model. However, a similar experiment substituting subsite I of Tn*3* *res* with subsite I of Tn*21* *res* failed to give

product when both resolvases were added (M.R. Boocock, personal communication).

Correct alignment of the crossover sites, resulting in resolution, was maintained when subsite I was made perfectly symmetrical in both copies of a Tn*3* *res* site oriented as direct repeats in a supercoiled plasmid DNA molecule (Bednarz *et al.*, 1990). Recombinant indicative of correct alignment was also the predominant product of the intermolecular reaction catalysed by resolvase when this modified *res* site was isolated on a linear DNA molecule. Two copies of the wild-type subsite I of *res*, with the accessory subsites deleted from both sites in a supercoiled DNA molecule, failed to recombine. However, deletion of the accessory subsites from one partner only resulted in the formation of resolution product regardless of whether the isolated subsite I and the intact *res* site were oriented as direct or inverted repeats (Bednarz *et al.*, 1990). Thus, the presence of the accessory subsites in both *res* sites was necessary to ensure correct alignment of the crossover sites, although the presence of accessory subsites in one partner only appeared sufficient to define the synapse topology (see Section 3.5).

An increase in spacing between subsites I and II of the γδ *res* site, representing the addition of two turns of the DNA helix, did not affect the efficient resolution of a substrate containing two copies of this modified site in direct repeat orientation (Salvo and Grindley, 1988). This represents further evidence of a quasi-independence of the accessory subsite synapse from events at the crossover site, suggesting that direct contact is not necessary. The role of the accessory subsites in synapsis is considered in Sections 3.5, 4.2, and in Chapter 6 of this thesis.

Information on the rate of synapsis by resolvase has been obtained using a novel method for assaying interactions between distant sites in DNA. Recombination between a pair of directly repeated *res* sites by Tn*3* resolvase was inhibited by the interaction of *lac* repressor with its operator sites provided one operator site was located in each domain of the resolvase substrate – the suggestion being that the *res* sites were topologically isolated on separate loops formed when the *lac* operator sites came together (Saldanha *et al.*, 1987). A system in which Tn*21* resolvase reported on interactions between the Tn*3* *res* sites was created by replacing the *lac* repressor/operators with Tn*21* resolvase/*res* sites and using reaction conditions in which Tn*21* recombination greatly outpaced

Tn*3* recombination (Parker and Halford, 1991). The requirement that there be no direct interaction between the systems was demonstrated.

In constructs where direct repeats of the Tn*21* *res* site were interspersed with either direct or inverted repeats of the Tn*3* *res* site, preincubations with Tn*3* resolvase reduced the extent of recombination by the subsequently added Tn*21* resolvase to about 25% of that seen when Tn*3* resolvase was not present (Parker and Halford, 1991). This inhibition of Tn*21* recombination was attributed to the isolation of the Tn*21* *res* sites on separate domains by synapsis of the Tn*3* *res* sites. The concentration dependency of the inhibitory effect was equivalent to that seen for recombination (maximal inhibition reached at 6 mol. Tn*3* resolvase dimer per mol. DNA). All of the substrate DNA that had formed a synapse with direct repeats of the Tn*3* *res* site (as assayed by the inhibition effect) went on to produce Tn*3* recombinant, despite it taking more than 3 hours for the Tn*3* reaction to reach completion under the reaction conditions used. In contrast, the inhibitory effect of inverted repeats of the Tn*3* *res* site was not long-lived, the inhibition breaking down with a half-time of about 5 minutes.

Under reaction conditions in which both resolvases functioned efficiently, the inhibition of Tn*21* recombination attributed to the interaction of Tn*3* *res* sites in direct repeat orientation was fully established when the preincubation with Tn3 resolvase was 0.5 seconds (Parker and Halford, 1991). Thus, under the reaction conditions used, a rapid and very stable interaction between Tn*3* *res* sites in direct repeat orientation was seen. The authors believed this interaction too rapid to permit a defined synaptic structure to arise from random collision of *res* sites in the manner proposed by the two-step model described earlier. Instead they debated the merits of slithering as a means of bringing the sites together in an ordered manner to form the correct synapse structure. Recognising the problem of reconciling this mechanism with the random collision of DNA sites thought to precede lambda integrase-mediated synapsis, they suggested that both ordered and random collisions could occur in a DNA molecule and that the predominance of one or the other as the means of bringing together the recombining sites in a particular system may be governed by the reaction kinetics of the recombinase.

I end this introductory chapter with an outline of an earlier reported investigation of the synaptic complex formed by Tn*3* resolvase, a study

that it was initially hoped would provide a stepping stone in the elucidation of further details of the synaptic intermediate (Benjamin and Cozzarelli, 1988). A putative synaptic intermediate was detected by its characteristic electrophoretic mobility in agarose gels in a yield reported to vary between 40 and 100% of the input substrate when the reaction temperature was lowered and the protein crosslinking reagent glutaraldehyde was added. This synaptic complex was only seen when the substrate DNA was negatively supercoiled and carried two *res* sites, although both direct repeats and inverted repeats of the *res* site gave complex. Addition of SDS prior to electrophoresis disrupted the complex, showing that stabilisation was indeed conferred by crosslinking of the protein component. Electron microscopy revealed that the *res* sites were complexed in a spherical mass estimated to be about 100 Å in diameter. Relaxation of the supercoiled DNA in the crosslinked synapsis reactions, using topoisomerase I, was used to determine the linking number difference trapped in the crosslinked synapse. The isolation and characterisation of a Tn*3* resolvase synaptic complex by Benjamin and Cozzarelli (1988) will be considered further in Chapters 3 and 4 of this thesis.

Chapter 2

Materials and methods

2.1 Bacterial strains.

The bacterial strains used for plasmid DNA amplification and resolvase expression were derivatives of *Escherichia coli* K-12.

Strain	Genotype	Source/reference
AB1157	*thr*1, *leu*6, *his*G4, *thi*1, *ara*14, *pro*A2, *arg*E3, *gal*K2, *sup*37, *xyl*15, *mtl*1, *tsx*33, *str*31	
DS941	AB1157, but *rec*F143, *sup*E44, *lac*ZΔM15, *lac*I^q	D.J. Sherratt
DS902 (AB2463)	AB1157, but *rec*A13	D.J. Sherratt
JM101	*sup*E, *thi*, D(*lac*, *pro*AB) [F', *tra*D36, *pro*AB, *lac*ZΔM15, *lac*I^q]	Yanisch-Perron *et al.*, 1985

2.2 Plasmids.

The plasmids used or constructed are listed in Table 2.1, beginning overleaf.

2.3 Chemicals.

The major sources of chemicals are listed below. Sources of specialised chemicals, buffers, and proteins are identified in the appropriate methods Sections.

Chemicals	Source
General chemicals, biochemicals, organic solvents	Aldrich/Sigma, BDH, May & Baker
Media	Difco, Oxoid
Agarose, acrylamide	BRL, FMC, Bio-Rad
Radiochemicals	ICN Biomedicals

2.4 Bacterial growth.

a) Media.

Growth was in L-Broth (10 g bacto-tryptone, 5 g bacto-yeast extract, 5 g NaCl made up to 1 litre with deionised water, and adjusted to pH 7.5 with NaOH), or on L-Agar (L-Broth with 15 g/l agar). The resolvase expression strain JM101(pMA6111) was maintained on minimal agar consisting of 1 x Davis & Mingioli (D & M) salts[1] and 1.5% agar, supplemented with 1 μg/ml thiamine (vitamin B1) and 0.2% glucose.

[1] 4 x D & M salts: 28 g $K_2HPO_4.3H_2O$, 8 g KH_2PO_4, 4 g $(NH_4)_2SO_4$, 1 g tri-sodium citrate.$2H_2O$, 0.4 g $MgSO_4.7H_2O$, made up to 1 litre with deionised water. D & M salts were sterilised at 120°C for 20 minutes.

Plasmid	Size (bp)	Antibiotic resistance markers	Description/derivation (reference is made to figures in this thesis showing maps of the various plasmids)	Source or Reference
pAL261	4848	Ap Tc	2381 bp *Pst*I/*Ava*I (*res* subsite I) pAL11 + 2467 bp *Pst*I/*Ava*I (wt *res*) pMA2615 (see Figure 3.25)	Bednarz *et al.*,1990
pAL265	4848	Ap Tc	2381 bp (*res* subsite I) pAL15 + 2467 bp *Pst*I/*Ava*I (wt *res*) pMA2615 (see Figure 3.25)	Bednarz *et al.*,1990
pAL3151	2750	Ap	Exonuclease III deletion of pAL31; subsites II/III (see Figure 3.23)	Bednarz,1989
pBR322	4363	Ap Tc	Vector derived from pMB1	Sutcliffe, 1978
pCM3	5451	Ap Tc	1119 bp *Eco*RI/*Hin*dIII (Tn*3* wt *res* + Tn*21* wt *res*) pCM1 + 4332 bp *Eco*RI/*Hin*dIII pBR322 (see Figure 3.10)	C. McDougall
pDB5	6652	Ap	1900 bp *Hin*dIII/*Acc*I (*galK*) + 4752 bp *Hin*dIII/*Eco*RV pAL225 (see Figure 3.25)	Blake, 1993
pGC1	4927	Ap Tc	pMA21 derivative (mutagenesis of crossover dinucleotide of pLS139-derived *res* site: AT→TA)	G. Calder
pGC4	4927	Ap Tc	pMA21 derivative (mutagenesis of crossover dinucleotide of both *res* sites: AT→TA)	G. Calder
pMA1441	2968	Ap	282 bp *Pvu*II (wt *res*) pLS138 + *Sma*I pUC18	M.R. Boocock
pMA21	4927	Ap Tc	1065 bp *Pst*I/*Hin*dIII pLS139 + 3862 bp *Pst*I/*Hin*dIII pMA44 (see Figure 3.16)	Bednarz *et al.*,1990
pMA2350	3326	Ap	282 bp *Pvu*II (wt *res*) and 358 bp *Hae*III (wt *res*) in *Sma*I and *Hin*cII pUC18 (see Figure 3.21)	Stark *et al.*,1989b
pMA2631	4927	Ap Tc	2460 bp *Pst*I/*Ava*I pMA21 + 2467 bp *Pst*I/*Ava*I pMA1961 (see Figure 3.16)	Bednarz *et al.*,1990
pMA44	4645	Ap Tc	282 bp *Pvu*II (wt *res*) pLS138 + *Pvu*II pBR322 (see Figure 3.16)	M.R. Boocock
pMA6111	5900	Ap	1324 bp *Eco*RI/*Pst*I (Tn*3* *tnpR*) +4600 bp *Eco*RI/*Pst*I pKK223-3	Blake, 1993

Table 2.1 Plasmids.

Plasmid	Size (bp)	Antibiotic resistance markers	Description/derivation (reference is made to figures in this thesis showing maps of the various plasmids)	Source or Reference
pMS2	5936	Ap	Dimer of pMA1441 (see Figure 3.38)	W.M. Stark
pMS11	4611	Ap	312 bp *Bam*HI/*Hin*dIII (*res*) pMA2350 + 4299 bp *Bam*HI/*Hin*dIII pMA44 (mutagenesis of crossover dinucleotide of pMA2350-derived *res* site: AT→AC) (see Figure 3.41)	W.M. Stark
pMS12	4611	Ap	312 bp *Bam*HI/*Hin*dIII (wt *res*) pMA2350 + 4299 bp *Bam*HI/*Hin*dIII pMA44 (see Figure 3.41)	W.M. Stark
pMW11	4455	Ap Tc	92 bp *Eco*RI pAL3151 (*res* subsites II/III) + *Eco*RI pBR322 (see Figure 3.23)	Section 3.5
pMW13	4551	Ap Tc	92 bp *Eco*RI pAL3151 (*res* subsites II/III) (filled-in) + *Pvu*II pMW11 [= direct repeats of *res* II/III]	Section 3.5
pMW14	4551	Ap Tc	92 bp *Eco*RI pAL3151 (*res* subsites II/III) (filled-in) + *Pvu*II pMW11 [= inverted repeats of *res* II/III]	Section 3.5
pUC18	2686	Ap	Vector derived from pBR322	Yanisch-Perron *et al.*, 1985

Table 2.1 Plasmids.

a) Media (continued from page 24).

Growth media were sterilised at 120°C for 15 minutes, $CaCl_2$ at 114°C for 10 minutes, and other supplements at 108°C for 10 minutes. Where required, growth media were supplemented with 0.2% glucose.

b) Antibiotics.

The following antibiotics were used in selective growth media: ampicillin (50-100 μg/ml), tetracycline (10 μg/ml), and streptomycin (50 μg/ml). Stock solutions were stored at 4°C.

c) Bacterial cultures.

Inoculation of liquid or solid media was with purified strains or with a single colony from non-purified strains. All liquid cultures were grown at 37°C with vigorous shaking. Growth on agar plates was at 37°C for a minimum of 12 hours. For long-term storage, cultures grown overnight in L-Broth were diluted 2-fold with 40% glycerol + 2% peptone, and were maintained at –70°C.

2.5 Transformation of *E.coli* with plasmid DNA.

1 ml of a stationary liquid culture was diluted 20-fold in L-Broth and grown to an OD_{600} (optical density at 600 nm wavelength) of about 0.35, which is equivalent to approximately 2×10^8 cells per ml. The cells were harvested by centrifugation (12 000 g, 4°C, 1 minute), resuspended in 10 ml ice-cold 50 mM $CaCl_2$, and pelleted again (centrifugation as above). The cells were then resuspended in 1 ml ice-cold 50 mM $CaCl_2$. This procedure results in a suspension of cells competent for uptake of DNA. The mechanism is poorly understood but it has been suggested that the cell envelope is rendered accessible to interaction with DNA by a combination of low temperature, making the normally fluid membrane structure more rigid, and divalent cations shielding the negative charges of phosphate groups of both the cell envelope and the subsequently added DNA (Hanahan, 1987).

About 0.5 μg plasmid DNA was added to 200 μl of the competent cell suspension. This transformation mixture was incubated on ice for 15 minutes, given a heat shock at 37°C for 5 minutes, then left a further 15 minutes on ice. Addition of 1 ml L-Broth was followed by incubation at 37°C for 60 minutes to allow recovery of cells and expression of exogenous

DNA. 100 µl aliquots of this culture (or appropriate dilutions thereof) were plated on medium selective for antibiotic resistance markers carried on the transforming plasmid DNA. For all transformations, non-transformed competent cells were plated on selective medium as a control.

2.6 Isolation of plasmid DNA from *E.coli.*

Methods utilised were adapted from Birnboim and Doly (1979)

a) Large-scale preparation.

Cells from a 200 ml liquid culture, grown to stationary phase (approximately 12 hours shaking at 37°C), were harvested by centrifugation (12 000 g, 4°C, 5 minutes). The pellet was resuspended in 4 ml GTE (50 mM glucose, 25 mM Tris-HCl (pH 8.0), 10 mM EDTA), and the cell suspension was incubated on ice for 5 minutes with gentle agitation. 8 ml of an alkaline sodium dodecyl sulphate (SDS) solution (200 mM NaOH, 1% SDS; freshly mixed) was added, and the suspension was incubated on ice for 4 minutes with gentle agitation by inversion. This treatment irreversibly denatures chromosomal DNA, but the topologically intertwined strands of the relatively small covalently closed circular plasmid DNA molecules quickly reform native superhelical molecules when the pH is returned to normal.

Chromosomal DNA, high molecular weight RNA, and potassium/SDS/protein/membrane complexes were precipitated by addition of 6 ml of ice-cold potassium acetate/acetic acid solution (0.6 vol. 5 M CH_3COOK, 0.115 vol. CH_3COOH made up to 1 vol. with H_2O). The precipitate was pelleted by centrifugation (39 200 g, 4°C, 30 minutes), and the supernatant was added to 12 ml isopropanol. Incubation at room temperature to allow precipitation of the DNA was for a minimum of 15 minutes, and this was followed by centrifugation (27 200 g, 20°C, 30 minutes). The supernatant was discarded, and the pellet was washed with 70% ethanol, then resuspended in 2 ml TE (10 mM Tris-HCl (pH 8.0), 1 mM EDTA) by shaking at 37°C for 1-2 hours. The suspension was centrifuged (27 200 g, 20°C, 5 minutes) to remove any undissolved material, and the supernatant was added to a solution of 5 g caesium chloride in 3 ml deionised water. 270 µl of 15 mg/ml ethidium bromide was added, and the resulting solution (with a density of about 1.58 g/ml) was transferred to an ultracentrifuge tube. Following addition of liquid paraffin to fill the tube and

heat sealing of the tube, the CsCl gradient was centrifuged in a Beckman Ti70 fixed-angle rotor at 200 000 g for 16 hours at 20°C.

DNA was visualised using a long-wave UV source (365 nm wavelength), and the band representing fractionated supercoiled plasmid DNA was removed using a 1 ml syringe. Generally two DNA bands were visible, with the band closer to the top of the ultracentrifuge tube representing nicked plasmid and contaminating chromosomal DNA. 2 ml of deionised water was added to the recovered DNA solution (typically about 0.8 ml volume), and the ethidium bromide was removed by repeated extraction with 0.75 vol. butanol. The aqueous solution was diluted two-fold by addition of deionised water, and the DNA was recovered by addition of two volumes of ethanol, incubation at –20°C for 30 minutes, and centrifugation (27 200 g, 4°C, 30 minutes). The DNA pellet was washed with 70% ethanol, left to dry at room temperature for a minimum of 2 hours, then resuspended in 200 µl TE buffer. Storage of plasmid DNA preparations was at 4°C.

b) Small-scale preparation.

All centrifugation steps utilised an Eppendorf microcentrifuge operating at 14 000 rpm. The solutions used were those described in the large-scale preparation (Section 2.6a).

Cells from 1.5 ml of a liquid culture, grown to stationary phase (approximately 12 hours shaking at 37°C), were harvested by centrifugation (30 seconds). The pellet was resuspended in 100 µl GTE, and the cell suspension was incubated on ice for 5 minutes with gentle agitation. 200 µl of alkaline SDS solution was added, and the suspension was incubated on ice for 5 minutes with gentle agitation. Addition of 150 µl of ice-cold potassium acetate/acetic acid solution was followed by 5 minutes incubation on ice. The precipitated cell debris was pelleted by centrifugation (3 minutes), and the supernatant was recovered.

The preparation was further purified from protein by two phenol extractions (see Section 2.7a). One chloroform extraction removed any traces of phenol remaining. Plasmid DNA (and contaminating low molecular weight RNA) was recovered by ethanol precipitation (see Section 2.7b), and the pellet was resuspended in 40 µl TE. Plasmid DNA prepared by this method is suitable for restriction endonuclease digestion and other *in vitro* techniques. Storage was at 4°C.

2.7 General *in vitro* manipulation of DNA.

a) Purification of DNA by phenol extraction.

Addition of an equal volume of phenol (equilibrated to a pH of 7.8-8.0) was followed by vigorous mixing, centrifugation in an Eppendorf microcentrifuge at 14 000 rpm for 3 minutes, and recovery of the aqueous layer. This process was repeated if necessary. Any trace amounts of phenol remaining were removed by repeating the above extraction procedure using chloroform instead of phenol.

b) Ethanol precipitation of DNA.

Where necessary, the salt concentration of the DNA solution was increased by addition of 300 mM sodium acetate. Addition of two volumes of ethanol was followed by mixing and incubation on ice for 15 minutes. Precipitated DNA was recovered by centrifugation in an Eppendorf microcentrifuge at 14 000 rpm for 30 minutes at an ambient temperature of 4°C. The supernatant was discarded and the pellet was washed with 70% ethanol and centrifuged (as above, but for 5 minutes), before removing the 70% ethanol and drying the pellet at room temperature for a minimum of 2 hours.

c) Restriction endonuclease digestion of DNA.

Commercial restriction endonuclease preparations were purchased from Bethesda Research Laboratories, Boehringer Mannheim, New England Biolabs, and Promega. Storage was as recommended (generally at –20°C).

For **general purpose digestion of DNA**, normal concentration restriction endonuclease preparations were used (i.e. ≤ 12 units/μl) in the suppliers' recommended buffer, with between 2-fold and 10-fold excess enzyme. Incubation at the recommended temperature was for 1 hour, and the reaction was terminated by addition of electrophoresis loading buffer containing SDS (see Section 2.9b), or by heating to 70°C for 5 minutes, or by phenol extraction (the method depending on the next step in the experiment).

For **restriction endonuclease digestion of plasmid DNA in resolvase-mediated synapsis reactions** containing ~20 μg/ml DNA, the digestion was under the reaction conditions pertaining after treatment with a protein crosslinking reagent (see Section 2.15c). If Mg^{2+} was not already present, 10 mM $MgCl_2$ was added at this stage.

Typically, the synapsis reaction volume was such that a number of aliquots were treated with different restriction endonucleases. Where possible, high concentration (50 units/µl) restriction endonuclease preparations from the above suppliers were used, added to give a final concentration of 3 units/µl. The restriction endonuclease digestion reaction was incubated at 37°C for 30 minutes, followed by addition of electrophoresis loading buffer or further manipulation, depending on the experiment (see Section 2.15c).

For **restriction endonuclease digestion of DNA in agarose gels**, high concentration *Eco*RV (~3000 units/µl) was the enzyme of choice. This preparation was a gift from Christian Parker and Steve Halford (University of Bristol).

Generally, a strip (about 5 x 5 x 90 mm in size) containing bands representing the protein-DNA complexes of interest was excised from the agarose gel (see Section 2.9g) and placed in a 15 ml Falcon tube. Initial incubation was at 37°C in a volume of 5 ml of the recommended buffer, 100 µg/ml bovine serum albumin (BSA) and *Eco*RV at ~2 units/µl, in the absence of Mg^{2+}. The capped tube was positioned horizontally with gentle agitation provided by a platform shaker to keep the agarose gel strip submerged in the minimum reaction volume.

After 2 hours, 10 mM $MgCl_2$ and additional *Eco*RV (~1 unit/µl) were added, and the reaction continued for a further 3 hours. The initial incubation in the absence of Mg^{2+} allows the restriction endonuclease to diffuse into the agarose gel, with the presence of BSA to saturate any non-specific protein binding activity of the agarose. With the restriction endonuclease *in situ*, the addition of the faster-diffusing cation initiates digestion. A second dimension of electrophoresis commenced after the additional 3 hours incubation for digestion (see Section 2.9g).

d) Calf intestinal phosphatase (CIP) treatment of DNA.

Dephosphorylation of DNA restriction fragments in order to prevent self-ligation was achieved by addition of 1 mM zinc sulphate and 0.5 units CIP to a 20 µl restriction digest after inactivation of the restriction endonuclease by heating to 70°C for 5 minutes (or following phenol extraction). After incubation at 37°C for 30 minutes, CIP was inactivated by addition of 0.5% SDS, 5 mM EDTA, and 100 µg/ml proteinase K, followed by incubation at 55°C for 30 minutes. One phenol and one

chloroform extraction were followed by ethanol precipitation. The DNA pellet was resuspended in TE.

e) Filling-in of 3' recessed ends of DNA restriction fragments.

Deoxynucleotide triphosphates (dNTPs) were purchased from Promega; the Klenow fragment of DNA polymerase I was supplied by BRL or New England Biolabs; [α-^{32}P]dNTPs were supplied by ICN Biomedicals. Storage was at –20°C.

This technique was used **to blunt 3' recessed ends prior to cloning of a DNA restriction fragment.** A 25 µl reaction containing about 0.5 µg DNA, 100 µM each of dATP, dGTP, dCTP, and dTTP, and 2 units of the Klenow fragment of DNA polymerase I in BRL REact 2 buffer (50 mM Tris-HCl (pH 8.0), 50 mM NaCl, 10 mM $MgCl_2$) was incubated for 30 minutes at room temperature. The reaction was stopped by heating to 70°C for 10 minutes and the DNA was recovered by ethanol precipitation.

The same technique was used in order **to add 3' end-label to a DNA molecule.** The DNA substrate (generally 0.1 µg or less of a restriction fragment with a recessed 3' end) in BRL REact 2 buffer (50 mM Tris-HCl (pH 8.0), 50 mM NaCl, 10 mM $MgCl_2$), with 5 µCi of an [α-^{32}P]dNTP (specific activity: 3000 Ci/mmol) and the remaining three non-radiolabelled dNTPs (10 µM each), was reacted with 1 unit of the Klenow fragment of DNA polymerase I in a reaction volume of 15 µl. After 20 minutes incubation at room temperature, all four non-radiolabelled dNTPs were added (at 150 µM each), and the reaction was incubated for a further 10 minutes at room temperature. The reaction volume was increased to 50 µl by addition of TE (10 mM Tris-HCl (pH 8.0), 1 mM EDTA), and one phenol extraction was followed by one chloroform extraction (see Section 2.7a). DNA was recovered by ethanol precipitation, and the pellet was dried for 15 minutes at room temperature before resuspending in an appropriate volume of deionised water.

f) DNase I nicking of DNA.

Bovine pancreatic deoxyribonuclease I (DNase I) was supplied by Boehringer Mannheim. Dilutions were made in 50 mM Tris-HCl (pH 8.2), 150 mM NaCl, 50% (v/v) glycerol.

DNase I treatment in the presence of ethidium bromide was used to limit the extent of cleavage to an average of one single-stranded break per plasmid DNA molecule. Supercoiled plasmid DNA at a concentration

of 20-100 μg/ml was treated with 1.6 μg/ml DNase I in 50 mM Tris-HCl (pH 8.2), 10 mM $MgCl_2$, 0.1 mM EDTA, and 300 μg/ml ethidium bromide. After incubation at 30°C for 90 minutes, the reaction was stopped by addition of 16 mM EDTA and one phenol extraction (see Section 2.7a). In the case of a large scale nicking reaction, this was followed by another two phenol extractions, a chloroform extraction, and ethanol precipitation to give a nicked plasmid DNA preparation resuspended in TE. In contrast, small volume nicking reactions destined to undergo electrophoresis as the next step (as in nicking of resolution product for example – see Section 2.15c) were extracted once with chloroform following the initial phenol extraction.

Treatment with DNase I in the absence of ethidium bromide, in order to produce more than one nick per DNA molecule, was in the same buffer, but the incubation of about 100 μg/ml plasmid DNA was with 2.0 μg/ml DNase I on ice for 1 hour. Other details were as described above.

g) Ligation of DNA.

T4 DNA ligase (1 unit/μl) was supplied by BRL.

For **general purpose ligation of DNA fragments in cloning**, the concentration of dephosphorylated vector DNA (see Section 2.7d) was 20-50 μg/ml and the approximate molar ratio of vector to insert DNA was 1:2 for ligation of cohesive termini and 3:1 for ligation of blunt ends. DNA was reacted with 1 unit of T4 DNA ligase in 25 μl BRL ligation buffer (50 mM Tris-HCl (pH 7.6), 10 mM $MgCl_2$, 1 mM ATP, 1 mM DTT, 5% (w/v) polyethylene glycol-8000) supplemented with 0.5 mM of a freshly-made solution of ATP. After incubation at room temperature overnight, 3 μl aliquots were used to transform competent *E.coli* cells (see Section 2.5).

For **ligation of nicked plasmid DNA after incubation with Tn*3* resolvase** (see Section 2.15e), 0.3 units of T4 DNA ligase in 2 μl BRL ligation buffer (see above) was added to a 20 μl reaction containing ~20 μg/ml nicked plasmid DNA and variable amounts of resolvase in buffer E (see Section 2.15b). After incubation at 37°C for 15 minutes, the reaction was stopped by addition of 0.2 mg/ml proteinase K. Addition of 0.2 volume of 5 x FLB (see Section 2.9b) was followed by agarose gel electrophoresis in the presence of 3μg/ml chloroquine (see Section 2.9e).

For **ligation of DNA in agarose gels**, a high concentration preparation of T4 DNA ligase (~50 units/µl) was used. This was a gift from Christian Parker and Steve Halford (University of Bristol).

A band representing synaptic complex cleaved with restriction enzymes to leave cohesive DNA ends was excised from an FMC SeaPlaque GTG low-melting-point agarose gel (see Section 2.10). The agarose gel slice (approximately 5 x 5 x 2 mm in size) was placed in a Nunc tube. Incubation was at room temperature in a volume of 250 µl containing 50 mM Tris-HCl (pH 8.2), 10 mM MgCl2, 0.05 mM EDTA, 5 mM spermidine.3HCl, 20% glycerol, 4 mM ATP, 100 µg/ml bovine serum albumin (BSA) and T4 DNA ligase at ~0.2 units/µl. After about 16 hours, the gel slice was transferred into a fresh reaction volume as above and the reaction proceeded for a further 4 hours. DNA was recovered from the low-melting-point agarose gel slice as described in Section 2.10c.

h) Purification of DNA by spun-column chromatography.

As described in Sambrook *et al.* (1989).

2.8 Single colony gel analysis.

A single bacterial colony was spread on a fresh plate of L-Agar (with appropriate antibiotic selection; see Section 2.4) to give a 1 cm square patch. After overnight incubation, cells were scraped from the patch and deposited in 150 µl sample buffer (2.5% Ficoll, 1.25% SDS, 0.05% bromophenol blue, 1 x TAE (see Section 2.9a)). Following centrifugation in an Eppendorf microcentrifuge at 14 000 rpm for 30 minutes, 40 µl of the supernatant was loaded directly onto a 1.2% agarose gel and analysed by electrophoresis (see Section 2.9d). This represents a rapid means of determining the plasmid DNA content of transformants.

2.9 Agarose gel electrophoresis.

a) Preparation.

Standard agarose was purchased from BRL ('Ultrapure') or from FMC Bioproducts ('SeaKem GTG'). Low-melting-point agarose was purchased from BRL or from FMC ('SeaPlaque GTG'). Agarose gels were prepared according to the manufacturer's instructions. All agarose gels were

electrophoresed using 1 x TAE running buffer (40 mM Tris-acetate (pH 8.2), 20 mM sodium acetate, 1 mM Na_2EDTA), prepared as a 50 x stock solution (1210 g Tris-base, 410 g sodium acetate, 93 g $Na_2EDTA.2H_2O$, 355 ml glacial acetic acid, made up to 5 litres with deionised water). A fresh dilution (with deionised water) of a volume sufficient for casting and electrophoresis of one agarose gel was prepared on each occasion.

Routinely, 150 x 200 mm horizontal slab gels were cast with 250 ml of melted agarose slurry to give either 0.8% or 1.2% agarose gels. This size of gel gave 22 adjacent sample wells, with fractionation of DNA through the longest dimension of the gel. The electrophoresis tank, not commercially available, required about 3 litres of 1 x TAE buffer to submerge the gel. Apparatus supplied by IBI International Biotechnologies and Hoeffer Scientific Instruments were used on occasion to run smaller size gels.

b) Loading buffers.

0.2 volume of the following were added to samples prior to loading on the agarose gel.

5 x FLB (10% Ficoll, 50 mM Tris-HCl (pH 8.2), 0.01% bromophenol blue) was added to aliquots from synapsis reactions prior to electrophoresis.

5 x FLB+SDS (as above but + 1% SDS), giving a final concentration of 0.2% SDS, was added to dissociate protein-DNA complexes. This was the general purpose loading buffer for analysis of DNA by agarose gel electrophoresis.

5 x FLB+SDS+K (as above, but + 1 mg/ml proteinase K; freshly prepared), giving a final concentration of 0.2 mg/ml proteinase K, was added prior to electrophoresis of resolvase resolution reactions.

c) DNA molecular weight standards.

Lambda DNA-*Hin*dIII digest and 1 kilobase ladder were purchased from BRL.

d) Electrophoresis.

For **general purpose analysis of DNA**, single colony gels (see Section 2.8), and resolvase resolution assays (see Section 2.15c), 1.2% agarose gels were run at an applied voltage of between 2 and 5 V/cm.

For **analysis of synapsis reactions**, 0.8% or 1.2% agarose gels were run at 3 V/cm for approximately 15 hours (ambient temperature of 4°C).

Electrophoretic resolution of small DNA-protein complexes was enhanced by a reduction in the run-time achieved by increasing the applied voltage to ~12 V/cm while using a pre-cooled 'Minnie-the-Gel-Cicle' apparatus (Hoeffer Scientific Instruments) and electrophoresis running buffer recirculated through ice.

e) Chloroquine gels for analysis of topoisomer distributions.

Both the 1.2% agarose gel and the electrophoresis running buffer were prepared with 3 μg/ml chloroquine (7-chloro-4-[4-diethylamino-1-methyl-butylamino]-quinoline) included. Chloroquine, a DNA intercalator, introduces positive writhe into covalently closed circular DNA molecules (see Section 4.2). Electrophoresis was at room temperature for approximately 15 hours at an applied voltage of 2 V/cm.

f) Visualisation of DNA and photography.

Agarose gels containing fractionated DNA molecules were stained with ethidium bromide by soaking for about 30 minutes in a 0.6 μg/ml solution made by dilution of a 3 mg/ml ethidium bromide stock solution with 1 x TAE electrophoresis buffer. Chloroquine gels were soaked in 1 x TAE buffer for 30 minutes prior to ethidium bromide staining to remove excess chloroquine. A destaining step consisting of about 45 minutes soaking in 1 x TAE buffer preceded visualisation of DNA by the enhanced fluorescence of DNA-bound ethidium.

If bands were to be cut from the gel, visualisation of DNA was by long-wave ultraviolet (UV) illumination (a 365 nm source); otherwise a 245 nm UV source was used. Documentation of gels was by photography, using Polaroid type 667 film and Ilford HP5 35 mm film, the latter up-rated to 1600 ASA and processed accordingly (as per the manufacturer's instructions with Ilford Microphen developer and Amfix fixative). A Kodak Wratten filter No. 23A was fitted to all cameras.

g) Two-dimensional gel electrophoresis.

Generally, entire lanes containing the bands of interest were cut from the first-dimension agarose gel as a strip approximately 5 x 5 x 90 mm in size. Bands were visualised by 365 nm UV illumination, either following ethidium bromide staining or, if DNA without bound ethidium was required, by removal and staining of adjacent marker lanes followed by reassembly of the gel and use of stained marker bands to locate unstained bands. Excised lanes were either treated with restriction endo-

nuclease (see Section 2.7c) or with SDS (soaked in a 15 ml Falcon tube in 10 ml of a solution of 5% SDS in TAE buffer (see Section 2.9a) for a minimum of 3 hours at room temperature).

The second dimension agarose gel was cast with a single continuous slot, 5 mm square in cross-section, replacing the wells. Following treatment with restriction endonuclease or SDS, the agarose gel strip from the first dimension of electrophoresis was placed in the slot. Typically, two strips were fitted in the slot, together with marker DNA bands cut as slices from an agarose gel, such that the direction of migration in the second dimension of electrophoresis was at 90^0 to that in the first dimension. Any gaps were filled with melted agarose slurry and care was taken to achieve an unbroken contact between faces of the agarose gel through which the DNA would migrate during electrophoresis. Electrophoresis was as described in Section 2.9d.

2.10 Recovery of DNA or protein from agarose gels.

Bands of interest were cut as slices of the smallest possible size from ethidium bromide-stained agarose gels viewed on a 365 nm UV trans-illuminator. If DNA without bound ethidium was required, removal and staining of adjacent marker lanes was followed by reassembly of the gel and use of stained marker bands to locate unstained bands. In attempts to recover the protein component of crosslinked synaptic complexes, the gel slice containing isolated complex was immersed in a solution of 1% SDS in TAE (see Section 2.9a) at room temperature for 3 hours prior to treatment by centrifugation or by melting.

a) Centrifugation.

The method of Heery *et al.* (1990) was either used as published or adapted by replacement of the siliconised glass wool with Miracloth filtration material (Calbiochem Corporation).

b) Electrophoresis onto DEAE-cellulose membrane.

The method described in Sambrook *et al.* (1989) was followed, using Schleicher & Schuell NA45 DEAE membrane. Attempts to elute protein from DNA-protein complexes trapped on the membrane involved soaking in either 2% SDS or in 8M urea for 1 hour, followed by precipitation of

protein (see Section 2.12), or direct loading onto a SDS-polyacrylamide gel (see Section 2.14), depending on the volume used.

c) Use of low-melting-point agarose.

An excised slice of low-melting-point agarose gel containing the DNA band of interest was transferred to a large Eppendorf tube and heated to 65°C. Attempts to recover protein from gel-isolated synaptic complex involved loading of the melted agarose into the wells of an SDS-polyacrylamide gel at this stage (see Section 2.14d). Alternatively, for recovery of DNA the volume of melted agarose gel was increased to 250 µl by addition of TE at 65°C. The remaining steps were carried out at room temperature. One phenol extraction (see Section 2.7a), carefully avoiding the powdered agarose at the interface, was followed by back-extraction of the organic phase and interface with 250 µl TE. The recovered aqueous phases were combined and another two phenol extractions and one chloroform extraction were performed. The purified DNA was concentrated by ethanol precipitation (Section 2.7b), and was resuspended in TE or in a buffer suitable for further manipulation.

2.11 Southern hybridisation.

Capillary transfer of DNA from agarose gel to membrane (Amersham Hybond-N) was as described in Sambrook *et al.* (1989). Radiolabelled probe was made using a random primed DNA labelling kit (Boehringer Mannheim) according to the manufacturer's instructions. Hybridisation of probe to DNA immobilised on Amersham Hybond-N membrane was according to the manufacturer's instructions. Autoradiography was as described in Section 2.19.

2.12 Precipitation of protein.

This was generally performed to concentrate protein from crosslinked synapsis reactions prior to analysis by SDS-polyacrylamide gel electrophoresis (see Section 2.14). Addition of 0.1% SDS and 300 mM potassium acetate was followed by 30 minutes incubation on ice , then centrifugation in an Eppendorf microcentrifuge at 14 000 rpm for 15 minutes. The pellet was resuspended in 30 µl glycerol/SDS protein sample buffer (see Section 2.14b).

2.13 Radioiodination of protein.

Iodine-125 in the form of NaI in NaOH (pH 10), specific activity: carrier free, was obtained from ICN Biomedicals. Iodogen (1,3,4,6-tetrachloro-3α, 6α-diphenylglycouril) was purchased from Sigma. Both were stored at 4°C.

This method was adapted from Tolan *et al.* (1980). Thanks to M.R. Boocock for advice and assistance. All centrifugation steps utilised an Eppendorf microcentrifuge operating at 14 000 rpm.

1% SDS was added to 50 µl of elutant from an agarose gel slice containing isolated crosslinked synaptic complex, obtained by centrifugation through Miracloth (see Section 2.10a), or to 50 µl of 4 µM Tn*3* resolvase in TAE (the latter a control; see Section 2.9a). After incubation at 80°C for 2 minutes, the sample was placed on ice. 10 µCi of ^{125}I was added to the sample. The iodination mix was transferred to a small glass tube pretreated to evaporate iodogen on the inside surface (20 µl of a freshly prepared solution of 0.9 mg/ml iodogen in chloroform was applied to the bottom of each tube, which was then vortexed until the solvent had evaporated leaving an even coat of iodogen; prepared tubes were stored overnight at –20°C prior to use). Iodogen provides the oxidising environment necessary for iodination of tyrosine residues, the most commonly modified amino acids. After 1 minute incubation on ice with gentle swirling, the iodination mix was returned to its original Eppendorf tube.

Addition of 10 µl of 10% β-mercaptoethanol (to quench unreacted iodine) and 6 µl of 3 M potassium acetate (to precipitate protein-SDS complexes) was followed by 10 minutes incubation on ice. The supernatant obtained after centrifugation (5 minutes) was discarded and 400 µl acid acetone (acetone + 0.1 M HCl) was added to the pellet. The acid conditions may dissociate protein-SDS complexes, allowing the SDS to go into solution while the protein is precipitated by the acetone. Addition of 10 µg bovine serum albumin (BSA; a carrier to improve the efficiency of recovery of the small amount of radioiodinated protein) was followed by mixing and centrifugation (5 minutes). A second acid acetone precipitation (400 µl acid acetone added to the pellet and centrifugation for 5 minutes) was followed by addition of 100 µl trichloroacetic acid (TCA) to the pellet, mixing, and incubation on ice for 30 minutes to precipitate the protein. After centrifugation for 5 minutes, the supernatant was discarded and

the pellet was washed with 100 µl acetone. Eppendorf tubes containing the sample pellets were stored at –20°C.

For SDS-polyacrylamide gel electrophoresis, the pellets were resuspended in urea/SDS protein sample buffer (see Section 2.14b). Molecular weight marker proteins, iodinated as above, were co-electrophoresed. Electrophoresis (15% polyacrylamide resolving gel), gel drying, and autoradiography were as described in Sections 2.14, 2.18, and 2.19, respectively.

2.14 SDS-polyacrylamide gel electrophoresis.

The SDS-discontinuous system of Laemmli (1970) was used. For further information, see Hames (1990).

a) Preparation.

30% acrylamide:0.8% bisacrylamide (w/v) was purchased as a ready-mixed solution from FMC Bioproducts. A vertical slab gel apparatus, not commercially available, permitted electrophoresis of 20 samples in a single run. Clamped gel plates, with 0.75 mm spacers, were sealed with a length of plastic tubing. Resolving gels were either 15% or 7% acrylamide in 375 mM Tris-HCl (pH 8.8), 0.1% SDS. Stacking gels were 4% acrylamide in 125 mM Tris-HCl (pH 6.8), 0.1% SDS. The acrylamide gel mix was de-gassed, and polymerisation was initiated by addition of 1.7 mg/ml ammonium persulphate and 0.75 µl of TEMED (*N,N,N',N'*-tetramethylethylenediamine) per ml of gel mix. Electrophoresis running (reservoir) buffer was 25 mM Tris, 192 mM glycine (pH 8.3), 0.1% SDS.

b) Protein sample buffers.

A minimum of 0.5 volume of the following were added to samples prior to loading on the polyacrylamide gel. Protein pellets were resuspended directly in these buffers.

Glycerol/SDS (50% glycerol, 5% SDS, 50 mM Tris-HCl (pH 6.8), 0.01% bromophenol blue). This was the general purpose SDS-PAGE sample buffer.

Urea/SDS (7.2 M urea, 1% SDS, 0.01% bromophenol blue).

c) Protein molecular weight standards.

Sigma low molecular weight markers (SDS-7), high molecular weight markers (SDS-6H), and a specially made mix of gel chromatography

calibration proteins (cytochrome c (12.5 kDa), chymotrypsinogen A (25.0 kDa), aldolase (39.5 kDa), ovalbumin (45.0 kDa), and bovine serum albumin (68.0 kDa); Boehringer Mannheim) were used as size markers.

d) Electrophoresis.

Samples were generally loaded within 1 hour of the stacking gel having set. Routinely, samples with loading buffer added were heated to 90°C for 10 minutes prior to loading. β-mercaptoethanol was usually omitted from resolvase samples, since there are no cysteine residues in the protein and the presence of the reducing agent was found to produce an artefact following silver staining (see Section 2.14f). However, β-mercaptoethanol was added to protein molecular weight standards before heating. On occasion, low-melting-point agarose gel chips containing isolated synaptic complex were heated to 80°C and were loaded as melted agarose.

Gels were run either at 30-40 mA constant current (for about 4 hours), or at 10-15 mA constant current (for about 15 hours). Electrophoresis ended when the dye front was close to or at the bottom of the resolving gel.

e) Coomassie Blue staining.

The gel containing fractionated protein was immersed in 0.1% Coomassie Blue R-250, 50% methanol, 10% acetic acid with gentle agitation on a platform shaker for at least 1 hour. This was followed by destaining in 10% methanol, 10% acetic acid with changes until the background was relatively clear.

f) Silver staining.

This non-diamine chemical method is based on the procedure devised by Sammons *et al.* (1981) with improvements by Schoenle *et al.* (1984).

The gel containing fractionated protein was immersed in a volume of 200 ml of the various solutions (all made with deionised water), in a glass dish at room temperature with gentle agitation provided by a platform shaker.

The gel was fixed in 50% methanol, 10% acetic acid for 30 minutes, then in 5% methanol, 7% acetic acid for a further 30 minutes. 30 minutes immersion in 10% glutaraldehyde was followed by two rinses with deionised water and a soak in deionised water for a minimum of 1 hour (or overnight if required), then immersion in fresh deionised water for another 30 minutes.

Following immersion in 5 μg/ml dithiothreitol (DTT) for 30 minutes, the solution was poured off without rinsing and a 0.1% silver nitrate solution was added. After 30 minutes immersion, the silver nitrate solution was poured off, the gel was rinsed once in a small volume of deionised water, then rinsed once in 200 ml of 3% sodium carbonate, 0.02% formaldehyde. After this rinse, the gel was immersed in another 200 ml of 3% sodium carbonate, 0.02% formaldehyde, and staining was monitored by visual inspection over a light box during which time there was constant agitation of the gel. When staining was judged complete, 10 ml of 2.3 M citric acid was added to the staining solution, followed by agitation of the gel for 10 minutes. The gel was rinsed several times with deionised water.

Several artefactual bands migrating at about 60 kDa (as determined by co-electrophoresed protein molecular weight standards) were seen only when samples had been treated with a reducing agent such as β-mercaptoethanol or dithiothreitol (see Figure 5.4). This is consistent with previous reports of contaminating bands detected by silver staining and proposed to be due to keratin-type proteins (Merril, 1990).

g) Photography.

Coomassie- or silver-stained polyacrylamide gels were photographed (immediately after staining, before drying) on a light box using Polaroid type 667 film and Ilford HP5 35 mm film, the later up-rated to 1600 ASA (see Section 2.9f).

2.15 *In vitro* resolvase-mediated synapsis and site-specific recombination.

All substrate plasmid DNA used in resolvase reactions was isolated by caesium gradient centrifugation (see Section 2.6a).

a) Resolvase.

Tn*3* resolvase was either a gift from M.R. Boocock, or was purified in the preparation described in Section 5.1. Tn*21* resolvase was a gift from Christian Parker and Steve Halford (University of Bristol).

Storage was at –20°C. Concentration of the Tn*3* resolvase stock, stored in buffer I diluted by addition of 50% (v/v) glycerol, varied between 150 and 400 μM depending on the preparation and fraction. Protein concentration

was estimated by Bradford assay (Bradford, 1976), and by amino acid analysis (Blake, 1993). However, determination of resolvase concentration by comparison with bovine serum albumin standards in the Bradford assay is believed to underestimate the amount of resolvase present (see Section 5.1 for details of the activity of purified resolvase).

Dilutions of the resolvase stock were in 1 M NaCl, 10 mM Tris-HCl (pH 7.5), 0.2 mM EDTA. These were stored on ice for up to 1 week. Determination of the optimal concentration of a given fraction of the resolvase stock in recombination and synapsis assays was by titration with a two-fold dilution series. Generally, 0.05 volume of a 2^{-3}, 2^{-4}, or 2^{-5} dilution of the resolvase stock was required in a standard resolution or synapsis reaction containing about 20 μg/ml pMA21 DNA.

b) Buffers for *in vitro* synapsis, recombination, and for purification of Tn*3* resolvase.

Buffers A-E were used for *in vitro* reaction of resolvase with plasmid DNA substrate. The NaCl concentration includes 50 mM NaCl introduced with 0.05 volume of resolvase in a 1 M NaCl buffer (see Section 2.15a).

A. 50 mM Tris-HCl (pH 9.4), 50 mM NaCl, 0.1 mM EDTA, 10 mM $MgCl_2$. The standard recombination buffer.

B. 20 mM triethanolamine-HCl (pH 7.5), 100 mM NaCl, 5 mM EDTA.

C. 50 mM MOPS-NaOH (pH 8.0), 100 mM NaCl, 1 mM EDTA. The standard synapsis buffer. 10 mM $MgCl_2$ was added on occasion (as detailed).

D. 50 mM MOPS-NaOH (pH 7.0), 100 mM NaCl, 1 mM EDTA.

E. 50 mM Tris-HCl (pH 8.2), 50 mM NaCl, 5 mM $MgCl_2$, 0.05 mM EDTA, 5 mM spermidine.3 HCl, 20% glycerol, 1 mM DTT, 0.4 mM ATP. This buffer was used for resolvase-mediated synapsis of nicked plasmid DNA substrate and subsequent treatment with T4 DNA ligase (see Section 2.15e).

Buffers F-I were used in the purification of Tn*3* resolvase described in Section 5.1.

F. KPM extraction buffer: 25 mM K_2HPO_4 (pH 7.0), 5 mM $MgCl_2$, 1 mM EDTA, 0.4 mM DTT, 1 mM benzamidine.

G. 'S-200 equilibration buffer': 20 mM Tris-HCl (pH 7.5), 2 M NaCl, 0.1 mM EDTA. This was the chromatography column equilibration buffer.

H. 20 mM Tris-HCl (pH 7.5), 100 mM NaCl, 0.1 mM EDTA, 0.1 mM DTT, 1.2 mM PMSF, 1% ethanol. Chromatography column fractions were dialysed against this buffer in order to precipitate resolvase.

I. 'Resolvase dissolving buffer': 20 mM Tris-HCl (pH 7.5), 2 M NaCl, 0.1 mM EDTA, 0.4 mM DTT. 1 volume of glycerol was added to produce the resolvase stock, resulting in final concentrations half the value of those given above.

Buffer J was used for crosslinking of resolvase in the absence of the *res* site (see Section 5.3).

J. 50 mM MOPS-NaOH (pH 8.0), 1 M NaCl, 1 mM EDTA.

c) Standard *in vitro* assays for Tn*3* resolvase activity.

Any departures from the standard assays described below are noted in the descriptions of individual experiments presented in this thesis.

Site-specific recombination catalysed by Tn*3* resolvase was assayed by addition of 0.05 volume of a dilution of the resolvase stock (see Section 2.15a) to pMA21 DNA (approximately 20 μg/ml) in buffer A. The typical reaction volume was 20 μl. After incubation at 37°C for 30 minutes, the reaction was stopped by heating to 70°C for 5 minutes.

The (–2) catenane resolution product, which migrates close to supercoiled substrate DNA when in the fully supercoiled state, was digested by treatment with appropriate restriction endonuclease(s). Routinely, *Pst*I was used to cleave the 2616 bp pMA21 product circle, giving supercoiled 2311 bp resolution product and linearised 2616 bp resolution product. 10 units of *Pst*I in 5 μl REact 2 buffer (BRL) was added to a 20 μl reaction, and incubation at 37°C was for 60 minutes. Restriction endonuclease digestion was stopped by addition of 0.2 volume of 5 x FLB+SDS+K (see Section 2.9b), and electrophoresis in a 1.2% agarose gel was as detailed in Section 2.9d. As an alternative to restriction endonuclease digestion, the catenane product was nicked by DNase I treatment prior to electrophoresis (see Section 2.7f).

Tn*3* resolvase-mediated synapsis was assayed by addition of 0.05 volume of a dilution of the resolvase stock (equivalent to approximately 0.8 μM resolvase) to substrate plasmid DNA (about 20 μg/ml) in buffer C. After incubation at 37°C for 10 minutes, 0.05% glutaraldehyde (Sigma EM grade; fresh dilutions of the 25% stock in deionised water) was added and the reaction was incubated for a further 5 minutes at 37°C. Addition

of 100 mM sodium borohydride (freshly prepared as a 1 M solution in deionised water) was followed by incubation at room temperature for 10 minutes. Alternative protein crosslinking reagents replaced glutaraldehyde in some experiments (see Section 2.15d).

Subsequent treatment was dependent on the experiment. Typically, the synapsis reaction volume was such that a number of aliquots were treated with different restriction endonucleases (Section 2.7c), then two equal volume aliquots were taken from each restriction digest to produce identical plus- and minus-SDS samples following addition of the appropriate loading buffer (see Section 2.9b). The final sample loaded on an agarose gel represented about 15 µl of the initial synapsis reaction. Agarose gel electrophoresis was as described in Section 2.9d.

Samples to be analysed by SDS-PAGE were generally loaded immediately after crosslinking (see Section 2.14d). This was occasionally preceded by treatment with DNase I (as noted in the legend to Figure 5.4) or with micrococcal nuclease (supplied by Boehringer Mannheim; 150 units added, together with 5 mM $CaCl_2$, to a 40 µl synapsis reaction containing 140 µg/ml pMA21 DNA, followed by incubation at 37°C for 15 minutes) in order to destroy the DNA component of the crosslinked synaptic complex.

d) Alternative protein crosslinking reagents utilised.

The *N*-hydroxysuccinimide (NHS) esters dithio*bis*(succinimidyl-propionate) (DSP) and ethylene glycol*bis*(succinimidylsuccinate) (EGS) were purchased from Pierce, as was 1-ethyl-3-(3-dimethylaminopropyl)-carbodiimide hydrochloride (EDC). Optimal concentration of crosslinking reagents and the reaction conditions required to trap a Tn*3* resolvase-mediated synaptic complex were empirically determined (see Section 3.1).

The NHS esters were prepared fresh as a 50 mM stocks in dimethyl sulphoxide (DMSO), and dilutions were in DMSO. Addition of DSP (50 µM) or EGS (100 µM) to the standard synapsis reaction was followed by incubation on ice for 60 minutes. 50 mM Tris-HCl (pH8.2) was added to quench the unreacted crosslinking reagent.

EDC was prepared fresh as a 750 mM stock in deionised water. Synapsis reactions destined to be crosslinked with EDC were in buffer D rather than buffer C, but were otherwise as described in Section 2.15c. Addition of EDC (75 mM) was followed by incubation at room temperature for 90

minutes. 100 mM Tris-HCl (pH8.2) was added to quench the unreacted EDC.

Subsequent treatment was dependent on the experiment, as outlined in Section 2.15c. Cleavage of DSP crosslinks by disulphide reduction was achieved by addition of 10 mM dithiothreitol (DTT) and incubation at 37°C for 30 minutes.

e) Determination of topological change introduced by interaction of resolvase with nicked plasmid DNA.

Plasmid DNA substrate was nicked by treatment with DNase I in the presence of ethidium bromide (see Section 2.7f). 0.05 volume of a dilution of the resolvase stock (or the dilution buffer alone) was added to nicked plasmid DNA (~20 μg/ml) in buffer E. The reaction volume was 20 μl. After 10 minutes incubation at 37°C, the reaction was treated with T4 DNA ligase as described in Section 2.7g, followed by agarose gel electrophoresis in the presence of 3 μg/ml chloroquine (see Section 2.9e).

f) Time-course assays of synapsis.

A 360 μl standard synapsis reaction was prepared (see Section 2.15c) and pre-incubated at the required temperature. However, before addition of resolvase, a 28.5 μl aliquot was removed to act as the zero time-point sample (see Section 3.9). This aliquot was added to 1.5 μl of 1% glutaraldehyde (0.05% final concentration), followed by mixing and the immediate addition of 1.5 μl of an appropriate dilution of the resolvase stock (equivalent to approximately 0.8 μM resolvase). Subsequent treatment of the zero time-point sample was identical to the other time-point samples (see below).

The time-course reaction was initiated by addition of 16.5 μl (i.e. 0.05 volume) of the resolvase stock dilution. 30 μl aliquots, taken during incubation at the required temperature at various times after initiation of the reaction, were added to 1.5 μl of 1% glutaraldehyde, followed by the standard crosslinking treatment, restriction endonuclease digestion, and electrophoresis (see Section 2.15c).

The temperature at which the reaction was incubated, the time-points at which samples were taken, and any departures from the above procedure are detailed in the presentation of individual experiments in Section 3.9.

2.16 Probing the synaptic complex with DNA footprinting reagents.

Standard Tn*3* resolvase synapsis reactions using pMS12 as substrate were digested with *Bam*HI + *Hin*cII or with *Hin*dIII + *Hin*cII, depending on the strand to be labelled (see Section 6.2).

a) Methylation protection footprinting.

0.1 volume of 10% dimethyl sulphate (DMS; a fresh dilution v/v in deionised water) was added to the digested synapsis reaction. After incubation at room temperature for 3 minutes, addition of 0.2 volume of 5 x FLB was followed rapidly by agarose gel electrophoresis (see Section 2.9). The required DNA-protein complex bands and free DNA bands were cut from the ethidium bromide-stained agarose gel (see Section 2.10). The elutant from an agarose gel slice, obtained by centrifugation through Miracloth (see Section 2.10a), was purified by one phenol and one chloroform extraction (see Section 2.7a) and the DNA was concentrated by ethanol precipitation (see Section 2.7b). The pellet was resuspended in 10 µl TE and was the substrate in a 3' end-labelling reaction with [α-^{32}P]dGTP (see Section 2.7e).

After 3' end-labelling at the *Bam*HI or *Hin*dIII sites, the DNA was resuspended in 20 µl deionised water. Cleavage at methylated guanine residues was by addition of 1 volume of 20% piperidine (a fresh dilution v/v in deionised water), followed by incubation at 90°C for 30 minutes. Piperidine was removed by evaporating the samples to dryness using a SpeediVac centrifugal desiccator, and resuspending the DNA in 20 µl deionised water. This procedure was repeated another two times, finally resuspending in 5 µl deionised water. These samples were loaded on a denaturing polyacrylamide gel as detailed in Section 2.17.

b) DNase I protection footprinting.

Restriction digests of the pMS12 synapsis reaction were each divided into five 18.5 µl samples. 2 µl of a dilution of DNase I (see Section 2.7f) was added to each sample to give final concentrations of zero, 1.0, 2.0, 3.0, and 4.0 µg/ml DNase I, respectively. DNase I digestion reactions were incubated at room temperature for 3 minutes and were stopped by addition of 20 mM EDTA. Addition of 0.2 volume of 5 x FLB was followed quickly by agarose gel electrophoresis (see Section 2.9).

The required DNA-protein complex bands and free DNA bands were cut from the ethidium bromide-stained agarose gel (see Section 2.10). The elutant from an agarose gel slice, obtained by centrifugation through Miracloth (see Section 2.10a), was purified by one phenol and one chloroform extraction (see Section 2.7a) and the DNA was concentrated by ethanol precipitation (see Section 2.7b). The pellet was resuspended in 10 µl TE and was the substrate in a 3' end-labelling reaction with [α-^{32}P]dGTP (see Section 2.7e).

After 3' end-labelling at the *Bam*HI or *Hin*dIII sites, the DNA was resuspended in 5 µl deionised water. Samples were loaded on a denaturing polyacrylamide gel as detailed in Section 2.17.

2.17 Denaturing polyacrylamide gel electrophoresis of DNA.

TBE buffer is 89 mM Tris-borate (pH 8.3), 2 mM Na_2EDTA. For a 10 x stock: 108 g Tris base, 55 g boric acid, and 9.3 g $Na_2EDTA.2H_2O$ were made up to 1 litre with deionised water.

For an 8% polyacrylamide/7 M urea gel, a mixture of 46 g of urea, 20 ml of a 40% (w/v) acrylamide solution (19:1 ratio of acrylamide to bisacrylamide; Bio-Rad), and 10 ml of 10 x TBE buffer was made up to 100 ml with deionised water. An IBI Base Runner sequencing gel kit was used and a 20 x 45 cm gel was poured by a sliding method. Briefly, the notched glass plate was arranged on top of the mirrored plate (the latter with spacers positioned) so that it overlapped by about 4 cm and was supported at the exact height required for it to slide freely along the length of the mirrored plate to complete the plate-spacer-plate assembly. The spacers were clamped to the mirrored plate at the opposite end from the overlap. 20 µl of TEMED and 335 µl of 10% (w/v) ammonium persulphate were added to 50 ml of the gel mix, and the solution was taken up into a 50 ml syringe body (no needle). The syringe was positioned at the gap between the overlapping plates, and the gel mix was squeezed out slowly. After the 4 cm overlap had filled, the notched plate was gradually pushed along to cover the mirrored plate, at the same time depositing sufficient gel mix to fill the increasing area of overlap between the plates. When the plates were completely overlapping, the assembly (fitted with comb) was clamped at the edges and left for about 45 minutes for polymerisation. The gel was prerun at 45 W (constant power) for 30 minutes.

Radiolabelled DNA samples (in deionised water) were aliquoted so as to obtain the required counts per second (cps; measured by hand-held monitor) in a volume of 1.5 µl. 1.5 µl of the formamide loading buffer supplied in the Sequenase kit was added to each sample, followed by incubation at 80°C for 10 minutes. 2 µl of each sample was loaded using a sharks-tooth comb, and electrophoresis was at 45 W (constant power) for 2-3 hours.

2.18 Drying polyacrylamide gels.

Denaturing polyacrylamide gels containing fractionated DNA or protein were dried under vacuum on a slab dryer (Bio-Rad), according to the manufacturer's instructions. Polyacrylamide/urea denaturing gels for DNA were immersed in a solution of 10% methanol, 10% acetic acid for 15 minutes prior to drying for fixation and removal of urea. Drying was at 80°C for 60 minutes.

2.19 Autoradiography.

Dried polyacrylamide gels containing fractionated radiolabelled DNA or protein, and Southern hybridisation membranes, were exposed to Fuji RX X-ray film in a film cassette, either at a temperature of –70°C using an intensifying screen (for shorter exposure time), or at room temperature without the intensifying screen (giving a sharper image but requiring a longer exposure time). Exposed film was developed in an X-OMAT automated processor (Kodak).

2.20 Additional details.

Autoradiographs were photographed on a light box using Ilford Pan F 35 mm film, which was processed according to the manufacturer's instructions. Photographic prints from 35 mm negatives were on Ilford Ilfospeed RC grade 3 photographic paper, processed manually according to the manufacturer's instructions.

This thesis was produced on a PC using Word for Windows v2.0 (Microsoft), CorelDraw v4.0 (Corel), PagePlus v2.0 (Serif), and EndNote Plus v1.0 (Niles & Associates). Text was set in New Century Schoolbook (12 point for the body text, 10 point for figure legends). PostScript files were downloaded to an Apple Personal LaserWriter NTR.

Chapter 3

Isolation and basic characterisation of synaptic complexes

Introduction.

Isolation and subsequent investigation of a protein-DNA complex generally utilises the technique of gel retardation or band shift analysis (Carey, 1991; Lane *et al.*, 1992). The altered mobility of a DNA molecule with protein bound (usually retarded relative to the unbound DNA) during gel electrophoresis under non-denaturing conditions is characteristic of such a complex. Often a small linear DNA fragment containing the known or putative recognition sequence of the site-specific DNA-binding protein is used, and separation is by polyacrylamide gel electrophoresis (PAGE). This approach has been used to investigate the protein-mediated interaction of DNA sites. Thus, a small linear DNA fragment containing two *lac* operators formed a looped structure in the presence of *lac* repressor (Krämer *et al.*, 1987). This looped structure, believed to comprise a tetramer of the *lac* repressor bound to the two operator sites, was significantly retarded relative to the fully occupied but unlooped DNA fragment. In addition to the looped single fragment complex, a 'sandwich' structure in which two DNA molecules were linked by two *lac* repressor tetramers was formed.

As discussed in Chapter 1, members of the integrase family of site-specific recombinases generally exhibit a relaxed substrate specificity, and will efficiently catalyse intermolecular recombination of non-supercoiled DNA molecules. Complexes containing lambda integrase and two copies of a small linear DNA fragment containing *att*L were isolated by non-denaturing polyacrylamide gel electrophoresis (Segall and Nash, 1993). Like the aforementioned *lac* repressor complexes, these lambda Int synaptic complexes were sufficiently stable to be isolated without the use of a protein crosslinking reagent. In contrast, glutaraldehyde crosslinking was required to stabilise a putative synaptic intermediate formed by the FLP recombinase and a linear DNA fragment containing direct repeats of the FRT site (Amin *et al.*, 1990).

The use of a small linear DNA substrate, together with separation of DNA-protein complexes from unbound DNA in a polyacrylamide gel, was not considered feasible as a means of isolating a Tn*3* resolvase synaptic complex in sufficient yield for further study for a number of reasons. Firstly, Benjamin and Cozzarelli (1988) reported that no complex was formed in their crosslinking assay when a plasmid DNA substrate containing *res* sites in direct repeat orientation was first nicked or

linearised, leading them to conclude that synapsis required supercoiling (see Chapter 1). Secondly, extensive studies of resolvase binding to the linearised *res* site did not reveal any complexes attributable to synapsis (Bednarz, 1989; Blake, 1993). Intermolecular synapsis of small linear DNA fragments containing a *res* site was observed when the spacing between subsites I and II was altered by a non-integral number of helical turns (see Chapter 1), (Salvo and Grindley, 1988; N.D.F. Grindley, personal communication). Furthermore, it has been reported that DNA fragments containing the wild-type *res* site form a synaptic complex in the presence of a mutant resolvase unable to form the compact single *res* site complex or resolvosome (Grindley, 1994), (see the introduction to Chapter 5). Thus, the inability to observe synapsis of linearised *res* sites in a polyacrylamide gel may be because the resolvase-single *res* complex is the more stable protein-DNA complex under these conditions. A further consideration influencing the decision not to attempt to isolate synaptic complexes by non-denaturing PAGE was the possibility that a synaptic complex formed with linearised *res* sites may differ from a genuine intermediate formed under conditions that promote efficient recombination.

The gel retardation assay has been used with supercoiled plasmid DNA molecules separated by agarose gel electrophoresis to investigate protein-mediated interaction of distant DNA sites in systems other than resolvase/*res*. The type 1 and type 2 transpososomes (the cleaved donor and strand transfer complexes, respectively), protein-DNA complexes involved in the *in vitro* transposition of bacteriophage Mu DNA, were identified by mobility shift during agarose gel electrophoresis (Surette *et al.*, 1987). No additional stabilisation in the form of protein crosslinking was required for isolation of these complexes in high yield, nor was crosslinking required for isolation of a synaptic complex formed prior to Mu donor DNA cleavage (Mizuuchi *et al.*, 1992).

A protein-DNA complex, migrating slightly faster than the supercoiled plasmid substrate in a 0.9% agarose gel, was isolated from a Hin inversion reaction (Heichman and Johnson, 1990; see also Lim and Simon, 1992). This putative inversion intermediate, stabilised by protein crosslinking, yielded products of cleavage at the recombination sites upon denaturation and proteinase treatment. On the basis of a requirement for the enhancer site and FIS protein, and analysis by electron microscopy, the isolated species was proposed to represent an invertasome in which

the Hin-bound recombination sites interact with the FIS-bound enhancer to form a three-looped complex (Heichman and Johnson, 1990), (see Chapter 1).

In view of the above considerations, it was decided as a first step to pursue a strategy for isolation of a Tn*3* resolvase synaptic complex that followed closely that of Benjamin and Cozzarelli (1988), using a supercoiled plasmid substrate, and protein crosslinking to stabilise a synaptic intermediate during agarose gel electrophoresis.

Results and Discussion.

3.1 Isolation of a synaptic complex formed by Tn*3* resolvase.

The standard reaction conditions employed in this laboratory to assay *in vitro* site-specific recombination catalysed by Tn*3* resolvase were adapted from Reed (1981), and are detailed in Section 2.15c. Purified resolvase is reacted with negatively supercoiled plasmid DNA substrate, containing two copies of the Tn*3* *res* site in direct repeat orientation, in 50 mM Tris-HCl (pH 9.4), 50 mM NaCl, 0.1 mM EDTA, and 10 mM $MgCl_2$ (buffer A). The reaction proceeds for 30 min. at 37°C.

A standard resolution substrate, pMA21 (Bednarz *et al.*, 1990), was selected for experiments to determine the reaction conditions required for efficient isolation of a synaptic intermediate in the Tn*3* resolvase-catalysed reaction. Figure 3.1 is a representation of this plasmid. Initial experiments adhered closely to the strategy employed by Benjamin and Cozzarelli (1988) in their isolation of a putative synaptic intermediate. However, in my case both the resolvase and the *res* sites were those of Tn*3*, thus addressing a criticism of the earlier work which analysed a synaptic complex formed by Tn*3* resolvase and γδ *res* sites.

Following the method of Benjamin and Cozzarelli (1988), the protein crosslinking reagent glutaraldehyde was used at 0.2% final concentration. Glutaraldehyde is a bifunctional reagent that reacts with amino and sulphydryl groups, albeit with low specificity (Figure 3.2), (Han *et al.*, 1984). The reactivity with primary amines obviously rules out the Tris buffering system used in the standard recombination assay, and efficient crosslinking also demands a lower pH in order to minimise

aldocondensation which forms polymers of glutaraldehyde that eventually precipitate from an alkaline solution. Therefore, 20 mM triethanolamine-HCl buffering at pH 7.5 was used initially (buffer B, see Section 2.15b). Mg^{2+} was omitted from the reaction and, since Benjamin and Cozzarelli (1988) had stressed low temperature as the most important factor in trapping their putative synaptic intermediate in a yield reported to vary between 40 and 100% of input substrate, the recommended temperature of 15°C was used. However, the yield of synaptic complex was very poor under these conditions (data not shown).

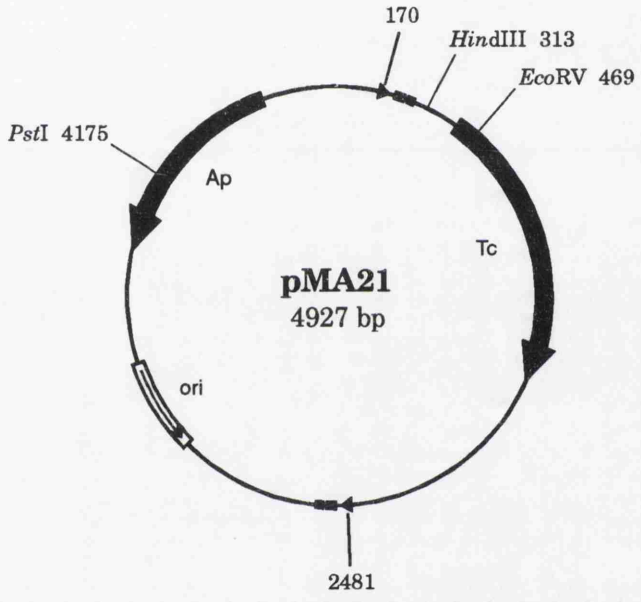

Figure 3.1 A simplified map of the Tn*3* resolvase resolution substrate pMA21 (Bednarz *et al.*, 1990). The locations of the *res* crossover sites which define the two domains of the synapsed substrate are shown, as are the unique restriction endonuclease sites used to generate the α- and χ-forms. Site locations are numbered (in bp) relative to the centre of the *Eco*RI site of pBR322 (designated zero; not shown). See Figure 3.16 for a more detailed map.

I II III denotes the res site in this and subsequent Figures.

Considerable manipulation of the reaction conditions, with a gradual improvement in yield along the way (data not shown), finally led to the following basic protocol for isolation of the synaptic complex (described in detail in Section 2.15c). Purified resolvase (approximately 0.8 μM) was reacted with pMA21 DNA (~20 μg/ml) in a buffer comprising 50 mM

MOPS-NaOH (pH 8.0), 100 mM NaCl, and 1 mM EDTA (buffer C). After incubation at 37°C for 10 minutes, 0.05% glutaraldehyde was added[1]. A further 5 minutes at 37°C was followed by addition of 100 mM sodium borohydride ($NaBH_4$), and the reaction was left at room temperature for 10 minutes. Sodium borohydride reduces the Schiff base formed by glutaraldehyde crosslinking (see Figure 3.2), thereby stabilising the crosslinked products, and inactivates unreacted glutaraldehyde by reduction (Jaenicke and Rudolph, 1989). This means of quenching excess glutaraldehyde permitted the subsequent addition of restriction endonuclease without an intervening gel filtration step. Most of the restriction endonucleases used cut to completion when added with Mg^{2+} at this stage. The finding that the isolation of synaptic complex was most efficient after initial incubation at 37°C conflicts with the report of Benjamin and Cozzarelli (1988) where increasing the reaction temperature above 15°C markedly reduced the yield, and synaptic complex was undetectable at 37°C.

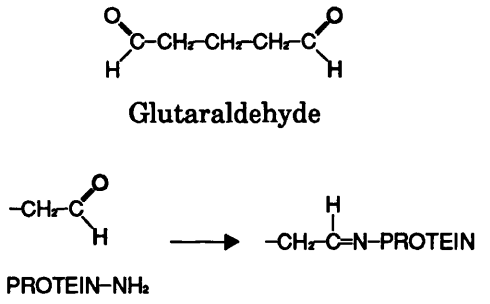

Figure 3.2 The chemical formula of glutaraldehyde and the formation of a Schiff base between the crosslinking reagent and the primary amine group of a protein.

Figure 3.3a shows the results after agarose gel electrophoresis of the glutaraldehyde-crosslinked synapsis reaction. An aliquot from this reaction loaded on the gel without further treatment produced protein-DNA complex slightly retarded with respect to the supercoiled protein-

[1] 0.05% glutaraldehyde was eventually shown to produce the most efficient crosslinking of the synapse, but some experiments presented in this thesis use 0.2% glutaraldehyde, as noted in the figure legend where applicable.

free substrate DNA (henceforth referred to as uncut retarded complex). Restriction endonuclease cleavage at a unique site in pMA21, e.g. using *Pst*I (see Figure 3.1), should produce an α-form complex from any plasmid in which the *res* sites were synapsed. The crosslinked α-form, remaining supercoiled in the uncut domain of the synapsed substrate, exhibited a characteristic mobility in the agarose gel, migrating between full-length linear substrate DNA and supercoiled substrate[2]. Also present after restriction endonuclease cleavage within a single domain was the relaxed α-form (Figure 3.3b), discussed further in Section 3.3. Restriction endonuclease cleavage within both domains of the synapsed substrate generated the χ-form of the complex, with four DNA 'arms' issuing from the nucleoprotein core.

Addition of SDS prior to electrophoresis resulted in the loss of all the aforementioned protein-DNA complex bands so that only bands representing protein-free substrate or product DNA remained (Figure 3.3b). This is consistent with the observation of Benjamin and Cozzarelli (1988), showing that only the protein component was crosslinked in the synapse and the DNA was freed upon treatment with a protein denaturant. Protein-DNA complex bands migrating a much shorter distance into the gel than those attributed to intramolecular synapsis are believed to arise from intermolecular synapsis. These will be considered in Section 3.7.

The reaction conditions outlined above for the isolation of a synaptic intermediate in the resolvase-catalysed reaction did not preclude recombination. Indeed, in the presence of Mg^{2+}, a crosslinked product synaptic complex was isolated in relatively high yield (see Section 3.8). This is in contrast to the conditions used by Benjamin and Cozzarelli (1988), primarily the reduced reaction temperature and the lower pH, which inhibited formation of product. Figure 3.4 shows a standard recombination assay with a resolvase titration (as detailed in Section 2.15) in the presence and absence of Mg^{2+}, comparing the extent of recombination in the standard recombination buffer (A) with that in the standard synapsis buffer (C).

[2] Throughout this thesis, unless specifically stated otherwise, the term 'α-form' will refer to the supercoiled form of this cleaved complex.

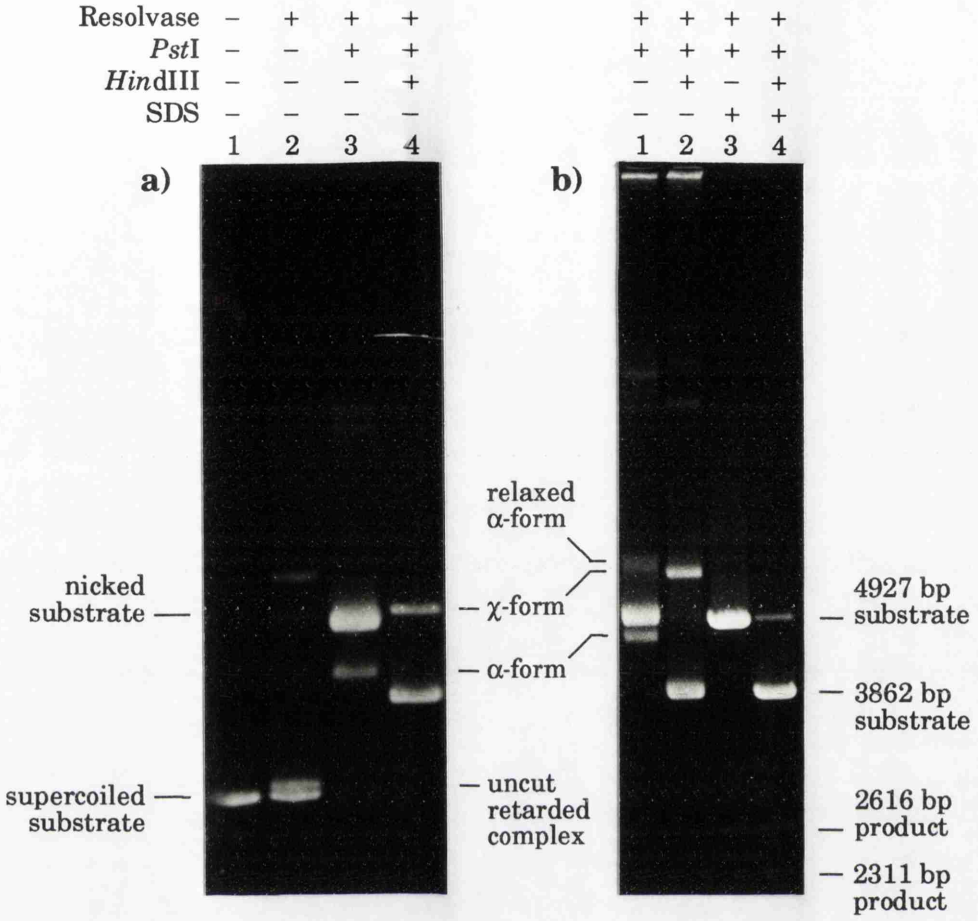

Figure 3.3 Agarose gel electrophoresis of glutaraldehyde-crosslinked pMA21 synapsis reactions: isolation of synaptic complex.

a) When restriction endonuclease treatment is omitted an uncut complex band is present (lane 2), retarded relative to the supercoiled substrate band identifiable from the minus-resolvase reaction sample (lane 1). Restriction endonuclease cleavage within one or both domains of the synapsed substrate generates the α- and χ-form of the complex, respectively (see text for further details).

Buffer C, minus-Mg^{2+}; 0.2 % glutaraldehyde; 0.8 % agarose gel.

b) Treatment with 0.2% SDS prior to gel electrophoresis results in the loss of all bands attributed to protein-DNA complexes (lanes 3 and 4). In addition, the effect of an increase in gel percentage on the mobility of the cleaved forms of the synapsed substrate is shown. The supercoiled α-form and the χ-form of the synaptic complex are shifted back relative to the free linear substrate DNA fragments, and the relaxed α-form, hidden behind full-length linear substrate DNA in a 0.8% agarose gel, is revealed.

Buffer C, minus-Mg^{2+}; 0.05% glutaraldehyde; 1.2% agarose gel.

Complexes due to intermolecular synapsis, migrating a shorter distance in the gel, are apparent (see Section 3.7).

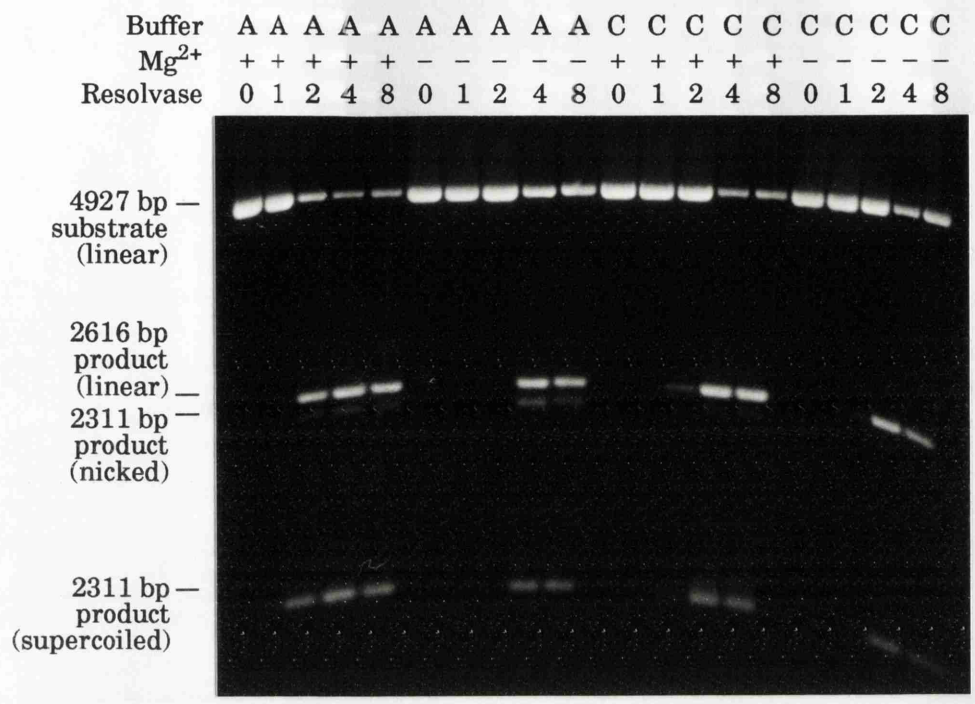

Figure 3.4 Agarose gel electrophoresis of pMA21 recombination reactions (see Section 2.15c) performed in the standard recombination buffer (A), or in the standard synapsis buffer (C), both in the presence and absence of 10 mM Mg^{2+}.
The increase in the concentration of resolvase through the titration was two-fold, as denoted by the numbering; 1 is equivalent to approximately 0.2 μM resolvase. Each sample was treated with *Pst*I in order to free the catenated products of recombination, giving one linearised 2616 bp product and one supercoiled 2311 bp product.

1.2% agarose gel.

In addition to glutaraldehyde, several other protein crosslinking reagents were used in the experimental work reported in this thesis. In general, they differ from glutaraldehyde in that they show greater specificity toward particular reactive groups in a protein molecule, and they are of defined length. The homobifunctional N-hydroxysuccinimide (NHS) esters react with the primary amine of lysine residues or with available N-terminus amines, forming a stable amide bond (Figure 3.5). Dithio*bis*-(succinimidylpropionate) (DSP) and ethylene glycol*bis*(succinimidyl-succinate) (EGS) differ in length (and so in the maximum distance across which they will crosslink: 12 Å and 16.1 Å, respectively), but are both cleavable (Lomant and Fairbanks, 1976; Abdella *et al.*, 1979). Thus, crosslinks can be broken by disulphide reduction (DSP) or hydroxylamine

treatment (EGS); this property is particularly valuable when analysing the crosslinked protein by SDS-polyacrylamide gel electrophoresis (see Section 5.4).

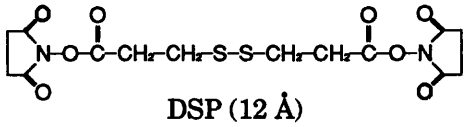

DSP (12 Å)

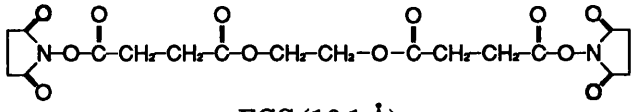

EGS (16.1 Å)

Figure 3.5 Chemical formulae of dithio*bis*(succinimidylpropionate) (DSP) and ethylene glycol*bis*(succinimidylsuccinate) (EGS). These crosslinking reagents react with a primary amine group of the protein to form an amide bond with the release of N-hydroxysuccinimide as by-product.

Figure 3.6 shows a synapsis reaction crosslinked with various concentrations of DSP and analysed by agarose gel electrophoresis. EGS crosslinking trapped the synaptic complex with comparable efficiency (optimally with 100 μM EGS; data not shown). Details of the various crosslinking reaction conditions are given in Section 2.15d.

1-Ethyl-3-(3-dimethylaminopropyl)carbodiimide hydrochloride (EDC), a so-called zero-length crosslinking reagent, catalyses the formation of an amide bond at salt bridges (Figure 3.7), (Yamada *et al.*, 1981). Therefore, the isolation of synaptic complex after EDC treatment (Figure 3.8) indicates that the crosslinking of resolvase monomers in intimate contact is sufficient to stabilise the synapse.

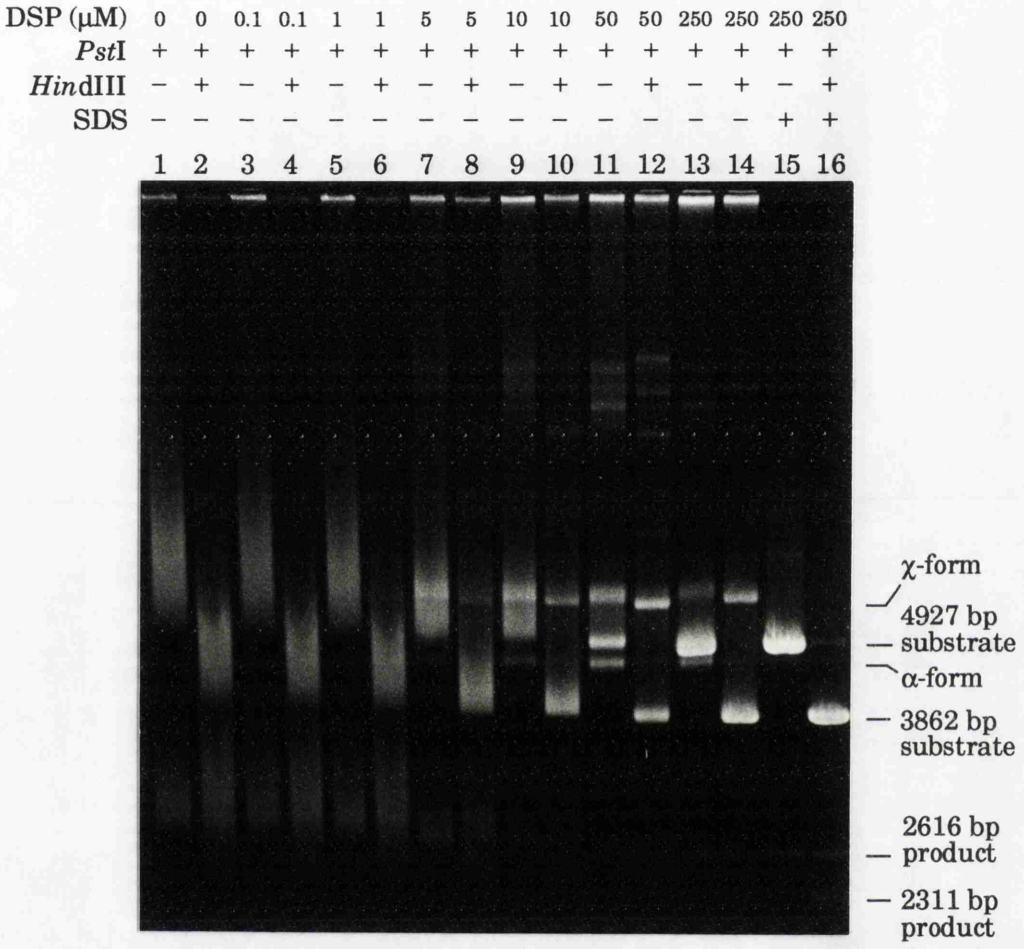

Figure 3.6 Agarose gel electrophoresis of a DSP-crosslinked pMA21 synapsis reaction.
A titration with DSP. The two lanes below each concentration value of DSP show a *Pst*I digestion to generate the α-form (on the left) and a *Pst*I + *Hin*dIII digestion to generate the χ-form (on the right). The best yield of synaptic complex is at 50 μM DSP (lanes 11 and 12). Considerable retardation and smearing of the DNA is apparent in the absence of, or at sub-optimal concentrations of, the crosslinking reagent (lanes 1-10).

Buffer C, minus-Mg^{2+}; 1.2% agarose gel.

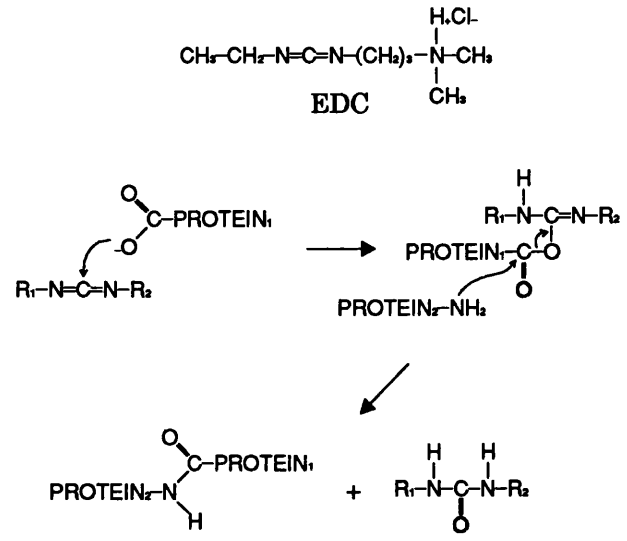

Figure 3.7 Chemical formula of 1-ethyl-3-(3-dimethylaminopropyl)-carbodiimide hydrochloride (EDC) and the activation of a protein carboxyl group which then reacts with an amino group to form an amide bond with the release of EDC as a urea derivative.

Figure 3.6 shows that a protein crosslinking reagent is required for the isolation of a discrete band representing a Tn*3* resolvase-*res* synaptic complex following restriction endonuclease cleavage. However, the general retardation and smeared appearance of all the DNA bands in the absence of DSP is indicative of an unstable interaction between resolvase and DNA. Very similar evidence of instability during electrophoresis was seen following treatment with sub-optimal concentrations of the other crosslinking reagents, while the addition of SDS produced the discrete bands characteristic of DNA only (data not shown). Furthermore, this may be a synapsis-dependent effect, since it did not occur when the plasmid had no *res* site (even when the resolvase:DNA ratio was high, and a non-specific interaction was demonstrated in an alternative assay – see Section 4.2), nor when the plasmid contained only a single *res* site (Figure 3.9).

However, an uncut complex band retarded with respect to the supercoiled pMA21 DNA, isolated without the use of a protein crosslinking reagent, failed to produce any of the α-form complex characteristic of synapsis when in-gel restriction endonuclease treatment was followed by a second

dimension of electrophoresis (see Figure 3.13). The nature of the uncut retarded complex band is discussed further in Section 3.2.

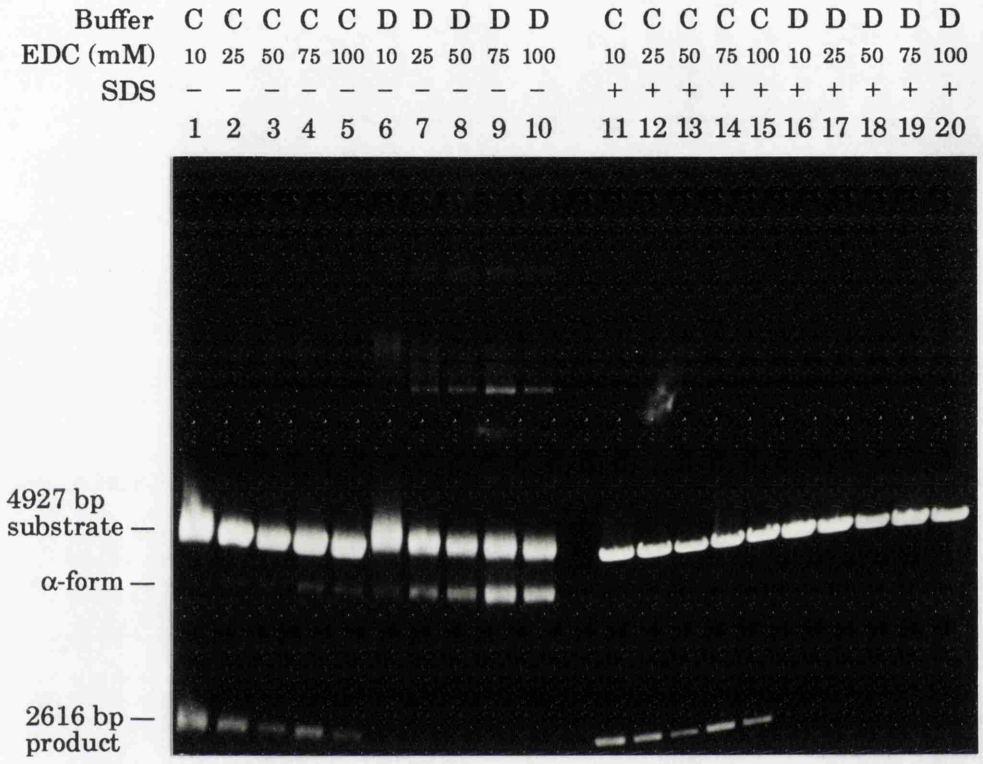

Figure 3.8 Agarose gel electrophoresis of a EDC-crosslinked pMA21 synapsis reaction (synapsis and crosslinking at pH 8.0 and at pH 7.0).
A titration with EDC. The best yield of synaptic complex (as assayed by *Pst*I cleavage to generate the α-form) was at pH 7.0 with 75 mM EDC (lane 9; EDC crosslinking is more efficient at lower pH). Note the deleterious effect of lowering the pH on the amount of resolution product formed.

Buffer C (pH 8.0) or buffer D (pH 7.0), both minus-Mg^{2+}; 0.8% agarose gel.

The requirement for crosslinking of resolvase in order to isolate the synaptic complex raises the question of the degree of involvement of the crosslinking reagent itself in the observed synapsis of *res* sites. Could it be simply linking protein-bound sites that come together only transiently, and not necessarily in the form of a genuine reaction intermediate? The ability to isolate the same nucleoprotein species (as least as assayed by

mobility in an agarose gel) efficiently following treatment with a variety of different crosslinking reagents, including the 'zero-length' EDC, suggests that a real synaptic interaction is trapped. It may be the case that a normally transient interaction is stabilised and thereby amplified during the time required for the crosslinking reaction to reach completion, since there is evidence that synapsis does not cease immediately on addition of the crosslinking reagent (see Section 3.9).

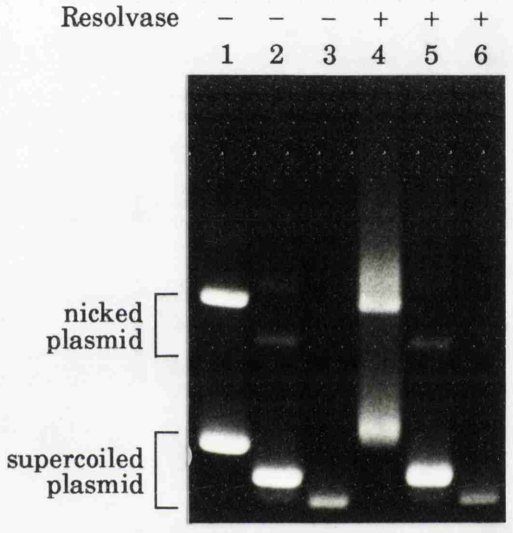

Figure 3.9 Agarose gel electrophoresis of non-crosslinked synapsis reactions showing the effect of resolvase on a plasmid with two *res* sites in direct repeat orientation (pMA2350; lanes 1 and 4; see Figure 3.21 for a map of this plasmid), a single *res* site plasmid (pMA1441; lanes 2 and 5), and a plasmid without a *res* site (pUC18; lanes 3 and 6). Only pMA2350 shows a resolvase-dependent effect in the absence of a crosslinking reagent, namely retardation of the supercoiled DNA and general smearing indicative of an unstable protein-DNA interaction (lane 4).

Buffer C, minus-Mg^{2+}; no restriction endonuclease treatment; 0.8% agarose gel.

In order to test the 'worst-case scenario', where the crosslinking reagent links protein-bound *res* sites that have come into proximity by chance, but would not normally interact further, the following experiment was designed. pCM3, a plasmid containing a single Tn*3* *res* site and a single Tn*21* *res* site in direct repeat orientation (represented in Figure 3.10),

was put into the standard synapsis assay using glutaraldehyde, the least specific of the crosslinking reagents described. It was shown that Tn*3* resolvase fails to bind to any of the subsites of the Tn*21 res* site and, while Tn*21* resolvase did bind to the three subsites of Tn*3 res*, there was no evidence of any interaction between the different sites, mediated by either resolvase (Avila *et al.*, 1990; Parker and Halford, 1991). However, a crosslinked synaptic complex was readily isolated when a plasmid containing two copies of the Tn*21 res* site was included in the standard synapsis assay with Tn*21* resolvase (data not shown).

Treatment of the crosslinked pCM3 reaction with the appropriate restriction endonucleases followed by agarose gel electrophoresis showed that the only protein-DNA interactions stabilised were those between each resolvase and its cognate *res* site (Figure 3.11). When both resolvases were present in the reaction, and both *res* sites were occupied, there was no evidence of synapsis between the sites, despite the optimal conditions for crosslinking of the synaptic complex. The complex formed by resolvase and a single *res* site, as evidenced by a crosslinking-dependent and SDS-labile species retarded with respect to restriction fragments containing one copy of the *res* site, is discussed further in Section 3.10.

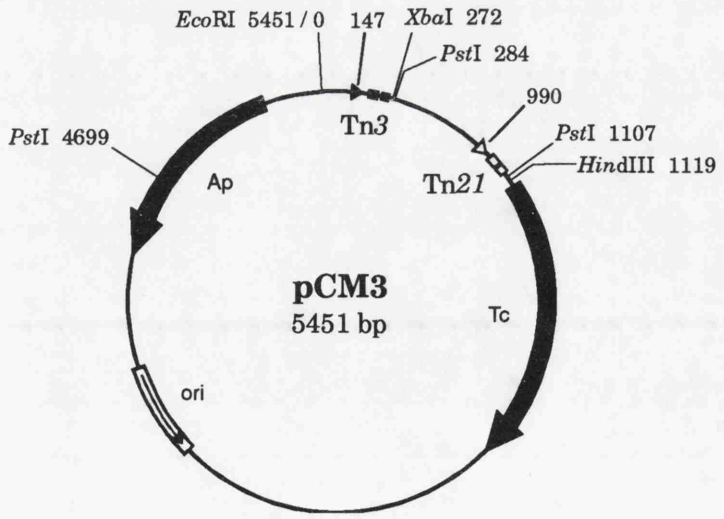

Figure 3.10 A simplified map of pCM3 (C. McDougall and W.M. Stark, personal communication), a plasmid containing a single Tn*3 res* site and a single Tn*21 res* site in direct repeat orientation. The location of the *res* sites is shown, as are the restriction endonuclease sites used in the experiment described in the text. Site locations are numbered (in bp) relative to the centre of the *Eco*RI site (designated zero).

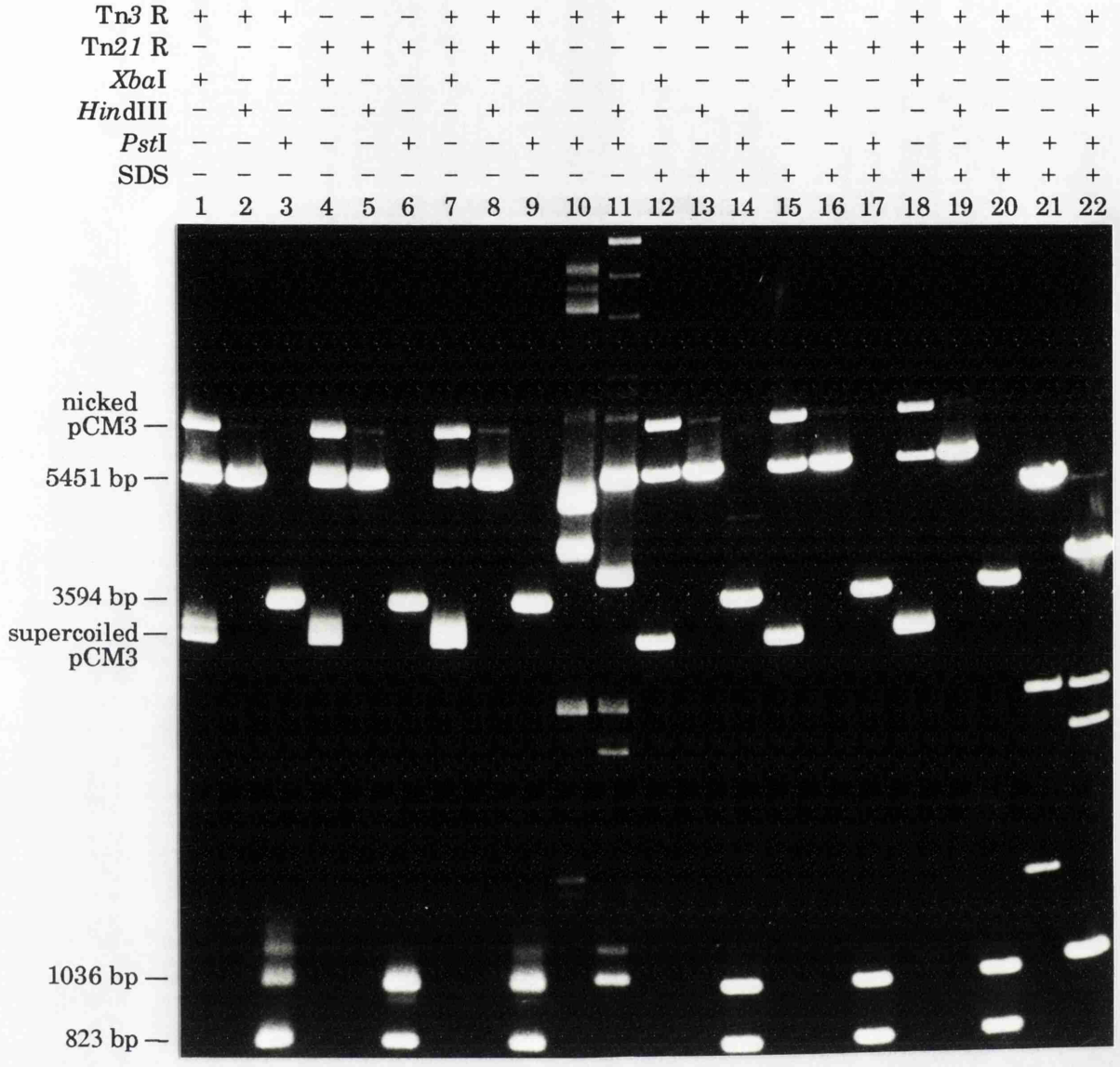

Figure 3.11 Agarose gel electrophoresis of a glutaraldehyde-crosslinked synapsis reaction showing the behaviour of pCM3 (single Tn*3* *res* site and single Tn*21* *res* site, in direct repeat orientation) in the presence of Tn*3* resolvase, Tn*21* resolvase, or both resolvases.
Each pCM3 reaction was divided into three aliquots and treated with *Xba*I, *Hin*dIII, or *Pst*I, respectively (from left to right in each group of three lanes; see Figure 3.10 for a restriction map). The *Xba*I digest is partial; uncut complex is present with either or both resolvases (lanes 1, 4, and 7). *Hin*dIII cleavage of pCM3 gives full-length linear plasmid (5451 bp; lanes 2, 5, and 8), and would give a faster-migrating α-form if the *res* sites were synapsed; no such complex is visible. *Pst*I cleavage gives a 1036 bp fragment containing the Tn*3* *res* site and a 823 bp fragment containing the Tn*21* *res* site (lanes 3, 6, and 9). Each resolvase forms a crosslinked complex only with its cognate *res* site (as evidenced by the presence of retarded complex behind the appropriate fragment). *Pst*I cuts in both domains of pCM3, but there is no sign of χ-form complex in any of the reactions. A crosslinked pMA21 synapsis reaction, cut with *Pst*I (lane 10) and *Pst*I + *Hin*dIII (lane 11) is included as a control, giving α-form and χ-form, respectively. SDS treatments are included (lanes 12-22).

Buffer C, minus-Mg^{2+}; 0.8% agarose gel.

The obvious way to show that a genuine intermediate in the site-specific recombination reaction has been trapped by the crosslinking strategy is to get the isolated substrate synapse to perform strand-exchange to generate product. However, like much of the subsequent analysis of the synaptic complex described in this thesis, attempts to achieve further reaction were complicated by an inability to get the crosslinked complex out of the gel and into solution intact. A variety of methods were tried to this end (see Section 2.10) but all failed, thus dictating the considerable use of in-gel reactions and two-dimensional gel electrophoresis. Clearly a possible weak link in this regard is the binding of resolvase to the *res* site since it is the protein that is crosslinked and not the interaction between protein and DNA.

It is perhaps surprising (and fortunate) that the crosslinked pMA21 synaptic complex was able to survive restriction endonuclease cleavage in one or both domains[3]. Two observations indicate that the cleaved pMA21 synaptic complex is relatively stable during agarose gel electrophoresis. Firstly, breakdown of the α- and χ-forms of the synaptic complex was minimal when isolated complexes were subjected to a second dimension of electrophoresis (see Section 3.2). Secondly, partial DNA restriction fragments arising from protection at restriction endonuclease sites within *res* in the synaptic complex were only present in the gel as synaptic complex following electrophoresis (see Section 6.1). Thus, any failure to reflect the amount of synapsed pMA21 present at the time of crosslinking is more likely to be due to inefficient crosslinking or instability during the subsequent restriction endonuclease digestion.

All attempts to obtain product, or even resolvase-dependent cleavage at the *res* site, following in-gel incubation of either uncrosslinked protein-DNA complexes or crosslinked substrate synaptic complex (following treatment to cleave the protein crosslinks) were unsuccessful (data not shown).

[3] There was some evidence that a crosslinked synaptic complex involving a plasmid containing closely-spaced res sites was relatively unstable during the post-crosslinking treatment to isolate the synapsed substrate (see Section 3.4).

3.2 Characterisation of the isolated synaptic complex by two-dimensional agarose gel electrophoresis.

The technique of two-dimensional agarose gel electrophoresis is introduced here as a means of characterising further the uncut and cleaved forms of the synaptic complex, the isolation of which was described in the Section 3.1. However, it is used throughout this Chapter and in Section 6.1 to obtain additional information on the various protein-DNA complexes isolated from synapsis reactions. Details of the technique, originally developed for rapid mapping of restriction sites in a DNA molecule (Kovacic and Wang, 1979), are given in Section 2.9g.

Glutaraldehyde-crosslinked pMA21 synapsis reactions were either undigested or treated with *Pst*I before the first dimension of electrophoresis (as described earlier and shown in Figure 3.3). Whole lanes containing the bands of interest were cut as strips from this gel and incubated with *Eco*RV (see Section 2.7c). Restriction endonuclease cleavage at the unique *Eco*RV site in pMA21 (Figure 3.1) converts uncut synapsed plasmid in the first-dimension gel into an α-form, and converts the *Pst*I-cleaved α-form into the χ-form of the synaptic complex. After incubation with *Eco*RV, the lanes excised from the first-dimension gel were set into a fresh agarose gel such that the direction of migration in the second dimension of electrophoresis was at 90° to that in the first dimension (see Section 2.9g).

Figure 3.12 shows that the α-form is derived from the uncut complex band that is retarded relative to the supercoiled protein-free substrate DNA after the first-dimension of electrophoresis. In Figure 3.12a the in-gel digestion with *Eco*RV was partial and about 30% of the species that were supercoiled in the first-dimension gel remained in the supercoiled state, either as free substrate or as retarded complex. In Figure 3.12b the *Eco*RV digest went further toward completion, showing that only about 40% of the uncut retarded complex was converted to the α-form, the remainder running as full-length linear substrate DNA. This could be due to the crosslinked synaptic complex falling apart during the treatment between the first and second dimensions of electrophoresis, or the uncut retarded complex band may represent a mixture of synapsed substrate and substrate with resolvase-bound to unsynapsed *res* sites, or both may apply.

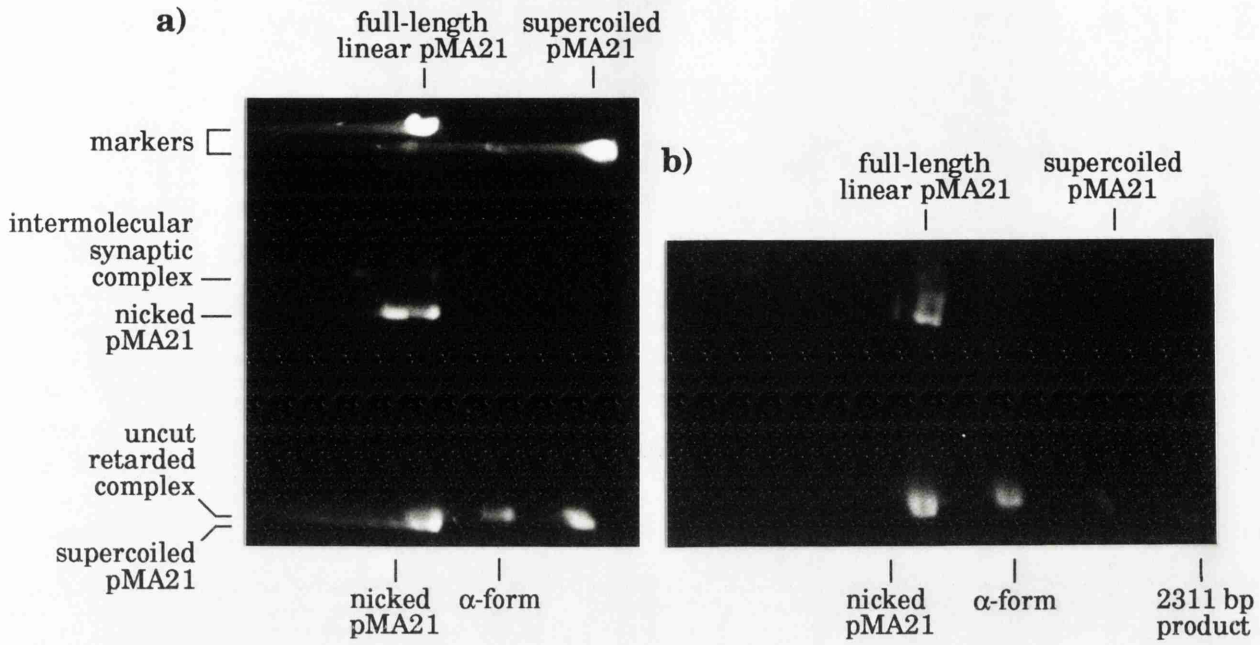

Figure 3.12 Two-dimensional agarose gel electrophoresis of glutaraldehyde-crosslinked pMA21 synapsis reactions.
The undigested synapsis reaction was loaded on a 0.8% agarose gel and run in the first dimension from top to bottom, giving results very similar to the undigested reaction lane in Figure 3.3a. The excised lane was treated with *Eco*RV and run in the second dimension from left to right.

a) The *Eco*RV digest is partial, so all the relevant species are present in the second-dimension gel. The α-form of the synaptic complex, with characteristic mobility between full-length linear and supercoiled substrate DNA is seen to issue from the material running as uncut retarded complex in the first dimension. A putative intermolecular synaptic complex, migrating at a slower rate than the nicked substrate DNA in the first-dimension, is converted into a number of even slower-migrating complexes by *Eco*RV treatment, as well as a portion being unaffected (i.e. remaining on a diagonal with the similarly unaffected nicked and supercoiled substrate bands) and the remainder migrating as full-length linear substrate (see Section 3.7).

b) Here, the *Eco*RV digest is almost complete. Approximately 40% of the uncut retarded complex band has been converted to the α-form, with the remainder of that cleaved running as full-length linear substrate.

Buffer C, minus-Mg^{2+}; 0.2% glutaraldehyde; 0.8% agarose gel in both dimensions.

Figure 3.13 shows the result of a similar experiment, differing only in that the synapsis reaction was not treated with a protein crosslinking

reagent. Despite this, a discrete uncut retarded complex band was obtained after the first dimension of electrophoresis. However, no *Eco*RV α-form was present after the second dimension of electrophoresis; all the cleaved complex migrated to the position of full-length linear substrate DNA.

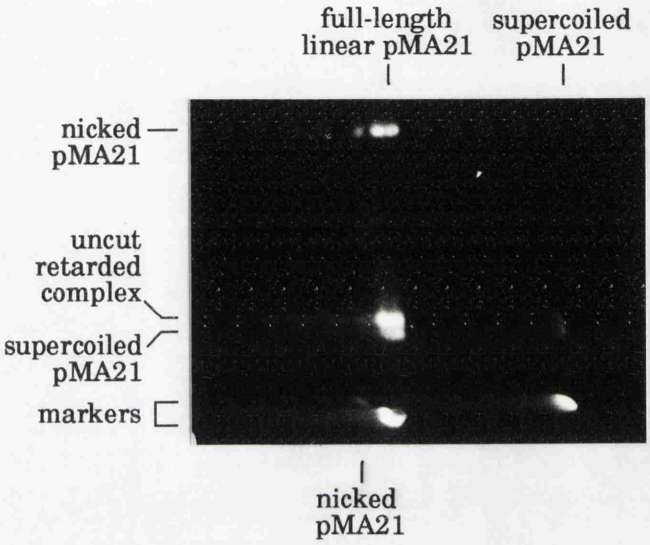

Figure 3.13 Two-dimensional agarose gel electrophoresis of a non-crosslinked pMA21 synapsis reaction.
The undigested synapsis reaction was loaded on a 0.8% agarose gel and run in the first dimension from top to bottom. A discrete uncut complex band was present at this stage. The excised whole lane was treated with *Eco*RV and run in the second dimension from left to right.
The in-gel *Eco*RV digest is virtually complete, with the uncut retarded complex band converted to full-length linear substrate, and no sign of α-form complex.

Buffer C, minus-Mg^{2+}; 0.8% agarose gel in both dimensions.

Figure 3.14 presents the data obtained from both 0.8% and 1.2% agarose second-dimension gels after in-gel *Eco*RV digestion of the first-dimension *Pst*I α-form of pMA21. The *Eco*RV digest is about 50% complete in both cases, as shown by the considerable amount of first-dimension free substrate DNA remaining as full-length linear. Points to note are:

- *Eco*RV digestion did indeed convert the *Pst*I α-form into a χ-form of the synaptic complex (the partial digest resulting in an approximately equal amount of each species).

- Dissociation of the α-form to full-length linear substrate, and of the χ-form to its component double-restriction DNA fragments of 3706 bp and 1221 bp was less than 10%. Thus, despite an inability to elute the synaptic complex from the agarose gel intact, it appears to be relatively stable in the gel.
- χ-form complex was also generated from the location of full-length linear substrate in the first-dimension gel – produced from the relaxed *Pst*I α-form which has the same mobility as full-length linear in the 0.8% agarose first-dimension (see Figure 3.3).
- Also in evidence is the aforementioned effect of agarose percentage on the mobility of the α- and χ-form of the synaptic complex, namely the decreased mobility of both complexes relative to linear DNA fragments in the higher percentage gel (see Figure 3.3).
- There was a considerable difference in the mobility of the *Eco*RV α-form (issuing from the uncut retarded complex band in the first dimension) and the PstI α-form (remaining due to the incomplete *Eco*RV digestion) in a 1.2% agarose gel. This interesting phenomenon, in which the mobility of the α-form of the synaptic complex is influenced by the relative length of the free arms and the amount of DNA remaining in the supercoiled state, is investigated further in Section 3.3.

The bands predicted from their mobility to represent protein-DNA complexes were cut from the second-dimension gels. SDS treatment followed by a third dimension of electrophoresis produced the expected DNA fragments from each complex (data not shown).

The relatively low level of breakdown of the α- and χ-form lends credence to the view that the conversion of the uncut complex into approximately equal amounts of α-form and full-length linear substrate following *Eco*RV digestion (Figure 3.12) was a reflection of a genuine mixture of synapsed and unsynapsed substrate, rather than being due to breakdown of the crosslinked synapse. Indeed, an uncut retarded complex indistinguishable from that obtained with a plasmid containing two *res* sites in direct repeat orientation was present after crosslinking of a synapsis reaction with plasmid containing a single *res* site (Figure 3.15). Therefore, restriction endonuclease cleavage to generate the α- or χ-form of the protein-DNA complex is necessary in order to show that the *res* sites are synapsed. The nature of the crosslinked complex formed by resolvase and a single *res* site is discussed in Section 3.10.

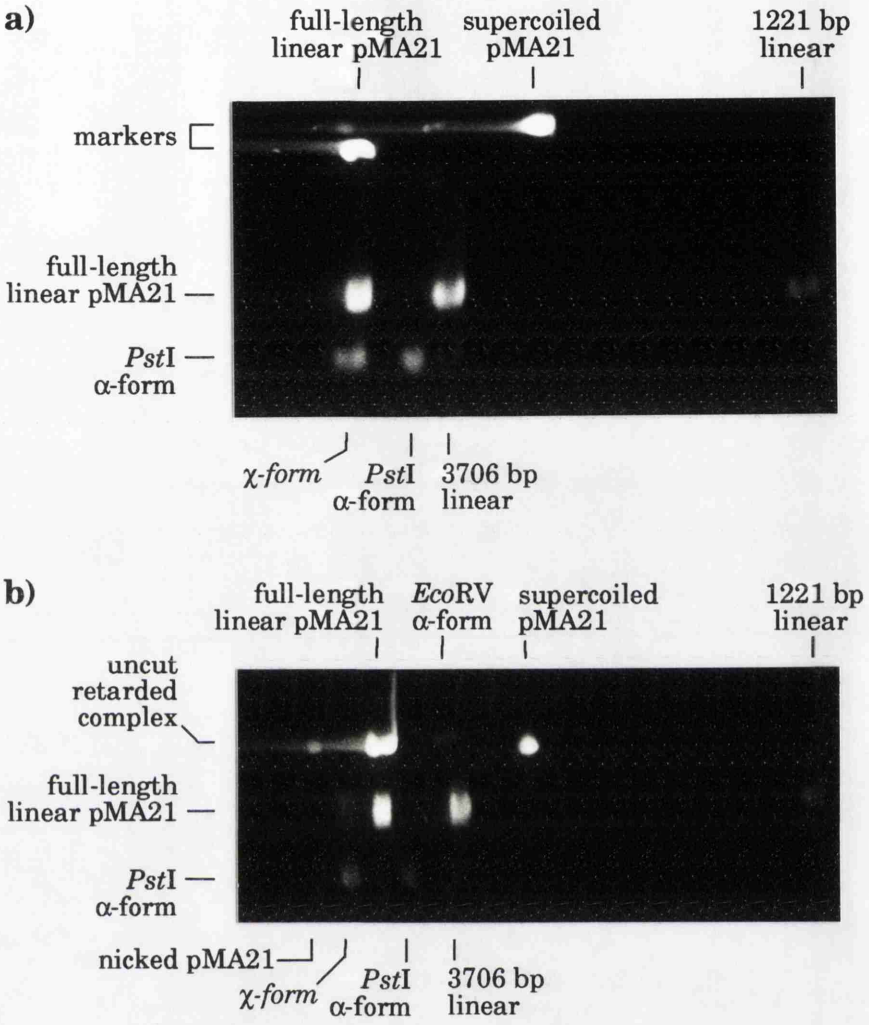

Figure 3.14 Two-dimensional agarose gel electrophoresis of glutaraldehyde-crosslinked pMA21 synapsis reactions.
The *Pst*I-digested synapsis reaction was loaded on a 0.8% agarose gel and run in the first dimension from top to bottom, giving results very similar to the analogous lane in Figure 3.3. The excised lane was treated with *Eco*RV and run in the second dimension from left to right. The in-gel *Eco*RV digest is partial.

a) 0.8% agarose second-dimension gel. About 50% of the *Pst*I α-form has been converted to the χ-form of the synaptic complex, with the characteristic change in mobility. See text for further details.

b) 1.2% agarose second-dimension gel. An identically-treated uncut complex band is included to show the different mobility of the *Eco*RV α-form compared to the *Pst*I α-form. See text for further details.

Buffer C, minus-Mg^{2+}; 0.2% glutaraldehyde.

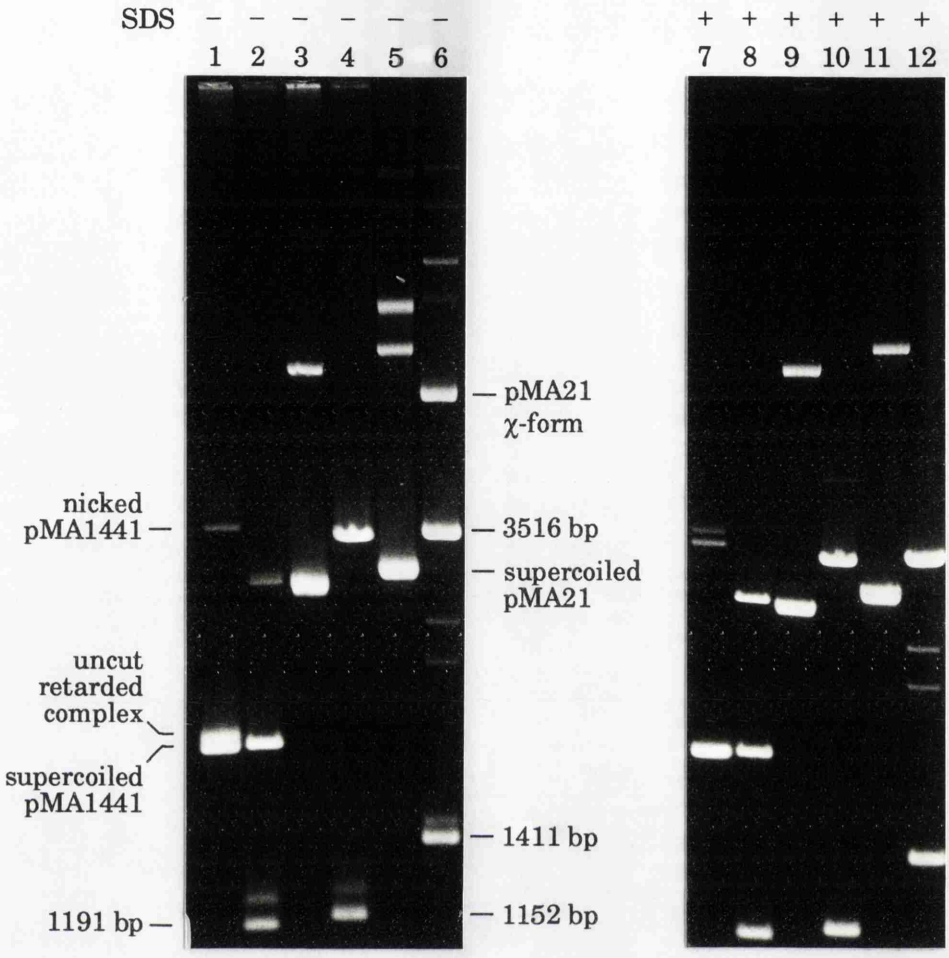

Figure 3.15 Agarose gel electrophoresis of glutaraldehyde-crosslinked synapsis reactions: a plasmid containing a single copy of the *res* site produces uncut retarded complex.
pMA1441 contains a single copy of the *res* site (inserted in the polylinker of pUC18). An undigested synapsis reaction (lane 1) reveals a discrete uncut complex band retarded with respect to the supercoiled substrate DNA. Digestion with *Sst*I + *Xmn*I (lane 2) isolates the *res* site on a 1191 bp restriction fragment, a portion of which is retarded by resolvase binding to form a discrete band. There is no detectable intermolecular synaptic complex.
pMA44 is identical to pMA21 except that the top *res* site (as shown in Figure 3.16) is absent, leaving a single *res* site. The uncut retarded complex of larger size plasmids does not migrate as a distinct band in a 1.2% agarose gel (lane 3; compare with Figure 3.3a). Digestion with *Ava*I + *Nde*I (lane 4) isolates the *res* site on a 1152 bp restriction fragment, a portion of which is retarded to form a discrete protein-DNA complex band.
pMA21 (undigested in lane 5; digested with *Pst*I + *Bam*HI in lane 6) produces both intra- and intermolecular synaptic complexes (as discussed in Section 3.1 and Section 3.7, respectively). Lanes 7-12 show SDS treatments of the above reactions in the same order.

Buffer C, minus-Mg^{2+}; 0.05% glutaraldehyde; 1.2% agarose gel.

3.3 Further characterisation of the synapsed substrate by restriction endonuclease treatment.

Figure 3.16 is a more detailed representation of the standard synapsis substrate pMA21 showing the increased repertoire of restriction endonuclease sites used in this Section.

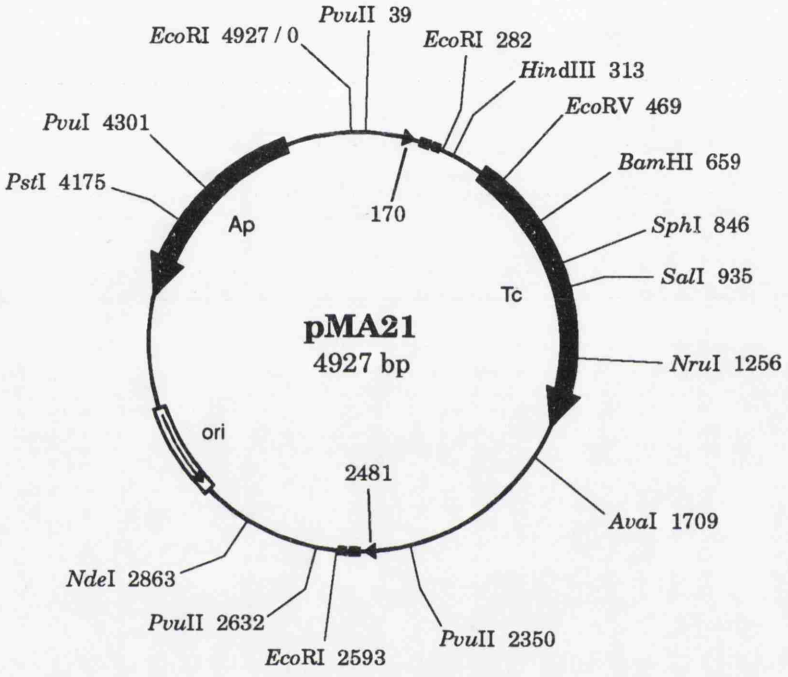

Figure 3.16 A restriction map of the Tn*3* resolvase resolution substrate pMA21 (Bednarz *et al.*, 1990). The locations of the *res* crossover sites which define the two domains of the synapsed substrate are shown, as are the restriction endonuclease sites used to generate various α- and χ-forms. Site locations are numbered (in bp) relative to the centre of the *Eco*RI site of pBR322 (designated zero).
In pMA44, the *Eco*RI fragment containing the top *res* site (as represented in the map) is absent, leaving a single *res* site.
In pMA2631, the bottom *res* site (on the *Pvu*II fragment) is inverted.

As can be seen from Figure 3.16, *Eco*RI cleavage of synapsed pMA21 will generate a χ-form with three short arms and one relatively long arm. Figure 3.17 shows the effect of a gradual reduction in the length of the

long arm on the gel mobility of the χ-form. This procedure culminates in the production of the *Eco*RI + *Pvu*II χ-form in which the synapsed *res* sites (about 115 bp in size) are on DNA fragments of 243 bp, with most of the non-*res* DNA on the subsite I side of each *res* site. This provides further evidence that the crosslinked synapse is specific to the *res* sites. Electron microscopy of a crosslinked χ-form of the synaptic complex revealed free DNA arms with the length expected if the *res* sites were within the central electron-dense structure (Benjamin and Cozzarelli, 1988).

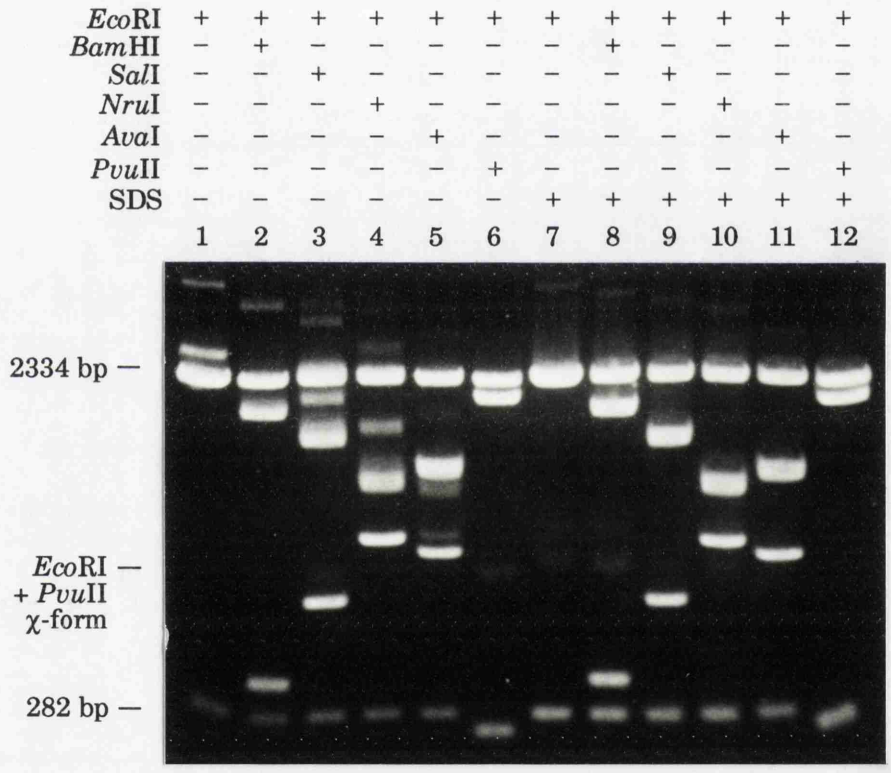

Figure 3.17 Agarose gel electrophoresis of a glutaraldehyde-crosslinked pMA21 synapsis reaction. Electrophoretic resolution of small complexes was enhanced through a reduction in run-time achieved using higher applied voltage in conjunction with a cooling system for the gel apparatus and the recirculating running buffer (see Section 2.9d).
The long arm of the *Eco*RI χ-form of the synaptic complex was gradually reduced in size by treatment with the named additional restriction endonucleases (see Figure 3.16). This produced successively smaller χ-forms, the smallest being the *Eco*RI + *Pvu*II complex in which the synapsed DNA fragments were both 243 bp in size (lane 6). The *Eco*RI + *Bam*HI χ-form migrated to the same position as the 2334 bp substrate DNA fragment and was therefore hidden (lane 2).

Buffer C, minus-Mg^{2+}; 0.05% glutaraldehyde; 0.8% agarose gel.

The *Eco*RI + *Pvu*II χ-form of the crosslinked pMA21 synaptic complex is small enough to be isolated by non-denaturing polyacrylamide gel electrophoresis. Exploiting this in the future may provide a means of eluting the intact complex from the gel, and of obtaining the protein and DNA components in a cleaner form than has been possible from agarose gels (thus facilitating protein stoichiometry and footprinting studies; see Chapters 5 and 6). This small χ-form produced from supercoiled substrate could also be used as a positional marker for studies on the synapsis of small linear DNA fragments, visualised by non-denaturing PAGE.

The results of experiments investigating the effect of restriction endonuclease cleavage within the *res* site on the crosslinked synaptic complex are presented in Section 6.1.

When a crosslinked pMA21 synapsis reaction is divided and each aliquot is treated with a different restriction endonuclease that cuts at a unique site in the plasmid, the α-forms generated all comprise the same amount of DNA. However, they differ in the relative length of the arms freed by cleavage, and they may also differ in respect of the domain cut by the restriction endonuclease. Since the two domains defined by the *res* cross-over sites of pMA21 differ in size (2616 bp and 2311 bp, see Figure 3.16), the amount of DNA remaining supercoiled in the crosslinked α-form will depend on which domain remains uncut. Taking the generally-quoted figure for specific linking difference (σ) of plasmid DNA of –0.06 and a helical repeat of 10.5, the number of trapped negative supercoils will differ by about 2.

Figure 3.18 reproduces the results of agarose gel electrophoresis of a number of aliquots from the same pMA21 synapsis reaction treated with different unique-cutting restriction endonucleases. Figure 3.19 presents the data on relative mobility of the resulting α-complexes in graphical form. Considering first the effect of altering the relative arm-length by use of different restriction endonucleases that cut in the same domain; due to restriction site availability, the best data were for the 2311 bp domain of pMA21. Gel mobility of the α-form was at a maximum when the restriction site was close to a *res* site, and decreased gradually to reach a minimum with the *Nru*I α-form. Of the restriction sites utilised, the *Nru*I site was closest to a position midway between the *res* sites. Thus, it appears that an α-form with one long arm and one short arm migrates fastest in an agarose gel and that mobility decreases gradually

as the arms approach equality in length. The relative mobility of α-forms generated by cleavage at different sites in the 2616 bp domain of pMA21 was consistent with this interpretation. Indeed, it appeared that the effect on mobility was greater when making a change in relative arm length by cleavage in the 2616 bp domain than was the case when making a similar change by cutting in the 2311 bp domain (see Figure 3.19), although a more even distribution of unique restriction sites would have been informative in this regard.

A very similar effect on the gel mobility of the pMA21 χ-form of the synaptic complex was seen when restriction endonuclease cleavage was maintained at the same site in one domain, while the cleavage site within the other domain was varied (data not shown). There was a less pronounced overall variation in mobility than was seen for the α-form, but once again the effect was greatest when the relative length of the arms that formed the 2616 bp domain of the synapsed substrate was altered. This may be due to the fact that more of the total DNA is redistributed when the relative arm length is changed in the larger domain of the synapsed substrate. Speculation on any significance in terms of synapse structure awaits further information on the path of the DNA in the complex and the spatial arrangement of the DNA 'arms' upon exit from the nucleoprotein core. The latter property could be investigated by determining whether there is any preferential pattern of religation of a χ-form generated by treatment with a single restriction endonuclease, although the arms created would have to be short enough to be constrained, but not immobilised, by their spatial geometry. Electron microscopy of the χ-form of a resolvase synaptic complex did not reveal any unique arrangement of arms issuing from the core (Benjamin and Cozzarelli, 1988).

A decrease in the rate of migration during gel electrophoresis when two free arms issuing from the core of the cleaved synaptic complex were changed from being very different in length to being approximately equal in length is not surprising when one considers the effect of bend position on the electrophoretic mobility of a DNA molecule. If the nucleoprotein core of the synapsed DNA molecule is analogous to the site of a bend in a DNA fragment, then the act of changing the relative arm length can be considered analogous to the technique of permutation analysis. This method for localising protein-induced bends exploits a similar gradual reduction in the rate of gel migration as the site of bending is moved

stepwise from an end to the centre of a DNA fragment (Lane *et al.*, 1992). Although the effect of bends on the electrophoretic mobility of DNA molecules has been reported as being apparent only in polyacrylamide gels, this is probably due to the use of DNA molecules too small for the effect to be observed in agarose gels (Calladine *et al.*, 1991). The effect of relative arm length on the electrophoretic mobility of the α-form of the synaptic complex also appeared to be enhanced when the intact domain was supercoiled (Figure 3.19).

The relaxed α-form was visible in the 1.2% agarose gel (Figure 3.18). Its presence made it possible to differentiate between the effect of relative arm length described above and the effect of the amount of DNA remaining in the supercoiled state on the mobility of the α-form. When represented graphically (Figure 3.19), it can be seen that the relative mobility of the relaxed α-form was uniformly dependent on the relative arm length, regardless of the domain cleaved (allowing for the aforementioned heightened effect when the 2616 bp domain was cut). In contrast, the mobility of supercoiled α-forms with a similar relative arm length differed considerably when the restriction sites utilised were in different domains of pMA21. This is the effect of supercoiling: α-forms created by restriction endonuclease cleavage within the 2616 bp domain of pMA21 have less of the total amount of DNA trapped in the supercoiled state than those generated by cleavage in the 2311 bp domain, and so their rate of migration is reduced.

Formation of the relaxed α-form of the synaptic complex could be due to a number of processes. Some of that seen (Figure 3.3b, Figure 3.18) will certainly have arisen from synapsis of nicked substrate DNA already present in the preparation used, as this has been shown to occur (see Section 3.6). In addition, either resolvase-dependent or resolvase-independent processes may result in loss of supercoiling. Thus, there could be nicking of the DNA at the *res* crossover site, or possibly relaxation by the topoisomerase I activity of resolvase under the reaction conditions used; and a form of the so-called 'star activity' reported for a number of restriction endonucleases appears to be involved (Fuchs and Blakesley, 1983) – see the legend for Figure 3.18. In the face of this uncertainty, I have elected to call this species 'relaxed' rather than 'nicked' α-form. The two bands at the position of relaxed α-form in Figure 3.18 probably reflect the presence of relaxed product α-form in addition to the faster-migrating relaxed substrate α-form. The relaxed α-forms

exhibit a clear difference in mobility between the substrate and product complexes, in contrast to the corresponding supercoiled α-forms which migrate to about the same position in the agarose gel (see Section 3.8).

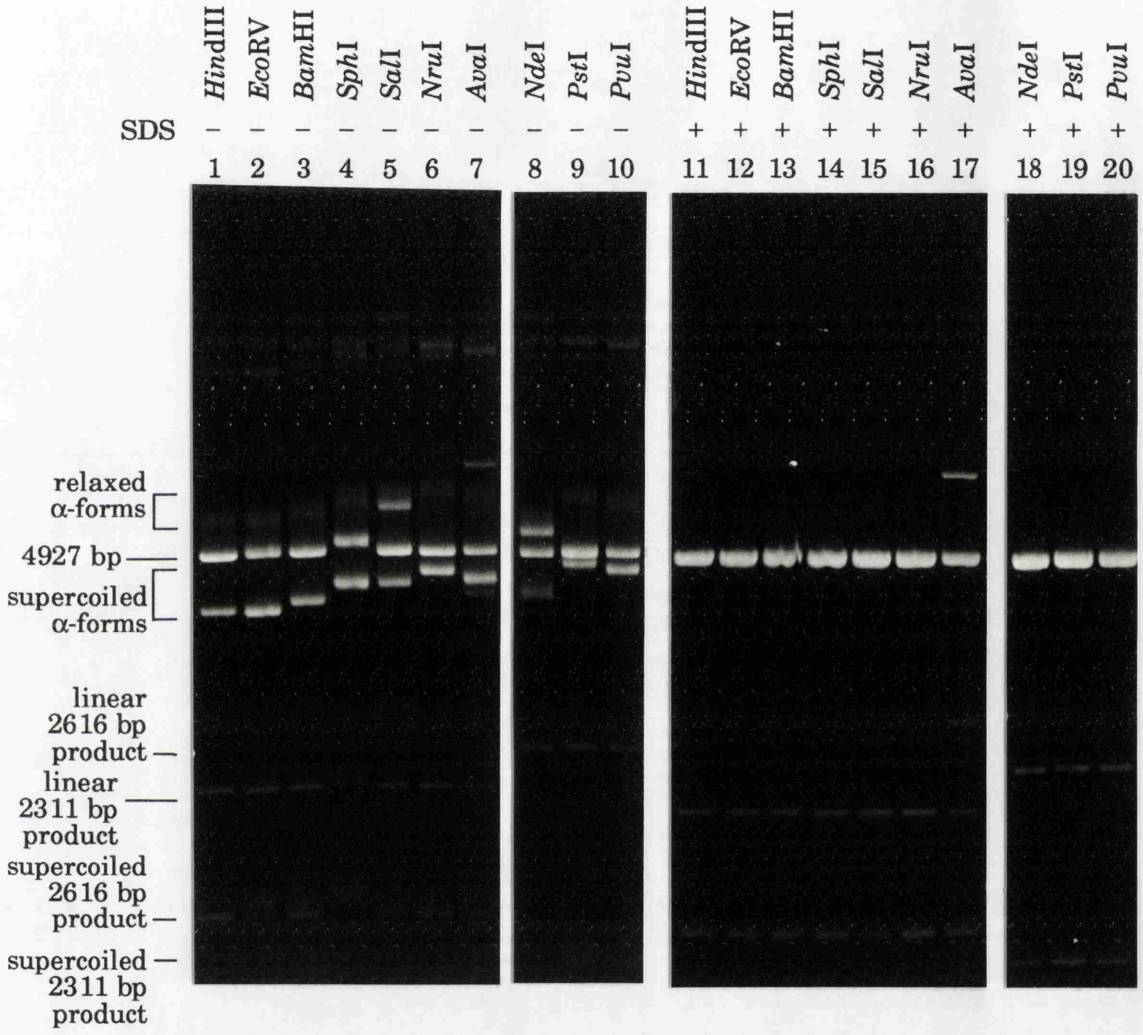

Figure 3.18 Agarose gel electrophoresis of a glutaraldehyde-crosslinked pMA21 synapsis reaction: the relative mobility of the α-form is dependent on the site of restriction endonuclease cleavage.
Aliquots from the synapsis reaction were treated with a number of restriction endonucleases that cut at unique sites in pMA21 as shown; SDS treatments are included. See the text for details.
Use of *Sal*I or *Nde*I reproducibly increases the amount of relaxed α-form, probably due to nicking at a cryptic recognition site in the other domain from that cleaved since there also appears to be a small amount of a double restriction substrate DNA fragment present in each case. There is a general retardation of bands in the *Sph*I digest, indicating a DNA-binding activity arising from the restriction endonuclease preparation. The *Hin*dIII and *Ava*I restrictions are partial, leaving nicked and supercoiled substrate and, in the case of *Ava*I, singly-nicked synaptic complex running immediately ahead of the α-form, and singly-nicked catenane following the SDS treatment.

Buffer C, minus-Mg^{2+}; 0.05% glutaraldehyde; 1.2% agarose gel.

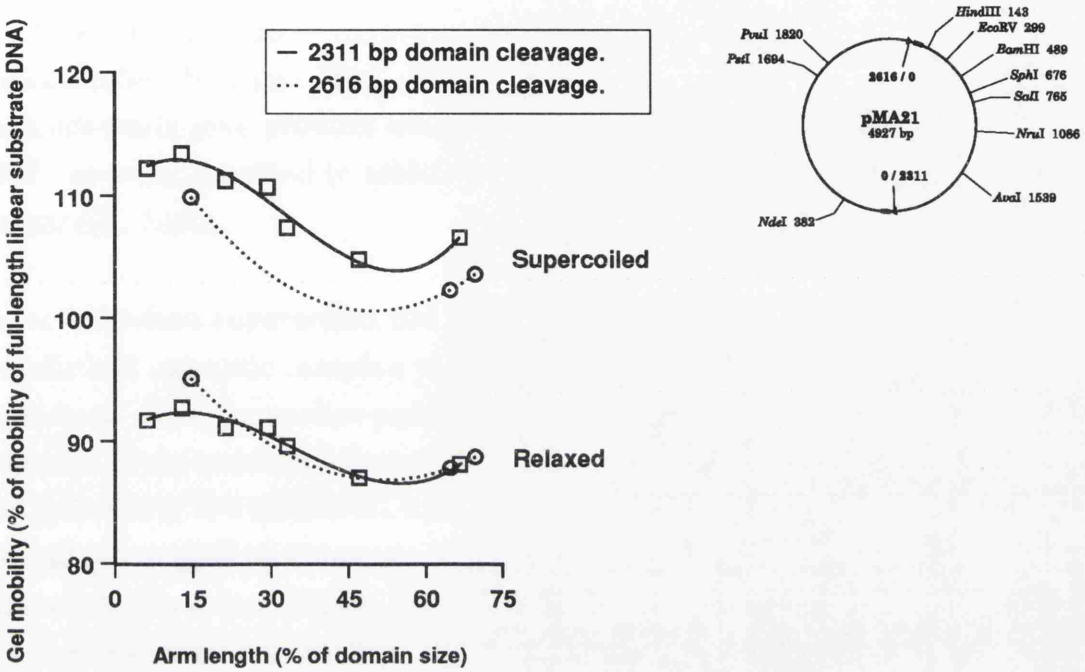

Figure 3.19 Graph showing the relative mobility of pMA21 α-forms resulting from cleavage with different restriction endonucleases and isolated in the gel reproduced in Figure 3.18.

The distance of migration of the relaxed and supercoiled α-forms is normalised to that of full-length linear substrate DNA. The relative length of the two arms freed by restriction endonuclease cleavage is represented by expressing the distance between the *res* crossover site and the restriction site (measured clockwise from the appropriate *res* site on the map of pMA21) as a percentage of the domain size. Thus, in this model, the crosslinked synapse is treated as a point-attachment at the crossover sites, and 50% arm length is equivalent to an α-form with arms of equal length. The relationship between gel mobility and relative arm length is demonstrated, as is the reduced mobility of a supercoiled α-form cut in the 2616 bp domain of pMA21 relative to one cut in the 2311 bp domain (see the text for details).

3.4 Effect of *res* site orientation and spacing on synapsis.

pMA2631 is identical to pMA21 with one exception: the bottom *res* site (as represented in Figure 3.16) is in the reverse orientation (Bednarz *et al.*, 1990). Resolution or inversion of supercoiled pMA2631 was undetectable (Bednarz *et al.*, 1990); such inverted site substrates have been shown to give product when nicked or linearised (Boocock *et al.*, 1987), or when knotted in addition to being supercoiled (Dröge and Cozzarelli, 1989).

However, when supercoiled pMA2631 was assayed for synapsis, crosslinked synaptic complex was obtained (Figure 3.20). This result was consistent with the earlier published study of resolvase-mediated synapsis (Benjamin and Cozzarelli, 1988). In terms of gel mobility, the α- and χ-forms of the pMA2631 synaptic complex were identical to those of pMA21 generated by cleavage at the same restriction sites, but the yield was markedly lower (Figure 3.20). Although inverted *res* sites interacted in a synapse that was stabilised by protein crosslinking, the block on recombination of pMA2631 could arise from mispairing of the *res* sites in the synapse. An inverted site synaptic structure in which the two *res* sites are aligned in antiparallel such that subsite I of one site is paired with subsite III of the other site has been proposed (Benjamin and Cozzarelli, 1988). Alternatively, a crosslinked synaptic complex formed by inverted repeats of the *res* site may be identical to that proposed for direct repeats in terms of subsite interactions, with the block on recombination due to instability arising from a tangled DNA conformation outside the synapse (Stark *et al.*, 1989a), (see Figure 3.27). The topological arrangement of the DNA in the crosslinked pMA21 and pMA2631 synaptic complexes is probed further in Chapter 4.

pMA2350 contains two copies of the *res* site in direct repeat orientation, but the crossover sites of *res* are separated by only 219 bp (Figure 3.21). This substrate was recombined efficiently by resolvase (Stark *et al.*, 1989b). However, the yield of crosslinked synaptic complex in numerous assays was generally poor, as Figure 3.22 shows. This reduced yield may be a reflection of breakdown of the closely-spaced *res* site synaptic complex occurring during post-crosslinking treatment, perhaps as a result of the very differently-sized domains causing instability, rather than an indication of any fundamental difference between synapsis of pMA2350 and pMA21. Indeed, there was generally more evidence of

complex breakdown during electrophoresis of pMA2350 synapsis reactions than was seen following synapsis of pMA21, and the pMA2350 α-form did not survive intact a second dimension of electrophoresis (data not shown). The rapid migration of the α-form generated by restriction endonuclease cleavage in the 219 bp domain of pMA2350 demonstrates well the effect of the amount of DNA remaining trapped in the super-coiled state on the gel mobility of the α-form of the synaptic complex (Figure 3.22).

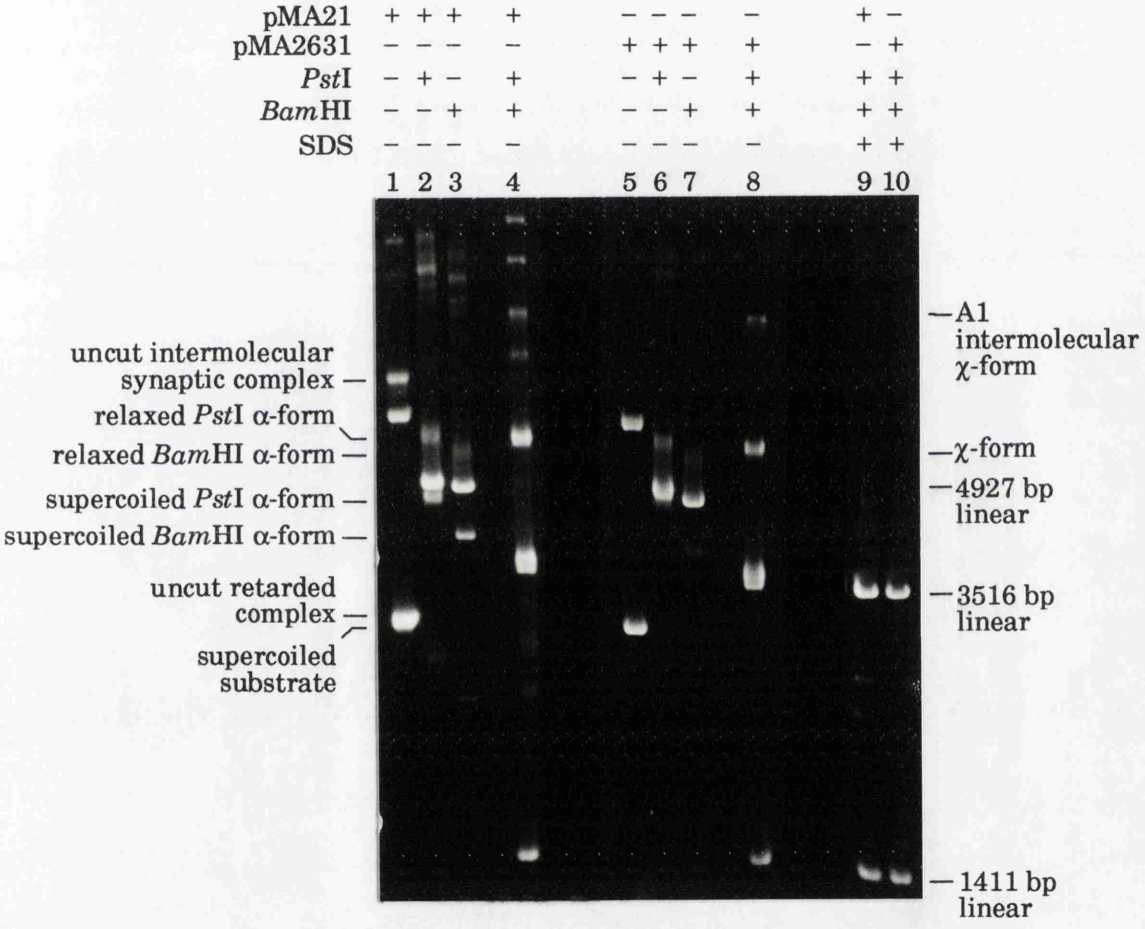

Figure 3.20 Agarose gel electrophoresis of a glutaraldehyde-crosslinked pMA2631 synapsis reaction: a synaptic complex is formed by a plasmid containing inverted repeats of the *res* site.
Synapsis reactions containing either pMA21 or pMA2631 were digested with *Pst*I or with *Bam*HI (to generate α-forms of the synaptic complex exhibiting a different gel mobility), or with *Pst*I + *Bam*HI (to generate the χ-form). SDS treatments of the *Pst*I + *Bam*HI digest of both plasmids are included (lanes 9 and 10). See the text for further details.
Note that following the *Pst*I + *Bam*HI digest, while there are four distinct bands representing intermolecular synapsis of pMA21 (lane 4), only one of these four bands is present in significant amount in the pMA2631 reaction (lane 8). This band represents the 'A1' intermolecular synaptic complex shown in Figure 3.32; see Section 3.7 for further discussion.

Buffer C, minus-Mg^{2+}; 0.2% glutaraldehyde; 1.2% agarose gel.

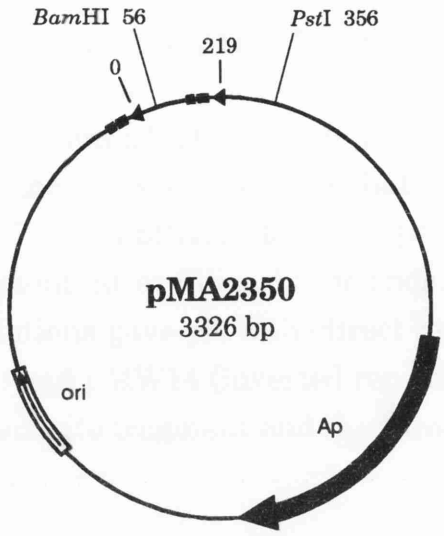

Figure 3.21 A simplified map of the Tn*3* resolvase resolution substrate pMA2350 (Stark *et al.*, 1989b). The locations of the *res* crossover sites which define the two domains of the synapsed substrate are shown, as are the unique restriction endonuclease sites used to generate the α- and χ-forms. Site locations are numbered (in bp) relative to the centre of one of the crossover sites.

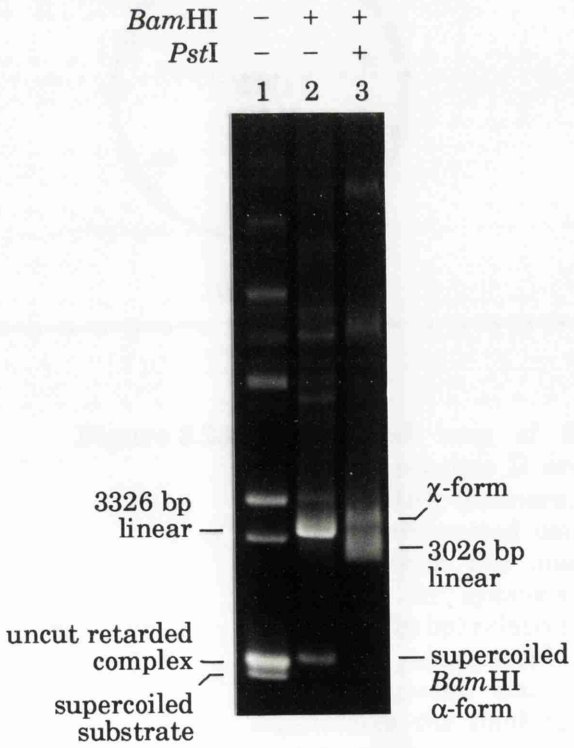

Figure 3.22

Agarose gel electrophoresis of an EGS-crosslinked pMA2350 synapsis reaction: isolation of a synaptic complex formed by a plasmid containing closely-spaced *res* sites.

A high yield of uncut retarded complex (lane 1) was not reflected in the amount of fast-migrating α-form generated following *Bam*HI cleavage within the 219 bp domain (lane 2). The α-form produced by cleavage in the 3107 bp domain of pMA2350 is yet to be seen, possibly due to additional instability introduced when the arms forming the large domain are freed, leaving the other domain as a small loop formed by the synapsed *res* sites.

Buffer C, minus-Mg^{2+}; 1 mM EGS; 0.8% agarose gel.

3.5 Synapsis characteristics of plasmids with partial *res* sites.

The 92 bp *Eco*RI fragment from pAL3151 (Bednarz, 1989), containing subsites II and III of *res* (the accessory subsites) but lacking subsite I, was cloned into the *Eco*RI site of pBR322 to create pMW11. Subsequent cloning of the same fragment, after filling-in the ends, into the *Pvu*II site of pMW11 in both orientations gave pMW13 (direct repeats of the accessory subsites of *res*) and pMW14 (inverted repeats). Figure 3.23 diagrams the accessory subsite fragment and the three plasmids constructed.

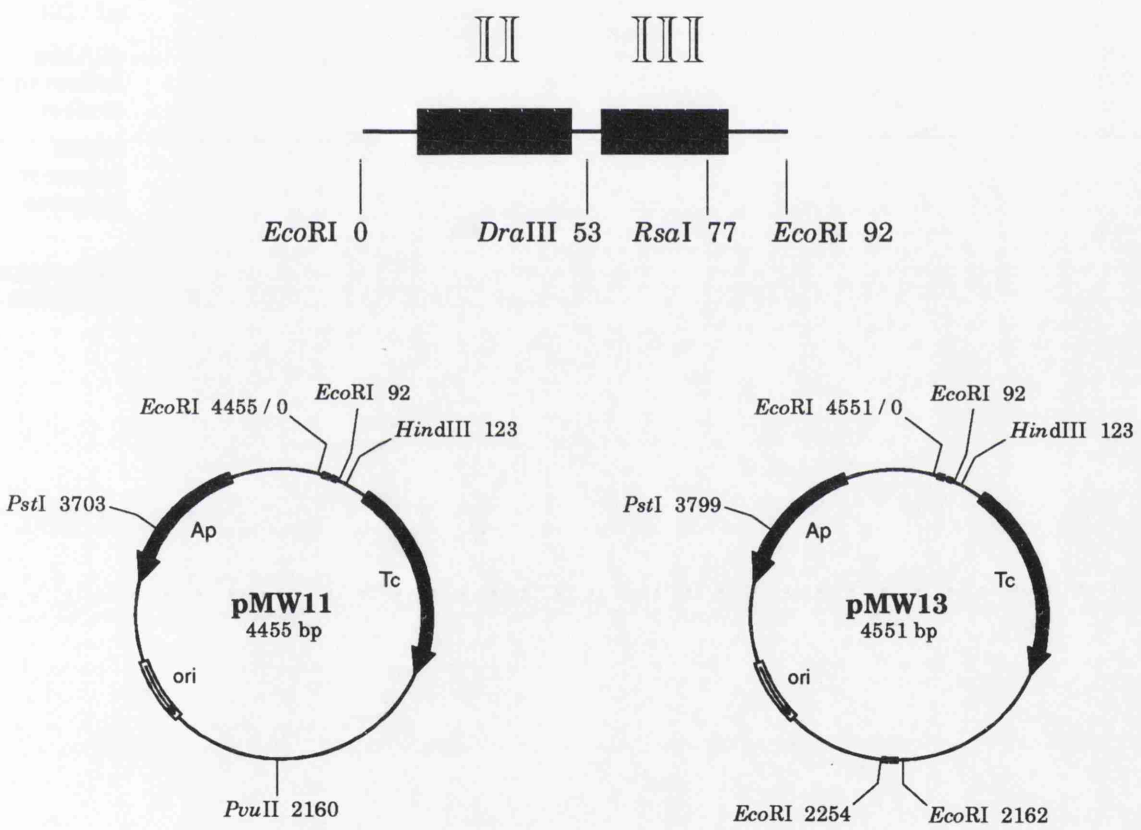

Figure 3.23 A simplified map of the 92 bp *Eco*RI fragment containing subsites II and III of the *res* site, derived from pAL3151 (Bednarz, 1989). Also shown are the plasmids constructed using this *res* accessory subsite fragment, with the unique restriction endonuclease sites used in synapsis assays. Site locations are numbered (in bp) relative to the centre of the *Eco*RI site of pBR322 (designated zero). Inserting the filled-in *Eco*RI fragment into the *Pvu*II site of pMW11 regenerates the flanking *Eco*RI sites. pMW13 (direct repeats of the accessory subsite fragment, as shown) and pMW14 (inverted repeats) differ only in the orientation of the fragment inserted in the *Pvu*II site.

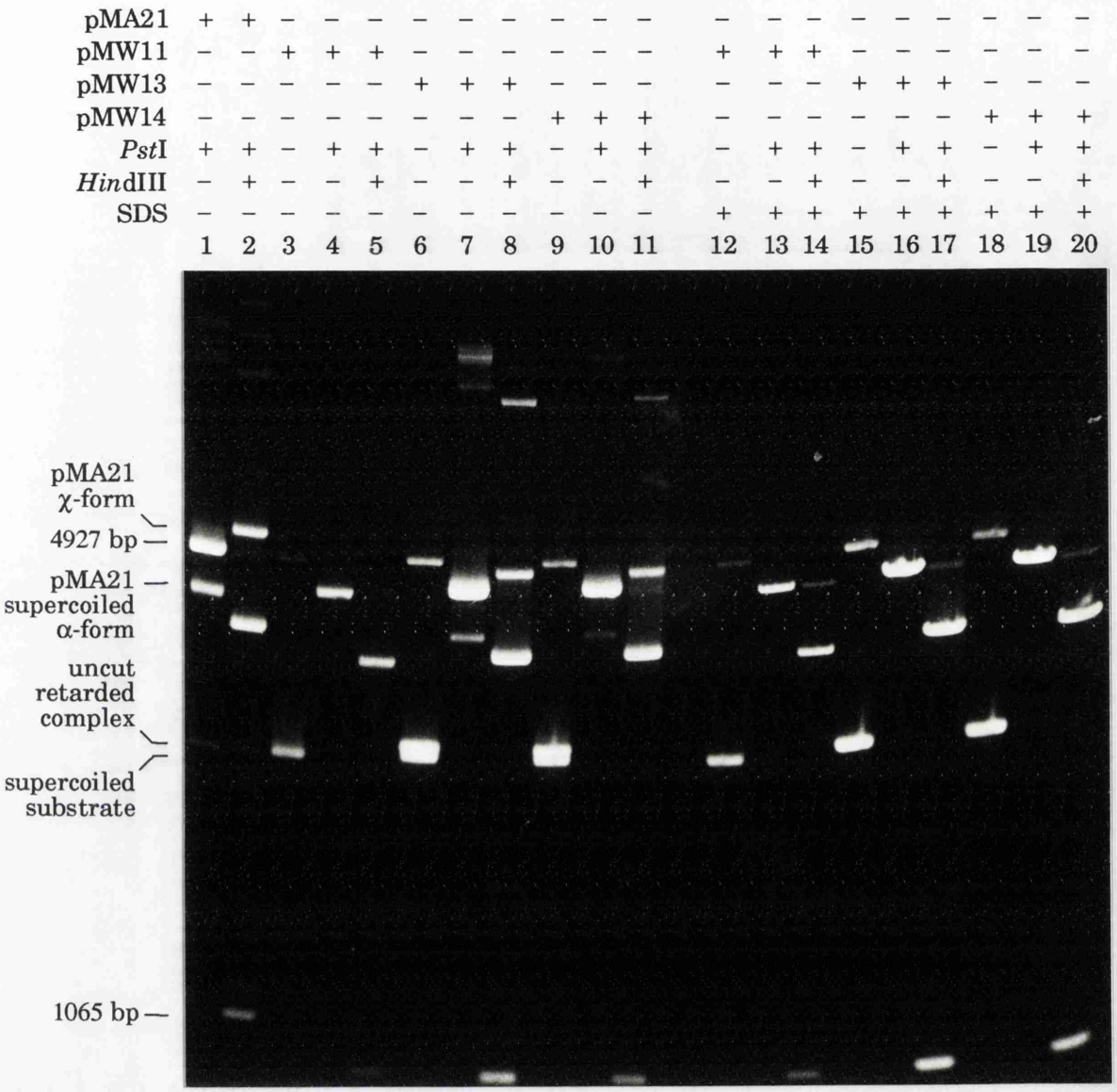

Figure 3.24 Agarose gel electrophoresis of glutaraldehyde-crosslinked synapsis reactions: isolation of a synaptic complex formed by plasmids containing direct and inverted repeats of *res* subsites II and III.

Synapsis reactions with pMW11 (single copy of the *res* accessory subsites), pMW13, and pMW14 (direct and inverted repeats of the accessory subsites, respectively) are compared with pMA21 (direct repeats of the intact *res* site). pMW11 shows no evidence of synapsis, although one might have expected to see some sign of intermolecular synapsis. In contrast, both pMW13 and pMW14 form synaptic complexes indicative of both intra- and intermolecular synapsis. The phenomenon of intermolecular synapsis is discussed further in Section 3.7.

Buffer C, minus-Mg^{2+}; 0.05% glutaraldehyde; 0.8% agarose gel.

Figure 3.24 shows the results of agarose gel electrophoresis of synapsis assays on the three accessory subsite plasmids. Both plasmids containing two copies of subsites II and III showed evidence of intramolecular synapsis, with more of the α- and χ-form produced by pMW13 (direct repeats) than by pMW14 (inverted repeats). This similarity to the behaviour of the analogous intact *res* site plasmids (pMA21 and pMA2631, respectively) suggests an important role for the accessory subsites in synapsis of the intact *res* site, a view consistent with the two-step model for the resolvase-catalysed site-specific recombination reaction (see Chapter 1).

pDB5 contains two copies of the isolated *res* subsite I in direct repeat orientation (Figure 3.25), (Blake, 1993). There was no detectable recombination between either direct or inverted repeats of an isolated subsite I of *res* in a supercoiled substrate (Bednarz *et al.*, 1990). When the standard synapsis assay was performed there was likewise no detectable α- or χ-form of the synaptic complex, at least within the limitations of ethidium bromide staining and ultraviolet visualisation (Figure 3.26a). Again, this finding is consistent with a fundamental role in synapsis for subsites II and III of *res*.

pAL265 contains one copy of the intact *res* site and one copy of the isolated subsite I in direct repeat orientation, while pAL261 has the same complement of intact *res* versus subsite I in inverted repeat orientation (Bednarz *et al.*, 1990), (Figure 3.25). Direct or inverted repeats of an intact *res* site and subsite I in a supercoiled plasmid recombined very slowly (using the 'permissive' reaction conditions that promote recombination of non-supercoiled substrates), with both orientations giving only resolution product (supercoiled two-noded catenane) (Bednarz *et al.*, 1990). Resolution of the inverted site substrate was indicative of incorrect alignment of the crossover sites in the productive synapse at the time of strand-exchange, and the failure of pMA2631 (inverted repeats of the intact *res* site) to recombine suggested that the presence of accessory subsites in both partners blocked this reaction.

Crosslinking of a pAL265 synapsis reaction after the standard 10 minutes incubation at 37°C resulted in the isolation of the χ-form of the synaptic complex formed by interaction of the intact *res* site and subsite I in direct repeat orientation (Figure 3.26b, lane 2). A considerably lower, although still detectable, amount of the χ-form was produced by the

inverted site plasmid, pAL261 (lane 4). However, the same χ-form is produced following restriction endonuclease cleavage of both the intramolecular synaptic complex and the 'A2' intermolecular synaptic complex (see Section 3.7). The presence of a band representing the 'A1' complex shows that these plasmids did form a two-site intermolecular synaptic complex in relatively high yield, albeit the complex formed by interaction of two intact *res* sites. The α-form, uniquely diagnostic of intramolecular synapsis, was present in very low yield. The greater apparent yield of the χ-form may be because the α-form is partitioned between supercoiled and relaxed states, as is generally observed (Section 3.3) – the relaxed α-form would be obscured by the full-length linear plasmid DNA in the 0.8% agarose gel shown in Figure 3.26b. However, the low yield of supercoiled α-form may reflect an instability during the post-crosslinking treatment similar to that seen with pMA2350, the substrate containing closely-spaced *res* sites (Section 3.4); hardly surprising in view of the imbalance of the interacting sites in pAL265 and pAL261. Product topology was consistent with synapsis trapping three negative supercoils, suggesting that non-specific DNA sequences substituted inefficiently for subsites II and III of one *res* site in the modelled interwrapped synapse structure (Bednarz *et al.*, 1990), (see Figure 3.27c).

The crosslinked synaptic complex formed by pAL261 (Figure 3.26b) could contain the two copies of subsite I (one isolated, one part of an intact *res* site) aligned in parallel, in which case it would represent an unproductive complex, since no detectable inversion product is formed (Bednarz *et al.*, 1990). Such a complex may be similar in structure to that proposed for pMA2631, which contains two copies of the intact *res* site in inverted repeat orientation (Figure 3.27b). Alternatively, the crossover sites could be misaligned in an antiparallel orientation in the isolated crosslinked pAL261 synaptic complex, as is required to generate the observed slowly-formed resolution product (Figure 3.27c), (Bednarz *et al.*, 1990). The block on resolution of pMA2631 may be due to the presence of two sets of accessory subsites dictating the formation of an inverted site synaptic structure that is unproductive, possibly because an energetically unfavourable 'tangle' of the substrate DNA results (Boocock *et al.*, 1986), (see Figure 3.27).

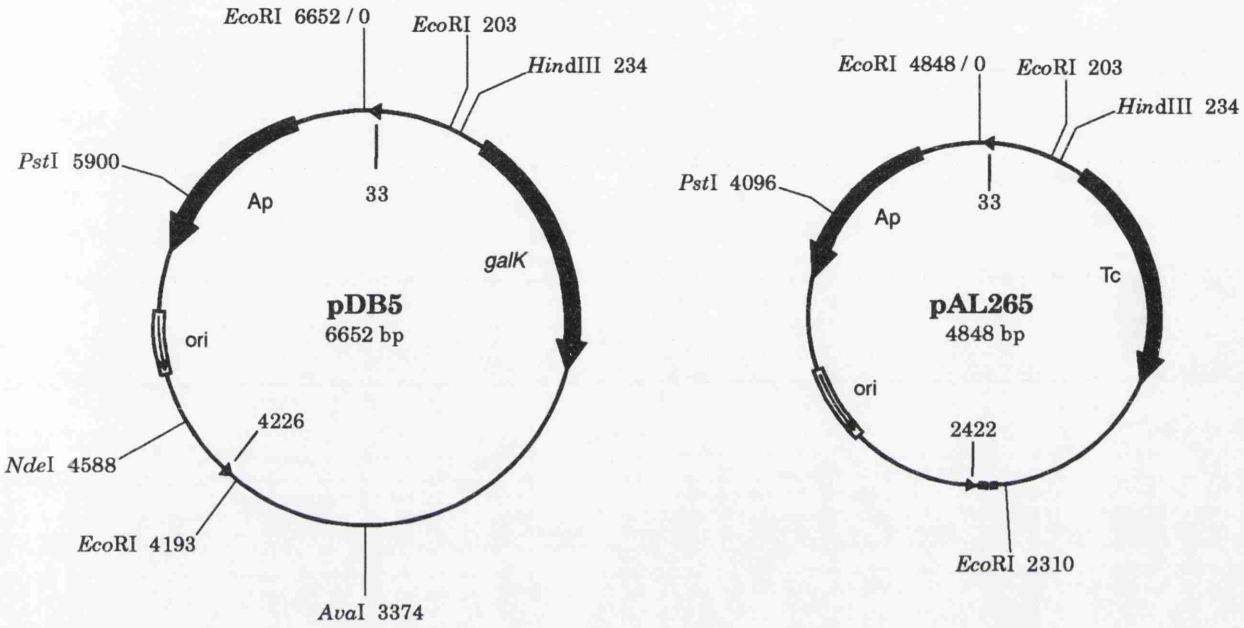

Figure 3.25 Simplified maps of plasmids containing the isolated subsite I of *res*. pDB5 contains two copies of subsite I in direct repeat orientation (Blake, 1993). pAL265 contains one copy of subsite I and one copy of the intact *res* site in direct repeat orientation (Bednarz *et al.*, 1990). pAL261 is identical to pAL265 with one exception, the isolated subsite I is inverted. The locations of the *res* crossover sites are shown, as are the unique restriction endonuclease sites used in synapsis assays. Site locations are numbered (in bp) relative to the *Eco*RI site of pBR322 (designated zero).

The isolated subsite I of *res* is shown as an arrowhead (the convention used to depict the intact *res* site is as described in the legend to Figure 3.1).

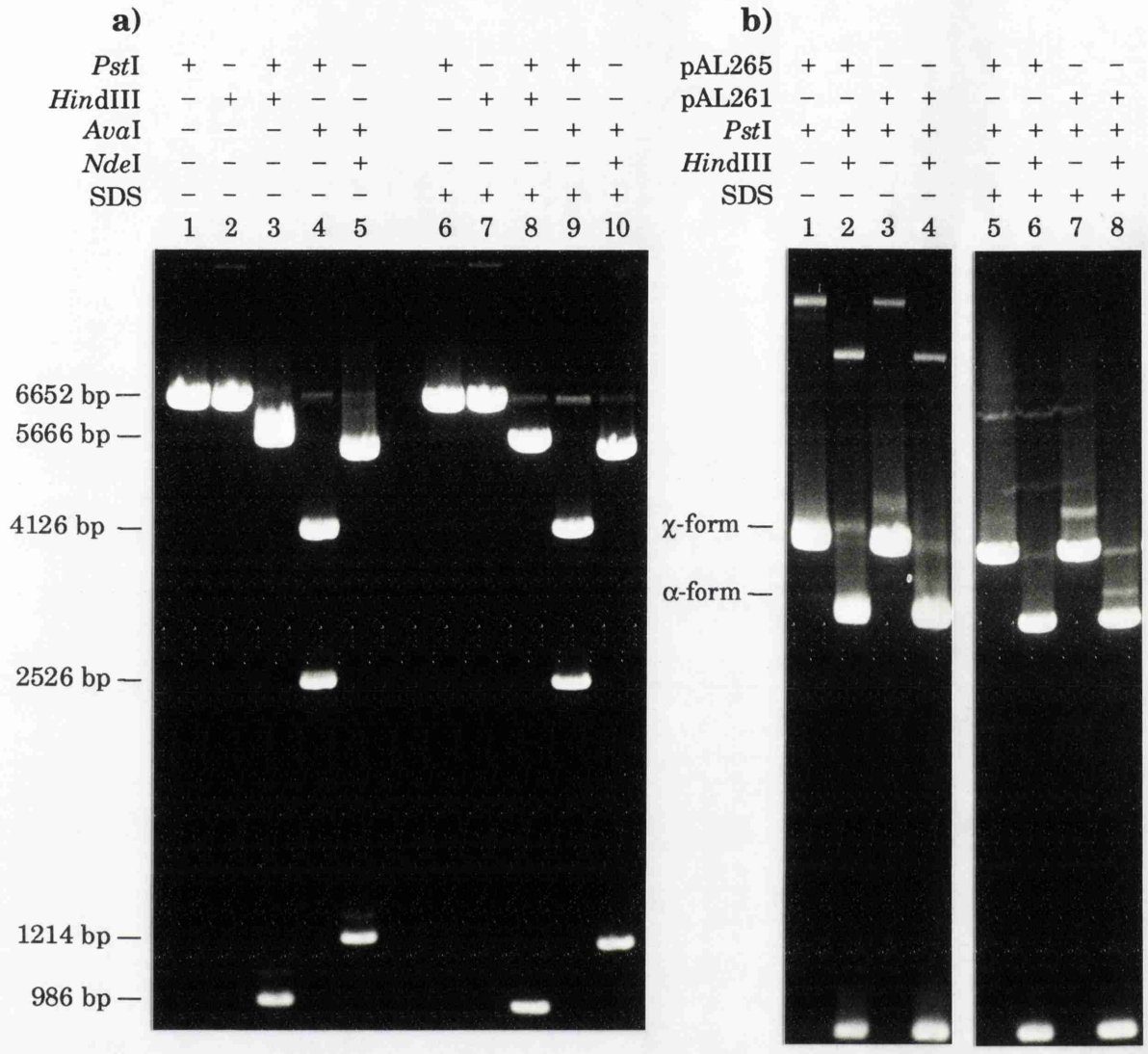

Figure 3.26 Agarose gel electrophoresis of glutaraldehyde-crosslinked synapsis reactions: two copies of an isolated *res* subsite I do not form detectable amounts of synaptic complex, but the isolated subsite I does show evidence of synapsis with a copy of the intact *res* site.

a) Synapsis reactions on pDB5, a plasmid containing two copies of an isolated *res* subsite I in direct repeat orientation, were treated with various restriction endonucleases. *Pst*I or *Hin*dIII alone should produce the α-form complex from any synapsed plasmid, while the double restrictions should result in χ-form. There is no evidence of synapsis, although a crosslinked single *res* site complex is clearly visible (see Section 3.10).
Buffer C, minus-Mg^{2+}; 0.05 % glutaraldehyde; 1.2 % agarose gel.

b) Both pAL265 and pAL261 (one isolated subsite I and one intact *res* site in direct or inverted repeat orientation, respectively) form detectable amounts of intramolecular synaptic complex. Once again, the plasmid containing direct repeats (pAL265) produces significantly more crosslinked synaptic complex than does the plasmid containing inverted repeats (pAL261). Note the single discrete band representing intermolecular synaptic complex, formed by both plasmids. This represents the 'A1' complex shown in Figure 3.32; see Section 3.7 for further discussion.
Buffer C, minus-Mg^{2+}; 0.05% glutaraldehyde; 0.8% agarose gel.

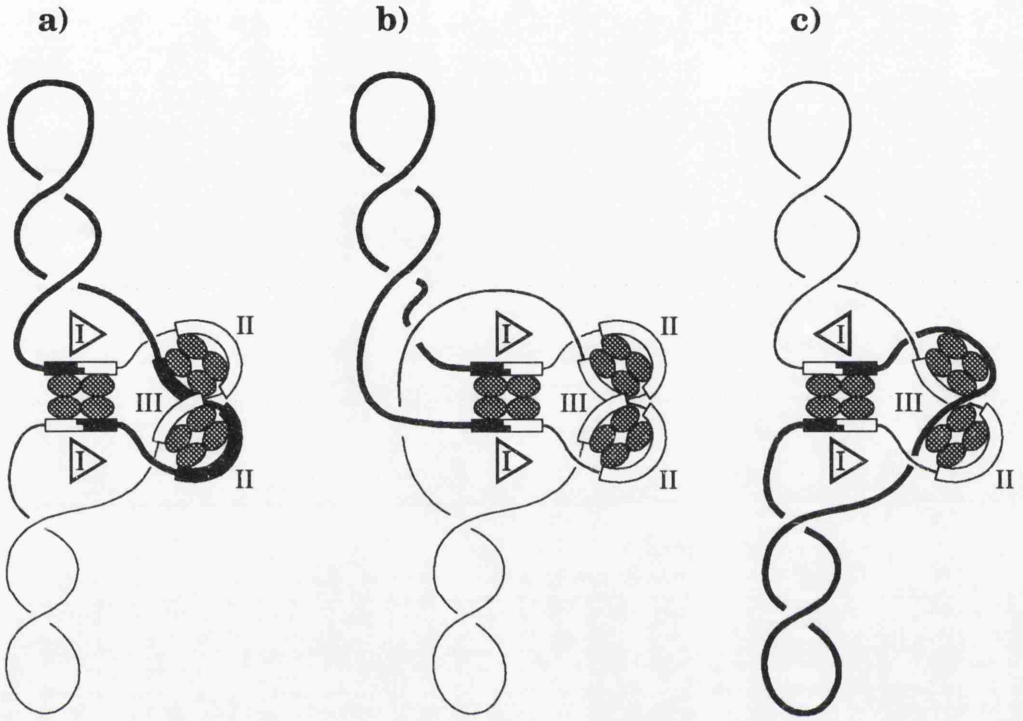

Figure 3.27 Models proposed for the structure of the synaptic complex (see Chapter 1). The relative orientation of the crossover sites is indicated by the triangles.

a) A synaptic complex formed during resolution of a plasmid containing two copies of the intact *res* site in direct repeat orientation, such as pMA21.

b) An unproductive synaptic complex that may be formed by a plasmid containing two copies of the intact *res* site in inverted repeat orientation, such as pMA2631. Strand exchange would result in inversion.

c) A synaptic complex formed during resolution of a plasmid containing one copy of the intact *res* site and one copy of the isolated subsite I in inverted repeat orientation, such as pAL261. The two copies of subsite I are aligned in the antiparallel orientation, with non-specific DNA sequences substituting for subsites II and III of one *res* site.

Figure adapted from Stark *et al.* (1989a) and Bednarz *et al.* (1990).

3.6 Synapsis of non-supercoiled plasmid substrate.

Intramolecular recombination of nicked or linearised plasmid containing two copies of the *res* site in direct repeat orientation has been observed, albeit at a lower frequency than is seen with the same substrate in the supercoiled state (Boocock *et al.*, 1986). Some intermolecular recombination of linearised substrate was also detected (Boocock *et al.*, 1986). However, in an earlier study of Tn*3* resolvase-mediated synapsis, it was reported that no crosslinked synaptic complex was isolated when the substrate plasmid was nicked or linearised (Benjamin and Cozzarelli, 1988). It was concluded that the synaptic complex only formed if the substrate DNA was supercoiled.

Supercoiled pMA21 (Figure 3.16) was treated with DNase I in the presence of ethidium bromide in order to generate singly-nicked plasmid DNA (see Section 2.7f for details). Figure 3.28 shows the result of agarose gel electrophoresis of a standard glutaraldehyde-crosslinked synapsis reaction using the nicked plasmid as substrate (see Section 2.15c). When an aliquot from this reaction was digested with the appropriate restriction endonucleases, a discrete SDS-labile band identical in gel mobility to the χ-form isolated from synapsis reactions containing supercoiled substrate was obtained. The yield of the χ-form obtained from nicked substrate was generally about 20% of that obtained from a reaction containing the same amount of input DNA in the supercoiled state. The presence of more than one protein-DNA complex band when the reaction was undigested or cut in one domain to produce the relaxed α-form of the synaptic complex probably reflects the existence of topoisomers due to supercoiling trapped in the intact (i.e. un-nicked) domain upon synapsis.

Full-length linear pMA21 DNA was created by cleavage with *Pst*I (see Figure 3.16). Use of this DNA as substrate in the glutaraldehyde-crosslinked standard synapsis assay[4] produced evidence of both intra- and intermolecular synapsis (Figure 3.29). The absence of a band that could be attributed to intermolecular synapsis of the two copies of the *res* site nearest an end of the linearised substrate DNA (922 bp separating

[4] In this experiment, the initial incubation of substrate DNA with resolvase at 37°C was for 60 minutes rather than the standard 10 minutes, as this increase in incubation time was found to slightly improve the yield of isolated synaptic complex from linearised pMA21 (data not shown).

the crossover site and the end of the DNA molecule) may reflect a bias against this interaction (shown as complex 'A3' in Figure 3.29). The resulting small χ-form may be poorly resolved during electrophoresis, although alternative restrictions that produce a larger χ-form failed to demonstrate a detectable amount of the 'A3' intermolecular synaptic complex (see Figure 3.33). However, an 'end effect' was not apparent in the experiment described next where the single *res* site is almost the same distance from an end of the DNA molecule. Furthermore, recombination between a linear DNA molecule containing a single *res* site and a supercoiled molecule also containing a single *res* site was unaffected when the distance between the *res* site and the end of the linear DNA molecule was varied (data not shown).

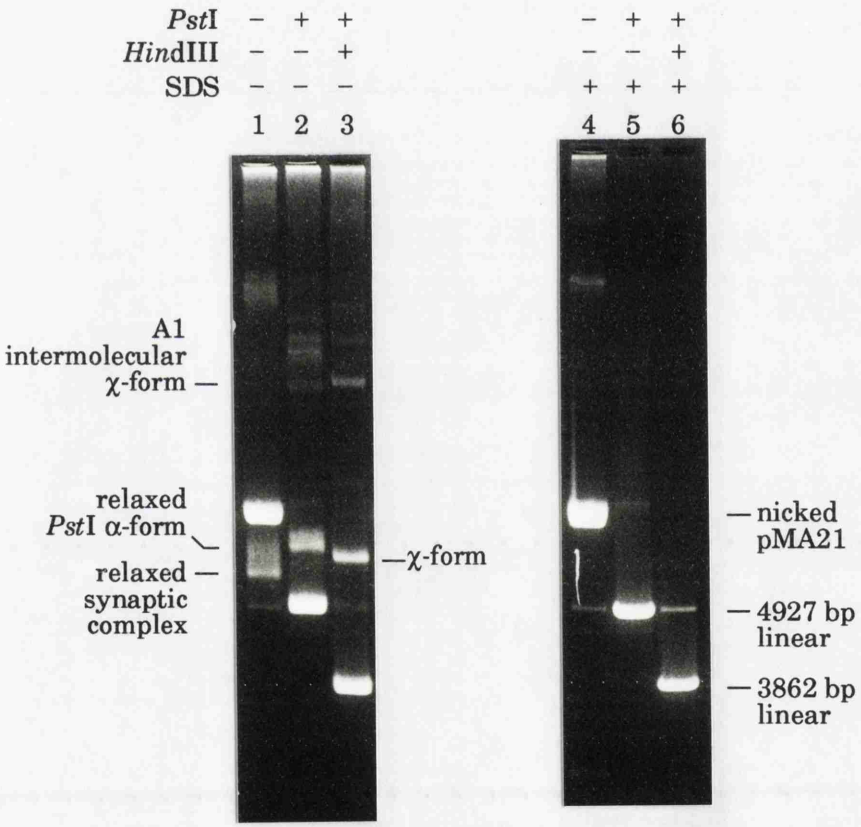

Figure 3.28 Agarose gel electrophoresis of a glutaraldehyde-crosslinked synapsis reaction: isolation of a synaptic complex formed by nicked pMA21.

pMA21 DNA treated with DNase I in the presence of ethidium bromide was included in the standard synapsis assay. Undigested, a discrete band migrating between the positions of nicked and full-length linear substrate DNA in the 1.2% agarose gel, with diffuse band(s) migrating immediately behind, represents the relaxed synaptic complex (lane 1). *Pst*I cleavage produces the relaxed α-form (lane 2). *Pst*I + *Hin*dIII digestion produces the characteristic discrete χ-form band (lane 3). All these bands attributed to protein-DNA complexes fail to appear when SDS treatment precedes electrophoresis (lanes 4-6).

Buffer C, minus-Mg^{2+}; 0.05% glutaraldehyde; 1.2% agarose gel.

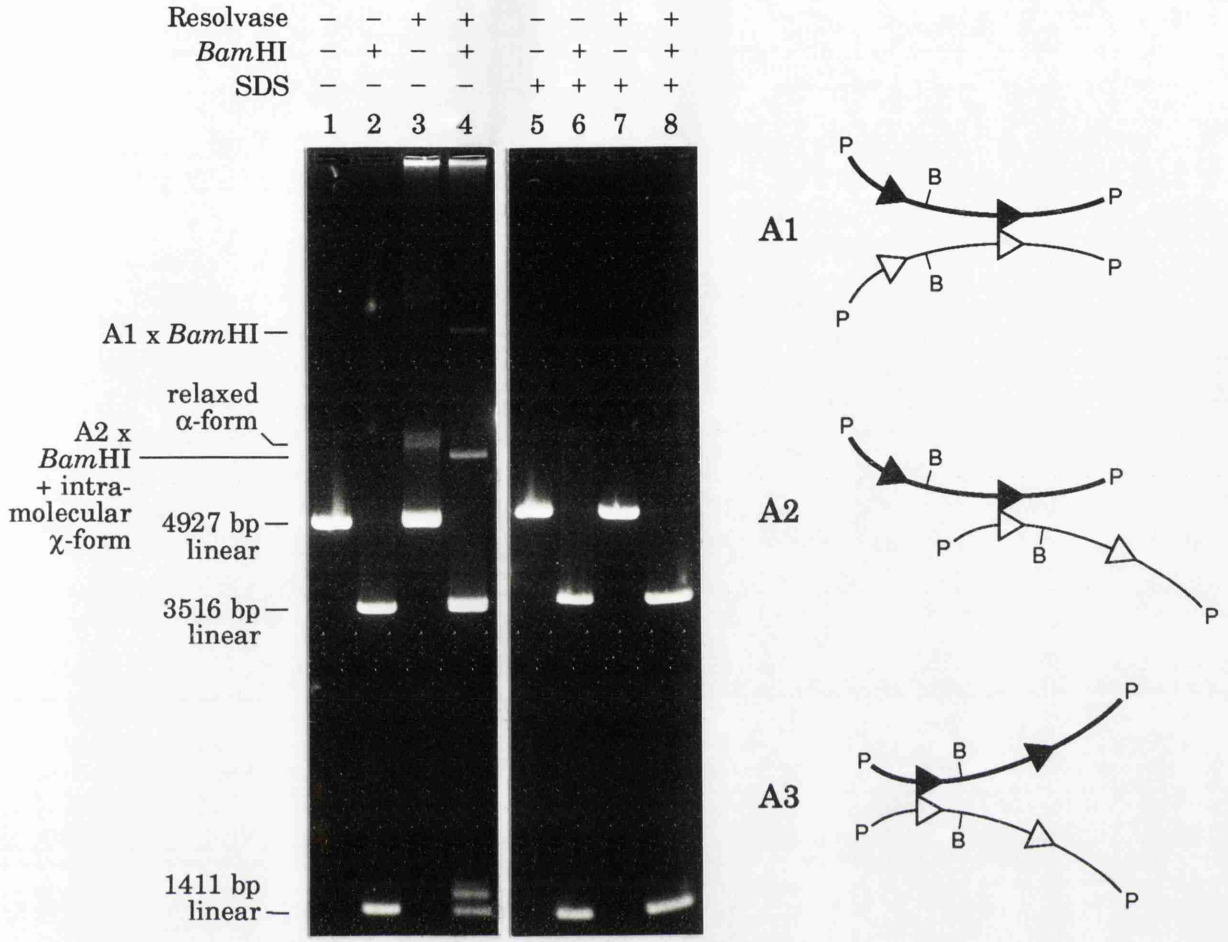

Figure 3.29 Agarose gel electrophoresis of a glutaraldehyde-crosslinked synapsis reaction: isolation of synaptic complex formed by linearised pMA21. *Pst*I-cleaved full-length linear pMA21 DNA (4927 bp) was the substrate in a synapsis assay. When undigested, diffuse band(s) migrate to the position characteristic for relaxed α-form of the synaptic complex (lane 3). This species is resolvase-dependent and SDS-labile, and is therefore proposed to represent intramolecular synapsis of the linearised substrate DNA, with the failure to appear as a single band attributed to the presence of topoisomers as discussed in the text. Of the predicted χ-forms resulting from intermolecular synapsis of two *res* sites in the various combinations (diagrammed above (P = *Pst*I, B = *Bam*HI); the identification A1, A2, A3 is used in the discussion of intermolecular synapsis in Section 3.7), some or all of these may be represented by the slow-migrating diffuse band(s).

*Bam*HI digestion produces a χ-form complex with characteristic gel mobility – this can arise from the 'A2' intermolecular synaptic complex (as shown above), as well as from the intramolecular α-form. The predicted slower-migrating *Bam*HI-cleaved χ-form ('A1' complex) is also present, but the fastest-migrating of these χ-forms, arising from intermolecular synapsis of two copies of the *res* site nearest to an end of the linear substrate DNA (the 'A3' complex) is not visible.

Note the presence of a protein-DNA complex band representing resolvase bound to the 1411 bp restriction fragment of pMA21 containing a single *res* site (see Section 3.10).

Buffer C, minus-Mg^{2+}; 60 minutes incubation for synapsis; 0.05% glutaraldehyde; 1.2% agarose gel.

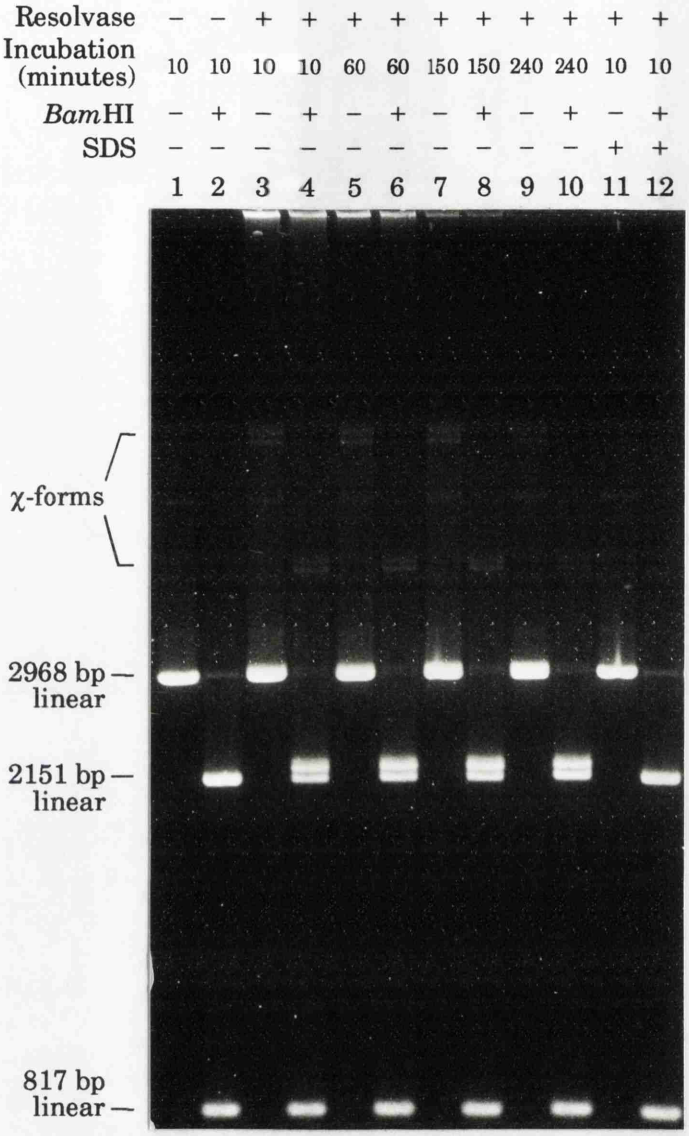

Figure 3.30 Agarose gel electrophoresis of a glutaraldehyde-crosslinked synapsis reaction: isolation of synaptic complex formed by linearised pMA1441 (single *res* site).
*Xmn*I-cleaved full-length linear pMA1441 DNA (2968 bp) was the substrate in a synapsis assay. The incubation for synapsis was for 10, 60, 150, or 240 minutes, followed by crosslinking. A small amount of the predicted intermolecular χ-form is seen in the undigested samples, and (with a predictable change in gel mobility) following *Bam*HI cleavage. The yield of synaptic complex has declined at 240 minutes. The presence of two discrete bands, representing closely-migrating protein-DNA complexes, may indicate that intermolecular synapsis has occurred with the crossover sites paired in both the parallel and antiparallel orientations (see the text for details). The restriction fragment containing the single *res* site (2151 bp in size) is readily identified by the presence of a retarded resolvase-bound complex.

Buffer C, minus-Mg^{2+}; Incubation for synapsis as detailed; 0.05% glutaraldehyde; 1.2% agarose gel.

In contrast to synapsis reactions containing supercoiled pMA21 DNA as substrate, the yield of two-plasmid complexes arising from intermolecular synapsis of three or four *res* sites was very low when linearised pMA21 was the substrate DNA. This observation is discussed further, and made use of for identification purposes, in Section 3.7.

pMA1441, a 2968 bp pUC18 derivative, contains a single copy of the intact *res* site. Full-length linear pMA1441 DNA was created by cleavage with *Xmn*I. Synapsis assays using this DNA as substrate produced a small amount of the predicted intermolecular χ-form (Figure 3.30). The presence of two discrete protein-DNA complex bands may indicate that intermolecular synapsis has occurred in two different arrangements. The 'correct' parallel alignment of crossover sites was strongly favoured in intermolecular recombination reactions between linear substrates containing a single *res* site, although there was some evidence that a small amount of product (less than 10% of the total) arising from 'incorrect' antiparallel alignment was formed (Bednarz *et al.*, 1990).

3.7 Intermolecular synapsis.

Intermolecular recombination catalysed by Tn*3* resolvase has not been observed using supercoiled substrates, but was readily detected when one or both of the *res* sites were located on a linear DNA molecules (Boocock *et al.*, 1986). A much lower frequency of intermolecular recombination occurred when the DNA substrate was in the form of a nicked circle containing a single *res* site (Boocock *et al.*, 1987). The most efficient example of resolvase-catalysed intermolecular recombination so far detected was between the *res* sites on the fully nicked form of the (–2) catenane product of the standard resolution reaction. Typically, more than 80% of the catenane was converted to circular product within 1-2 hours (Stark *et al.*, 1989b). Synapsis of the (–2) catenane is investigated in Section 3.8.

An earlier investigation reported evidence of intermolecular synapsis mediated by resolvase only when the supercoiled substrate plasmid contained one or three *res* sites (Benjamin and Cozzarelli, 1988). It was concluded that intermolecular synapsis occurred only when a *res* site was unable to pair with another site in the same molecule, either because there were no other sites or because the other sites were already part of

an intramolecular synaptic complex. However, it was not stated whether there was any evidence of intramolecular synapsis of two *res* sites in the three site plasmids paired in the observed intermolecular synaptic complex.

The results of agarose gel electrophoresis of crosslinked synapsis reactions displayed in the previous Sections have shown that this is not an interpretation that can be drawn from my experiments. There was evidence of resolvase-mediated intermolecular synapsis with virtually all of the DNA substrates used.

Figure 3.31 shows the results of agarose gel electrophoresis of a supercoiled pMA21 synapsis reaction, with the bands representing intermolecular synapsis marked. It should be pointed out that the amount of the larger intermolecular synaptic complexes seen in Figure 3.31a was greater than that typically seen (and was used for demonstration purposes). However, the yield of the putative two-plasmid synaptic complexes was of the order generally observed in the crosslinked synapsis assay. When supercoiled, the two-plasmid intermolecular synaptic complexes migrated as a single discrete band behind the nicked substrate DNA. This changed following treatment with a restriction endonuclease cutting at a unique site in pMA21, whereupon a group of bands representing the different forms of the two-plasmid intermolecular synaptic interaction appeared. These cleaved forms exhibited a considerably reduced rate of migration in the agarose gel due to loss of supercoiling, and their derivation from the single undigested complex band was confirmed by two-dimensional gel electrophoresis (see Figure 3.12).

Concentrating on the interaction of two plasmid molecules, Figure 3.32 illustrates the different forms of intermolecular synaptic complex predicted to arise from pMA21, and the effect of restriction endonuclease cleavage. Since the two-site complexes were the predominant intermolecular synaptic complexes detected in synapsis assays on linearised pMA21 (see Section 3.6), these provided markers for identification of the same complexes in the supercoiled pMA21 reaction (Figure 3.33).

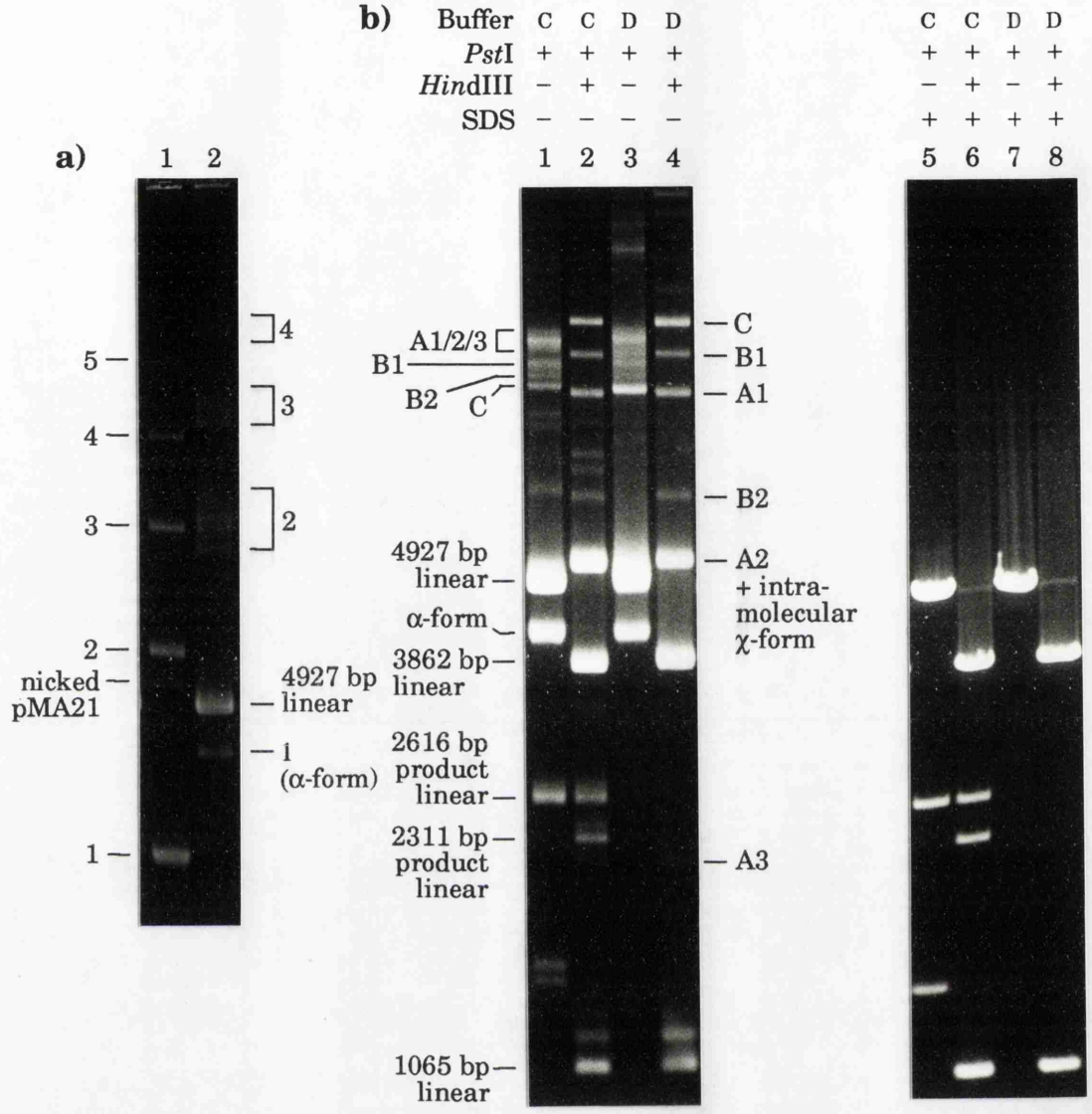

Figure 3.31 Agarose gel electrophoresis of a crosslinked pMA21 synapsis reaction: isolation of intermolecular synaptic complexes.

a) Undigested, a ladder of intermolecular synaptic complexes is present (lane 1). This is believed to represent a simple multimeric series of the supercoiled plasmid. The proposed number of interacting plasmids in each complex is indicated, starting with 1 for the 'intramolecular' uncut retarded complex band. Following *Pst*I cleavage (lane 2), each discrete uncut band breaks down to a group of bands (again marked with the proposed number of interacting plasmids) representing species with a considerably reduced gel mobility, as expected when supercoiling is lost.
Buffer C, minus-Mg^{2+}; 1 mM EGS; 0.8% agarose gel.

b) The effect of additional *Hin*dIII digestion on the group of bands resulting from *Pst*I cleavage of the two-plasmid intermolecular synaptic complexes. The effect of synapsis at pH 7.0 as well as the standard pH 8.0 is shown. All protein-DNA complex bands are absent following treatment with SDS (lanes 5-8). See text and Figure 3.32 for details of the identification of intermolecular synaptic complexes.
Note also the effect of the reduction in the pH of the reaction on the amount of product formed and on the amount of the crosslinked complex formed by resolvase bound to a single *res* site on the 1065 bp pMA21 restriction fragment (see Section 3.10).
Buffer C (pH 8.0) or buffer D (pH 7.0), both minus-Mg^{2+}; 0.05% glutaraldehyde; 0.8% agarose gel.

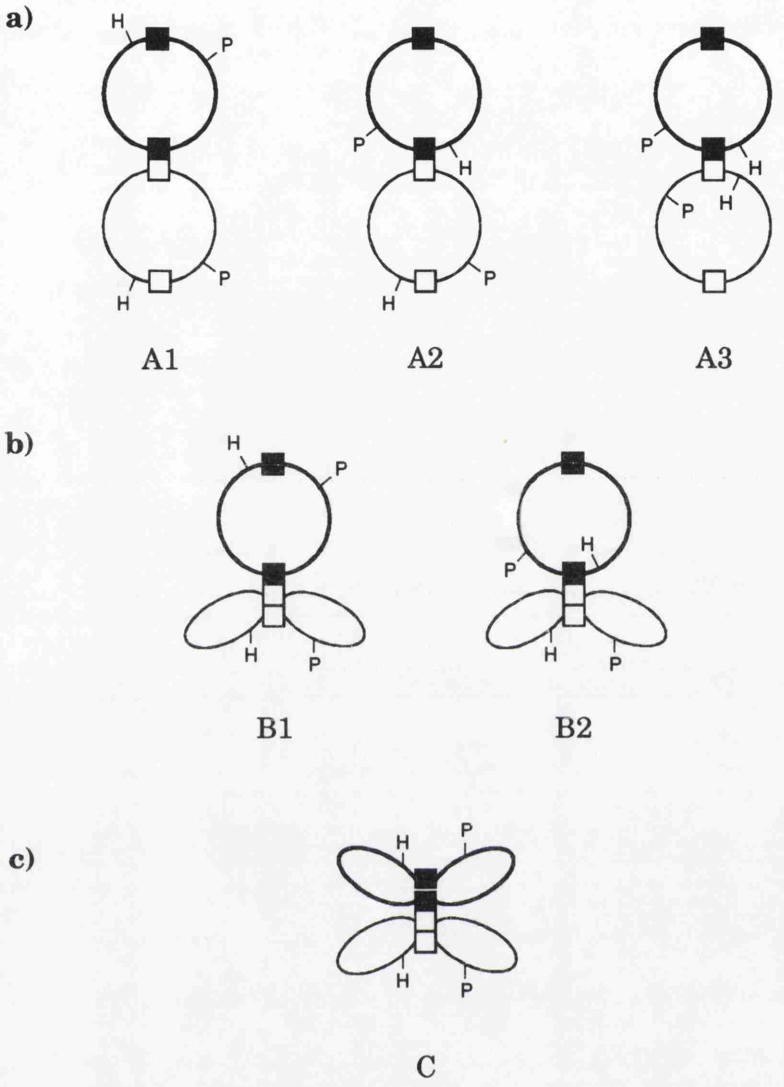

Figure 3.32

Proposed intermolecular synapsis interactions involving two pMA21 molecules. Although supercoiling is omitted for simplicity, the DNA is in the supercoiled state in these synaptic complexes. The *res* sites are represented by squares, black for one plasmid, white for the other plasmid. Since all of these synaptic complexes contain the same amount of DNA, restriction endonuclease cleavage is required to differentiate between them in terms of mobility in an agarose gel. The restriction endonuclease sites utilised are shown (P = *Pst*I, H = *Hin*dIII).

a) Two sites synapsed. There are three possible synaptic complexes (identified as A1, A2, and A3). Following cleavage by the appropriate restriction endonuclease(s), these complexes are identical in gel mobility to synaptic complexes formed by linearised pMA21 (Figure 3.33; the synaptic complexes formed by linearised pMA21 are diagrammed in Figure 3.29, where they are identified similarly). Following digestion with *Pst*I + *Hin*dIII, there is a loss of 2130 bp of DNA from complex A1, 4927 bp from complex A2 (which is now, superficially at least, identical to the intramolecular χ-form), and 7724 bp from complex A3.

b) Three sites synapsed. There are two possible synaptic complexes (B1 and B2). In contrast to the two-site complexes, which lose all supercoiling when cut at a unique restriction site, these three-site intermolecular complexes will maintain about 25% of the total DNA in the supercoiled state (in one topologically closed domain). After digestion with *Pst*I alone, complex B2 is predicted to migrate slightly faster in an agarose gel than does complex B1 (see Figure 3.31). This is because the free DNA arms resulting from *Pst*I cleavage of the plasmid molecule containing an unsynapsed *res* site will be more disparate in length in complex B2 than in complex B1 (see

Section 3.3). Following digestion with *Pst*I + *Hin*dIII, there is a loss of 1065 bp of DNA from complex B1 and 3862 bp from complex B2.

c) Four sites synapsed. The single possible synaptic complex (superficially, since the detailed interaction of more than two *res* sites is a mystery, so there may well be more than a single form of the complex) maintains about 50% of the total DNA in the supercoiled state when cut at a unique restriction site. There is no loss of DNA upon digestion with *Pst*I + *Hin*dIII.

The various two-plasmid intermolecular synaptic complexes can also be distinguished by observing the effect on gel mobility of substituting alternative restriction endonucleases for *Hin*dIII in the double digest (see Figure 3.16). Using either *Bam*HI, *Sal*I, or *Ava*I, respectively, with *Pst*I results in successively more DNA deleted from the A1 and B1 complexes, and successively less DNA deleted from the A3 and B2 complexes. In contrast, these changes in the restriction endonuclease used in combination with *Pst*I do not alter the total amount of DNA remaining in the A2 or C complexes, although the relative lengths of the DNA arms will alter. The effect on gel mobility of the intermolecular complexes is shown in Figure 3.33. See the text for further details.

With the band representing the 'A1' two-site intermolecular synaptic complex in the gel shown in Figure 3.31b established, the identity of bands representing the other intermolecular complexes were considered in terms of the predicted relative gel mobility of these complexes (see Figure 3.32). Thus, the four-site complex ('C') will be the fastest migrating intermolecular complex following *Pst*I digestion (because it will retain the greatest proportion of total DNA in the supercoiled state), but it will be the slowest of the two-plasmid complexes after digestion with *Pst*I and *Hin*dIII (because it is the only complex that does not lose DNA). Similar consideration of the effect on gel mobility of the amount of supercoiling retained after *Pst*I cleavage, and the amount of DNA lost after the double digest enabled the other intermolecular synaptic complex bands to be identified (Figure 3.31b).

The effect of a change of the restriction endonuclease used with *Pst*I in the double digest on the gel mobility of intermolecular synaptic complexes was consistent with the assignment of bands to the various complexes (Figure 3.33; see also the legend to Figure 3.32). Thus, there was very little change in the mobility of the four-site complex ('C'), as expected if the only effect was a redistribution of arm length in the intermolecular χ-form. The rate of migration of the 'A1' and 'B1' complexes increased stepwise after cleavage with *Hin*dIII, *Bam*HI, *Sal*I, and *Ava*I, respectively – consistent with a greater loss of DNA with each subsequent cleavage. In contrast, the rate of migration of the 'B2' complex decreased as the same

changes in cleavage site resulted in a gradual reduction in the amount of DNA lost from the complex.

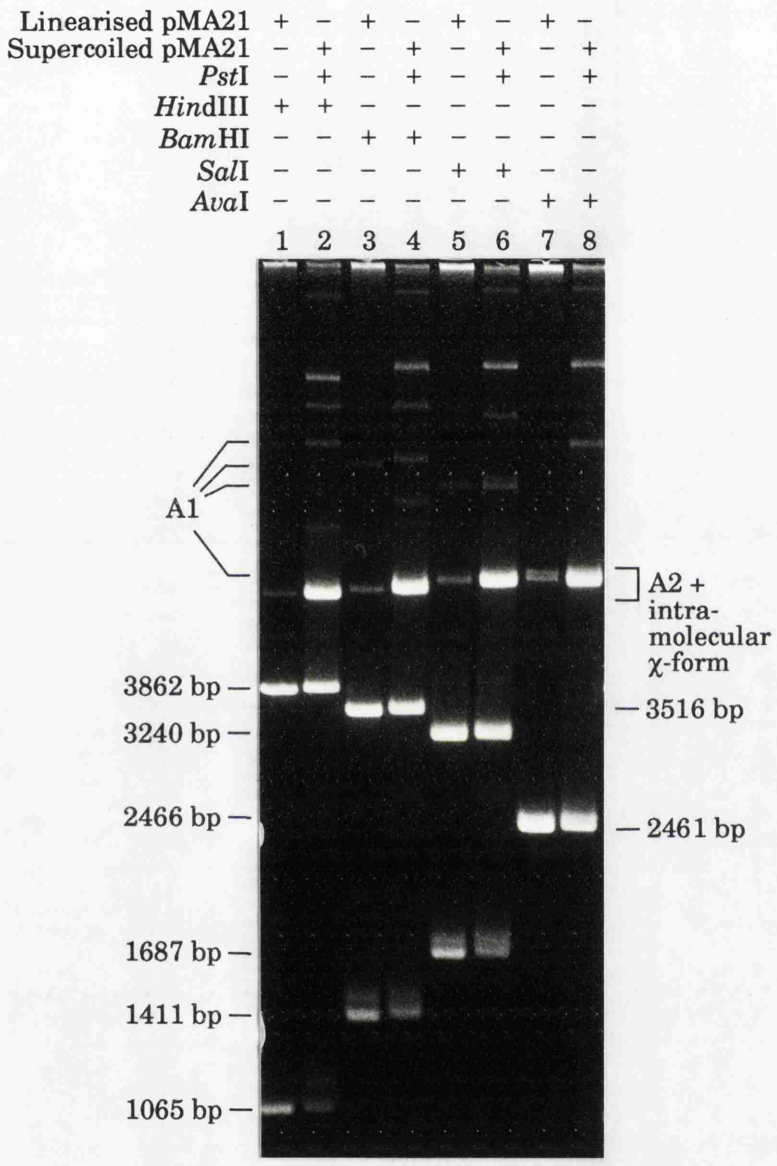

Figure 3.33 Agarose gel electrophoresis of glutaraldehyde-crosslinked synapsis reactions: use of two-site intermolecular synaptic complexes formed by synapsis of linearised pMA21 to identify similar complexes in the reaction of supercoiled pMA21.

*Pst*I-cleaved full-length linear pMA21 DNA was the substrate in a synapsis assay (see Section 3.6). Subsequent treatment with the appropriate restriction endonuclease (see Figure 3.16 for a restriction map) should produce intermolecular synaptic complex bands identical in gel mobility to similar complexes formed by supercoiled pMA21 after cleavage by *Pst*I and the same second restriction endonuclease. This is the case, and the complexes are identified using the code introduced in Figures 3.29 and 3.32. The effect of changing the second cleavage site (with *Pst*I digestion maintained) on the gel mobility of intramolecular complexes formed from supercoiled pMA21 is discussed in the text.

Buffer C, minus-Mg^{2+}; 60 minutes synapsis incubation for the linear pMA21 reactions, 10 minutes for the supercoiled pMA21 reactions; 0.05% glutaraldehyde; 1.2% agarose gel.

Electron microscopy of these crosslinked intermolecular synaptic complexes would provide additional confirmation of the number of *res* sites interacting. In addition, a determination of the multimeric state of the crosslinked resolvase may shed light on the interactions that operate when more than two *res* sites come together.

Comparing the various crosslinked two-plasmid intermolecular synaptic complexes obtained from a reaction containing supercoiled pMA21 (Figure 3.31) with those arising from intermolecular synapsis of the other DNA substrates assayed is informative. When the substrate was nicked pMA21, although the same bands were all present, the relative yield of the four-site complex 'C' was considerably reduced (see Figure 3.28). Supercoiled pMA2631 (two intact *res* sites in inverted repeat orientation) gave only two-site intermolecular synaptic complex in a yield comparable to that obtained from supercoiled pMA21, while the three-site complex bands were very faint and four-site complex was absent (Figure 3.20). Supercoiled plasmids containing direct and inverted repeats of an intact *res* site and an isolated subsite I (pAL265 and pAL261, respectively) produced only two-site intermolecular synaptic complexes, with the 'A1' complex (representing synapsis of the intact *res* sites of these plasmids) present in a similar yield to that obtained from pMA21 and pMA2631 (Figure 3.26). Plasmids containing two copies of the accessory subsites of *res* in direct and inverted repeat orientation (pMW13 and pMW14, respectively) produced two- and three-site intermolecular complexes only, with pMW13 giving a relatively large amount of the two-site complexes (Figure 3.24). Surprisingly, plasmids containing a single intact *res* site at best produced a very poor yield of intermolecular synaptic complex (Figure 3.34), and such complex was often absent (data not shown).

Several observations suggested that the intermolecular synaptic complexes isolated represented a genuine interaction, rather than an example of excessive crosslinking. Firstly, the finding that the lowest efficiency of isolation of these complexes occurred when the DNA substrate was a supercoiled plasmid containing a single *res* site. Secondly, the fact that intermolecular synaptic complexes were isolated with all the crosslinking reagents used, including EDC (see Figure 3.8). Thirdly, the failure of an increase in the concentration of crosslinking reagent to significantly increase the yield of these complexes (data not shown). Thus, in common with the bias against recombination of *res* sites in inverted repeat orientation, the block preventing intermolecular

recombination may also operate at a later point than an initial synaptic interaction that is sufficiently stable to be crosslinked.

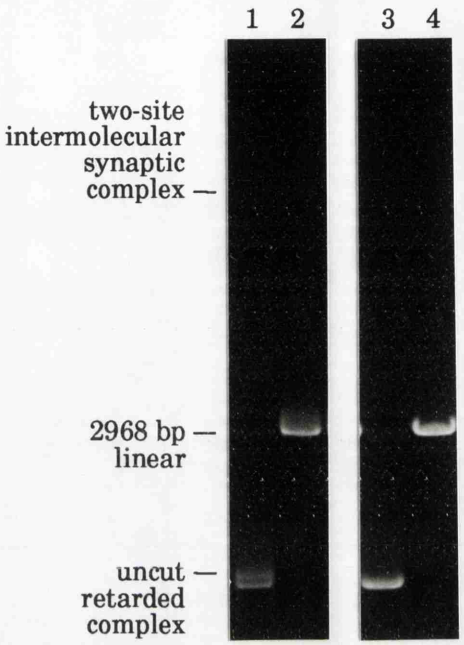

Figure 3.34 Agarose gel electrophoresis of a glutaraldehyde-crosslinked synapsis reaction: a supercoiled plasmid containing a single copy of the intact *res* site produces intermolecular synaptic complex in low yield.
pMA1441 (2968 bp) has a single *res* site inserted in the polylinker of pUC18. An undigested synapsis reaction (lane 1) reveals a discrete uncut retarded complex band; however, the supercoiled intermolecular synaptic complex is barely detectable. Cleavage at the unique *Bam*HI site (lane 2) produces the predicted reduction in the rate of migration of the two-site intermolecular synaptic complex. Lanes 3 and 4 show SDS treatments of the reactions loaded in lanes 1 and 2, respectively.

Buffer C, minus-Mg^{2+}; 1 mM EGS; 0.8% agarose gel.

The two-plasmid, four-site intermolecular synaptic complex, in which two intramolecular synaptic complexes are paired, is seen in by far the highest yield when the *res* sites are in direct repeat orientation on a supercoiled DNA molecule. However, it is not formed by the plasmids containing two copies of the *res* accessory subsites, despite their forming a significant amount of intramolecular synaptic complex. One can speculate as to whether the four-site intermolecular complex plays any part in the recombination reaction, but more information on the structure is required before anything can be concluded. The yield of the intermolecular synaptic complexes when assayed at various time-points during a resolvase reaction is investigated in Section 3.9.

3.8 Isolation and characterisation of a product synaptic complex.

When a standard pMA21 synapsis assay was carried out in the presence of 10 mM $MgCl_2$, there was an increase in the amount of resolution product formed during the 10 minutes incubation at 37°C prior to addition of the crosslinking reagent. In addition, following treatment with *Pst*I and *Bam*HI to generate the χ-form of the pMA21 synaptic complex, a band representing a novel protein-DNA complex appeared (Figure 3.35a). This cleaved protein-DNA complex migrated at a slower rate in a 1.2% agarose gel than did the identically treated substrate synaptic complex characterised in earlier Sections, resulting in two close-migrating but discrete bands. Excision of these bands, followed by in-gel treatment with SDS and electrophoresis in a second dimension (see Section 2.9g), revealed that, while the previously characterised synaptic complex (the predominant form in the absence of Mg^{2+}) dissociated to give the appropriate substrate restriction fragments, the slower-migrating complex broke down to give linearised product circles (Figure 3.35b). These complexes were homogeneous to the limits of ethidium staining and ultraviolet visualisation, and this remained true when the sensitivity was increased by probing a Southern blot (see Figure 3.44). Thus, after 10 minutes at 37°C in the presence of Mg^{2+}, a product synaptic complex can be isolated in a yield similar to that of the substrate synaptic complex (see Figure 3.36).

Figure 3.36 shows that the substrate and product synaptic complexes could also be seen as discrete bands following treatment with a restriction endonuclease that cuts at a unique site in pMA21 to generate the α-form. However, it was generally the case that the supercoiled α-form only gave discrete bands representing substrate and product synaptic complex when the yield of synapsed material was low; with a higher yield of complex the close-migrating bands merged. In contrast, the relaxed α-form typically formed discrete substrate and product complex bands (Figure 3.37). Although there was good separation of the substrate and product synaptic complexes when in the χ-form, the extent of separation was sensitive to the restriction endonuclease cleavage sites utilised (data not shown). Thus, with the 2616 bp domain cleavage constant at the *Pst*I site of pMA21, separation was best when the arms forming the 2311 bp domain were at their most disparate in length and

the separation decreased as the arms approached equality in length (and the rate of migration of the χ-form reached a minimum – see Section 3.3).

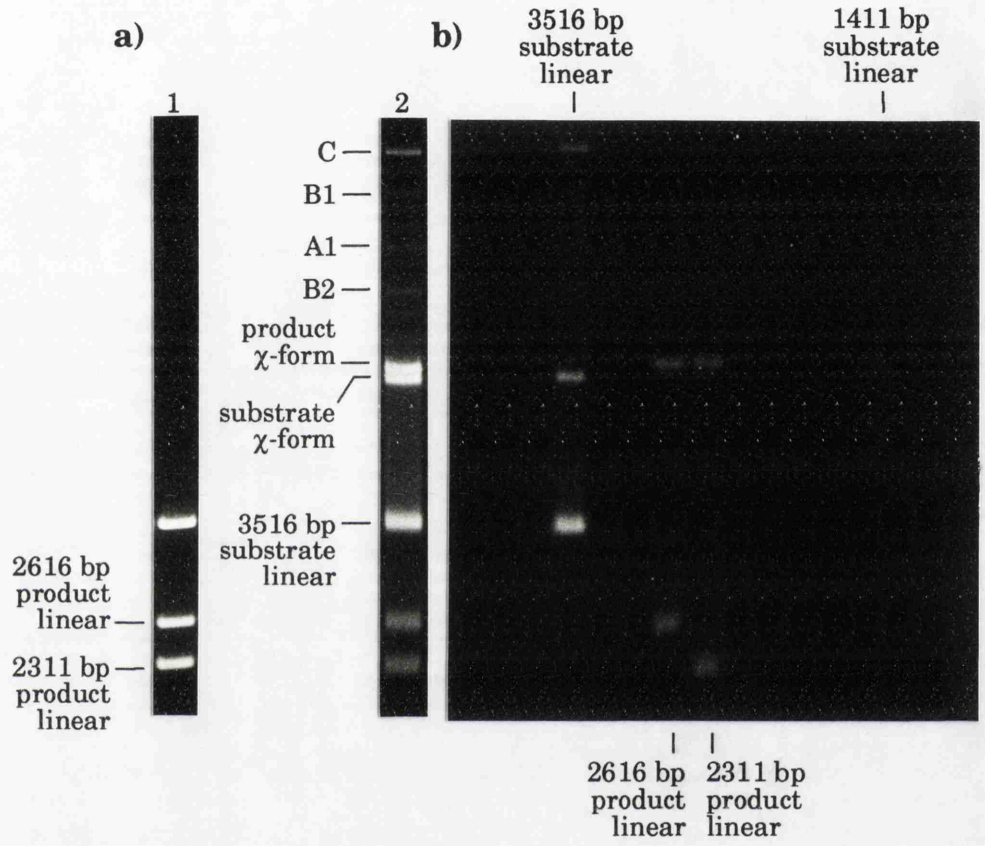

Figure 3.35 Agarose gel electrophoresis of a crosslinked pMA21 synapsis reaction: isolation and characterisation of synaptic complexes formed in the presence of Mg^{2+}.

a) Following digestion with *Pst*I + *Bam*HI, two discrete bands migrate to the position characteristic of the χ-form of the intramolecular synaptic complex (lane 2). These bands, and the slower-migrating species arising from intermolecular synapsis (see Section 3.7), are not present when 0.2% SDS is added prior to electrophoresis (lane 1).

Buffer C + 10 mM $MgCl_2$; 0.05% glutaraldehyde; 1.2% agarose gel.

b) Lane 2 was cut from the gel (as shown), soaked in SDS, and run in a second dimension of electrophoresis from left to right. The slower-migrating of the intramolecular χ-forms is composed of the linearised product circles, identified by their co-migration with the free product. The faster-migrating χ-form is the previously characterised substrate complex.

1.2% agarose gel.

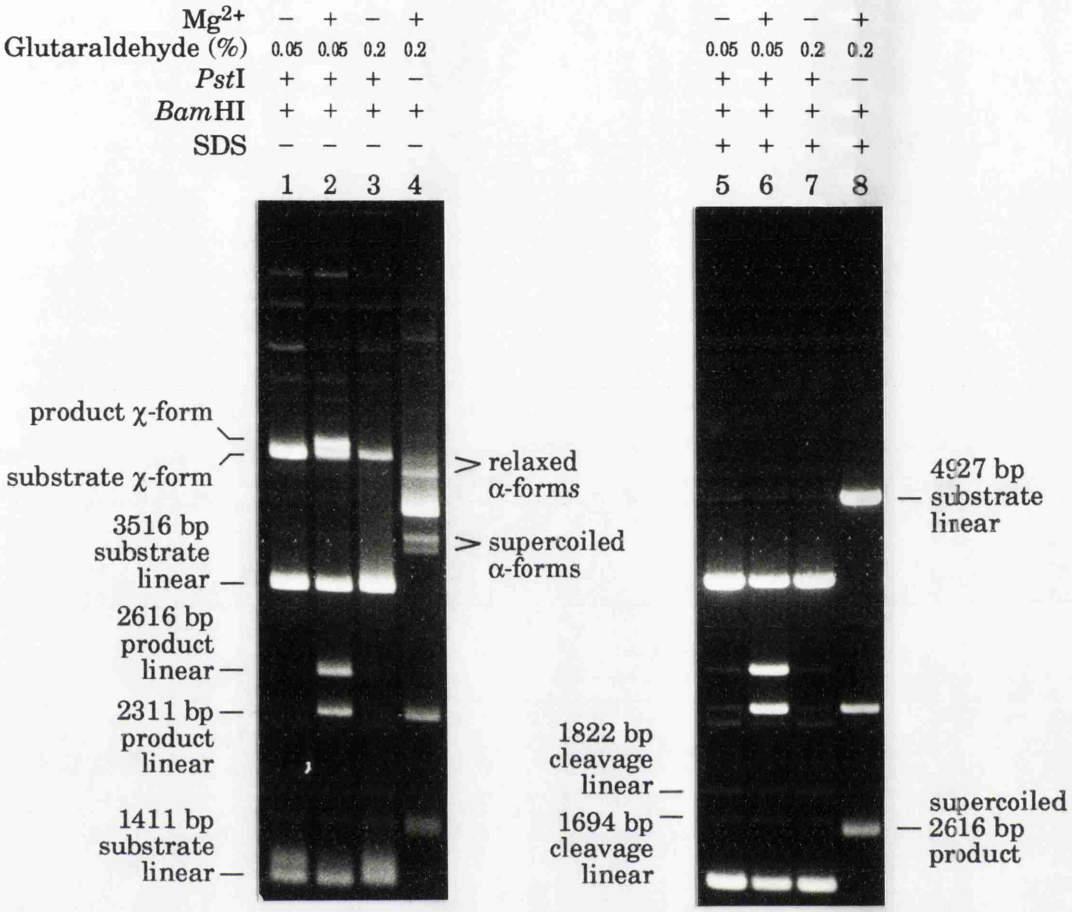

Figure 3.36 Agarose gel electrophoresis of glutaraldehyde-crosslinked pMA21 synapsis reactions: a comparison of synapsis in the presence and absence of Mg^{2+}.
Synapsis reactions were treated with 0.05% glutaraldehyde (lanes 1 and 2), or with 0.2% glutaraldehyde (lanes 3 and 4), following the standard 10 minutes incubation for synapsis. A detectable amount of product synaptic complex is only isolated following incubation in the presence of 10 mM Mg^{2+} (lane 2). The lower yield of complex isolated when using 0.2% glutaraldehyde (seen by comparing lane 3 with lane 1) enables observation of discrete bands representing the close-migrating supercoiled α-forms of the substrate and product synaptic complex (lane 4). SDS treatments are included (lanes 5-8). Products of resolvase-mediated cleavage at both crossover sites ('cleavage linears') are apparent. Such cleavage products were rarely detected in standard synapsis reactions, and are discussed further in Sections 3.9 and 5.4.

Buffer C, +/–10 mM $MgCl_2$; 0.05% or 0.2% glutaraldehyde; 1.2% agarose gel.

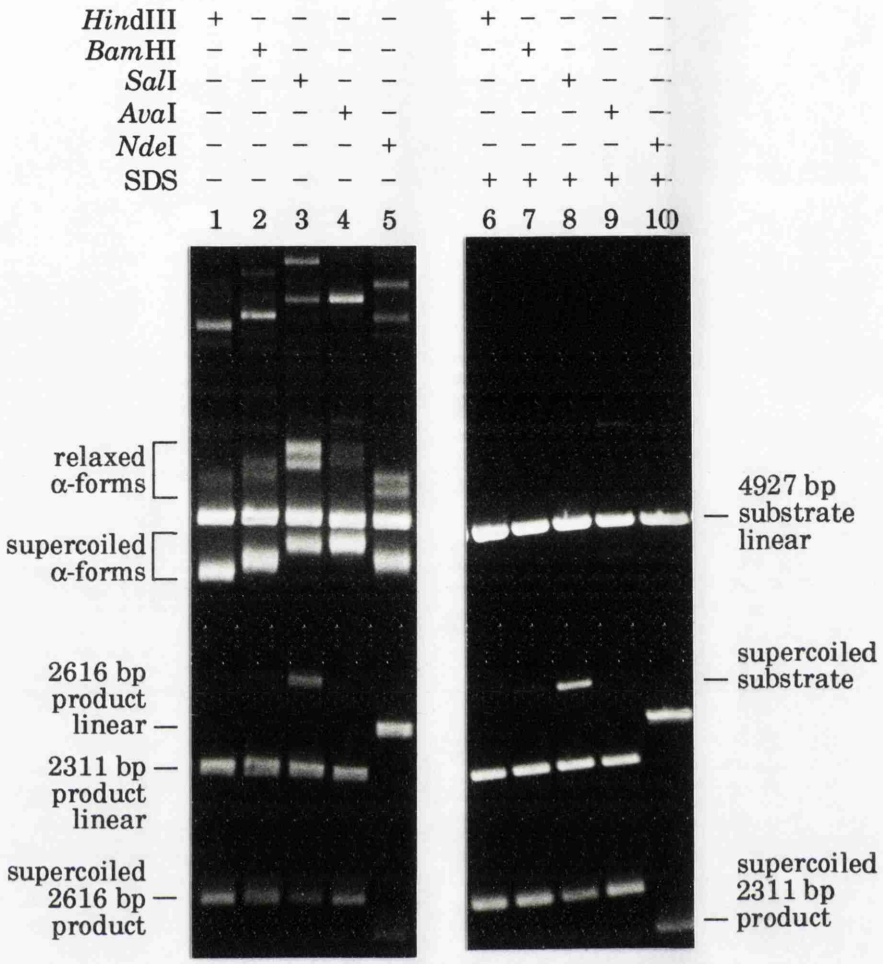

Figure 3.37 Agarose gel electrophoresis of a glutaraldehyde-crosslinked pMA21 synapsis reaction: substrate and product synaptic complexes are better separated when the α-form is relaxed. The enhanced separation of the relaxed α-forms of the substrate and product synaptic complex is best seen following digestion with *Sal*I or *Nde*I (lanes 3 and 5, respectively), enzymes previously shown to produce a relatively large amount of the relaxed α-form (see Figure 3.18). See Figure 3.16 for a restriction map of pMA21.

Buffer C + 10 mM $MgCl_2$; 0.05% glutaraldehyde; 1.2% agarose gel.

The sensitivity of the relative rate of migration of the χ-form to the sites of restriction endonuclease cleavage invites speculation on whether the difference in mobility between the cleaved forms of the substrate and product synaptic complex is due at least in part to the difference in relative arm length brought about by strand exchange. To test whether a structural difference in the nucleoprotein core of the two synaptic

complexes has a discernible effect on relative gel mobility, it was necessary to remove this effect of the change in relative arm length. This was achieved by using a resolvase substrate constructed by dimerisation of pMA1441, a plasmid containing a single *res* site. The symmetrical nature of the resulting plasmid, pMS2, ensured that the substrate χ-form had the same relative arm length as the product χ-form (see Figure 3.38). Despite cleavage at various sites, pMS2 produced only a single band representing the χ-form of the synaptic complex formed in the presence of Mg^{2+} (Figure 3.38). This strongly suggests that the difference in the gel mobility of the pMA21 substrate and product χ-form generated by *Pst*I + *Bam*HI cleavage was due to the change in the relative arm length brought about by strand exchange. Attempts to create a substrate χ-form with relative arm lengths resembling those of the *Pst*I + *Bam*HI product χ-form, and thereby swap the positions of substrate and product χ-form bands in the gel, failed due to a shortage of suitable restriction sites in pMA21 (data not shown).

The isolated product synaptic complex may represent an intermediate on the pathway from free substrate to free catenane product, trapped after strand exchange but before dissociation of the product synapse by the action of the crosslinking reagent. Another possibility is that the isolated product synaptic complex was formed by re-synapsis of the released catenane product. A preparation of the (–2) catenane resulting from resolution of pMA21 was used as substrate in a standard synapsis assay. Figure 3.39 shows that the catenane formed a crosslinked protein-DNA complex migrating to the same position in the gel as the χ-form of the product synaptic complex formed in a synapsis reaction starting with pMA21 as substrate. The observation that the catenane product of the Tn*3* resolvase reaction forms a synaptic complex provides another example of a block on recombination occurring after initial synapsis, since there is no detectable fusion of the catenated products when in the supercoiled state (Krasnow and Cozzarelli, 1983).

While there was obviously some synapsis of the catenane, the yield of the complex was poor even when compared to the yield obtained from a reaction in which pMA21 had formed less product (Figure 3.39). Therefore, this result does not exclude the possibility that some of the isolated product synaptic complex represents a genuine intermediate in the resolvase-catalysed reaction.

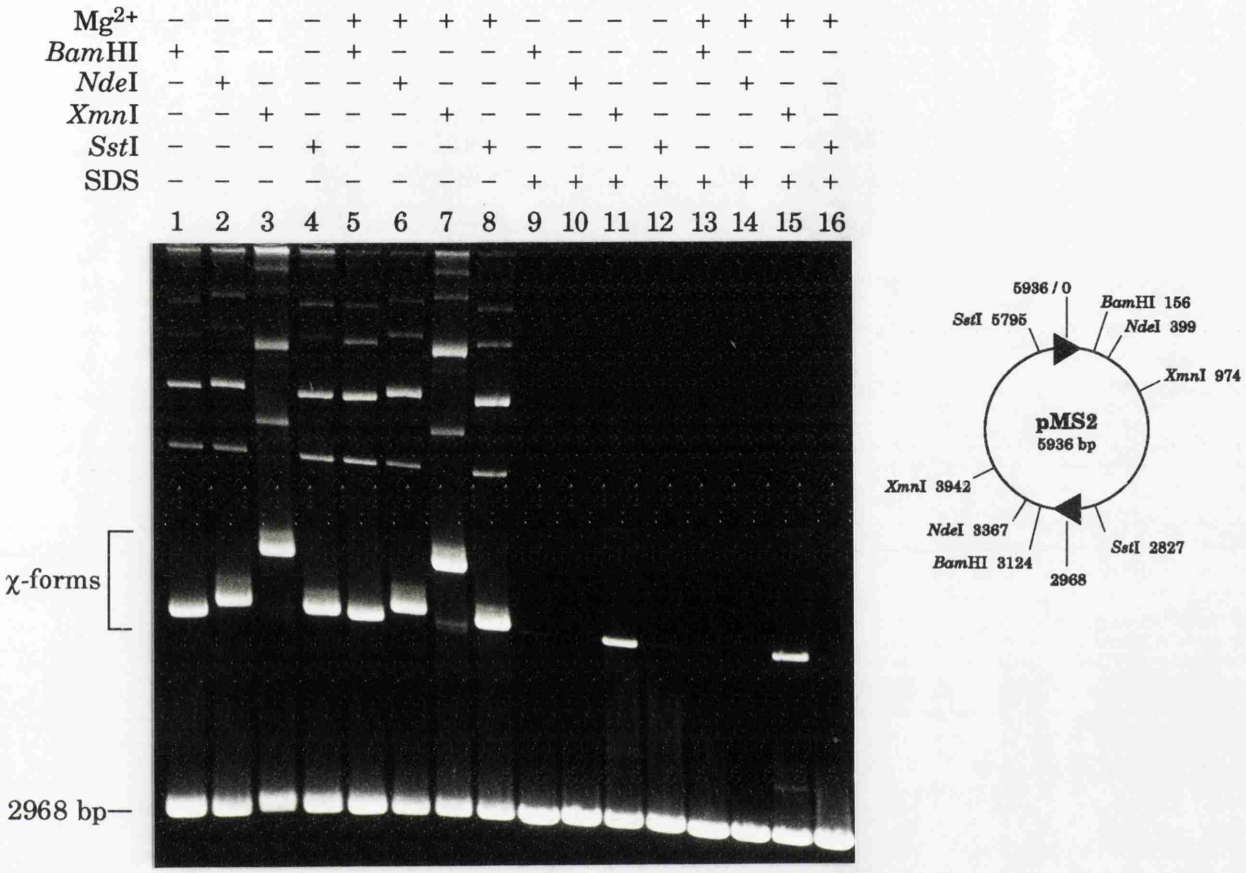

Figure 3.38 Agarose gel electrophoresis of a glutaraldehyde-crosslinked pMS2 synapsis reaction: substrate and product synaptic complexes do not migrate differently when in the χ-form.
Following synapsis in the presence and absence of Mg^{2+}, pMS2 (a dimer of the single *res* site plasmid pMA1441) was digested with a number of different restriction endonucleases in order to produce χ-forms with different mobility (restriction map shown). Although there is some material above the single χ-form band, this does not differ in amount between plus- and minus-Mg^{2+} reactions. Since recombination of pMS2 is increased in the presence of Mg^{2+} (data not shown), all the $+Mg^{2+}$ χ-form bands (lanes 5-8) probably represent a mixture of the substrate and product synaptic complexes. Therefore, when the difference in relative arm length of the χ-forms, brought about by strand exchange, is prevented by using a dimer substrate, the substrate and product complexes do not exhibit a detectable difference in mobility in the agarose gel.

Buffer C, +/–10 mM $MgCl_2$; 0.05% glutaraldehyde; 1.2% agarose gel.

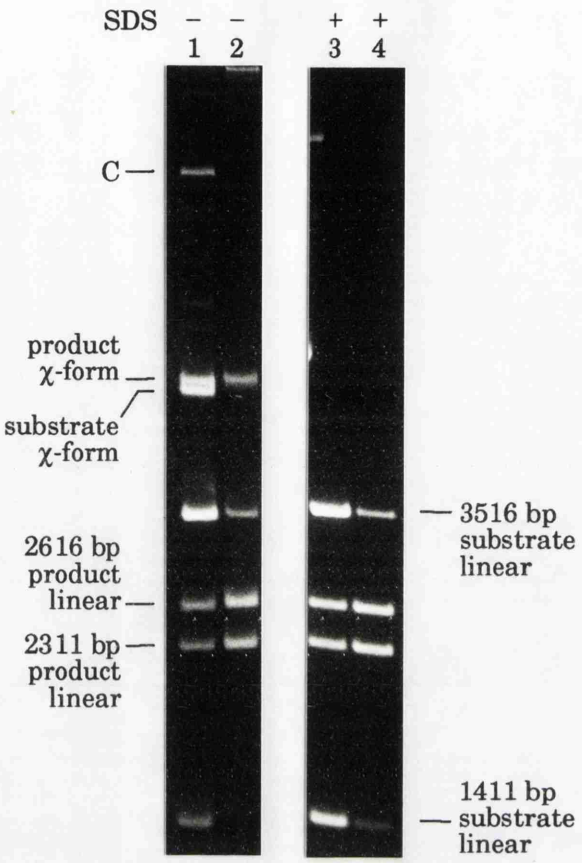

Figure 3.39 Agarose gel electrophoresis of a glutaraldehyde-crosslinked pMA21-catenane synapsis reaction: synapsis of the (–2) catenane produces a species migrating to the same position as the product χ-form obtained from the 'forward reaction'. Synapsis reactions differed only in the starting substrate, either supercoiled pMA21 (lane 1) or the supercoiled (–2) catenane product from the pMA21 resolution reaction (lane 2). A small amount of pMA21 remains in the catenane preparation. Following *Pst*I + *Bam*HI cleavage to produce the χ-form, pMA21 gives substrate and product synaptic complexes, while the pMA21-catenane crosslinks to give a band co-migrating with the product complex. However, the pMA21-catenane gives significantly less of the product χ-form, despite there being more product than is present after the 10 minute synapsis reaction with pMA21 as substrate. Lanes 3 and 4 show SDS treatments of the reactions loaded in lanes 1 and 2, respectively.

Buffer C + 10 mM $MgCl_2$; 0.05% glutaraldehyde; 1.2% agarose gel.

Figure 3.40 shows the effect of altering the concentration of resolvase on the yield of substrate and product synaptic complexes. With approximately 0.4 μM resolvase (lane 3), the substrate synaptic complex was

present, but there was virtually no product synaptic complex, despite there being a substantial amount of free product. A doubling of the resolvase concentration to the optimum for recombination resulted in the appearance of the product synaptic complex in relatively high yield. This suggests that there is a minimum concentration of resolvase required for stabilisation of the product synaptic complex by protein crosslinking, regardless of whether this complex is trapped immediately after strand exchange in the substrate synapse or following re-synapsis of the freed catenane. Furthermore, this concentration of resolvase is greater than that required to stabilise the substrate synaptic complex or to catalyse some (albeit not optimal) recombination.

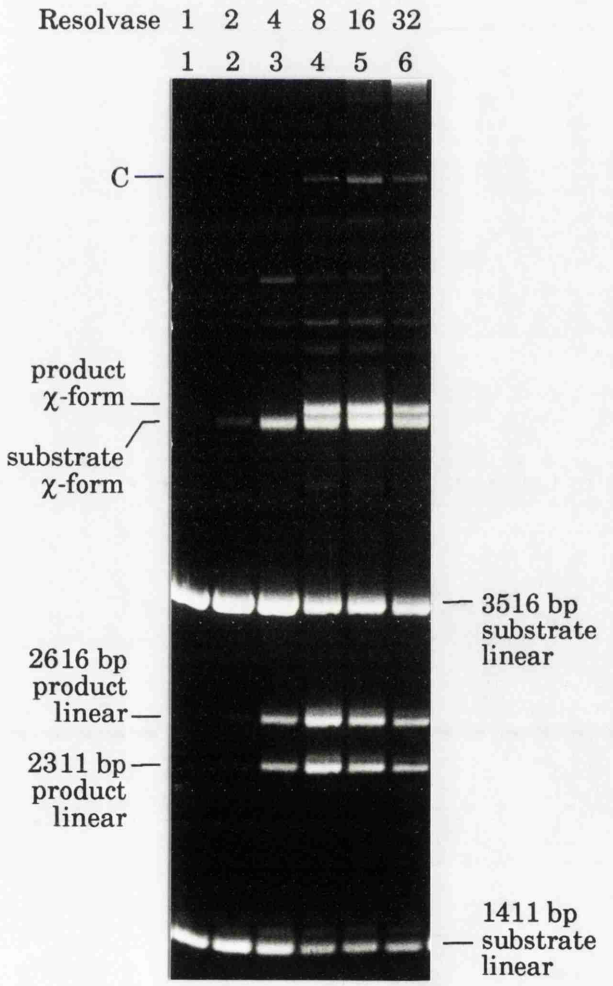

Figure 3.40

Agarose gel electrophoresis of glutaraldehyde-crosslinked pMA21 synapsis reactions: the effect of altering the resolvase concentration on the yield of substrate and product synaptic complexes.
The *Pst*I + *Bam*HI χ-form was used to assay the amount of substrate and product synaptic complex through a resolvase titration. The increase in the concentration of resolvase through the titration is two-fold, as denoted by the numbering; 1 is equivalent to approximately 0.1 μM resolvase.

Buffer C + 10 mM $MgCl_2$; 0.05% glutaraldehyde; 1.2% agarose gel.

pMS12 and pMS11 are identical in all but one respect. Both plasmids contain two copies of the *res* site in direct repeat orientation, but while

pMS12 contains two wild-type *res* sites, pMS11 contains one wild-type *res* site and one mutagenised *res* site containing an AC central overlap dinucleotide within subsite I in place of the wild-type AT (W.M. Stark, personal communication). Similarly, pGC1 and pGC4 differ from the wild-type substrate pMA21 in having the central dinucleotide mutagenised to TA in one *res* site and in both sites, respectively (G. Calder and W.M. Stark, personal communication). These plasmids are diagrammed in Figure 3.41.

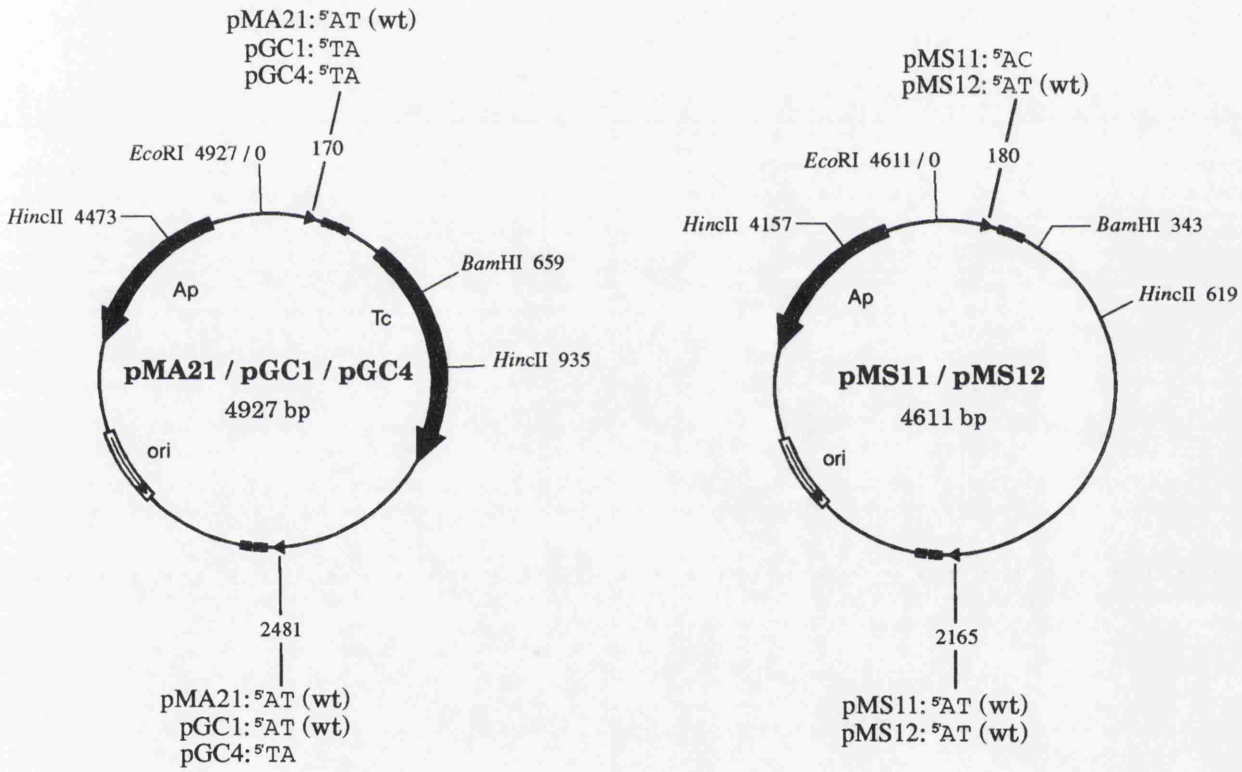

Figure 3.41 Simplified maps of plasmids containing copies of the wild-type *res* site and/or mutant *res* sites in which the subsite I central overlap dinucleotide is altered.
pMS12 contains two wild-type *res* sites. pMS11 contains one wild-type *res* site and one mutagenised *res* site containing an AC central overlap dinucleotide in place of the wild-type AT. pGC1 and pGC4 differ from the wild-type substrate pMA21 in having the central dinucleotide mutagenised to TA in one *res* site and in both sites, respectively.

A Tn*3* resolvase-catalysed reaction between *res* sites differing at one position in the central dinucleotide produced little recombinant (which contains mismatched base pairs), but gave large amounts of non-recombinant knots, starting at four nodes and increasing in complexity mainly in steps of four nodes (Stark *et al.*, 1991). This result is consistent with the 'simple rotation' model for strand exchange (see Chapter 1). The reaction of pMS11 (AC × AT) proceeded at a faster rate than did the reaction of pGC1 (TA × AT), while resolution of pGC4 (TA × TA) was very slow (W.M. Stark, personal communication). The reduced reactivity of pGC1 and pGC4 may be due to the demonstrated reduced binding affinity of resolvase towards a copy of subsite I containing the TA mutation in the central dinucleotide (Hatfull *et al.*, 1988).

In the standard synapsis assay, all these plasmids formed the substrate synaptic complex in equivalent yield, but only the wild-type substrates pMS12 and pMA21 produced the characteristic product synaptic complex (Figure 3.42). There was no evidence of any non-recombinant knot synaptic complex formed by the mismatch plasmids, but any trapped positive nodes may have been dissipated upon restriction enzyme cleavage of the crosslinked synaptic complex. Even if this was not the case, a non-recombinant synaptic complex of greater complexity may not migrate differently from the substrate synaptic complex following restriction endonuclease cleavage because strand exchange will not have changed the relative arm lengths, shown to be the major factor in the differential migration of the substrate and recombinant product synaptic complexes in agarose gels. The yield of substrate synaptic complex obtained from pGC1 and pGC4 was not markedly lower than that from the other plasmids, so any loss of binding affinity to subsite I of *res* did not appear to be manifested in a failure to trap either inter- or intra-molecular synaptic complex (Figure 3.42).

In conclusion, there is somewhat contradictory evidence on whether the isolated product synaptic complex represents a genuine intermediate in the site-specific recombination reaction. Its failure to appear at a concentration of resolvase that catalysed formation of a considerable amount of product might suggest that a higher concentration of resolvase is required to stabilise the transient intermolecular synapsis of catenane sufficiently for crosslinking. However, this could be equally true of a transient post strand-exchange intermediate. Furthermore, synapsis of catenane does not appear efficient enough to explain all of the cross-

linked product synaptic complex routinely isolated, although re-synapsis immediately after dissociation of newly formed product may be more efficient. This discussion will be continued in the light of results presented in the next Section.

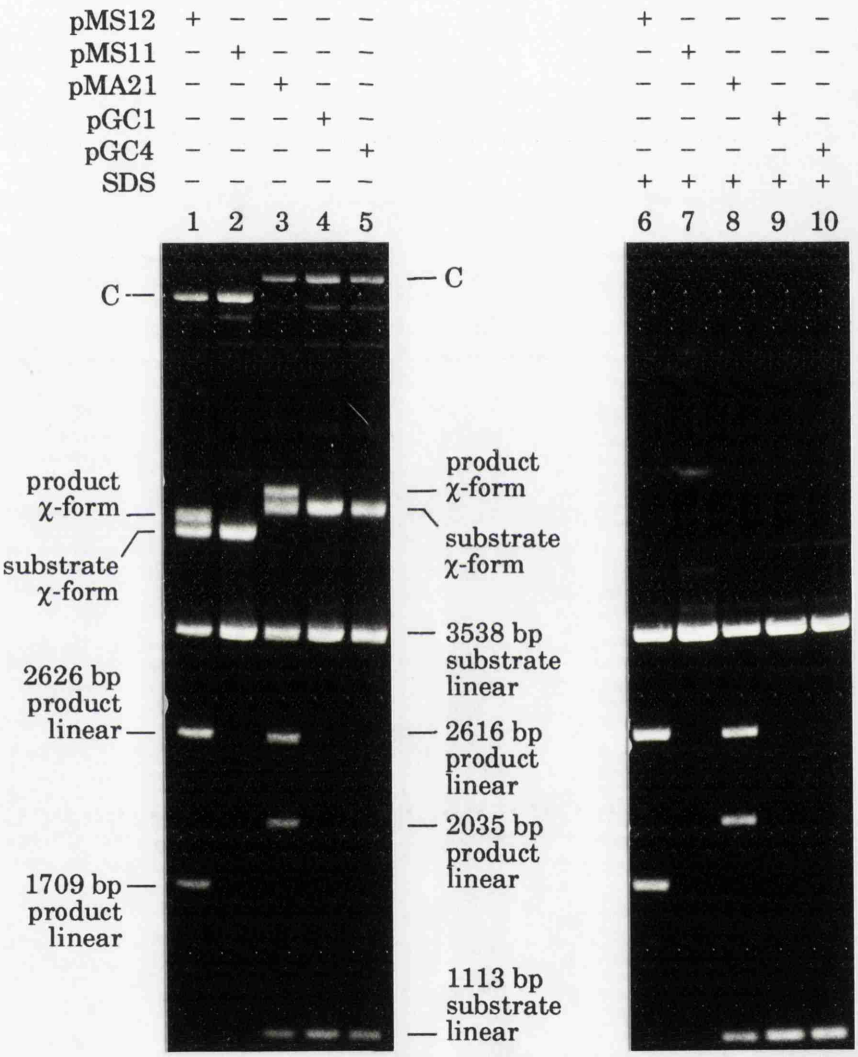

Figure 3.42 Agarose gel electrophoresis of glutaraldehyde-crosslinked synapsis reactions: the effect of altering the *res* subsite I central overlap dinucleotide.
The *Bam*HI + *Hin*cII χ-form was used to assay the amount of substrate and product synaptic complex obtained from the various plasmids diagrammed in Figure 3.41. See the text for details.

Buffer C + 10 mM $MgCl_2$; 0.05% glutaraldehyde; 1.2% agarose gel.

3.9 The rate of synapsis.

Before embarking on time-course assays to monitor the relative yield of the various synaptic complexes characterised in previous Sections at different stages of the Tn*3* resolvase-catalysed reaction, several problems had to be addressed.

Firstly, which cleaved form of the synaptic complex to monitor? It was decided to assay synaptic complex in the χ-form; *Pst*I + *Bam*HI digestion of pMA21 resulted in good separation of the substrate and product intramolecular synaptic complexes, and well-characterised migration of cleaved intermolecular synaptic complexes (see Sections 3.7 and 3.8). Furthermore, all of the intramolecular substrate synaptic complex migrated as a single band when in the χ-form, whereas the α-form was distributed between supercoiled and relaxed species, making it more difficult to estimate relative total yield at different time-points. However, it should be noted that the χ-form band representing intramolecular synapsis will also contain some complex arising from intermolecular synapsis in the 'A2' conformation (see Section 3.7).

Secondly, addition of crosslinking reagent did not immediately halt synapsis. The zero time-point sample in the time-course assays presented in this Section was produced by addition of crosslinking reagent to an aliquot of the reaction mixture containing the substrate DNA immediately before addition of resolvase (see Section 2.15f). However, in numerous experiments, the yield of substrate χ-form in this zero time-point sample was not exceeded in the first genuine time-point sample (for example, see Figure 3.43). Thus, there appeared to be sufficient time for synapsis to occur before an already-present crosslinking reagent inactivated resolvase.

Various changes were made to the crosslinking reaction conditions in an attempt to obtain a 'complex-less' zero time-point sample (data not shown). These included shortening the crosslinking reaction time, and using a higher concentration of glutaraldehyde while incubating the crosslinking reaction on ice. The standard conditions for isolation of synaptic complex (as described in Section 2.15c) were returned to when these changes not only failed to prevent synapsis in the zero time-point sample, but also failed to duplicate the efficiency of crosslinking obtained in earlier experiments.

However, it did appear that the synapsis occurring in the zero time-point sample was taking place in a short period of time, rather than at length during the crosslinking reaction incubation time of 5 minutes at 37°C. Therefore, the zero time-point sample is perhaps better described as an 'early' time-point, demonstrating the rapidity of formation of a synaptic interaction that can be stabilised by protein crosslinking.

Figure 3.43 shows the results of agarose gel electrophoresis of aliquots crosslinked with glutaraldehyde at various times between 30 seconds and 160 minutes after addition of resolvase to a standard supercoiled pMA21 synapsis reaction incubated at 37°C in the presence of 10 mM Mg^{2+} (see Section 2.15f). *Pst*I + *Bam*HI digestion showed the intramolecular substrate synaptic complex to be present in maximal yield, representing 40-50% of input substrate, in the zero time-point sample (see the above discussion). From this point in the reaction there was a gradual decline in the yield of the substrate synaptic complex until only a small amount remained after 160 minutes. The yield of the slower-migrating χ-form of the product synaptic complex increased gradually to reach a maximum at the 40 minute time-point, concomitant with a similar rate of increase in the amount of free resolution product. Throughout this stage of the reaction, 50-60% of the resolution product was in the form of a synaptic complex. However, while the yield of free resolution product continued to increase through to the 160 minute time-point, the amount of product synaptic complex declined through the 80 and 160 minute time-points.

The inability to stop synapsis very rapidly was most intrusive when attempting to assay the rate of formation of the substrate intramolecular synaptic complex. Attempts to assay changes in yield of putative synaptic intermediates during the early stages of the resolvase-catalysed reaction by lowering the reaction temperature failed (data not shown). Even when the reaction was incubated on ice, inhibiting formation of the product synaptic complex, the maximal yield of the crosslinked substrate synaptic complex was present from the outset (in the zero time-point sample). Similarly, when the reaction was incubated at 37°C in the absence of Mg^{2+}, a constant amount of substrate intramolecular synaptic complex present from the outset to the 10 minute time-point only declined very gradually thereafter when product began to form (data not shown). It is not known whether this crosslinked substrate synaptic complex, involving about 50% of input substrate, represented all (or part) of a long-lived population of stably-synapsed molecules or a continually changing

population in which the synaptic interaction was unstable. As described in Chapter 1, the results of Parker and Halford (1991) suggest the former, while the inhibition of recombination between non-adjacent sites in plasmids containing four *res* sites in direct repeat orientation (Brown, 1986) suggests an instability consistent with the two-step model for synapsis (Boocock *et al.*, 1986; Boocock *et al.*, 1987).

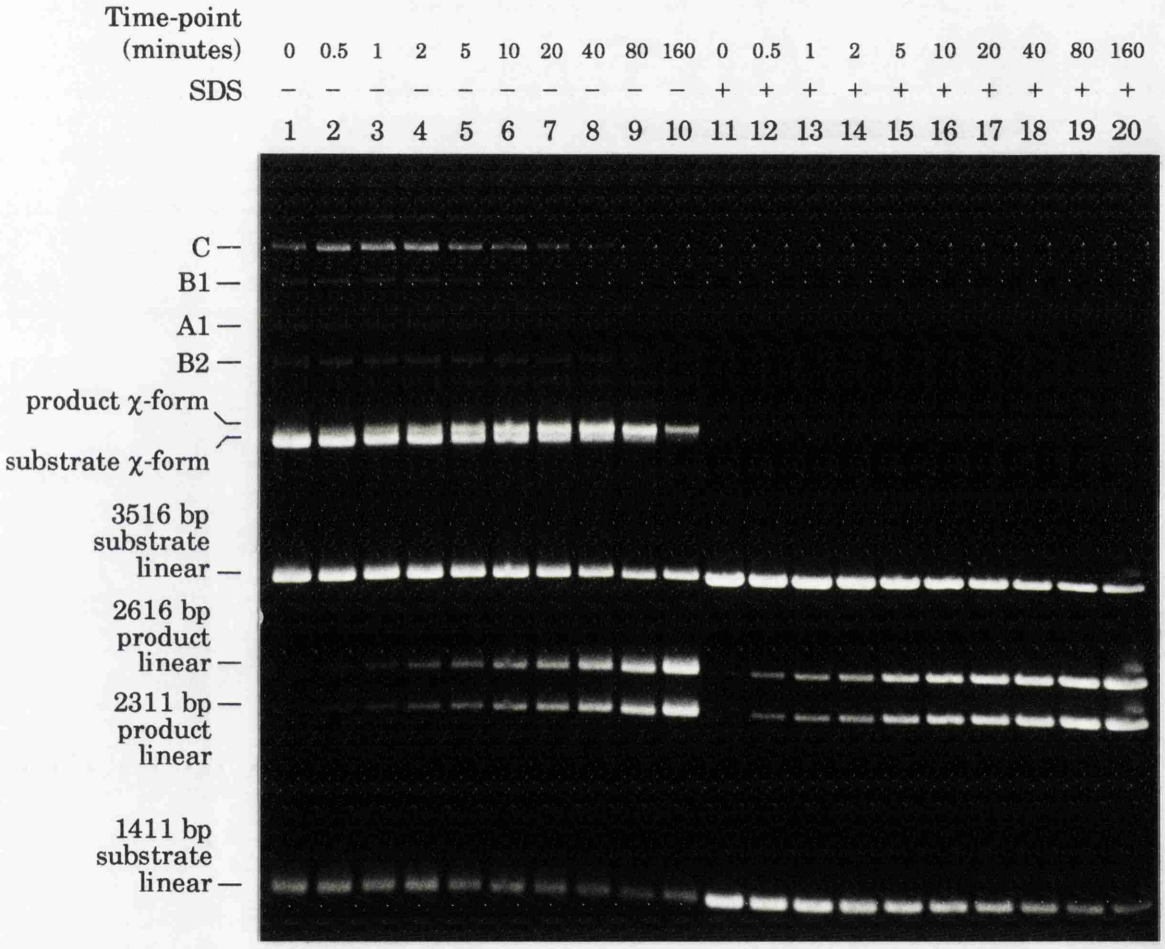

Figure 3.43 Agarose gel electrophoresis of a glutaraldehyde-crosslinked pMA21 synapsis reaction: a time-course at 37°C in the presence of 10 mM Mg^{2+}.
After initiation of the reaction by addition of resolvase, aliquots were taken at the times shown and, after crosslinking, were digested using *Pst*I + *Bam*HI (see Section 2.15f for details). The zero time-point sample was obtained by addition of glutaraldehyde to an aliquot of the reaction mix followed immediately by resolvase. SDS treatments of each sample are on the right (lanes 11-20). The intermolecular synaptic complexes are identified by the code outlined in Section 3.7 (see Figure 3.32). See the text for further discussion of these data.

Buffer C + 10 mM $MgCl_2$; 0.05% glutaraldehyde; 1.2% agarose gel.

As noted in Section 3.8, it is difficult to determine whether the isolated product synaptic complex represents an intermediate arising from DNA strand exchange occurring in the substrate synaptic complex, or whether it is formed by re-synapsis of free catenane. However, it is interesting to note that the amount of product synaptic complex remaining at the 160 minute time-point (Figure 3.43), by which stage the amount of substrate synaptic complex and the rate of product formation had declined considerably, was of the order expected to be formed by re-synapsis of the available free product if the efficiency of the reaction was similar to that seen in synapsis reactions starting with the pMA21 catenane (see Section 3.8). If this represented the maximal amount of product synaptic complex arising from re-synapsis, the higher yield at the earlier time-points shown in Figure 3.43, and a large part of the observed change in yield, may have been due to the isolation of a genuine recombinant synaptic intermediate.

In order to obtain more information on the nature of the protein-DNA complexes present at various time-points of the resolvase-catalysed reaction, whole lanes representing the 30 second, 1, 5, and 80 minute time-points from the gel shown in Figure 3.43 were treated with SDS and electrophoresed in a second dimension (see Section 2.9g). Southern blots were prepared to detect any species present in low yield. Autoradiographs from two-dimensional gels of the 1 minute and 80 minute time-points are reproduced in Figure 3.44. The more sensitive detection method confirmed that the two close-migrating χ-form bands characterised in Section 3.8 were composed solely of synapsed product and substrate, respectively. Species representing products of cleavage at both *res* sites of pMA21 are present in very low yield at 80 minutes only (Figure 3.44b). These DNA fragments may have resolvase covalently linked as do the cleavage products isolated in greater yield in the presence of a high concentration of ethylene glycol (data not shown), but there is no evidence of their being crosslinked in a slower-migrating synaptic complex at any of the time-points. The appearance of these products of *res* site cleavage only at a late time-point suggests that they may represent abortive recombination due to dissociation of the synapse before the cleaved strands are religated by resolvase.

Figure 3.44 *Facing.*

A second dimension of agarose gel electrophoresis (from left to right as shown) followed SDS treatment of selected lanes cut from the gel shown in Figure 3.43. SDS treatment dissociates the protein-DNA complexes, allowing their component DNA fragments to be visualised after a second dimension of electrophoresis. Autoradiographs of Southern blots probed with ^{32}P-labelled pMA21 DNA are reproduced (see Sections 2.9g and 2.11 for details).

Species of interest are identified. Restriction fragments characteristic of resolution product are released from species migrating as intermolecular synaptic complexes in the first dimension of electrophoresis. These product fragments increase in amount through the time course. The product and substrate fragments released enable a partial characterisation of the two-site intermolecular synaptic complexes involving resolution product. Complex P1 represents synapsis between the 2616 bp circle of the (–2) catenane and a substrate DNA molecule. This species co-migrates with complex B2 following *Pst*I + *Bam*HI digestion, and SDS treatment frees only the 3516 bp substrate linear and the 2616 bp product linear. Two novel bands appearing at later time-points in the first dimension migrating between complex B2 and the intramolecular product χ-form (see Figure 3.43) are similarly identified. Complex P2 represents a two-site synaptic interaction between the 2311 bp circle of the (–2) catenane and a substrate DNA molecule. Complex P3 represents synapsis of two catenanes involving the 2616 bp circles only. Three- and four-site intermolecular product synaptic complexes have migrated at a slower rate in the first dimension of electrophoresis following *Pst*I + *Bam*HI digestion.

The sensitive detection method has picked up traces of full-length linear substrate and product resulting from incomplete restriction endonuclease digestion and migrating as α-form of the synaptic complex between the substrate χ-form and the 3516 bp substrate linear in the first dimension of electrophoresis.

See the text for further discussion.

a) The 1 minute time-point.

b) The 80 minute time-point.

1.2% agarose gels.

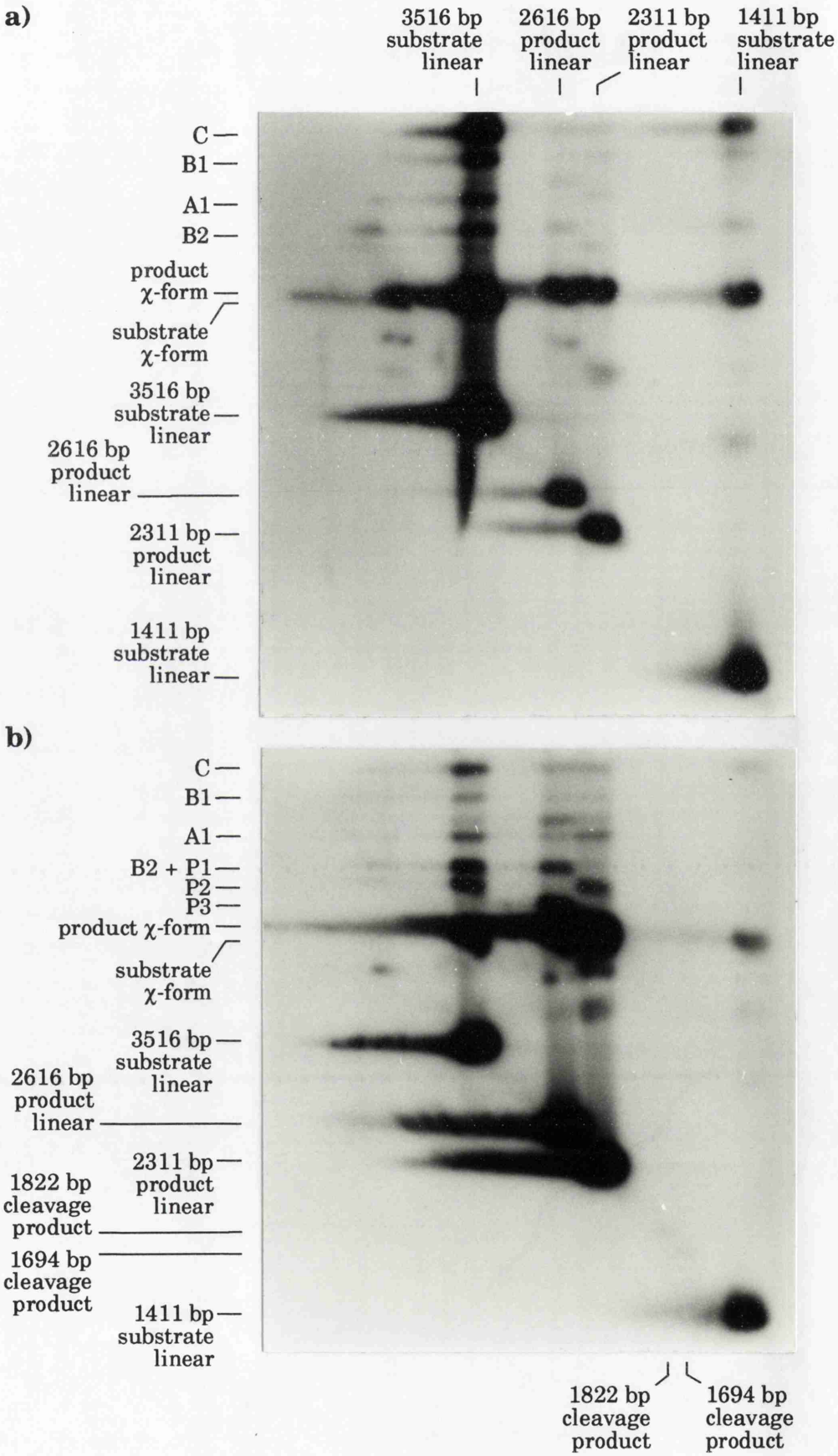
a)
3516 bp substrate linear
2616 bp product linear
2311 bp product linear
1411 bp substrate linear
C
B1
A1
B2
product χ-form
substrate χ-form
3516 bp substrate linear
2616 bp product linear
2311 bp product linear
1411 bp substrate linear
b)
C
B1
A1
B2 + P1
P2
P3
product χ-form
substrate χ-form
3516 bp substrate linear
2616 bp product linear
2311 bp product linear
1822 bp cleavage product
1694 bp cleavage product
1411 bp substrate linear
1822 bp cleavage product
1694 bp cleavage product

A feature only revealed by the more sensitive detection method was the prevalence at later time-points of intermolecular synaptic complexes containing resolution product (Figure 3.44b). In some cases, these co-migrated with the previously characterised intermolecular substrate synaptic complexes (see Section 3.7) and presumably arose by synapsis of catenane, either with another catenane or with substrate, although there exists the possibility of intramolecular recombination taking place in an intermolecular substrate synaptic complex.

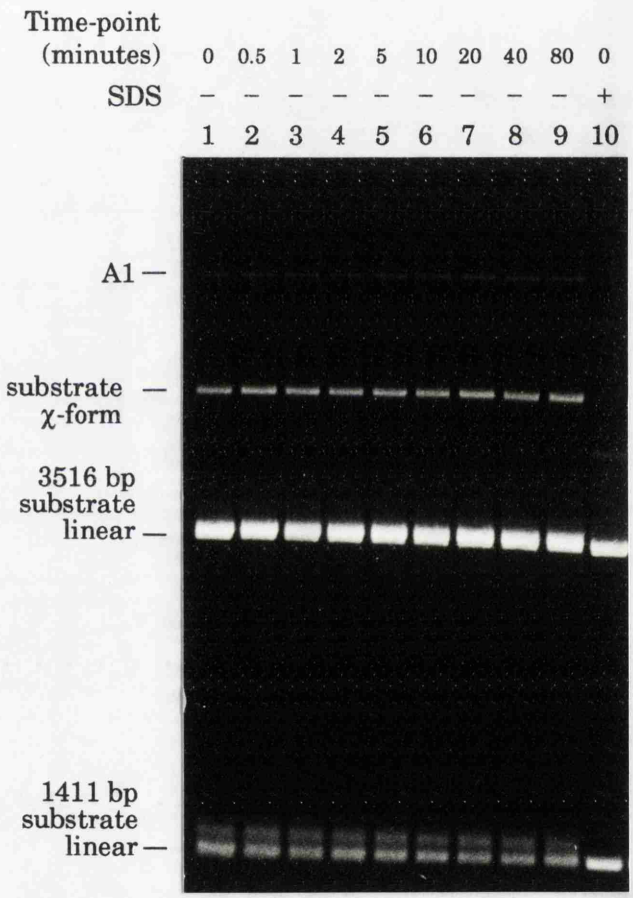

Figure 3.45 Agarose gel electrophoresis of a glutaraldehyde-crosslinked synapsis reaction: a time-course at 37°C in the absence of Mg^{2+} using nicked pMA21 as the substrate.
Experimental details are as outlined in the legend to Figure 3.43 (restriction endonuclease digestion was with *Pst*I + *Bam*HI). Only the SDS treatment of the zero time-point is shown (lane 10). Note the relatively high yield of the crosslinked resolvase-single *res* site complex (retarded relative to the 1411 bp substrate linear) discussed in Section 3.10. See the text for further discussion of these data.

Buffer C, minus-Mg^{2+}; 0.05% glutaraldehyde; 1.2% agrose gel.

Figure 3.45 shows a time-course in which the substrate DNA was nicked pMA21 (prepared by DNase I treatment in the presence of ethidium bromide as described in Section 2.7f). The reaction was incubated at 37°C in the absence of Mg^{2+}. The crosslinked substrate synaptic complex was present in maximal amount in the zero time-point sample and the yield remained constant throughout the 80 minute reaction. No product formed during this time; the recombination of non-supercoiled substrate generally requires a longer incubation and is promoted by the presence of glycerol and spermidine in the reaction mix (so-called 'permissive' reaction conditions). Although the yield of substrate synaptic complex seen in Figure 3.45 was considerably lower than that obtained from a reaction containing supercoiled substrate, the similar rapid appearance of the maximal amount of complex is of interest. Within the limitations of this assay (and acknowledging the failure to show that the isolated synaptic complex is productive), there was no apparent difference in the rate of formation of a synaptic complex whether starting from supercoiled substrate or from nicked substrate.

In an attempt to further investigate intermediates in the resolvase-catalysed reaction, an initial incubation of supercoiled pMA21 at 37°C in the absence of Mg^{2+} was followed by the addition of 10 mM Mg^{2+}. Throughout this reaction, aliquots were assayed at various timepoints and the result of agarose gel electrophoresis is shown in Figure 3.46. The first three time-points were in the absence of Mg^{2+}, and recombination was minimal during this 10 minute period. There did appear to be slightly less of the intramolecular substrate synaptic complex present in the zero time-point sample than was visible at the 30 second time-point on this occasion. However, a more dramatic change had occurred within 30 seconds after the addition of Mg^{2+}, in the form of a burst of recombination resulting in the appearance of synapsed and free resolution product. This was followed by little further recombination during the ensuing 2 minutes, then a gradual increase to a maximal yield of both synapsed and free product 80 minutes after the addition of Mg^{2+}.

This rapid formation of an amount of resolution product not normally seen until 2 minutes after the initiation of a resolvase-catalysed reaction in the presence of Mg^{2+} is suggestive of the accumulation of an intermediate during the incubation without Mg^{2+}. There did not appear to be a concomitant decrease in the amount of substrate synaptic complex immediately after addition of Mg^{2+}; indeed a more obvious decline

occurred in the amount of unsynapsed substrate – perhaps indicative of trapping of a constant amount of synapsed substrate from a larger pool by crosslinking, such that recombined substrate was rapidly replaced. The decrease in the amount of the resolvase-single *res* site complex upon addition of Mg^{2+} was striking, and the nature of this complex is considered in Section 3.10.

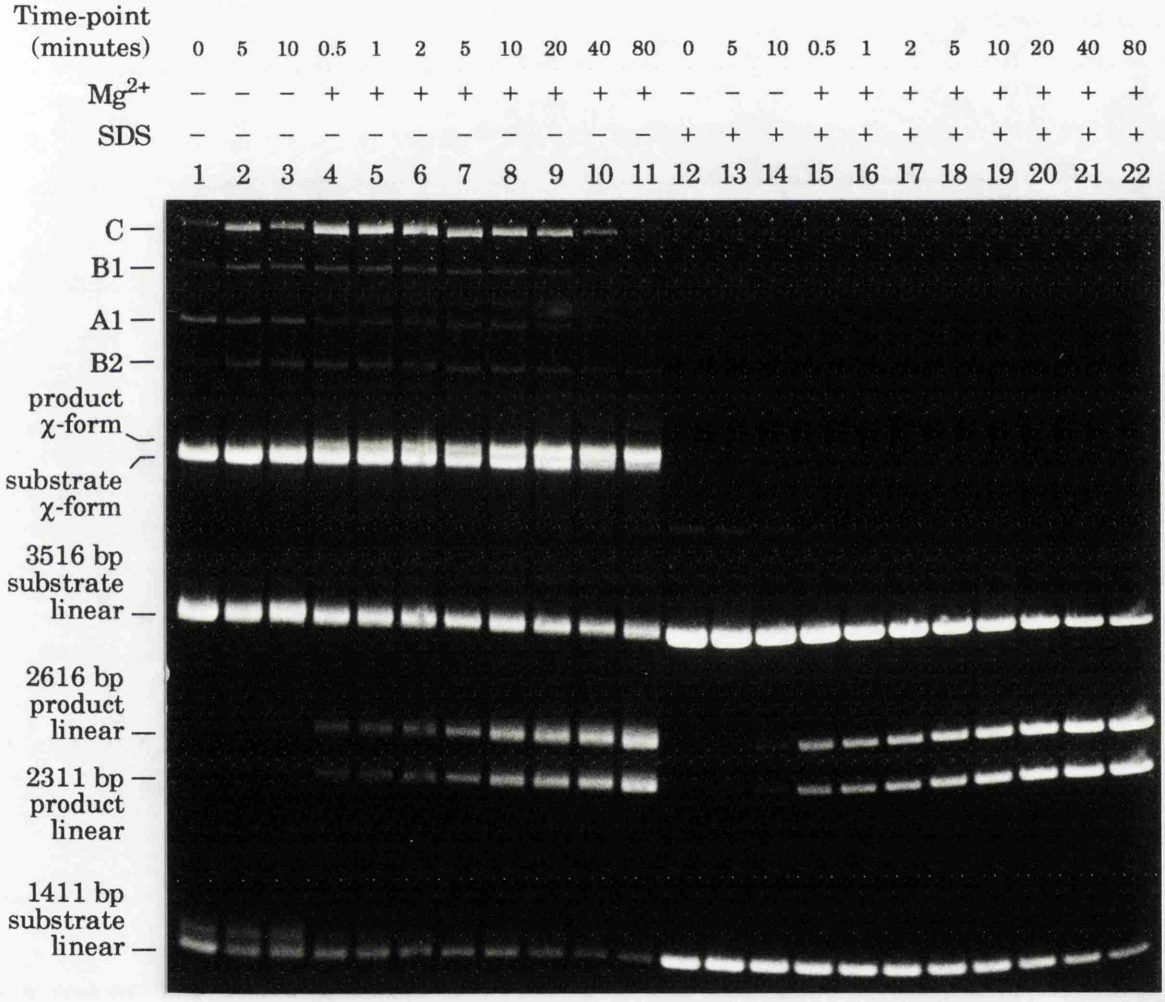

Figure 3.46 Agarose gel electrophoresis of a glutaraldehyde-crosslinked pMA21 synapsis reaction: a time-course at 37°C; 10 mM Mg^{2+} was added 10 minutes after addition of resolvase. Experimental details are as outlined in the legend to Figure 3.43 (restriction endonuclease digestion was with *Pst*I + *Bam*HI). The first three timepoints are relative to the addition of resolvase, while subsequent timepoints are measured from the addition of Mg^{2+}. See the text for further discussion.

Buffer C, minus-Mg^{2+} for 10 minutes, then + 10 mM $MgCl_2$; 0.05% glutaraldehyde; 1.2% agarose gel.

3.10 The complex formed by resolvase and a single *res* site.

In addition to the synaptic complexes isolated in experiments described in the preceding Sections, a retarded complex formed by resolvase and a single *res* site was often present. This complex was observed both with plasmids containing a single *res* site and with plasmids containing two *res* sites, and was significantly retarded when isolated as a supercoiled species, and particularly when a *res* site was left on a small DNA fragment by restriction endonuclease digestion (Figure 3.15). The resolvase-single *res* site complex also formed on nicked and linear DNA molecules (Figure 3.45 and Figure 3.29, respectively).

Protein crosslinking was required for the isolation of the resolvase-single *res* site complex in agarose gels under the conditions used to isolate synaptic complex (Figure 3.9), although this was not the case when binding of resolvase was to linear DNA fragments and separation was by non-denaturing PAGE (Bednarz *et al.*, 1990; Salvo and Grindley, 1988). As with the synaptic complex, dissociation of the resolvase-single *res* site complex in the presence of SDS (Figure 3.15) showed that there was no additional stabilisation of the complex by crosslinking of protein to DNA. These observations are consistent with the isolation of a complex in which resolvase bound at more than one subsite of *res* interacts, possibly to form a wrapped structure as was proposed for the resolvosome (Salvo and Grindley, 1988; Hughes *et al.*, 1990), (see Chapter 1).

The resolvase-single *res* site complex was invariably present in higher yield when the reaction conditions were such that resolution was inhibited. Thus, a reduction in pH from 8.0 to 7.0, or the absence of Mg^{2+}, increased the amount of this retarded complex (Figure 3.31b and Figure 3.36, respectively). The decrease in the yield of the resolvase-single *res* site complex when conditions favoured resolution was shown best when Mg^{2+} was added to an ongoing resolvase reaction, as noted in Section 3.9 (Figure 3.46). The resolvosome appears to be relatively stable and two preformed resolvosomes have been shown to recombine with high efficiency (Dröge *et al.*, 1990).

However, the model of the resolvosome as a wrapped structure with resolvase bound at subsite I of *res* interacting with resolvase bound at the accessory subsites (as described in Chapter 1) does not accord with the observation of an equivalent single-site complex when only the accessory

subsites of *res* were present (Figure 3.24). Even more perplexing was the isolation of a retarded resolvase-single-site complex when the plasmid contained only subsite I of *res*, albeit in relatively low yield (Figure 3.26a). It is more difficult to envisage how protein crosslinking could stabilise a complex with resolvase bound at a single subsite of *res*.

It may be that an interaction between resolvase and non-specific DNA sequences adjacent to the isolated *res* subsite allowed a wrapped structure to form, and that protein crosslinking stabilised this 'pseudo-resolvosome.' Such non-specific interactions were proposed to operate during synapsis of an intact *res* site and an isolated subsite I, in order to account for the formation of product indicative of a synapse topology identical to that proposed for the pairing of two intact *res* sites (Bednarz *et al.*, 1990), (see Section 3.5). However, since a plasmid containing a single subsite of *res* has not been assayed for single-site complex formation in the absence of crosslinking it is possible that the protein-DNA interactions are more stable when protein-protein interactions between resolvase-bound subsites of *res* are absent. Thus, a protein-DNA complex composed of resolvase bound to a single subsite of *res* might remain intact through the synapsis assay procedure. This interpretation is consistent with the finding that the stability of a fully occupied subsite II-III fragment during electrophoresis was increased when either the subsites were moved apart or a mutant resolvase deficient in an essential interdimer interaction was used (Grindley, 1994). The resolvase-single *res* site complex is discussed further in subsequent Chapters.

Chapter 4

Topology of the synaptic complex

Introduction.

Virtually all of the information on the DNA topology of reaction intermediates in Tn*3* resolvase-catalysed site-specific recombination has come from the study of product DNA topology, as discussed in Chapter 1. The topological analysis presented in this Chapter can be divided into two main parts. Section 4.1 describes an attempt to obtain information on the path of the DNA in the isolated crosslinked synaptic complex. Although topological analysis of a putative synaptic intermediate following isolation from unsynapsed material is the preferred approach, it has proved extremely difficult in practice to achieve this when dealing with the resolvase reaction (see page 66).

Benjamin and Cozzarelli (1988) described treatment of their glutaraldehyde-crosslinked Tn*3* resolvase synapsis reaction with topoisomerase I in order to relax the supercoiled substrate DNA. Topology was determined following agarose gel electrophoresis by comparing the resulting topoisomer distribution with that obtained following identical treatment of a minus-resolvase reaction. Assumptions were that a failure of topoisomerase I to relax an appropriate DNA substrate to the same extent in the presence of resolvase as in its absence was due to the entrapment of supercoils in the crosslinked synapse, and that the proportion of synapsed substrate was sufficiently high for study of the whole reaction to be informative.

Assaying plasmid substrates containing one, two (both direct and inverted repeats), and three *res* sites (direct repeats) in the absence of glutaraldehyde, the linking number difference ($Lk - Lk_0$)[1] between the minus- and plus-resolvase resolvase samples was reported as approximately –0.5 per *res* site, a change attributed to resolvase binding to unsynapsed *res* sites (Benjamin and Cozzarelli, 1988). Glutaraldehyde crosslinking was reported to have no effect on the $Lk - Lk_0$ observed for the single *res* site plasmid, whereas both orientations of two sites and the three site substrate produced an additional $Lk - Lk_0$ of –2 relative to the uncrosslinked control reactions. This difference was attributed to synapsis, stabilised only in the presence of the crosslinking reagent. The reported linking number difference of approximately –3 for plasmids containing two *res* sites in either orientation was consistent with the

[1] The linking number difference ($Lk - Lk_0$) is relative to relaxed linkage (Lk_0) defined under particular conditions, normally those of gel electrophoresis (Wang *et al.*,1984).

model of the synapse derived from study of product topology (Figure 1.4), and with the isolation of crosslinked synaptic complexes using the same plasmids (Benjamin and Cozzarelli, 1988). These results are discussed further, in the light of my own experimental data, in Section 4.1.

The remainder of Chapter 4 describes the results of an alternative approach that not only provides information on the changes in DNA topology brought about by the interaction of resolvase with various plasmid substrates, but also represents a novel assay for synapsis. Benjamin and Cozzarelli (1988) reported that the use of nicked circular plasmid DNA as the substrate for resolvase, followed by treatment with DNA ligase to trap any resolvase-induced change in topology, failed to show evidence of synapsis. The linking number difference was said to mirror that seen with supercoiled plasmid DNA in the absence of glutaraldehyde, with an $Lk - Lk_0$ of about –0.5 per *res* site. However, similar experiments carried out in this laboratory indicated otherwise (W.M. Stark, personal communication), and this approach was followed up in the work reported in Section 4.2.

The effect of protein-DNA interactions on the topology of the DNA has been investigated in other systems. Activation of transcription of the transposon-encoded mercury resistance operon, *mer*, was proposed to result from reorientation of sub-optimally phased promoter elements, a change brought about by underwinding of the intervening DNA upon binding of the transcription factor MerR complexed with its allosteric effector Hg(II) (Ansari *et al.*, 1992). This effect on DNA topology, amplified by the use of a plasmid containing 15 tandem copies of the MerR binding site, was demonstrated by an Hg-MerR-dependent shift in the topoisomer distribution following topoisomerase I relaxation. The same effect was seen when an Hg-MerR reaction containing nicked circular plasmid was treated with DNA ligase (Ansari *et al.*, 1992). A similar approach was used to show that a mutant of the Gin invertase exhibiting a FIS- and enhancer-independent phenotype induced localised unwinding of the DNA upon binding (Klippel *et al.*, 1993). This topological change was proposed to be brought about by FIS and the enhancer in order to aid strand exchange during the inversion reaction catalysed by wild-type Gin (see Chapter 1).

Results and Discussion.

4.1 The topology of the crosslinked synaptic complex.

This experiment was an attempt to test one aspect of a detailed model for the Tn*3* resolvase synaptic complex proposed by J.L. Brown, M.R. Boocock and D.J. Sherratt (unpublished; see Chapter 1). In the favoured variant of this model, a positive node is created by interwrapping of the paired copies of subsite I of *res* (Figure 1.6 and Figure 4.1a); an alternative variant, with an additional turn of the DNA helix in the subsite I-II spacer region (local frame), produces a negative node (Figure 4.1b). In each case, wrapping of the DNA around a tetramer of resolvase with 222 symmetry at subsite I is expected to create an additional node of the same sign as the DNA exits from the synapse (Figure 4.1).

Interwrapping of the DNA at the crossover site is predicted to influence the topology of products obtained following ligation of a χ-form of the crosslinked synaptic complex generated by cleavage at a unique restriction endonuclease site within each domain. Thus, ligation of a χ-form of the direct repeat synapse (such as that produced by *Pst*I + *Hin*dIII cleavage of synapsed pMA21 – see Figure 3.16) should give 4-node knot as the preferred product if two positive nodes flanking the crossover sites were trapped by crosslinking (Figure 4.1a). In contrast, if the trapped subsite I nodes were negative in sign, the simplest outcome is a 5-node knot (Figure 4.1b). If the subsite I DNA is not wrapped around a resolvase tetramer in a manner analogous to that proposed for the accessory subsites, or if the two copies of subsite I are not paired in the crosslinked χ-form of the synaptic complex, then the preferred product of ligation would be unknotted circular plasmid.

Determination of the number of knot nodes in the products of ligation was by differential migration during agarose gel electrophoresis after nicking of the DNA to ensure that only knot nodes remain trapped. However, the possibility of additional tangling of the free arms of the χ-form altering the topology trapped by ligation should be noted, particularly since a tendency to consider the model as drawn (Figure 4.1) does not reflect the reality of the synaptic complex in three-dimensional space.

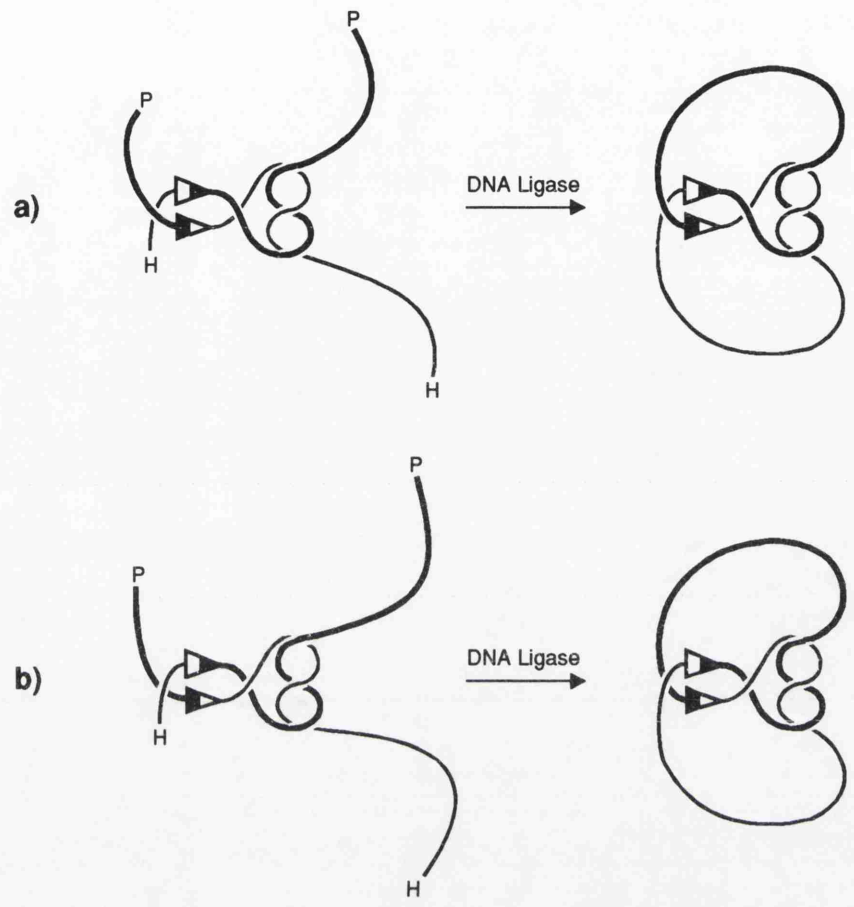

Figure 4.1 Variants of the model for the Tn*3* resolvase synaptic complex proposed by J.L. Brown, M.R. Boocock and D.J. Sherratt (unpublished; see Chapter 1).
Each variant is predicted to result in a different knot topology when a χ-form of the crosslinked synaptic complex generated by cleavage at a unique restriction endonuclease site within each domain is treated with DNA ligase. Thus, **(a)** is predicted to give 4-node knot as the major ligation product, while **(b)** favours the formation of 5-node knot. In the above representation of synapsed pMA21, the crossover sites are shown, as are the restriction endonuclease sites utilised (P = *Pst*I, H = *Hin*dIII). See the text for further details.

As discussed in Section 3.1, all attempts to elute the intact crosslinked synaptic complex from agarose gels failed. Treatment of the synapsis reaction with DNA ligase immediately after restriction endonuclease digestion was problematic because the conditions did not favour efficient ligation. Therefore, the isolated *Pst*I + *Hin*dIII χ-form of the pMA21 synaptic complex was reacted with DNA ligase in a low-melting-point agarose gel slice, as detailed in Section 2.7g. The problem of obtaining

sufficient material to visualise after a second fractionation by gel electrophoresis was solved by pooling a number of χ-form bands extracted after in-gel ligation. Prior to electrophoresis, the samples were treated with DNase I to nick the DNA so that only knot nodes remained trapped in the ligated plasmid molecules (see Section 2.7f).

Figure 4.2 shows the results of agarose gel electrophoresis of various samples. Judging from the high proportion of *Pst*I-cleaved full-length linear pMA21 DNA converted to unknotted circular plasmid (lane 2), the in-gel ligation was efficient. This was confirmed by a second ligation control consisting of the 3862 bp and 1065 bp linear fragments that make up the *Pst*I + *Hin*dIII digested χ-form of pMA21 (lane 7). These DNA fragments were cut from the low melting point agarose gel, melted together, and set into a single block of agarose which was then treated in an identical fashion to the synaptic complex bands cut from the same gel. Most of the material ligated to give a 9854 bp linear DNA molecule, twice the size of full-length linear pMA21 and therefore indicative of efficient religation at both restriction sites, although the reason for the preferred formation of this particular ligation product is not known.

Species representing intra-complex ligation in both domains of the *Pst*I + *Hin*dIII χ-form of pMA21 were apparent, predominantly unknotted circle with traces of trefoil knot and 4-node knot (Figure 4.2, lanes 3 and 4). The presence of the minor species was confirmed by Southern blot (data not shown). Although about 80% of the sample shown in lane 3 had ligated, most was present either as full-length linear pMA21 (presumably singly-ligated χ-form) or as slower-migrating species arising from inter-complex ligation. Thus, although the distribution of the product arising from intra-complex ligation in both domains of the χ-form was consistent with only nodes arising from interaction of the accessory subsites being trapped by glutaraldehyde crosslinking, the low proportion of the total amount of χ-form represented makes any conclusion unreliable. When intra-complex ligation is so inefficient one has to consider the stability of the synaptic complex, as even the demonstrated low level of breakdown of crosslinked complex in the gel will be significant (see Section 3.2).

When the experiment was repeated with pMA2631, a plasmid containing two copies of the *res* site in inverted repeat orientation (see Figure 3.16), the observed products of intra-complex ligation in both domains of the χ-

form were unknotted circle and barely detectable trefoil knot; 4-node knot was not present (Figure 4.2, lanes 5 and 6).

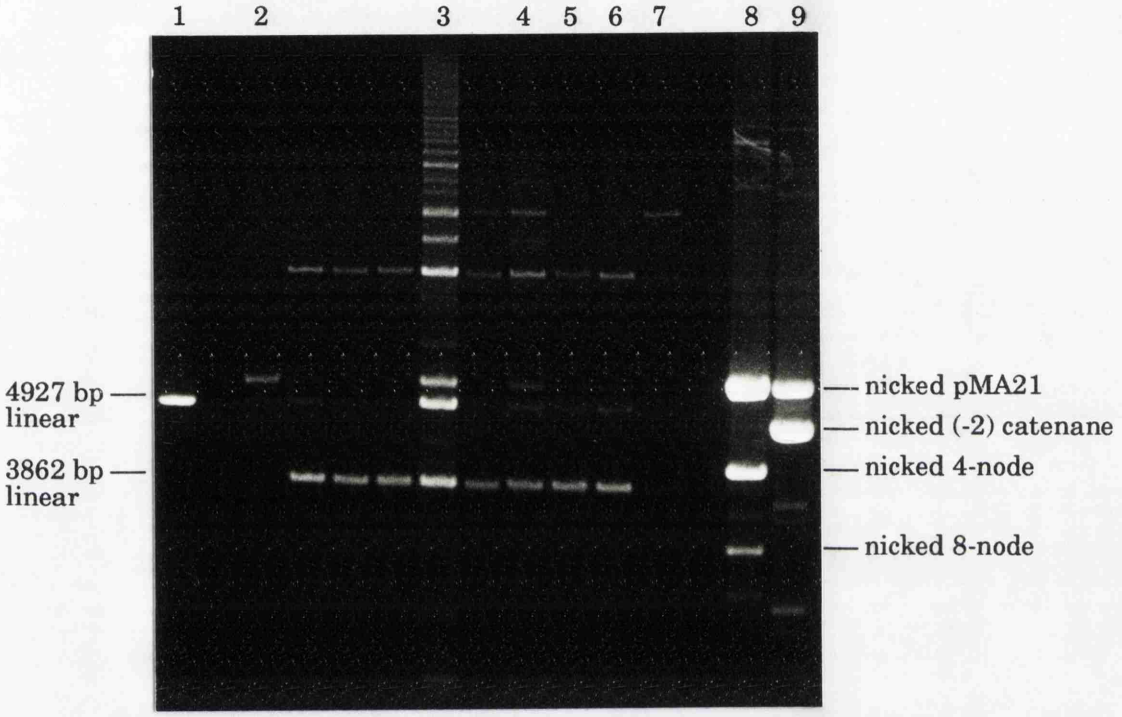

Figure 4.2 Agarose gel electrophoresis of DNA extracted from low-melting-point agarose after in-gel ligation of the crosslinked χ-form of the synaptic complex. The samples were treated with DNase I in order to nick the DNA, and with 0.2% SDS prior to electrophoresis.
The results of two independent experiments using the *Pst*I + *Hin*dIII χ-form of pMA21 (lanes 3 and 4), and the *Pst*I + *Hin*dIII χ-form of pMA2631 (lanes 5 and 6) are shown. Lanes 1 and 7 show in-gel ligation controls: *Pst*I-cleaved full-length linear pMA21, and the fragments of *Pst*I + *Hin*dIII digestion of pMA21, respectively. The un-numbered lanes show treatments of intermolecular synaptic complex bands; species present conform to those expected from the analysis presented in Section 3.7 and these data are not considered further. Lane 1 shows full-length linear pMA21, lane 8 a knotting reaction, and lane 9 a resolution reaction; the identity of the DNA markers generated is shown. Further details are given in the text.

0.8% agarose gel.

Modelling the inverted site synapse as identical to the direct repeat synapse in terms of antiparallel alignment of the accessory subsites and parallel alignment of the two copies of subsite I (see Figure 3.27b), results in any interwrapping of DNA in the subsite I synapse having no effect on knot topology following intra-complex ligation; trefoil knot is the simplest outcome. However, an even lower proportion of χ-form was ligated so as to regenerate circular pMA2631 DNA.

The preponderance of inter-complex ligation observed was probably due to a high local concentration of the χ-form in the excised electrophoretic band, and is therefore indicative of further problems arising from the inability to get the crosslinked synaptic complex out of the gel and into solution intact. Ligation of a χ-form with shorter-arms than those produced by *Pst*I + *Hin*dIII digestion of pMA21 would reduce the afore-mentioned possibility of tangling, but real progress on the elucidation of DNA topology in the crosslinked synapse awaits the isolation of stable synaptic complex at high yield in solution.

Benjamin and Cozzarelli (1988) investigated the topology of their cross-linked synaptic complex by topoisomerase I-mediated relaxation of the DNA followed by gel electrophoresis to compare the topoisomer distribution obtained from reactions in the presence and absence of resolvase. However, a number of details in the published report of these experiments were rather puzzling. Although the reported linking number difference of about –3 was apparent when a crosslinked resolvase synapsis reaction using a plasmid containing two *res* sites in direct repeat orientation was assayed, the shift in the topoisomer distribution appeared identical when the plasmid assayed contained only one *res* site. Furthermore, in the absence of resolvase, glutaraldehyde treatment had a marked effect on the topoisomer distribution as reproduced in the published paper, equivalent to a linking number difference of +1 (Benjamin and Cozzarelli, 1988). My own attempts to investigate the topological consequences of synapsis by measuring the linking number difference following topoisomerase I-mediated relaxation of the crosslinked synaptic complex were abandoned in the face of inconsistent results (data not shown).

4.2 Topological change introduced by interaction of resolvase with nicked plasmid DNA.

Plasmid DNA (~20 μg/ml), nicked by treatment with DNase I in the presence of ethidium bromide as described in Section 2.7f, was reacted with resolvase in a buffer containing 50 mM Tris-HCl (pH 8.2), 50 mM NaCl, 5 mM $MgCl_2$, 0.05 mM EDTA, 5 mM spermidine.3 HCl, 20% glycerol, 1 mM DTT, and 0.4 mM ATP (buffer E). After 10 minutes at 37°C, 0.3 units of T4 DNA ligase was added. This was followed, after an additional 15 minutes at 37°C, by 0.2 mg/ml proteinase K (see Section 2.15e). Although the ligation reaction was routinely left for 15 minutes, additional experiments revealed that the observed activity occurred within 10 seconds of the addition of ligase (data not shown). Samples were loaded on a 1.2% agarose gel with 3 μg/ml chloroquine in the gel and in the TAE buffer; electrophoresis (at room temperature), ethidium bromide staining, and photography were as described in Section 2.9. The presence of chloroquine, a DNA intercalator, results in positive supercoiling of the ligated plasmid DNA such that a topoisomer that was fully relaxed prior to electrophoresis migrates faster than topoisomers that contained trapped negative supercoils.

Figure 4.3 shows the results of this assay using pBR322 (no *res* site), pMA44 (one copy of the *res* site), and pMA21 (two copies of the *res* site in direct repeat orientation; see Figure 3.16). In each case, a titration with resolvase showed the effect of resolvase concentration on the topoisomer distribution obtained after ligation. Densitometry plots in the Y axis of each lane[2] are reproduced in Figure 4.4. For determination of the Gaussian centre of each topoisomer distribution, band intensities were taken from peak heights (Richardson *et al.*, 1988) (Figure 4.5); integration of peak area gave identical results. Each topoisomer differs from its neighbour by one unit of linking number (Lk). Therefore, the linking number difference ($Lk - Lk_0$) due to interaction of resolvase with the nicked plasmid DNA is determined by measuring the distance between

[2] After digitising a photographic print of the gel (Polaroid type 667 film) to obtain a 400 dpi TIF image file with 256 grey levels, half the lane width was sampled as a central bar in the Y axis of each lane (as orientated in Figure 4.3). This area (approximately 25 mm x 1.5 mm) was integrated across the image X axis in order to produce a single dimension data trace on the Y axis. The resulting densitometry plots have the image Y axis transferred to the X axis, such that the direction of electrophoresis is from left to right (see Figure 4.4). NIH Image version 1.41 (on the Apple Macintosh) and Quantiscan version 2.0 (Microbial Systems Ltd., on the PC) were used for the image analysis.

the centre of the distribution formed in the absence of resolvase and that formed in the presence of resolvase on a scale represented by the topoisomer bands (Figure 4.5). Following electrophoresis in the presence of chloroquine, if the centre of the topoisomer distribution formed in the presence of resolvase is retarded relative to that formed in the absence of resolvase, then Lk – Lk_0 is negative.

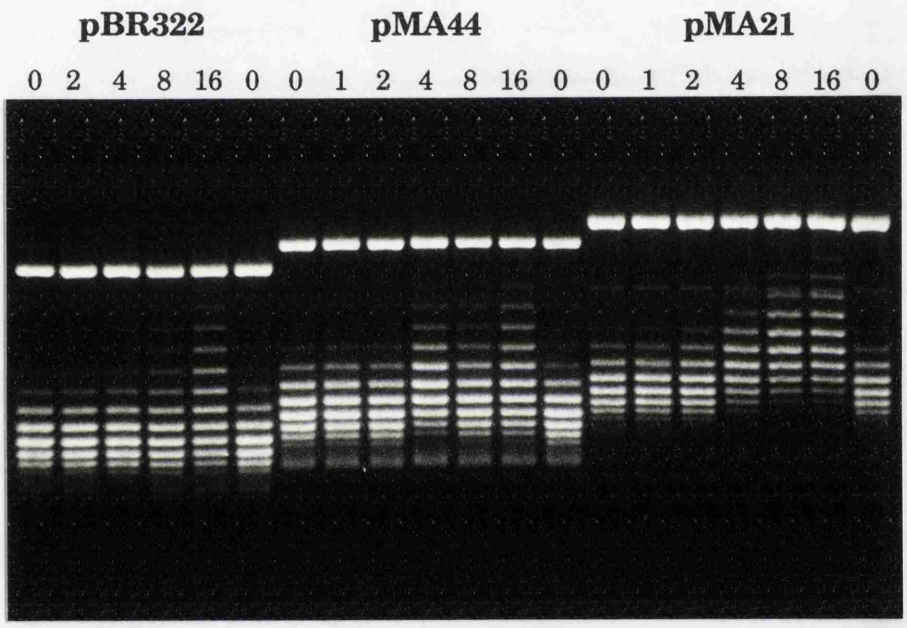

Figure 4.3 Agarose gel electrophoresis of nicked plasmid DNA reacted with resolvase, then ligated. A substantial shift of the centre of the topoisomer distribution in the presence of resolvase, equivalent to a linking number difference of about –2, is only seen when the plasmid contains two *res* sites in direct repeat orientation.
pBR322, pMA44, and pMA21 were assayed as described in the text. The increase in the concentration of resolvase through each titration is two-fold, as denoted by the numbering; 1 is equivalent to approximately 0.1 μM resolvase.

1.2% agarose gel; 3 μg/ml chloroquine.

Figure 4.4

Densitometry plots of individual lanes from the gel reproduced in Figure 4.3. The plots are oriented such that the direction of electrophoresis is from left to right. The approximate concentration of resolvase ([resolvase]) is given. The centre of the minus-resolvase topoisomer distribution is marked (dashed line). See the text for further details.

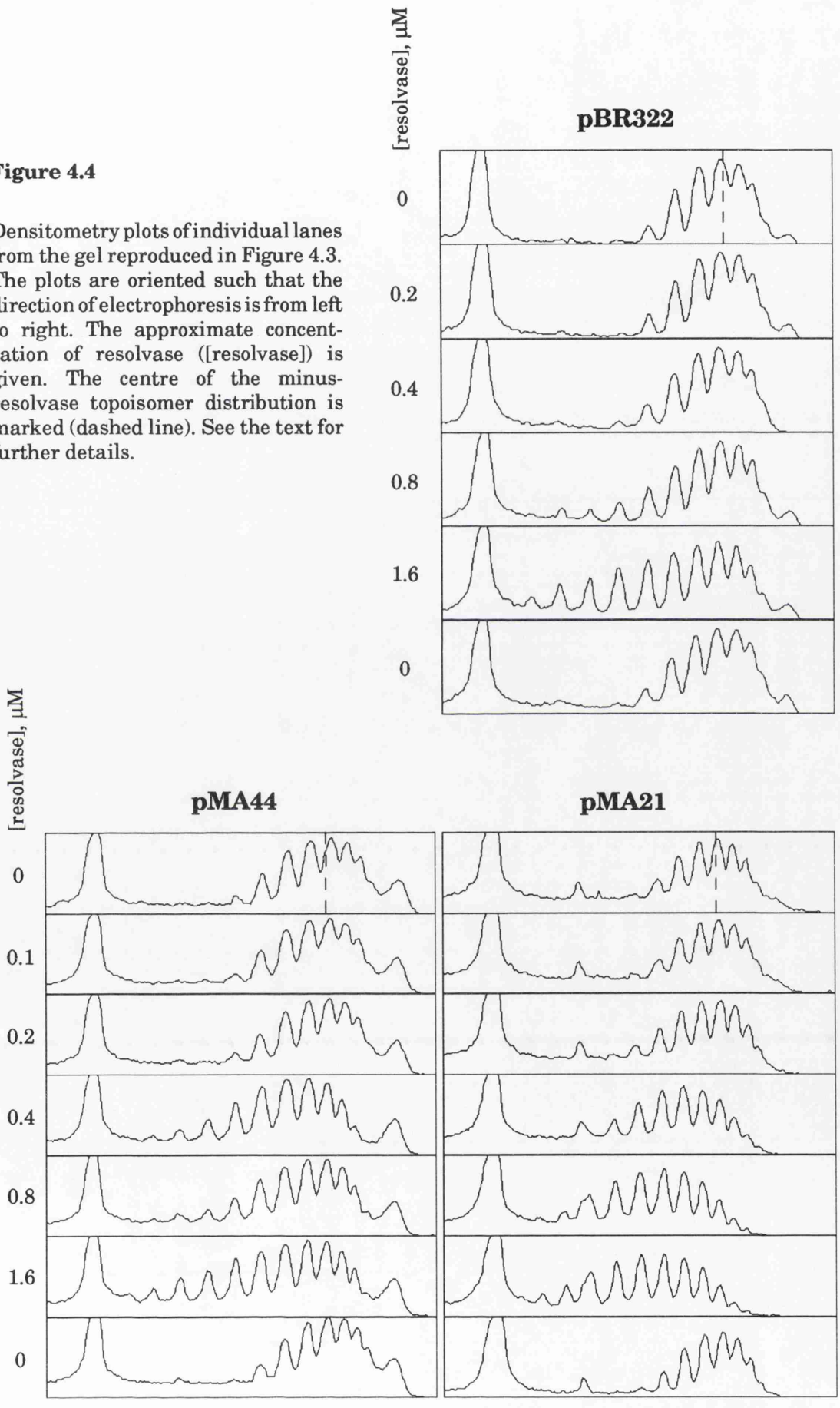

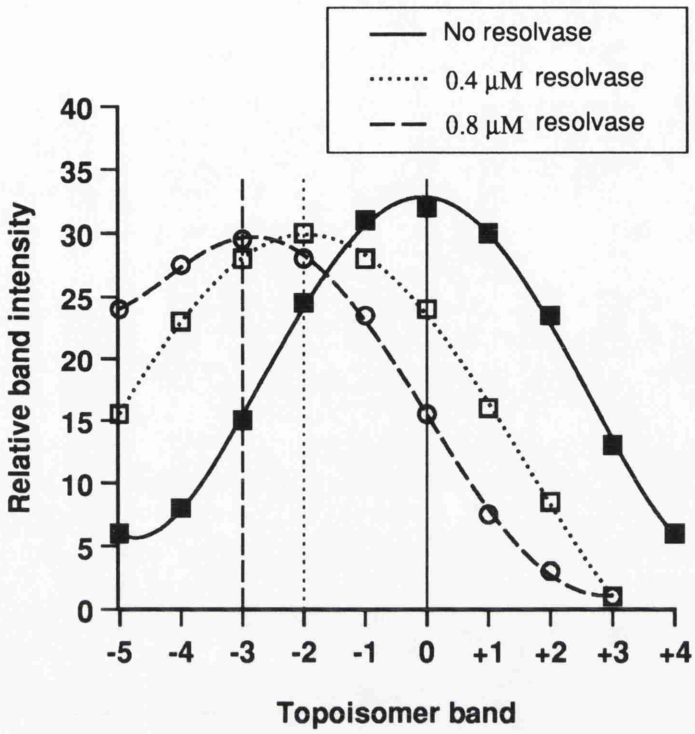

Figure 4.5 The shift of the centre of the pMA21 topoisomer distribution in the presence of resolvase. Topoisomer bands are numbered relative to the most intense band in the minus-resolvase topoisomer distribution, designated zero. Relative band intensity was determined from the height of peaks in the densitometry plot shown in Figure 4.4 (units are arbitrary); integration of peak area gave identical results. See the text for further details.

The linking number difference determined from densitometry plots derived from photographic prints of ethidium-stained gels as described above should be regarded as an approximate rather than an accurate measurement of $Lk - Lk_0$. Inaccuracies may be introduced by a non-linear response of the photographic film, by the digitisation procedure, and by the densitometry software.

Considering the data presented in Figures 4.3 and 4.4, the following points can be made:

- The presence of resolvase had no effect on the pBR322 topoisomer distribution, except at the highest concentration (approximately 1.6 μM resolvase), where a spreading out of the distribution occurred as more negatively supercoiled topoisomers increased in amount (Figure 4.4). The resulting shift of the centre of the topoisomer

distribution was equivalent to a linking number difference of about –0.5. This effect was consistently observed (with plasmids containing the *res* site as well as those lacking the *res* site), and was manifested at lower concentrations of resolvase when the concentration of DNA was reduced (data not shown); it probably results from the non-specific DNA binding activity of resolvase. In view of this 'non-specific' distortion of the topoisomer distribution, and the aforementioned inaccuracies inherent in the methodology, values of linking number difference ascribed to an interaction between resolvase and *res* site(s) are approximate.

- The observed shift of the centre of the pMA44 topoisomer distribution in the presence of resolvase, corresponding to a linking number difference of about –0.5, was consistent with that reported in a similar assay involving ligation of nicked plasmid containing a single *res* site (Benjamin and Cozzarelli, 1988). This shift occurred at a lower concentration of resolvase (0.4 μM) than the non-specific effect described above.
- In contrast to the behaviour of pBR322 and pMA44, the centre of the pMA21 topoisomer distribution shifted dramatically between the 0.2 μM and the 0.4 μM concentrations of resolvase (Figure 4.4). In the assay shown here, the shift was initially equivalent to an $Lk - Lk_0$ of –2, but changed to approximately –3 in the presence of 0.8 μM resolvase (Figure 4.5). However, this additional change in the linking number difference was not observed on other occasions, when the assay showed a single shift equivalent to an $Lk - Lk_0$ of approximately –2 which was maintained with increases in the resolvase concentration (see Figure 4.6). The observation of a discrete shift in the linking number difference, rather than a gradual change in response to the increasing concentration of resolvase, is indicative of the trapping of a specific interaction between resolvase and the DNA substrate.

The linking number difference of approximately –2, generally observed when pMA21 was assayed by this method, was four times that seen with a plasmid containing a single *res* site, and is proposed to indicate synapsis. In contrast, an $Lk - Lk_0$ of –1 determined for pMA2350 in the ligation assay (data not shown), is consistent with resolvase interacting with unsynapsed *res* sites. It may be that a failure to detect resolution of nicked pMA2350 when assayed under 'permissive' conditions (M.R. Boocock, personal communication) reflects an instability of the synaptic

complex formed by closely-spaced direct repeats of the *res* site. A failure to detect synapsis in the ligation assay is also consistent with the proposed instability of the synaptic complex formed by pMA2350, as judged by the results of crosslinking assays on supercoiled substrate (see Section 3.4). Although pMA2350 is resolved efficiently when in the supercoiled state, a failure to achieve the degree of synapse stability demanded by the crosslinking assay may indicate an inherent instability of the synapse that is manifested when the plasmid is relaxed.

Buffer E, similar to the 'permissive' buffers concocted to facilitate interaction of sites in DNA molecules, but with DTT and ATP present for the subsequent ligation reaction, was not essential for observation of the pMA21 linking number difference. When buffer E was replaced with the standard synapsis buffer (buffer C), supplemented with ATP, the linking number difference shown by pMA21 in the presence of resolvase at a concentration of 0.4 μM or above was about –2 (data not shown). However, the topoisomer distribution was better defined using buffer E, and the lower level of background fluorescence was advantageous for densitometry measurements.

Singly-nicked plasmid DNA (the predominant product of DNase I digestion in the presence of ethidium bromide) may produce an anomalously low linking number difference in this assay because of topology trapped in the un-nicked domain at synapsis (see Section 3.6). Therefore, pMA21 DNA was treated with DNase I in the absence of ethidium bromide in order to increase the occurrence of nicks in both domains of the plasmid (see Section 2.7f for details). When this preparation of nicked pMA21 was compared with a preparation nicked by DNase I treatment in the presence of ethidium bromide, the ligation assay produced identical results: a resolvase-dependent linking number difference of about –2 in each case (data not shown).

Figure 4.6 compares the shift of the pMA21 topoisomer distribution in the presence of resolvase with that of pMW13, a plasmid containing direct repeats of the accessory subsites of *res* (see Figure 3.23 for details of the construction of this plasmid). The densitometry plots revealed a linking number difference of –1.8 for pMA21, and about –1.3 for pMW13. In both cases, the transition from the topoisomer distribution seen in the absence of resolvase to one showing the full shift occurred over one doubling of the resolvase concentration, and there was no change when the resolvase

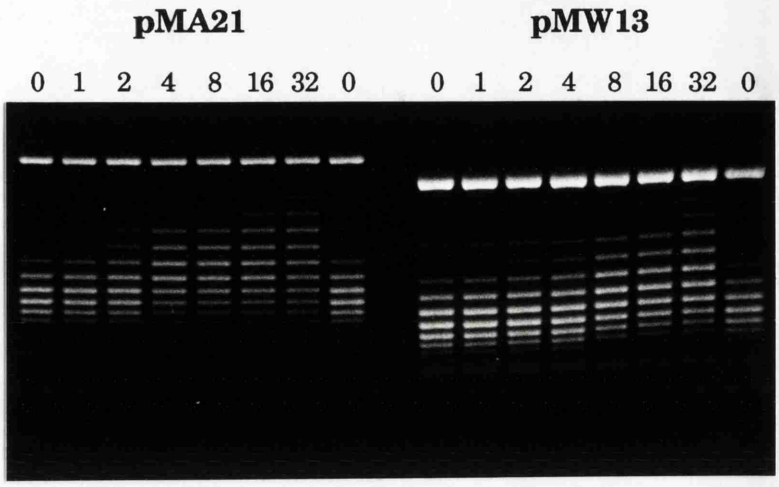

Figure 4.6 *above.* Agarose gel electrophoresis of nicked plasmid DNA reacted with resolvase, then ligated: the effect of increasing the concentration of resolvase on a plasmid containing two copies of the accessory subsites of *res* in direct repeat orientation (pMW13). pMA21 and pMW13 were assayed as described in the text. The increase in the concentration of resolvase through each titration is two-fold, as denoted by the numbering; 1 is equivalent to approximately 0.1 μM resolvase.

below. Densitometry plots of individual lanes taken from the gel reproduced above. The plots are oriented such that the direction of electrophoresis is from left to right. The approximate concentration of resolvase ([resolvase]) is given. The centre of the minus-resolvase topoisomer distribution is marked (dashed line). See the text for further details.

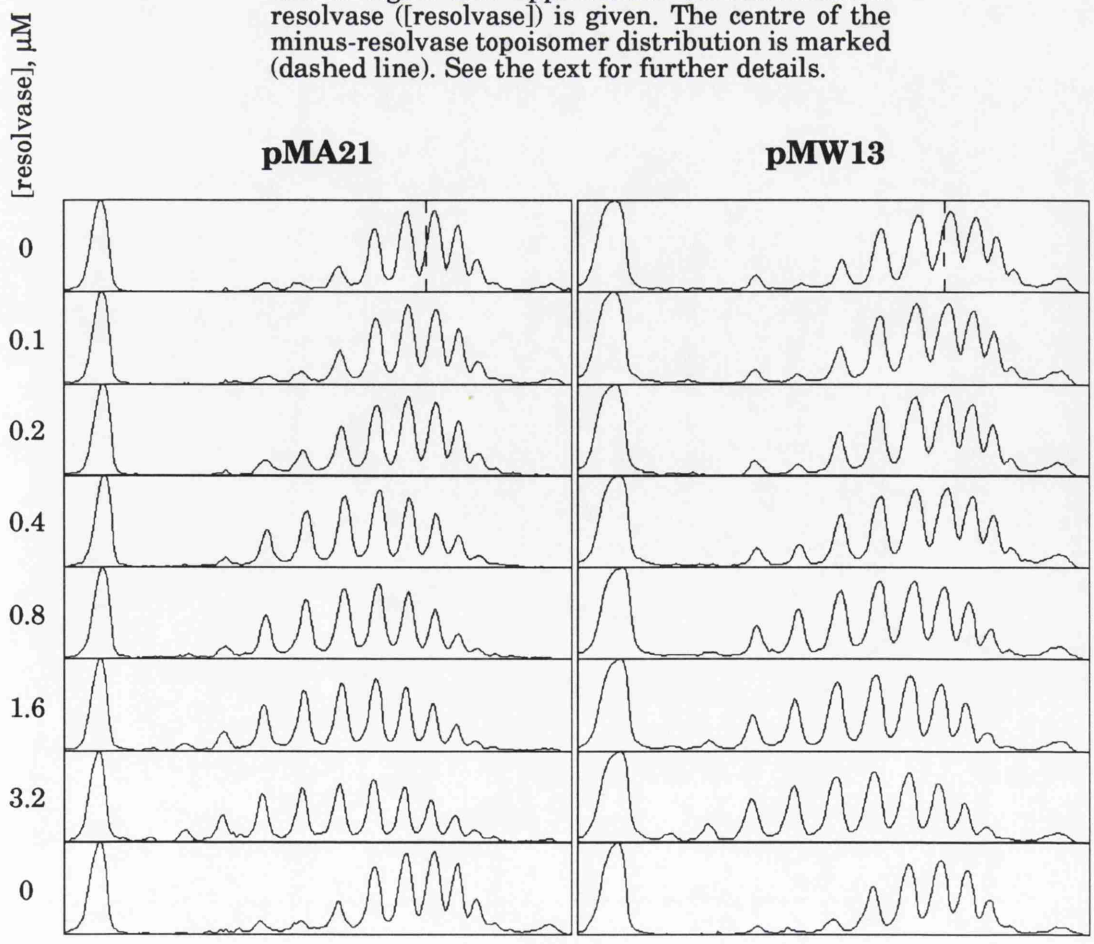

concentration was increased further. This transition occurred between 0.2 and 0.4 μM resolvase for pMA21, and between 0.4 and 0.8 μM resolvase for pMW13. This difference may be a reflection of the greater stability of the synapse formed when subsite I of *res* was present, consistent with the isolation of a higher yield of crosslinked synaptic complex from reactions containing pMA21 than was isolated from pMW13 reactions (see Figure 3.24).

The linking number difference of about –1.3 for pMW13 contrasts with no detectable shift for pMW11 (containing a single copy of the accessory subsites of *res*), and no shift for pMW14 (two copies of the accessory subsites in inverted repeat orientation; see Figure 3.23 for details of construction). This suggests that the $Lk - Lk_0$ of –1.3 observed for pMW13 was due to synapsis of the accessory subsites. The failure to observe a linking number difference when resolvase was added to pMW11 may result from instability of the single *res* site complex in the absence of subsite I, or a complex formed by subsites II and III alone may not trap the $Lk - Lk_0$ of about –0.5 characteristic of the single intact *res* site complex. A wrapped structure proposed for the resolvosome requires subsite I to be present as resolvase bound at this subsite is modelled as interacting with the resolvase-bound accessory subsites (Salvo and Grindley, 1988; Hughes *et al.*, 1990). Similarly, the failure to detect a linking number difference for pMW14 in the presence of resolvase may be because an inverted site synapse is not sufficiently stable in this assay. Indeed, the ligation assay failed to detect any linking number difference when nicked pMA2631, a plasmid containing inverted repeats of the intact *res* site (see Figure 3.16), was the substrate for resolvase (data not shown).

Figure 4.7 shows a time-course, with the addition of DNA ligase 10 seconds, 60 seconds, and 10 minutes after addition of resolvase to nicked pMA21 at 37°C. The demonstrated rapidity of the ligation reaction, probably an important factor in the detection of synapsis in an assay that does not involve protein crosslinking, suggested this to be a viable means of measuring the rate of synapsis. A linking number difference of approximately –1 was seen after 10 seconds in the presence of about 0.8 μM (or higher) resolvase, while the $Lk - Lk_0$ was about –1.8 when the incubation with resolvase was for 60 seconds or for 10 minutes (Figure 4.8). This may be an indication that there was a point as late as 10 seconds into the reaction of nicked substrate DNA when the synaptic

complex had either not yet formed in a yield required for detection in this assay, or was present as a structure differing from that detected after 1 minute.

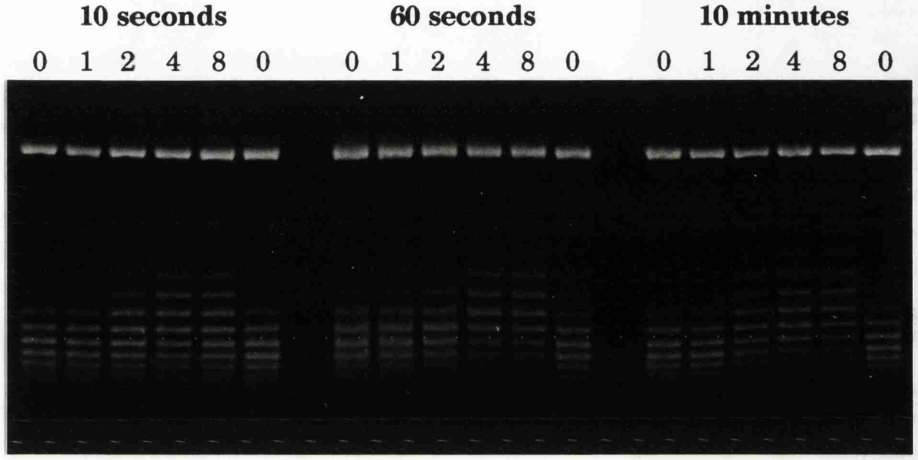

Figure 4.7 Agarose gel electrophoresis of nicked pMA21 DNA reacted with resolvase, then ligated after 10 seconds, 60 seconds, or 10 minutes.
The increase in the concentration of resolvase through each titration is two-fold, as denoted by the numbering; 1 is equivalent to approximately 0.2 μM resolvase. See the text for details.

1.2% agarose gel; 3 μg/ml chloroquine.

Isolation of the maximal amount of crosslinked synaptic complex formed from nicked pMA21 was achieved in the time required for the already present crosslinking reagent to stop the reaction (see Section 3.9). However, the yield of crosslinked synaptic complex obtained from nicked plasmid substrate was less than 10% of the input DNA. In the ligation assay, the proportion of subsequently ligated plasmid DNA present in a form that traps a linking number difference of about –2 must be high in order to produce a shift in the Gaussian centre of the topoisomer distribution. The synaptic complex trapped by protein crosslinking may differ in detail from a synaptic interaction reported by the ligation assay, since there is likely to be more than one substrate synaptic intermediate on the pathway to resolution product.

Figure 4.8

Densitometry plots of individual lanes from the gel reproduced in Figure 4.7. The plots are oriented such that the direction of electrophoresis is from left to right. The approximate concentration of resolvase ([resolvase]) is given. The centre of the minus-resolvase topoisomer distribution is marked (dashed line). See the text for further details.

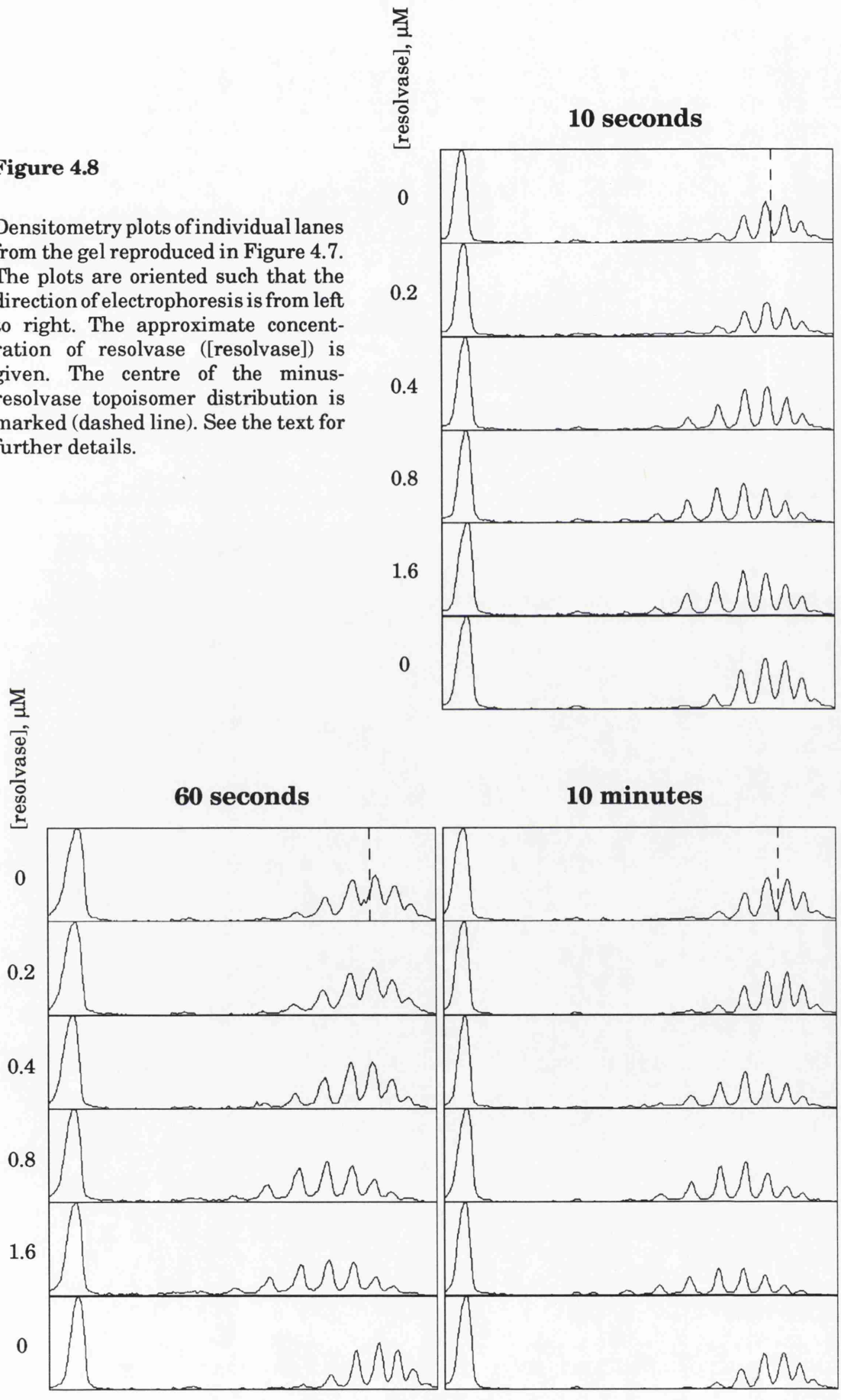

Because the ligation assay reports on the linking number difference of the DNA in the whole reaction mixture rather than an isolated synaptic complex, measurements will be influenced by any heterogeneity present. Thus, there exists the possibility that a number of different synaptic structures (perhaps including both genuine intermediates in the recombination reaction and unproductive complexes), as well as unsynapsed DNA molecules, contribute to an observed linking number difference in the presence of resolvase.

Chapter 5

Resolvase in the synaptic complex

Introduction.

Experiments presented in this Chapter were designed to elicit information on the multimeric state of crosslinked resolvase in the isolated synaptic complex. However, the requirement for large quantities of Tn*3* resolvase necessitated the preparation of a new batch of the purified protein. The opportunity was taken to modify the method used to date in this laboratory (M.R. Boocock, unpublished), primarily in order to increase the amount of purified resolvase obtained from a single run. Details of the procedure, derived from previously published methods (Reed, 1981; Symington, 1982; Krasnow and Cozzarelli, 1983), are given in Section 5.1.

The stoichiometry of the synaptic complex was estimated at 12 resolvase monomers per pair of *res* sites from the amount of Tn*3* resolvase required to generate maximal inhibition of Tn*21* resolvase-catalysed recombination in the synapsis assay of Parker and Halford (1991), described in Chapter 1. This figure is consistent with estimates of the concentration dependency of the resolvase-catalysed site-specific recombination reaction (Castell *et al.*, 1986).

Crosslinking of the protein component was required for the isolation and characterisation of resolvase-*res* synaptic complexes, as described in Chapter 3. This was also the case when Tn*3* resolvase-mediated synapsis of *res* sites was investigated by other workers (Benjamin and Cozzarelli, 1988). However, to date the only information on the multimeric state of resolvase in the synapse is in the form of inference from the interactions of γδ resolvase monomers in the absence of DNA, as revealed by X-ray crystallography, combined with studies of the behaviour of resolvase mutants produced by single amino acid substitutions. This powerful approach has recently shown that the 2-3' interface, an interaction between dimers represented in the crystal structure of the N-terminal domain of γδ resolvase, is not required for catalysis of strand exchange at subsite I (Grindley, 1993), (see Figure 5.3). Thus, it is unlikely that the crystalline 2,3/2',3' tetramer with 222 symmetry represents the resolvase assembly that mediates synapsis of the two copies of subsite I of *res*. The 2-3' interaction is required for recombination, presumably to fulfil a structural role elsewhere in the synapse (Grindley, 1994). This finding implicates the 1,2 dimer in catalysis in addition to its earlier identification as the solution and DNA-binding form of γδ resolvase

(Hughes *et al.*, 1993), (see Chapter 1). However, the means of interaction of subsite I-bound 1,2 dimers to form a catalytic assembly remains a mystery as there is no evidence of an appropriate direct interaction of 1,2 dimers in the crystal structure (Grindley, 1994).

In order to reconcile the absolute requirement for the 2-3' interaction in recombination with binding of the 1,2 dimer form of γδ resolvase to all the subsites of *res*, it was proposed that 1,2 dimers bound at each of the accessory subsites interact, each via one monomer, to form a single 2,3/2',3' tetramer (Hughes *et al.*, 1993). The resulting structure was represented in the crystal of γδ resolvase (Sanderson *et al.*, 1990). Thus, the subsite II/III synapse was modelled as an octamer of resolvase around which the DNA was wrapped to generate the predicted topology (Grindley, 1994), (Figure 5.1). However, there does not appear to be a corresponding absolute requirement for the 2-3 interactions that operate in the crystalline 2,3/2',3' tetramer. A mutation at the 2-3 interface of γδ resolvase (at L50 – see Figure 5.3) reduced the efficiency of recombination, but there was evidence that its deleterious effect on the single *res* site complex was more pronounced (Hughes *et al.*, 1993). When substituted for wild-type resolvase in gel retardation assays, the L50R mutant mediated intermolecular synapsis of linear fragments containing a single *res* site rather than formation of the resolvosome (Grindley, 1994). Further study, preferably by substitution of alternative amino acid residues, is required to gauge the importance of the 2-3 interface in synapsis.

It should be noted that experiments described in this Chapter were undertaken primarily in order to determine the multimeric state of resolvase as covalently crosslinked in the isolated synaptic complex. Although sufficient to increase the stability of the synaptic interaction under the conditions used to isolate synaptic complex, the crosslinking reagent will not necessarily have covalently linked all the monomers interacting in the form of a catalytically and/or structurally important multimer of resolvase. This will depend on the proximity of amino acid residues that are potential targets for the crosslinking reagent, complicated by the likely competition between inter- and intramolecular crosslinking reactions (see Section 5.2). Thus, determination of the multimeric state of crosslinked resolvase in the isolated synaptic complex does not allow one to distinguish definitively between models postulating assemblies of four, eight, or twelve interacting subunits of resolvase in

the synapse. However, the number of monomers crosslinked represents an important fact to be considered, alongside data from X-ray crystallography and a future determination of absolute stoichiometry, when attempting to model the synaptic complex formed by resolvase.

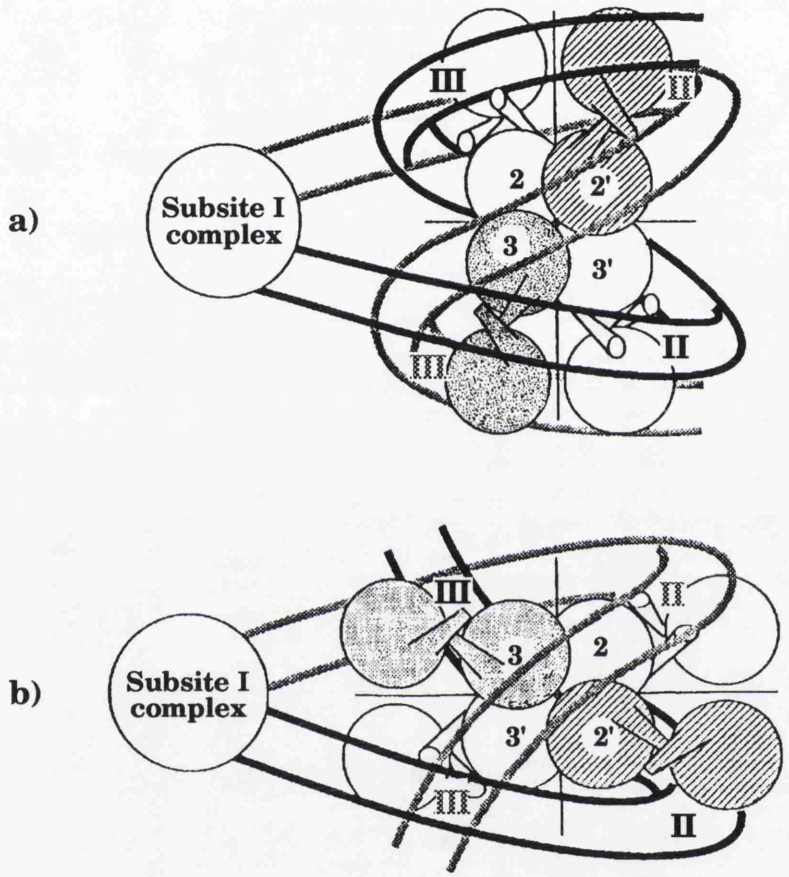

Figure 5.1 Alternative proposals for the involvement of a resolvase 2,3/2',3' tetramer in synapsis of the accessory subsites of *res*. In each case, subsites II and III of both *res* sites are bound by 1,2 dimers of resolvase, with only the N-terminal domains shown (each represented as a sphere with a protuberance to indicate the α-helix that mediates dimerisation – see Figure 5.3). The four 1,2 dimers interact, each via one monomer, to form the central tetramer. The structure of the subsite I synapse is not shown; at present the means of interaction of subsite I-bound 1,2 dimers to form a catalytic assembly is not clear. See the text for further details.
The organisation shown in **(b)** was proposed by Rice and Steitz (1994), who suggest that the subsite I-bound resolvase dimers sandwich the crossover site DNA in an assembly that is stabilised by a 2-3 interaction between subsite I- and subsite III-bound dimers. This model for pairing of the two copies of subsite I and the ensuing DNA strand exchange step is discussed in Chapter 1 (see Figure 1.8).

This figure was taken from the review of resolvase-mediated site-specific recombination by Grindley (1994).

The multimeric state of γδ resolvase *in vitro* in the absence of DNA was investigated by protein crosslinking followed by SDS-polyacrylamide gel electrophoresis (Liu *et al.*, 1993). The identification of the solution form of γδ resolvase as a dimer is consistent with data from chromatography and mutant studies (Grindley, 1994). Although there is evidence from chromatography experiments that Tn*3* resolvase is predominantly a dimer in solution (Symington, 1982), gel retardation experiments indicate that it binds DNA in the monomeric state (Blake, 1993).

There are few accounts in the literature of crosslinking of the protein component of a nucleoprotein complex in order to determine the multimeric state of the protein. This technique was used to investigate the quaternary structure of the MuA protein in the various intermediates isolated from the *in vitro* bacteriophage Mu DNA transposition reaction. The transposase, MuA, which exists as a monomer in the absence of DNA and when bound to unsynapsed Mu ends under normal conditions, was crosslinked in the form of a tetramer in the Type 0, 1, and 2 transpososomes (the stable synaptic, cleaved donor, and strand transfer complexes, respectively), (Lavoie *et al.*, 1991; Mizuuchi *et al.*, 1992; Baker *et al.*, 1993). The absolute stoichiometry determined for the Type 1 transpososome was consistent with there being a single tetramer bound to each DNA molecule (Baker *et al.*, 1993).

Despite the use of a number of experimental strategies, I was unable to establish the multimericity of crosslinked resolvase under the conditions used to isolate synaptic complex. However, the experiments presented in this Chapter resulted in some noteworthy observations that will hopefully contribute to future studies.

Results and Discussion.

5.1 Large-scale purification of Tn*3* resolvase.

The Tn*3* resolvase overproducing strain JM101(pMA6111), in which resolvase expression is under the control of the IPTG-inducible *tac* promoter, is described by Blake (1993). Growth of JM101(pMA6111) was in L-broth supplemented with 0.2% glucose, plus 100 μg/ml ampicillin to maintain selection for the plasmid. Throughout, 400 ml cultures were grown in 2 litre flasks with constant vigorous agitation at 37°C.

An overnight culture was diluted 1:40 to produce a starter culture which was grown to an OD_{600} (optical density at 600 nm wavelength) of 1.0. The starter culture was then diluted 1:40 into twenty 400 ml cultures which were grown to an OD_{600} of 1.9, whereupon expression of resolvase was induced. Induction of each culture was by addition of 400 ml L-broth containing 0.2% glucose, 100 μg/ml ampicillin, and 0.5 mM IPTG (giving a final concentration of 0.25 mM IPTG). Harvesting of cells began 4 hours after induction when the OD_{600} had reached 2.0.

Cells were harvested by centrifugation at 10 000 g for 5 minutes. Six pellets obtained from 16 litres of culture were each resuspended in 250 ml 20 mM K_2HPO_4 (pH 7.0), centrifuged as above, and the supernatant was removed. The total yield of cells (wet weight) was 88 g. Cell pellets were stored at –20°C.

The cell pellets were resuspended in 132 ml buffer F [KPM extraction buffer: 25 mM K_2HPO_4 (pH 7.0), 5 mM $MgCl_2$, 1 mM EDTA, 0.4 mM DTT, 1 mM benzamidine; 1.5 ml per gram of cells (wet weight)]. 1 ml of a 15 mg/ml solution of phenylmethyl sulphonyl fluoride (PMSF) in ethanol was added to the resuspended cells, dropwise with swirling. PMSF was added at various stages throughout the preparation to prevent proteolytic cleavage of resolvase in partially purified samples; in each case, PMSF was dissolved in ethanol immediately prior to addition. The cell suspension was sampled *[Sample A]*.

Throughout the above procedure the cell suspension was kept on ice; likewise, throughout this purification protocol, all solutions were maintained chilled on ice. Samples taken at various stages of the purification (noted as above) were analysed by SDS polyacrylamide gel electrophoresis (Figure 5.2), had the protein concentration estimated by Bradford assay (Bradford, 1976), and were assayed for resolvase activity (Table 5.1).

The cell suspension was passed through a French Press three times (maximum pressure set to 950 psi). 1 ml of 15 mg/ml PMSF was added after the first pass was completed and again after the third pass was completed. This resulted in 200 ml of a suspension of broken cells which was sampled *[Sample B]*.

100 ml of buffer F was added to the suspension of broken cells, followed by centrifugation at 48 000 g for 30 minutes at 4°C to remove cell debris. The supernatant was filtered through siliconised glass wool, the centrifugation step was repeated (15 minutes), and the supernatant was

again filtered through siliconised glass wool. 1 ml of 15 mg/ml PMSF was added to this crude extract (260 ml volume).

6.5 ml (1/40 total volume) of 200 mM spermine was added to the crude extract, dropwise with swirling. The solution was left for 15 minutes on ice after sampling *[Sample C]*. Addition of spermine (5 mM final concentration) leads to precipitation of DNA with resolvase bound, an established means of purifying resolvase (Reed, 1983). After centrifugation (48 000 g for 10 minutes at 4°C), the supernatant was removed and sampled *[Sample D]*. This discarded 'spermine supernatant' was visibly depleted in resolvase when compared with the crude extract by SDS-PAGE (Figure 5.2), while retaining a large proportion of the total protein (Table 5.1).

The pellet was resuspended in 120 ml '0.4 M NaCl cut buffer' (buffer F + 400 mM NaCl, 5 mM spermine, 0.6 mM PMSF, 0.5% ethanol) and centrifuged (48 000 g for 10 minutes at 4°C); the supernatant was removed and sampled *[Sample E]*. This process was repeated two more times, sampling the discarded supernatant each time *[Samples F and G]*. At a concentration of 0.4 M NaCl, resolvase remains bound to DNA, allowing purification from proteins that do not share this property. Some resolvase was lost with each of these 0.4 M NaCl cuts but they resulted in considerable purification of the resolvase remaining in the final pellet (see Figure 5.2).

The pellet was resuspended in 80 ml '1 M NaCl cut buffer' (buffer F +1 M NaCl, 5 mM spermine), and left on ice for approximately 90 minutes. The increase in the NaCl concentration allows resolvase to dissociate from the insoluble spermine-DNA complex. After centrifugation (48 000 g for 10 minutes at 4°C) to remove the spermine-DNA complex, the supernatant (78 ml volume) was recovered and sampled *[Sample H]*. The discarded pellet was also sampled *[Sample I]*. Again, loss of a significant amount of resolvase in the pellet was necessary in order to achieve further purification (Figure 5.2).

39 ml (½ volume) of a 90%-saturated ammonium sulphate solution was gradually added to the '1 M NaCl supernatant' stirring on ice. This 30% ammonium sulphate cut was left stirring on ice for 15 minutes. This step achieves further purification of resolvase. After centrifugation (48 000 g for 15 minutes at 4°C), the supernatant (112 ml volume) was recovered and sampled *[Sample J]*. The discarded pellet was also sampled *[Sample K]*.

270 mg/ml of solid ammonium sulphate was added gradually to the supernatant stirring on ice. This 50% ammonium sulphate cut was left stirring on ice for 20 minutes to allow precipitation of resolvase. After centrifugation (48 000 g for 15 minutes at 4°C), the supernatant was removed and sampled *[Sample L]*. This supernatant was estimated to contain less than 0.05 mg/ml protein (Table 5.1).

The pellet was resuspended in the minimum (12 ml) of 'AS resuspending buffer' (buffer F + 2 M NaCl, 1.2 mM PMSF, 1.0% ethanol). After centrifugation (to 48 000 g momentarily at 4°C), the supernatant was recovered. The discarded pellet was sampled *[Sample M]*. A considerable amount of resolvase remained in this pellet, estimated to contain about 50 mg of protein with a resolvase specific activity of some 18 000 units/mg (Table 5.1).

60 µl of a 20 mg/ml solution of PMSF was added to the supernatant. After centrifugation (60 000 g for 5 minutes at 4°C), the supernatant was recovered. The discarded pellet was sampled *[Sample N]*. Protein was not detected by Bradford assay, suggesting the resolvase detected by SDS-PAGE would not resuspend unless denatured.

The recovered supernatant was dialysed against buffer F + 200 mM NaCl, 1.2 mM PMSF, and 1.0% ethanol for about 4 hours to precipitate resolvase. After centrifugation (60 000 g for 5 minutes at 4°C), the supernatant was removed and sampled *[Sample O]*. Protein concentration was estimated at 0.32 mg/ml, while SDS-PAGE analysis indicated efficient precipitation of resolvase (Figure 5.2).

The large white pellet was resuspended in 6 ml buffer G ('S-200 equilibration buffer': 20 mM Tris-HCl (pH 7.5), 2 M NaCl, 0.1 mM EDTA). After centrifugation (60 000 g for 5 minutes at 4°C), the supernatant was recovered and sampled *[Sample P]*. This gave 6 ml of a solution suitable for fractionation by gel filtration chromatography, estimated to contain approximately 14 000 units/mg resolvase specific activity. The discarded pellet was sampled *[Sample Q]*. From the relative amount of resolvase in samples P and Q, as assayed by SDS-PAGE, more than 80% of the precipitated resolvase appeared to be resuspended (Figure 5.2).

Chromatography utilised a Pharmacia C 26/100 column packed with Sephacryl S-200 HR, according to the manufacturer's instructions, to give a bed height of 91 cm (packed gel volume = 482.3 cm^3). A Pharmacia P-1 peristaltic pump was connected. Throughout the chromatography run,

the pump setting was 4 x 10, giving a flow rate of approximately 22.5 ml/hour with the 1 mm internal diameter tubing used. The column was equilibrated with buffer G.

Column output was via a Waters 490E programmable multiwavelength detector with independent channels set to monitor absorbance at 280 nm, 215 nm, 260 nm, and the 260/280 nm absorbance ratio, respectively. A high 260/280 nm absorbance ratio is an indicator for the presence of DNA; the value was about 1.9 during elution of DNA, but fell to 0.9 when resolvase eluted from the column. The absorbance at 280 nm and 215 nm wavelength was recorded on a Goerz Metrawatt SE-120 chart recorder throughout the chromatography run for hard copy.

Column fractions were collected using a Pharmacia RediFrac fraction collector set to timed collection mode. A setting of 15 minutes per fraction was used throughout the period during which resolvase eluted from the column (as indicated by increase in absorbance at 215 nm and 280 nm wavelength). Chromatography was performed at an ambient temperature of about 4°C and the setup is illustrated below:

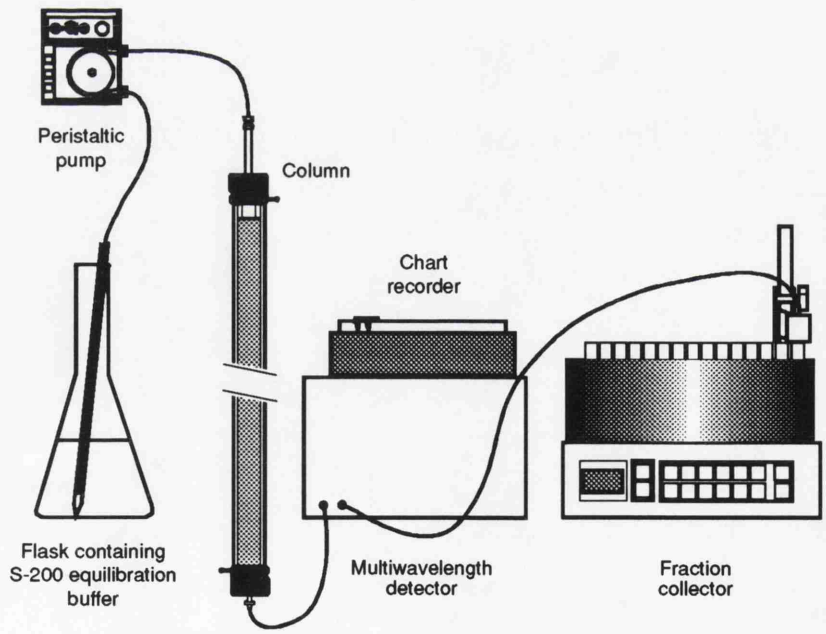

The 6 ml sample was applied to the column. DNA eluted from the column about 7 hours after the sample was loaded. Resolvase eluted about 10.5 hours after application of the sample, initiating a peak in absorbance at 215 nm and 280 nm that spanned eight 15 minute fractions (fractions 29-36). Each of these fractions was sampled and the samples were pooled

[Sample R]. Sampled fractions were also analysed individually by SDS-PAGE (Figure 5.2). In addition, the DNA peak (fraction 18) was sampled *[Sample S]*; the protein concentration of this sample was too low to be estimated by Bradford assay.

Fractions 29-36 were dialysed against buffer H (20 mM Tris-HCl (pH 7.5), 100 mM NaCl, 0.1 mM EDTA, 0.1 mM DTT, 1.2 mM PMSF, 1% ethanol) for approximately 5 hours to precipitate resolvase. The dense white precipitate was recovered by centrifugation in an Eppendorf microfuge at 14 000 rpm for 5 minutes. The supernatant was discarded, and the pellets resuspended in buffer I ('resolvase dissolving buffer': 20 mM Tris-HCl (pH 7.5), 2 M NaCl, 0.1 mM EDTA, 0.4 mM DTT). The five fractions that produced the centre of the resolvase absorbance peak were each resuspended in 300 µl of buffer I, while the other three fractions were resuspended in half that volume. The resuspended resolvase fractions were left on ice for about 45 minutes, then centrifuged (Eppendorf microfuge at 14 000 rpm for 5 minutes). 1 volume of glycerol was added to the recovered supernatant (there was no visible pellet), and the resolvase fractions were stored at -20°C.

Standard *in vitro* resolution assays (described in Section 2.15c) were performed on selected samples, and the resolvase activity present at various stages of the purification was determined[1]. This information is presented in Table 5.1. The total yield of resolvase was estimated to be about 27 mg; however, determination of resolvase concentration by comparison to bovine serum albumin standards in the Bradford assay is believed to underestimate the amount of resolvase present. Resolvase specific activity in the pooled column fractions (sample R) was estimated at ~7500 units/mg. The activity of the peak fraction (f 31) in its final form (plus-glycerol) was assayed at approximately 70 units/µl (Table 5.1).

---

[1] Resolvase activity is expressed in units.
1 unit = the amount of resolvase required for 50% resolution of 1 µg of pMA21 substrate DNA in a fixed time, under standard conditions.

The concentration of substrate DNA in the standard resolution assay is ~20 µg/ml.
At titration point, by definition, the concentration of resolvase ≡ 20 units/ml.

Therefore, the concentration of resolvase in a sample = $\frac{20 \times 20}{2^{-n}}$ units/ml

1/20 vol. of the sample dilution is present in the reaction

n = sample dilution at the titration point

The high resolvase activity in the sample taken from the suspension of broken cells (sample B; see Table 5.1) prompted speculation as to whether another component of the cell extract, lost with subsequent purification, was having a stimulatory effect on resolvase-catalysed site-specific recombination. There was some evidence of increased resolvase activity in the early stages of previous Tn*3* resolvase preparations (M.R. Boocock, personal communication). However, crude extract made from JM101 (albeit from cells broken by sonication rather than using the French Press) did not have any effect on the activity of purified resolvase in the *in vitro* resolution assay (data not shown).

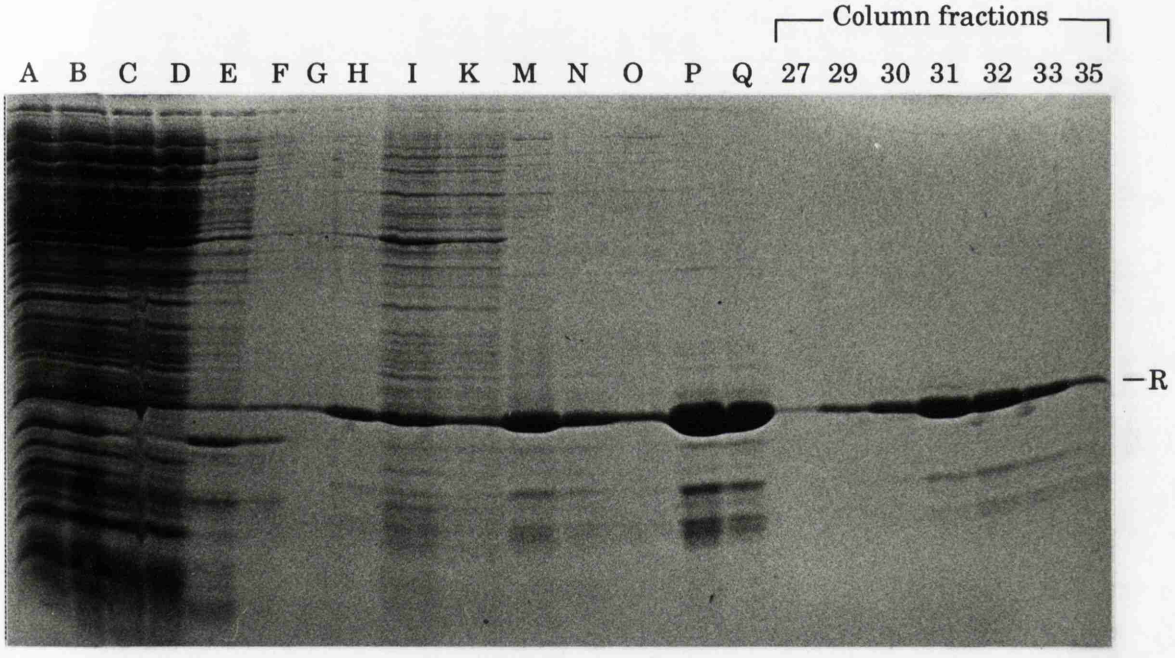

Figure 5.2 SDS-PAGE of selected samples taken at various stages of the Tn*3* resolvase purification. Samples are identified by the letter code used throughout the text, and are listed in Table 5.1. Fractions sampled direct from the chromatography column are identified by number.
The estimated fraction loaded of the total volume from which each sample was taken is given in Table 5.1 The position of resolvase is marked (R). See the text for further details.

15% polyacrylamide resolving gel; Coomassie stained.

Sample		Total vol. (ml)	[Protein] (mg/ml)	Protein (mg)	Units/ml	Units (yield)	Specific activity (units/mg)	Fraction loaded
Resuspended cells	A	ND	ND	ND	ND	ND	ND	2.5×10^{-5}
Broken cells (centrifuged)	B	200	ND	ND	>51200	$>102.4 \times 10^5$	ND	2.5×10^{-5}
Crude extract + spermine	C	260	15	3900	ND	ND	ND	1.9×10^{-5}
Spermine supernatant	D	266.5	15	3998	ND	ND	ND	1.9×10^{-5}
0.4 M cut 1	E	114	1.5	171	ND	ND	ND	8.3×10^{-5}
0.4 M cut 2	F	118	0.6	71	ND	ND	ND	8.3×10^{-5}
0.4 M cut 3	G	120	0.25	30	ND	ND	ND	8.3×10^{-5}
1.0 M NaCl supernatant	H	78	1.0	78	4526	3.53×10^5	4526	1.3×10^{-4}
Spermine pellet	I	260	ND	ND	ND	ND	ND	1.3×10^{-4}
30% AS supernatant	J	112	0.67	75	ND	ND	ND	-
30% AS pellet resusp.	K	6	ND	ND	ND	ND	ND	1.7×10^{-3}
50% AS supernatant	L	130	≤ 0.05	≤ 0.6	ND	ND	ND	-
50% AS pellet resusp.1	M	13.4	4.0	53.6	72408	9.70×10^5	18102	7.5×10^{-4}
50% AS pellet resusp.2	N	2	ND	ND	ND	ND	ND	5.0×10^{-3}
Low salt supernatant	O	18	0.32	5.8	ND	ND	ND	5.6×10^{-4}
S-200 load	P	6	5.0	30.0	72408	4.35×10^5	14482	1.7×10^{-3}
S-200 pellet resusp.	Q	2	ND	ND	ND	ND	ND	5.0×10^{-3}
S-200 pool (f29–f36)	R	$8 \times 5.6 = 44.8$	0.6	26.9	4526	2.03×10^5	7538	1.8×10^{-3} (individually)
S-200 fraction 18 (DNA peak)	S	5.6	<<0.05	-	ND	ND	ND	-
R28 fraction 31 (+ glycerol)	-	0.6	ND	ND	72408	0.43×10^5	ND	-

Table 5.1 Purification table for Tn*3* resolvase protein preparation R28. Samples were taken at various stages of the purification as noted in the text. Protein concentration was estimated by Bradford assay (Bradford, 1976); determination of resolvase activity (units/ml) is described in the text. ND = not determined. The 'fraction loaded' column refers to the amount of selected samples loaded on the gel shown in Figure 5.2, expressed as a fraction of the total volume from which the sample was taken.

5.2 The isolation of synaptic assemblies of resolvase: preliminary considerations.

Before presenting experiments designed to determine the multimeric state of resolvase, it will be informative to discuss several theoretical points that have a bearing on the experimental work.

As discussed in Chapter 1 and in the introduction to this Chapter, despite the lack of an obvious candidate for a synaptic assembly, the structure determined for γδ resolvase by X-ray crystallography has provided some insight into the interactions between subunits that may operate in the synaptic complex. Using published data (Sanderson *et al.*, 1990; Rice and Steitz, 1994), it is possible to consider the relative location in the crystal structure of amino acid residues that are the most likely targets for the crosslinking reagents used.

The primary amine group of lysine is the specific target of *N*-hydroxy-succinimide esters such as DSP and EGS, and is believed to be a preferred target for glutaraldehyde crosslinking (see Section 3.1). There are twelve lysine residues per Tn*3* resolvase monomer, ten of which are in the N-terminal domain as defined by limited proteolysis (Abdel-Meguid *et al.*, 1984). Figure 5.3 shows an α-carbon backbone representation of the crystal structure of γδ resolvase (amino acids 1-122) with seven lysine residues conserved in the primary sequence of γδ and Tn*3* resolvase marked. The remaining three lysine residues in the N-terminal domain of Tn*3* resolvase, at positions 134, 136, and 139 in the amino acid sequence, are in a region that is disordered in the crystal structure and may represent a flexible hinge linking the two domains of resolvase (see Chapter 1). These lysines may be crucial in crosslinking of a 1,2 dimer form, since the corresponding residues in different subunits could remain sufficiently close, although not located at the interface. In contrast, more than 20 Å separates lysine residues located in the N-terminal 120 amino acids of interacting monomers in the crystal structure of the 1,2 dimer (Sanderson *et al.*, 1990; Hughes *et al.*, 1993). This is too great a distance to be bridged by either DSP or EGS, which have maximum crosslinking distances of 12 Å and 16.1 Å, respectively. However, it is difficult to predict the range over which glutaraldehyde can crosslink because it is believed to act as a heterogeneous polymer, providing a wide spectrum of distances between the reactive groups (Jaenicke and Rudolph, 1989). Another unpredictable factor in the crosslinking reaction is the effect of

competing intra-subunit crosslinking on attempts to trap multimeric forms of resolvase.

The possibility of crosslinking resolvase subunits associated at the 2-3' interface between dimers appears more favourable, with lysine residues at positions 29 and 54 located at or close to the interface as represented in the crystal structure (Figure 5.3).

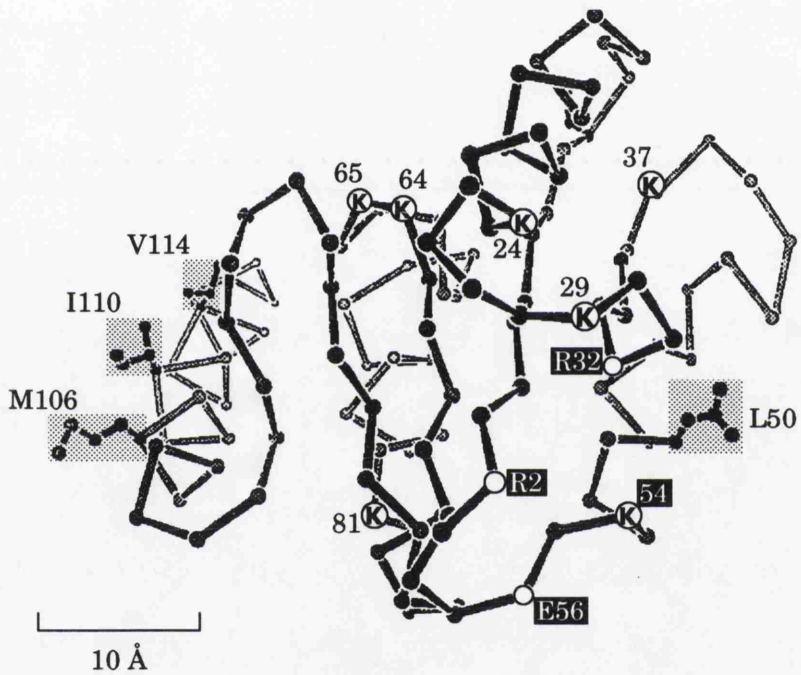

Figure 5.3 An α-carbon backbone representation of a single subunit from the crystal structure of the N-terminal domain of γδ resolvase; amino acids 1-122 are shown (Sanderson *et al.*, 1990). The locations of lysine (K) residues present in the primary sequence of Tn*3* resolvase are marked; in addition, γδ resolvase has lysines at positions 46 and 105. Several lysine residues are located in the putative hinge region that is disordered in all crystal structures determined to date (not shown).
Amino acid residues located at subunit dimerisation interfaces in the crystal structure have their side chains shown and are highlighted (grey boxes). M106, I110, and V114 lie at the 1-2 interface, while L50 is positioned at 2-3 interface. The α-carbons of R2, R32, K54, and E56, residues lying at the 2-3' interface (an interaction between resolvase dimers), are marked. See the text for further details.

This figure was adapted from Hughes *et al.* (1993).

An important consideration before any attempts were made to isolate crosslinked synaptic assemblies of resolvase was the means of detecting the protein following gel electrophoresis. Similar experiments carried out to determine the crosslinked form of the bacteriophage Mu transposase in synaptic intermediates, discussed in the introduction to this Chapter, used Western blotting and immunodetection to visualise the protein. However, antibodies to resolvase were not available and it was decided, after some preliminary experiments, that silver staining of polyacrylamide gels was a sufficiently sensitive means of detecting resolvase. The method of silver staining used, a non-diamine chemical protocol (Hames, 1990), is described in Section 2.14f. Briefly, fixation of protein bands in the gel is followed by reaction of protein groups with silver ions provided by addition of silver nitrate under acidic conditions. The principal reactive groups in the protein are believed to be free amines and those containing sulphur, although the process is poorly understood (Merril, 1990). Silver ions are reduced to metallic silver by the addition of formaldehyde under alkaline conditions. Image development, monitored by visual inspection, is halted by acidification.

The amount of monomeric resolvase readily detected by this silver staining procedure was estimated to be below 10 ng (data not shown). Although this represents some 30-fold less resolvase than is present in a 20 µl aliquot from a standard 0.8 µM resolvase synapsis reaction (20 µl being the volume normally loaded on an agarose gel), the amount of resolvase that is in the form of isolated intramolecular synaptic complex after crosslinking is considerably lower. Given the amount of pMA21 DNA present as χ-form in the standard synapsis assay, and assuming that twelve monomers of resolvase are involved in a synaptic complex, approximately 5% of the input resolvase was estimated to be present in the χ-form of the intramolecular synaptic complex isolated by agarose gel electrophoresis[2]. This is equivalent to about 16 ng of resolvase. In view of

---

[2] Approximately 35% of 0.6 µg of input pMA21 DNA (as determined by absorbance at 260 nm) is generally present as the χ-form of the intramolecular synaptic complex in a standard synapsis assay, i.e. about 0.2 µg of pMA21 DNA.
1 mole pMA21 ≈ 4927 x 660 ≈ 3.3×10^6 g.
Therefore, approximately $(2 \times 10^{-7} / 3.3 \times 10^6) \times 6.02 \times 10^{23} = 3.7 \times 10^{10}$ molecules of pMA21 are present as χ-form, each having 12 resolvase molecules bound.
Therefore, $(12 \times 3.7 \times 10^{10}) / 6.02 \times 10^{23} = 7.4 \times 10^{-13}$ moles of resolvase are present as χ-form. [N.B. This is equivalent to $7.4 \times 10^{-13} \times 2.15 \times 10^4 = 1.6 \times 10^{-8}$ g resolvase].
20 µl of 0.8 µM resolvase is equivalent to 1.6×10^{-11} moles of resolvase input.
Therefore, approximately 5% of the input resolvase is present as χ-form of the intramolecular synaptic complex in a standard synapsis assay.

the possibility of increasing the yield of synaptic complex by increasing the volume of the reaction and/or the concentration of reactants, silver staining was considered a feasible means of detection of the protein component.

Finally, the potential problem of determining the number of resolvase monomers participating in an isolated crosslinked species is worthy of discussion. In the experiments presented in the remainder of this Chapter, bands obtained following SDS-polyacrylamide gel electrophoresis (SDS-PAGE) were sized by comparing the gel mobility with that of protein molecular weight standards. However, crosslinking can lead to anomalous behaviour of proteins during SDS-PAGE. Inter- and intramolecular crosslinks can interfere with denaturation of the protein and prevent saturation with SDS (Hames, 1990). A resulting aberrant charge density will affect mobility during electrophoresis and this, combined with any effect on gel mobility of the loss of a fully extended polypeptide conformation, may render any size determination by co-migration with other proteins inaccurate. However, the number of crosslinked monomers represented by a given band can be determined if all the crosslinked forms from dimer up to the species of interest are also present in the gel. This may be the case without any experimental intervention or, if not, it can be achieved by limited cleavage of crosslinks prior to electrophoresis, an approach used in determining the multimeric state of MuA in a DNA transposition reaction intermediate (Lavoie *et al.*, 1991).

5.3 Crosslinking of resolvase in the absence of the *res* site.

Before presenting experiments that attempted to identify the crosslinked form of resolvase present in the isolated synaptic complex, I will describe observations made following crosslinking of resolvase in the absence of DNA or in the presence of non-specific DNA. As discussed in the introduction to this Chapter, there is good evidence that γδ resolvase exists as a dimer in solution, but the picture is not as clear for Tn*3* resolvase.

At the time the experiments presented in Chapter 5 were undertaken there was no published analysis of the effects of protein crosslinking on resolvase. Recently, SDS-polyacrylamide gel electrophoresis (SDS-PAGE)

following glutaraldehyde crosslinking of γδ resolvase in the absence of DNA was reported to show that both the intact protein and the N-terminal proteolytic fragment exist as dimers in solution (Liu *et al.*, 1993). However, in the absence of published gel photographs or any reference to the efficiency of crosslinking, it is impossible to comment on the yield of crosslinked multimeric forms of resolvase obtained by these workers.

Figure 5.4 shows the result of SDS-PAGE after glutaraldehyde crosslinking of approximately 20 μM Tn*3* resolvase in a reaction volume of 12 μl. Reactions were in buffer C, the standard synapsis assay buffer, both in the absence of DNA and in the presence of about 60 μg/ml pBR322. Various concentrations of glutaraldehyde were used, as detailed in the figure legend, and the crosslinking reaction was as described in Section 2.15c. Electrophoresis and silver staining of the polyacrylamide gel were as described in Section 2.14.

In the absence of DNA, treatment with 0.001% glutaraldehyde resulted in the appearance of four close-migrating bands at a position corresponding to between 39.5 and 45 kilodaltons (kDa), as determined by comparison of gel mobility with protein markers of known molecular weight (Figure 5.4, lane 2). Also apparent at this concentration of glutaraldehyde was a faint band migrating to the position expected for a larger crosslinked multimer of resolvase, with an estimated molecular weight of about 95 kDa suggesting it represents either an anomalously slow-migrating tetramer or a fast-migrating pentamer.

Despite the readily-detected amount of the 39.5-45 kDa species, which may represent forms of dimeric resolvase differing in gel mobility as a result of variation in intra- or intermolecular crosslinking interactions, most of the input resolvase remained in the monomeric state (~20.5 kDa) following treatment with 0.001% glutaraldehyde. An increase in the concentration of glutaraldehyde resulted in the loss of resolvase from the gel; at 0.01% glutaraldehyde only a trace of the monomeric form remained (Figure 5.4, lane 3), and at 0.1% glutaraldehyde there was no detectable resolvase (lane 4). The same details were noted when the crosslinking of resolvase was carried out in the presence of pBR322 DNA, but a higher concentration of glutaraldehyde was required for their observation (Figure 5.4, lanes 5-8). Thus, 0.01% glutaraldehyde was necessary to obtain a similar maximal yield of crosslinked species in the

gel, ten times the concentration required in the absence of DNA, and the protein failed to appear in the gel only after treatment with 0.1% glutaraldehyde, rather than with 0.01%.

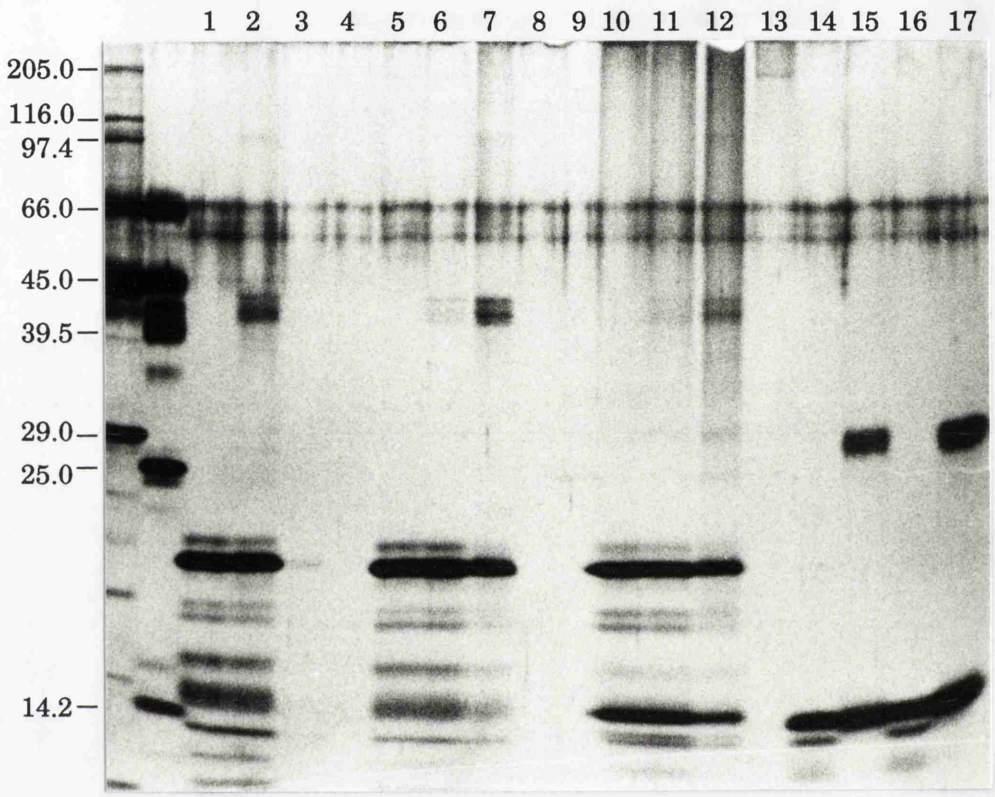

Figure 5.4 SDS-PAGE followed glutaraldehyde crosslinking of resolvase, or the N-terminal proteolytic fragment of resolvase, in the absence of DNA or in the presence of pBR322.
Lanes 1-4 show 20 μM resolvase reactions crosslinked in the absence of DNA; lanes 5-8 and lanes 10-13 both show reactions crosslinked in the presence of about 60 μg/ml pBR322 DNA, but differ in that the reactions shown in lanes 10-13 were treated with 2 μg/ml DNase I for 60 min. at 37°C prior to electrophoresis. The same amount of DNase I was loaded in lane 9 to identify proteins present in the nuclease preparation.
Lanes 14-17 show crosslinking reactions on the purified N-terminal proteolytic fragment of resolvase, in the absence of DNA (lanes 14 and 15) and in the presence of pBR322 (lanes 16 and 17).
The concentration of glutaraldehyde used was as follows: zero (lanes 1, 5, 10, 14, and 16), 0.001% (lanes 2, 6, and 11), 0.01% (lanes 3, 7, and 12), and 0.1% (lanes 4, 8, 13, 15, and 17). See the text for further details.
The sizes (kDa) of protein molecular weight standards are shown. The bands present in all lanes at about 60 kDa are artefacts commonly detected following silver-staining of protein gels (see Section 2.14f).

Buffer C; 15% polyacrylamide resolving gel; silver stained.

In a number of experiments involving titration of resolvase with different crosslinking reagents followed by SDS-PAGE, it was consistently the case that there was a relatively sharp transition going from most of the resolvase being present as monomer to most of the resolvase being absent from the gel (data not shown; see Section 5.4). The observation that this transition occurred at a lower concentration of crosslinking reagent in the absence of DNA suggested that precipitation of resolvase may be involved. In the absence of DNA, resolvase was reported to precipitate from solution when the NaCl concentration fell below about 500 mM (Reed, 1983; Krasnow and Cozzarelli, 1983). Indeed, purification of Tn*3* resolvase utilises this physical property, as described in Section 5.1.

The addition of glutaraldehyde at a concentration of 0.01% (or 0.1% in the presence of pBR322) may result in the formation of a crosslinked aggregate of resolvase too large to be resolved in a 15% polyacrylamide gel such as that reproduced in Figure 5.4. Indeed, there was no detectable protein in the 4% stacking gel, suggesting crosslinking of resolvase into a precipitate that remained insoluble despite the SDS-PAGE sample preparation treatment (heating to 90°C for 10 minutes in the presence of 2.5% SDS prior to electrophoresis).

In order to investigate whether aggregation of resolvase, followed by crosslinking to form an insoluble precipitate, was responsible for the absence of protein in the polyacrylamide gel, crosslinking was carried out in a buffer containing 1 M NaCl. The experiment was as described above, with the addition of a series of crosslinking reactions in buffer J (50 mM MOPS-NaOH (pH 8.0), 1 M NaCl, 1 mM EDTA) with no DNA present. In the absence of glutaraldehyde treatment, the amount of resolvase that migrated to the position of monomer in the gel appeared to be the same whether using buffer J (1 M NaCl) or buffer C (100 mM NaCl), (Figure 5.5, comparing lanes 1, 6, and 11). Thus, if precipitation occurred in buffer C in the absence of DNA, resolvase was efficiently redissolved by the aforementioned SDS-PAGE sample preparation treatment.

Crosslinking resulted in the loss of monomeric resolvase, regardless of whether the reaction was in buffer J, or in buffer C with or without pBR322 present (Figure 5.5). At the lowest concentration of glutaraldehyde used in this experiment (0.02%), there was no detectable monomeric resolvase following treatment in buffer C (lanes 7 and 12), while only a small amount was obtained from the buffer J reaction at this concentra-

tion of glutaraldehyde (lane 2). Subsequent experiments, in which crosslinks formed by treatment with dithio*bis*(succinimidylpropionate) (DSP) were cleaved prior to electrophoresis, showed that the disappearance of resolvase from the polyacrylamide gel was reversible (see Section 5.4).

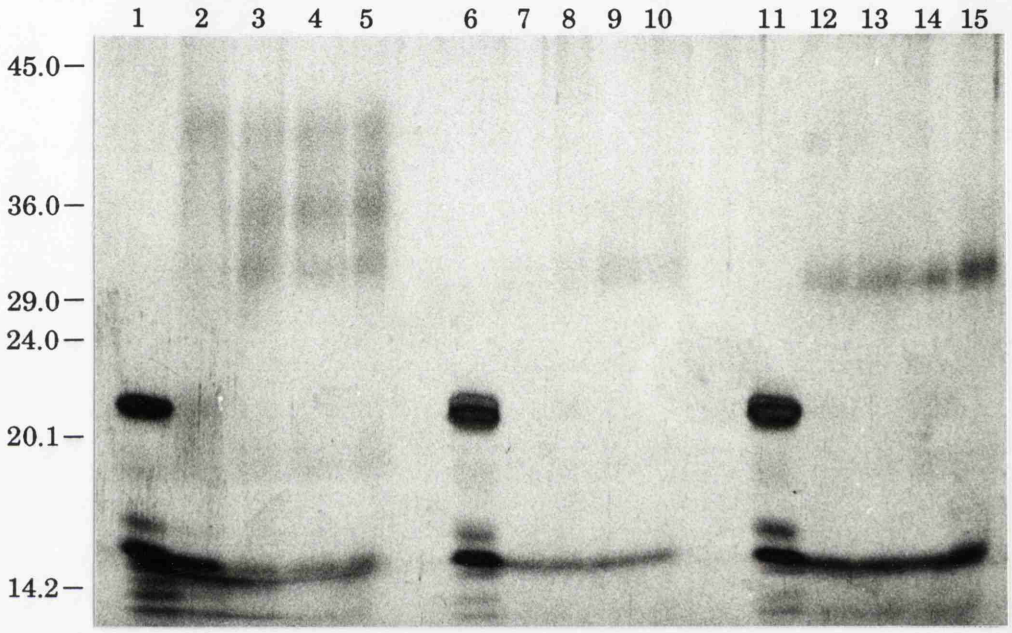

Figure 5.5 SDS-PAGE following glutaraldehyde crosslinking of resolvase in buffer J (1 M NaCl), or in buffer C (100 mM NaCl).
Lanes 1-5 show 20 μM resolvase reactions crosslinked in buffer J (1 M NaCl) in the absence of DNA. Lanes 6-10 and lanes 11-15 show reactions crosslinked in buffer C (100 mM NaCl), but differ in that the reactions shown in lanes 6-10 were crosslinked in the absence of DNA, while those shown in lanes 11-15 were crosslinked in the presence of about 60 μg/ml pBR322 DNA. The positions of co-electrophoresed protein molecular weight standards are shown (kDa).
The concentration of glutaraldehyde used was as follows: zero (lanes 1, 6, and 11), 0.02% (lanes 2, 7, and 12), 0.05% (lanes 3, 8, and 13), 0.1% (lanes 4, 9, and 14), and 0.2% (lanes 5, 10, and 15). See the text for further details.

Buffer C or buffer J; 15% polyacrylamide resolving gel; silver stained.

Species migrating at a lower rate than monomeric resolvase in the polyacrylamide gel were apparent following crosslinking, but the yield

was too low to account for the amount of monomeric resolvase lost (Figure 5.5). In buffer J, glutaraldehyde crosslinking produced very diffuse bands representing species of about 30, 35, and 42 kilodaltons (kDa) molecular weight. The 42 kDa species, believed to represent the crosslinked dimer of resolvase (although not present as four discrete bands as in Figure 5.4), predominated following treatment with 0.02% glutaraldehyde, while the 30 kDa and 35 kDa species appeared in greater yield as the concentration of glutaraldehyde was increased. After crosslinking in buffer C, only the 30 kDa species was present, with a considerable increase in amount when crosslinking of resolvase was in the presence of pBR322 DNA (Figure 5.5).

The 30 kDa and 35 kDa species were attributed to crosslinking of a homodimer formed by the N-terminal proteolytic fragment of resolvase, and a heterodimer formed by an interaction between intact resolvase and the N-terminal fragment, respectively. The preparation of purified resolvase used in this experiment contained more of the N-terminal proteolytic fragment than did the preparation used in the previous experiment. The 30 kDa and 35 kDa species were generally observed only when the resolvase used had a relatively large amount of the N-terminal fragment present as a contaminant. Furthermore, crosslinking of a preparation of the purified resolvase N-terminal fragment resulted in the efficient detection of a 30 kDa band which represented the only crosslinking-specific species (Figure 5.4, lanes 14-17).

The observations described suggest that the proposed aggregation of resolvase, leading to the formation of an insoluble precipitate after treatment with a protein crosslinking reagent, was aggravated by a reduction in the NaCl concentration from 1 M to 100 mM. This was hardly surprising in view of published data, although the loss of resolvase was considerable even at the higher NaCl concentration. In contrast, the N-terminal proteolytic fragment of resolvase was much less affected in this regard. Even in buffer C in the absence of DNA, a significant amount of uncrosslinked N-terminal fragment, and some of the 30 kDa homodimer, remained in the gel at all concentrations of glutaraldehyde used (Figure 5.5). Strikingly, in buffer C in the presence of pBR322, more than 50% of the N-terminal fragment appeared to be present, either in the uncrosslinked form or as the crosslinked 30 kDa homodimer, after treatment with 0.2% glutaraldehyde. When considered together with the observation of a complete absence of uncrosslinked

intact resolvase (or any crosslinked species of which it forms a part) following electrophoresis of the reactions carried out in buffer C, this suggests that the C-terminal DNA binding domain of resolvase may play a part in the proposed aggregation of the purified protein, even in the absence of DNA. This need not be a direct role in interactions between resolvase monomers, although the open question of how two 1,2 dimers interact in a catalytic assembly at subsite I of *res* does raise that possibility (see the introduction to this Chapter). Instead, a role in aggregation could be due to a contribution of the C-terminal domain toward the overall structure of resolvase which either increases the stability of interactions between monomers, or increases the potential of these interactions to be trapped by protein crosslinking.

In addition, a non-specific binding of resolvase to DNA could play a role in aggregation such that a crosslinked precipitate formed in the presence of pBR322 contains less of the N-terminal fragment, thus accounting for the observed enhanced selective retention of this species in the gel (Figure 5.5, lanes 11-15). Any DNA-mediated effect on crosslinking is not expected to involve covalent linkage of DNA and protein, since the DNA was readily freed when crosslinked synaptic complexes were treated with 0.2% SDS (Section 3.1). Indeed, there was no change in the amount of protein in the polyacrylamide gel when crosslinking reactions in the presence of pBR322 were treated with DNase I prior to electrophoresis (Figure 5.4, lanes 10-13).

Thus, the only major crosslinked form of resolvase observed in the absence of DNA or in the presence of DNA lacking the *res* site had a molecular weight of between 39.5 and 45 kDa as determined by co-electrophoresis of protein molecular weight standards. This is the size expected for a dimer of resolvase; but the yield of this species, comprising four close-migrating bands, was generally poor. The fact that crosslinking of the N-terminal fragment of resolvase into a dimer form was more efficient was probably not unconnected with the observation that it was considerably less prone to disappear from the gel when treated with crosslinking reagent.

The tendency for intact resolvase to fail to appear in the gel when treated with concentrations of glutaraldehyde above 0.02%, attributed to crosslinking of the aggregated protein, was not due simply to the high concentration of resolvase in the 12 µl volume crosslinking reactions. This

concentration of resolvase was dictated by a wish to have sufficient input resolvase for detection of minor crosslinked species, while being able to load the reaction onto the gel without any prior concentration of protein. However, when the resolvase concentration was reduced from 20 μM to 1.5 μM by increasing the crosslinking reaction volume to 160 μl, followed by precipitation of the protein in order to load a smaller volume onto the gel (see Section 2.12), there was no change in the concentration of cross-linking reagent required to give the same optimal yield of putative dimer form, or in the concentration that led to the total disappearance of resolvase from the gel (data not shown; see Figure 5.7).

Crosslinking of resolvase in the absence of DNA using 1-ethyl-3-(3-dimethylaminopropyl)carbodiimide hydrochloride (EDC) produced the 30 kDa, 35 kDa, and 40 kDa species in low yield, but did not result in the disappearance of resolvase at the concentrations used (up to 100 mM EDC; data not shown). However, treatment with EDC, which covalently links salt bridges (see Section 3.1), did have a profound effect on resolvase, producing considerable retardation of bands and a smeared appearance. This suggests that the major effect of EDC is to mediate intra- rather than intermolecular crosslinking of resolvase.

5.4 Crosslinking of resolvase in the presence of two copies of the *res* site in direct repeat orientation.

Figure 5.6 shows the result of SDS-PAGE after crosslinking of resolvase in the presence of pMA21 in buffer C. As in the experiments described in Section 5.3, crosslinking reactions were in 12 μl volume containing approximately 20 μM resolvase. However, in this experiment, the amount of DNA present (pMA21) was about 180 μg/ml, giving a resolvase:DNA ratio closer to that in the standard synapsis assay described in Section 3.1, albeit with both resolvase and pMA21 at a much higher concentration.

The observed behaviour of resolvase when crosslinked in the presence of pMA21 was similar to that seen in the presence of pBR322 (described in Section 5.3). A group of four bands at the position expected for a dimer of resolvase (migrating midway between the 39.5 kDa and 45 kDa protein markers) was present in maximal yield after crosslinking with 0.01% glutaraldehyde (Figure 5.6, lane 3). The slowest-migrating of these

species was present in greater amount than the other three, but the significance of this is unknown; as mentioned in Section 5.3, they may exhibit different gel mobility because of differential crosslinking of the dimer. The yield of these crosslinked dimer forms of resolvase is difficult to estimate, but probably represents less than 1% of the input resolvase. In addition, there were a number of other crosslinked species present in considerably lesser amounts: two faster-migrating species, and what appeared to be a ladder of slower-migrating multimeric forms corresponding in size to the trimer, tetramer, and pentamer of resolvase. Use of 0.1% glutaraldehyde once again resulted in the loss of most of the resolvase from the gel (Figure 5.6, lane 4). When otherwise identical reactions were performed in the presence of 10 mM $MgCl_2$, the results were virtually identical (lanes 5-8).

Crosslinking with dithio*bis*(succinimidylpropionate) (DSP), in a set of reactions corresponding to the minus-$MgCl_2$ glutaraldehyde-crosslinked reactions discussed above, produced similar results (Figure 5.6, lanes 9-13). The maximal yield of the dimer-sized crosslinked forms of resolvase followed treatment with 10 μM DSP. After crosslinking with 1 mM DSP virtually all of the resolvase had disappeared (Figure 5.6, lane 13). Treatment of the DSP crosslinked reactions with 10 mM dithiothreitol (DTT), followed by 30 minutes incubation at 37°C to cleave the crosslinks, resulted in loss of all the bands proposed to represent crosslinked multimers of resolvase (lane 15 shows a DTT treatment of the 10 μM DSP crosslinked reaction).

In addition, DTT treatment of the 1 mM DSP-crosslinked reaction effected a return of the absent resolvase, mostly to the position of monomer in the gel (with the smeared appearance indicating that some intramolecular crosslinks remained resistant to disulphide reduction), (Figure 5.6, lane 17). This is consistent with the hypothesis that the loss of resolvase was due to crosslinking to form an insoluble aggregate (see Section 5.3). Attempts to selectively cleave DSP crosslinks by titration with DTT did not result in the return of any multimeric form larger than the dimer; the reappearance of the bulk of input resolvase to the position of monomer in the gel was as sudden as its disappearance (data not shown).

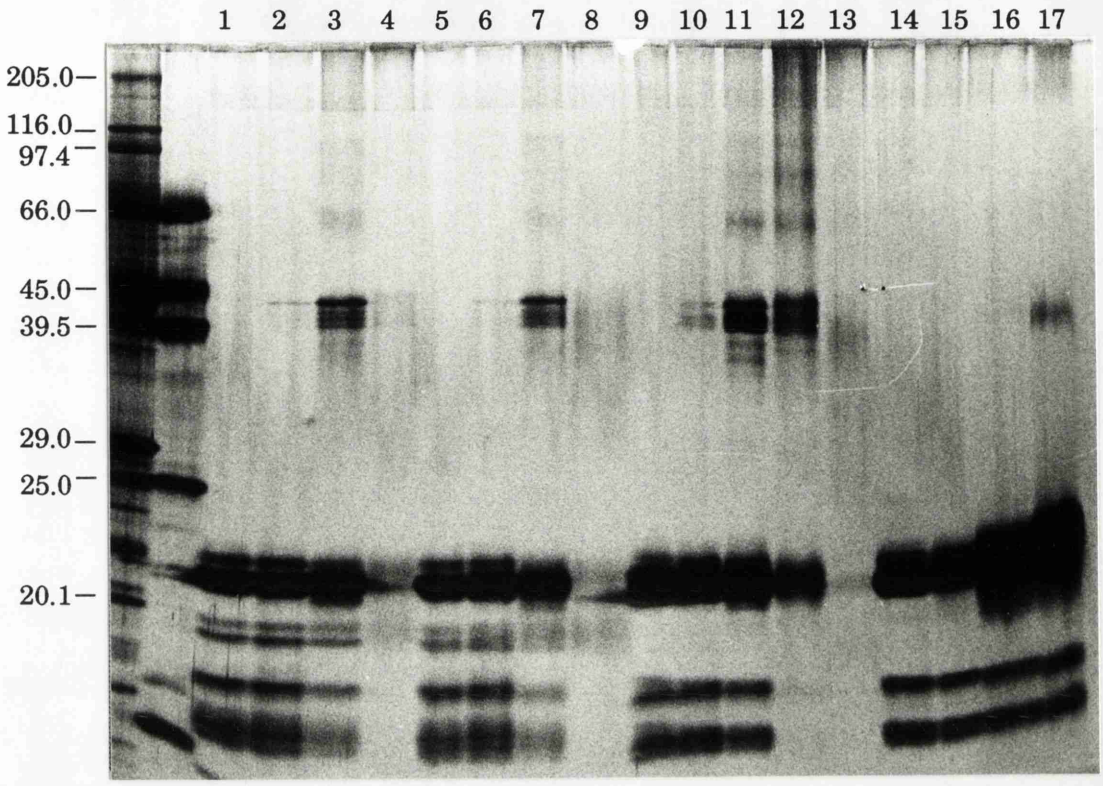

Figure 5.6 SDS-PAGE of glutaraldehyde- or DSP-crosslinked pMA21 synapsis reactions.
Lanes 1-4 show glutaraldehyde crosslinking of 20 μM resolvase in buffer C in the presence of about 180 μg/ml pMA21 DNA. Reactions shown in lanes 5-8 differ in that 10 mM $MgCl_2$ was included. The concentration of glutaraldehyde used was as follows: zero (lanes 1 and 5), 0.001% (lanes 2 and 6), 0.01% (lanes 3 and 7), and 0.1% (lanes 4 and 8).
Reactions shown in lanes 9-13 were crosslinked with DSP instead of glutaraldehyde, but were otherwise identical to those shown in lanes 1-4. Lanes 14-17 show DTT treatments of the reactions shown in lanes 9, 11, 12, and 13, respectively. The concentration of DSP used was as follows: zero (lanes 9 and 14), 1 μM (lane 10), 10 μM (lanes 11 and 15), 100 μM (lanes 12 and 16), and 1 mM (lanes 13 and 17). See the text for further details.
The sizes (kDa) of protein molecular weight standards are shown.

Buffer C +/– 10 mM $MgCl_2$; 15% polyacrylamide resolving gel; silver stained.

Figure 5.7 shows the result of DSP crosslinking in a larger reaction volume. 160 μl reactions containing 1.5 μM resolvase and 20 μg/ml pMA21 DNA were treated with various concentrations of DSP (see Section 2.15d). Protein was recovered by precipitation: addition of 0.1%

SDS and 300 mM potassium acetate was followed by 30 minutes incubation on ice, then centrifugation at 14 000 rpm for 15 minutes (Section 2.12). This procedure, in contrast to methods using acetone or ethanol to precipitate the protein, resulted in quantitative recovery of resolvase. The result obtained following SDS-PAGE was virtually identical to that seen when resolvase was crosslinked in the smaller reaction volume (as described above), with the maximal yield of crosslinked multimers obtained with 10 μM DSP (Figure 5.7, lane 3), and loss of resolvase at 1 mM DSP (lane 5).

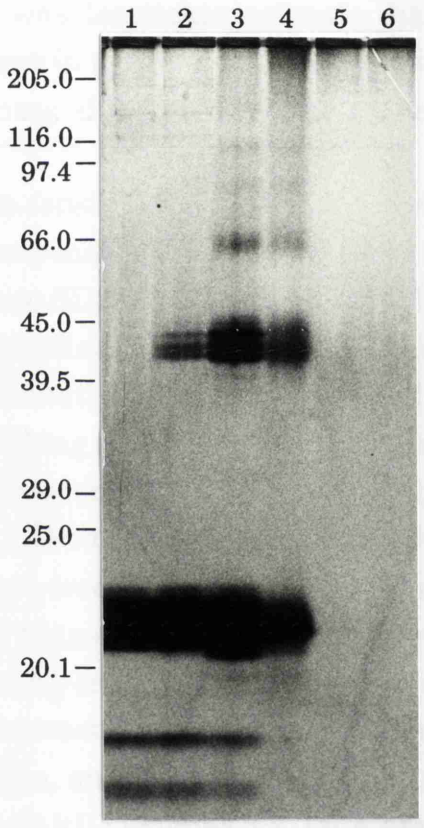

Figure 5.7 SDS-PAGE of DSP-crosslinked pMA21 synapsis reactions.
Lanes 1-6 show DSP crosslinking of 1.5 μM resolvase in buffer C in the presence of about 20 μg/ml pMA21 DNA. Protein was concentrated from the reaction volume of 160 μl by SDS/potassium acetate precipitation. The concentration of DSP used was as follows: zero (lane 1), 1 μM (lane 2), 10 μM (lane 3), 100 μM (lane 4), 1 mM (lane 5), and 2 mM (lane 6). See the text for further details.
The positions of co-electrophoresed protein molecular weight standards are shown (kDa).

Buffer C; 15% polyacrylamide resolving gel; silver stained.

Attempts to visualise the crosslinked protein component extracted from the χ-form of the intramolecular synaptic complex isolated by agarose gel electrophoresis were unsuccessful (data not shown). This was despite the use of various methods to extract protein from the agarose gel, or from DEAE membrane containing the electroeluted χ-form band (see Section 2.10). Loading an agarose gel chip containing isolated synaptic complex directly onto the polyacrylamide gel, either in the melted state or as solid agarose, did not produce any detectable protein after SDS-PAGE. All attempts to visualise the protein component by these means after increasing the yield of synaptic complex isolated in the agarose gel by 10-fold over that obtained in the standard synapsis assay similarly failed (data not shown). This was despite an estimate that there should be sufficient protein present in this amount of synaptic complex to be readily detected by silver staining after SDS-PAGE (see Section 5.2).

In order to increase the sensitivity of detection, it was decided to radio-iodinate the protein component extracted from the isolated crosslinked synaptic complex prior to SDS-PAGE, then detect fractionated protein by autoradiography. Radioiodination was as described in Section 2.13. The stock resolvase was efficiently labelled by this method; however there was evidence of crosslinking mediated by the iodination treatment (data not shown). Figure 5.8 reproduces an autoradiograph, the protein being derived from the α- or χ-form of the synaptic complex isolated in a standard glutaraldehyde-crosslinked synapsis assay; a lower concentration of the crosslinking reagent (0.01%) was used in addition to the standard 0.05%. Following crosslinking with 0.01% glutaraldehyde, radioiodination of the extracted χ-form produced faint diffuse bands at about 60 kDa and 20 kDa, and a more intense signal in the form of a sharper band at about 18 kDa (Figure 5.8, lane 1). A considerable amount of radioactive label remaining in the wells of the polyacrylamide gel and at the interface between stacking and resolving gels was apparent with all samples; its source is not known, although it may represent a radio-iodinated contaminant derived from the agarose. With 0.05% glutaralde-hyde, both the α- and χ-forms of the synaptic complex produced what appeared to be three diffuse bands migrating between 52 kDa (the stronger signal) and 70 kDa, together with a 30 kDa band unique to the χ -form (lanes 2 and 3).

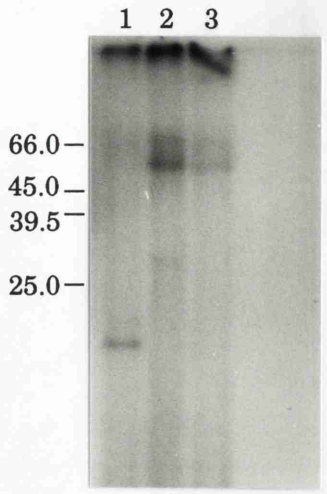

Figure 5.8 SDS-PAGE of the glutaraldehyde-crosslinked pMA21 substrate synaptic complex isolated by agarose gel electrophoresis: radioiodination of the protein component.
α- or χ-forms of the pMA21 substrate synaptic complex, isolated from standard synapsis reactions after glutaraldehyde crosslinking and agarose gel electrophoresis (as described in Section 3.1), were eluted from the agarose gel and iodinated. ^{125}I-labelled species were detected by autoradiography following SDS-PAGE.
Lane 1 shows material derived from 0.01% glutaraldehyde-crosslinked χ-form; lanes 2 and 3 show material derived from 0.05% glutaraldehyde-crosslinked α- or χ-forms, respectively. The positions of co-electrophoresed protein molecular weight standards are shown (kDa).

Buffer C; 0.01% or 0.05% glutaraldehyde; 1.2% agarose gel; 15% polyacrylamide resolving gel.

An interpretation of these results is that the species migrating between 52 and 70 kDa represent crosslinked resolvase multimers. Although they migrate around trimer size, the possibility of an aberrantly migrating dimer or tetramer should not be discounted (see Section 5.2). The observation that most of the signal in the resolving gel following crosslinking with 0.01% glutaraldehyde migrated to a position expected for an 18 kDa polypeptide is difficult to explain. This band could represent monomeric resolvase migrating at an increased rate due to intramolecular crosslinking. However, it was derived from an isolated crosslinked synaptic complex, presumably held together by inter-molecular crosslinking of resolvase despite being trapped with a lower concentration of glutaraldehyde than that determined optimal.

The aforementioned observation of intermolecular crosslinking of resolvase by the iodination treatment renders this an unsuitable method for the investigation of crosslinked multimers of resolvase. Use of a cleavable crosslinking reagent for the initial isolation of synaptic complex would enable the identification of protein multimers crosslinked prior to iodination. However, iodination of DSP-crosslinked synaptic complexes was problematic because a chemical reduction step, which results in cleavage of DSP crosslinks, was a necessary part of the iodination procedure (see Section 2.13).

Unable to determine the multimeric state of resolvase crosslinked in the synapse by electrophoresis of protein extracted from isolated synaptic complex, I returned to the approach of silver staining following SDS-PAGE analysis of crosslinked synapsis reactions on a preparative scale. Crosslinking of synapsis reactions containing different concentrations of resolvase was combined with assays of each sample by agarose gel electrophoresis as well as by SDS-PAGE. Thus, any protein species present in the polyacrylamide gel that exhibited the same changes in relative yield at different concentrations of resolvase as those shown by the previously characterised intramolecular synaptic complex in the agarose gel would be apparent. Restriction endonuclease digestion to generate the χ-form of the synaptic complex was only performed on aliquots subsequently loaded on the agarose gel; the bulk of each sample that was loaded onto the polyacrylamide gel remained undigested.

Figure 5.9 shows the results of this approach after crosslinking with either 0.05% glutaraldehyde or 100 μM DSP in buffer C in the presence of about 140 μg/ml pMA21 DNA and a wide concentration range of resolvase. The only crosslinked form of resolvase apparent in the polyacrylamide gel was the group of bands at the position of dimer noted in previous experiments (see Figure 5.6). However, the relative yield of these species obtained with different concentrations of resolvase was a closer match to the relative yield of the single *res* site complex in the agarose gel than it was to the χ-form of the synaptic complex (Figures 5.9 and 5.10).

Figure 5.9 *Facing.*

SDS-PAGE and agarose gel electrophoresis of glutaraldehyde- or DSP-crosslinked pMA21 synapsis reactions.

Various concentrations of resolvase were crosslinked in the presence of about 140 μg/ml pMA21 DNA. A 3 μl aliquot from each 40 μl reaction was digested with *Pst*I + *Bam*HI to produce the χ-form of the synaptic complex, then loaded onto an agarose gel (*bottom*). The remainder of each reaction was analysed by SDS-PAGE (*top*).

Lanes 1-9 show glutaraldehyde crosslinking; the reaction shown in lane 9 differed from the others in that 10 mM $MgCl_2$ was present from the outset. The monomeric resolvase band visible in lanes 1 and 2 of the polyacrylamide gel was due to contamination from an adjacent marker lane.

Lanes 10-14 show DSP crosslinking; the reaction shown in lane 13 differed from the others in that no DNA was present. Lane 14 shows a DTT treatment of the reaction shown in lane 11.

The relative concentration of resolvase is indicated; 1 is equivalent to approximately 0.05 μM resolvase.

A band proposed to represent full-length linear pMA21 DNA has entered the polyacrylamide resolving gel (*top*) and is marked (4927 bp), as are the bands proposed to represent products of resolvase-mediated DNA cleavage (C). The positions of co-electrophoresed 39.5 kDa and 45 kDa protein molecular weight standards are indicated.

On the agarose gel (*bottom*) the χ-form is marked, as are the various substrate and product DNA restriction fragments. Note the single *res* site complex retarded with respect to the 1411 bp substrate restriction fragment. See the text for further details.

Buffer C +/– 10 mM $MgCl_2$; 0.05% glutaraldehyde or 100 μM DSP; 15% polyacrylamide resolving gel, silver stained; 1.2% agarose gel, ethidium stained.

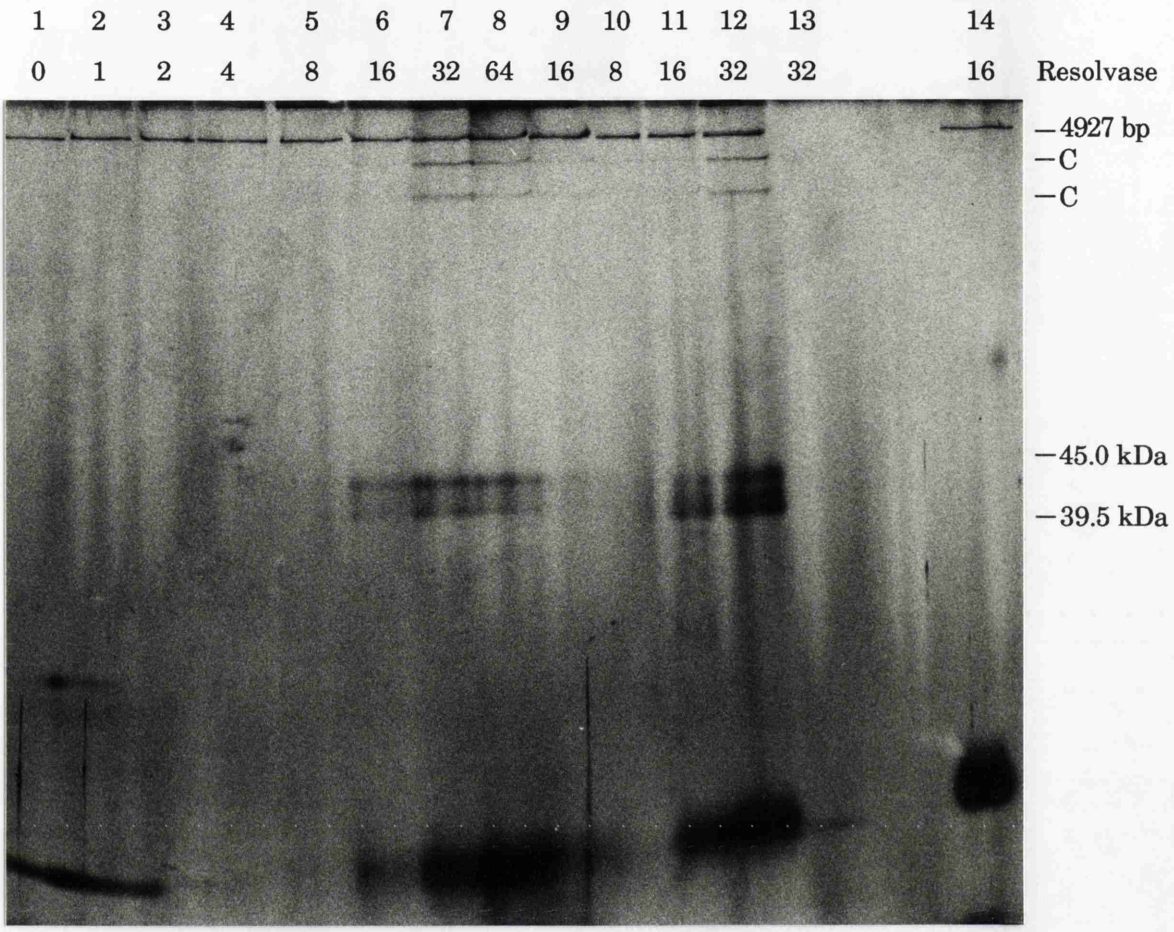
1 2 3 4 5 6 7 8 9 10 11 12 13 14
0 1 2 4 8 16 32 64 16 8 16 32 32 16
Resolvase
—4927 bp
—C
—C
—45.0 kDa
—39.5 kDa

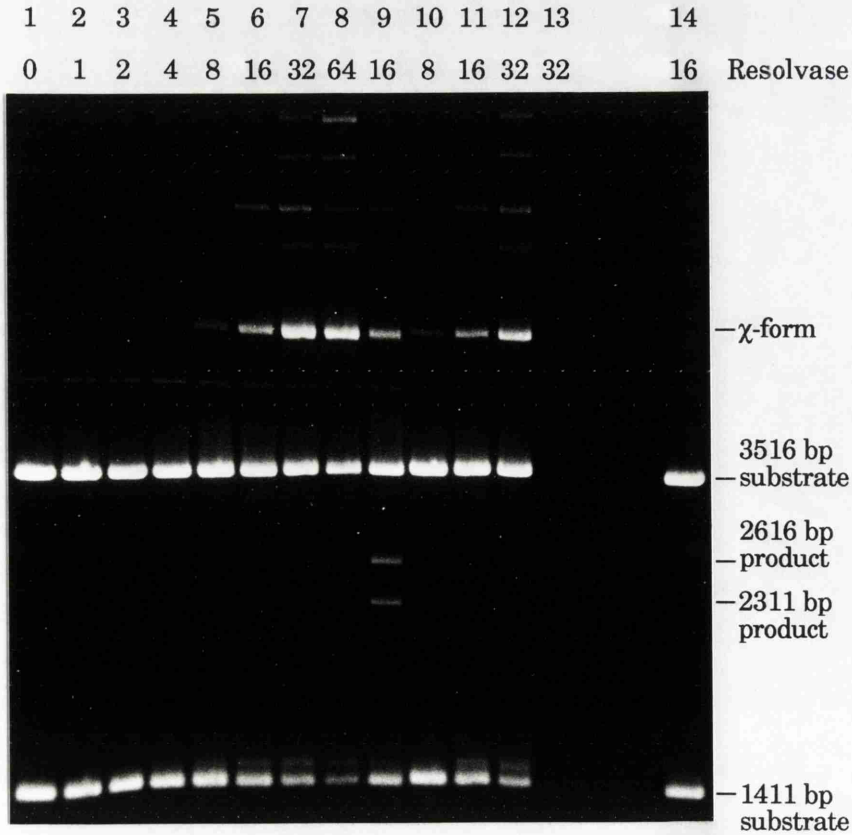
1 2 3 4 5 6 7 8 9 10 11 12 13 14
0 1 2 4 8 16 32 64 16 8 16 32 32 16
Resolvase
—χ-form
3516 bp
—substrate
2616 bp
—product
—2311 bp
product
—1411 bp
substrate

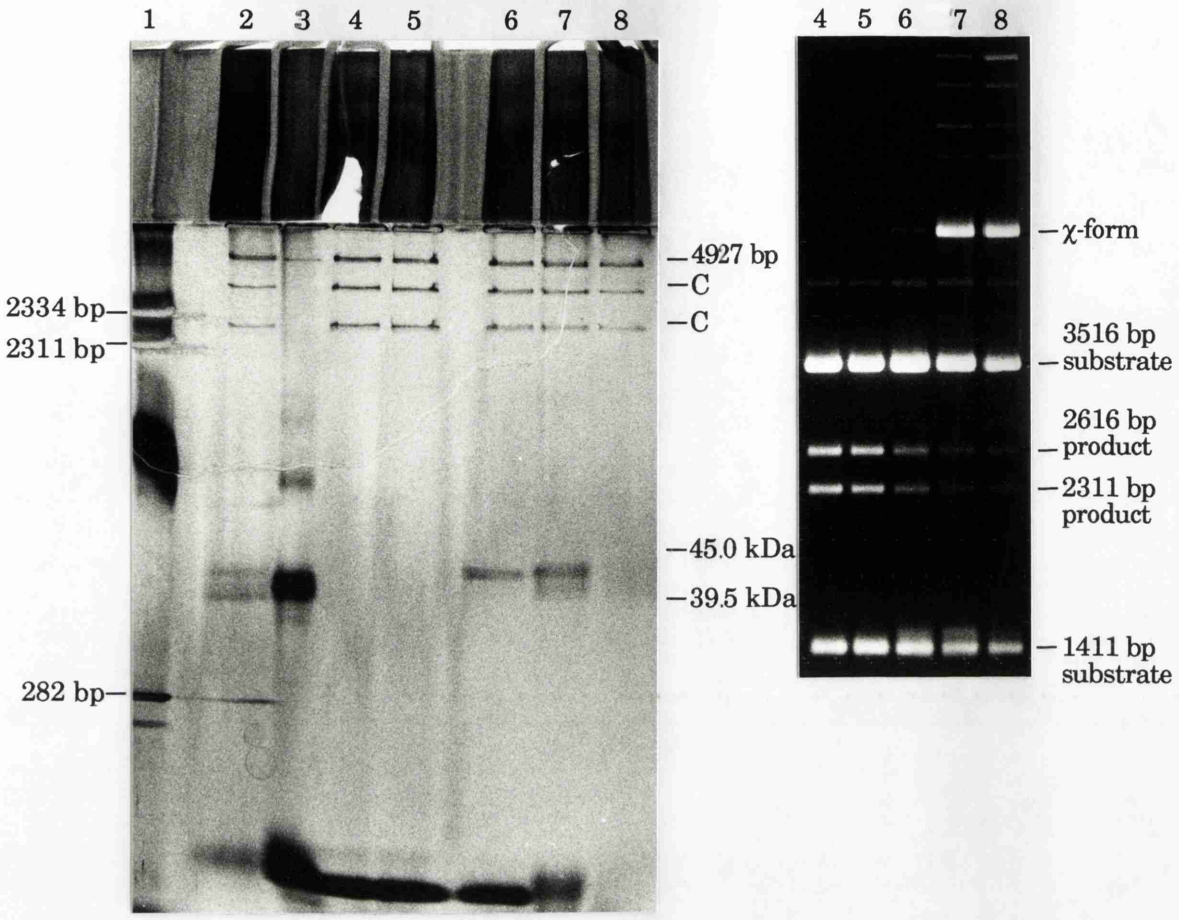

Figure 5.10 SDS-PAGE and agarose gel electrophoresis of glutaraldehyde-crosslinked pMA21 synapsis reactions.

The polyacrylamide gel (*left*) is shown complete with the stacking gel, where the supercoiled pMA21 DNA remains. A band proposed to represent full-length linear pMA21 DNA has entered the resolving gel and is marked (4927 bp). The positions of co-electrophoresed 39.5 kDa and 45 kDa protein molecular weight standards are indicated.

Lane 1 shows an *Eco*RI digestion of pMA21; the three DNA fragments generated have their sizes marked. The 2311 bp fragment is identical in size to the smaller DNA product obtained from resolvase-mediated cleavage at both *res* sites of pMA21. The bands in the polyacrylamide gel proposed to represent products of resolvase-mediated DNA cleavage are marked (C).

Lanes 2 and 3 show DSP-crosslinked reactions; that shown in lane 2 contained 1.5 μM resolvase, while that shown in lane 3 was a 15 μM resolvase reaction.

Lanes 4-8 show 1.5 μM resolvase reactions crosslinked with various concentrations of glutaraldehyde (zero, 0.001%, 0.01%, 0.05%, and 0.1%, respectively). Other details of the synapsis reactions are given in the legend to Figure 5.9.

The same samples were loaded on an agarose gel (*right*); the χ-form is marked, as are the various substrate and product DNA restriction fragments. Note the single *res* site complex retarded with respect to the 1411 bp substrate restriction fragment. See the text for further details.

Buffer C; glutaraldehyde (various concentrations) or 100 μM DSP; 15% polyacrylamide resolving gel, silver stained; 1.2% agarose gel, ethidium stained.

Two slow-migrating bands isolated in the polyacrylamide gel shown in Figure 5.9 did closely match the relative yield of synaptic complex isolated as χ-form in the agarose gel at different concentrations of resolvase. However, these are believed to represent DNA products of resolvase-mediated cleavage at both *res* sites, migrating faster than the full-length linear pMA21 present as contaminant in the DNA preparation (and therefore unchanged in amount in all the samples containing DNA). These two resolvase-dependent bands did not require protein crosslinking for their observation (Figure 5.10, lane 4), failed to appear when DNA was omitted from the reaction (Figure 5.9, lane 13), were present in reduced yield when Mg^{2+} was included in the reaction, and were no longer present when a reaction containing pMA21 was treated with micrococcal nuclease prior to electrophoresis (data not shown). The silver staining method used is a sensitive means of detection of DNA as well as protein (Hames, 1990). This accounts for the appearance of DNA species, not normally seen in ethidium-stained agarose gels, that represented only a small amount of the total DNA present (most of which remained in the supercoiled state, trapped in the stacking gel – see Figure 5.10).

The putative DNA cleavage products may have resolvase covalently linked as is the case when such DNA fragments are isolated in greater yield in the presence of ethylene glycol (data not shown). Indeed, the faster-migrating of the two DNA species appeared considerably retarded when its gel mobility was compared to that of a DNA restriction fragment identical in size to the smaller of those generated by cleavage at both crossover sites of pMA21 (Figure 5.10). However, if the two DNA bands do represent resolvase cleavage products, such species do not appear to interact in a complex sufficiently stable to be isolated in the standard synapsis assay (see Figure 3.44).

Thus, the number of resolvase subunits crosslinked in the isolated synaptic complex remains a mystery. When synapsis reactions containing about 2.5 μg of pMA21 DNA in the form of crosslinked synaptic complex were fractionated by SDS-PAGE, no crosslinked resolvase multimers larger than dimer were detected. This was equivalent to approximately 0.2 μg of resolvase present in the crosslinked synaptic complex (assuming each synapse contains 12 resolvase monomers – see Section 5.2), which should be readily detected by silver staining, even if partitioned among crosslinked species exhibiting different mobility in the polyacrylamide gel. The crosslinked synaptic complex was readily dissociated by SDS

treatment (see Section 3.1), so it seemed unlikely that a synaptic multimer of resolvase failed to appear in the polyacrylamide resolving gel due to its being trapped with the supercoiled DNA in the stacking gel. This was shown not to be the case by treating crosslinked preparative-scale synapsis reactions with micrococcal nuclease prior to SDS-PAGE (see Section 2.15c); the DNA was completely digested but there were no novel bands attributable to crosslinking of resolvase apparent in either the resolving or the stacking gel (data not shown).

It is not out of the question that the extent of crosslinking of resolvase required to stabilise the synaptic complex sufficiently for it to survive electrophoresis is such that dimers represent the largest crosslinked multimer obtained upon dissociation. In that case, it may be as much the failure to stabilise protein-protein interactions sufficiently as it is the failure to stabilise protein-DNA interactions that makes the crosslinked synapse fall apart when any attempt is made to elute it from the agarose gel (see Section 3.1). However, when the concentration of glutaraldehyde was varied, the yield of the slowest-migrating of the dimer-sized species changed in concert with the yield of the single *res* site complex rather than the synaptic complex (Figure 5.10, lanes 4-8). Future investigation of the resolvase component of the crosslinked synaptic complex may be best directed toward a resolvase-specific detection method such as the use of radiolabelled resolvase in the synapsis reactions (a necessity for determination of the absolute stoichiometry of the synapse), or immuno-detection.

Chapter 6

Resolvase-DNA interactions in the synaptic complex

Introduction.

In footprinting a protein bound to DNA, the pattern of chemically or enzymatically induced cleavage or modification of the DNA is compared in the presence and absence of bound protein. Differences in the pattern may be due to protection of the DNA by the bound protein or an alteration in the DNA conformation due to the interaction with the bound protein. Use of bovine pancreatic deoxyribonuclease I (DNase I) as a footprinting reagent is widespread (Galas and Schmitz, 1978); indeed, the three subsites forming the Tn*3* and γδ *res* sites were initially identified as resolvase binding sites by DNase I footprinting (Grindley *et al.*, 1982; Kitts *et al.*, 1983). Under standard conditions, DNase I cleaves a single strand of the DNA helix via attack in the minor groove. A crystal structure of the enzyme bound to an octanucleotide suggests that DNase I bends the DNA, widening the minor groove to permit access (Suck *et al.*, 1988). Despite its relatively large size (~31 kDa), DNase I is a sensitive probe of alterations in DNA conformation in addition to its facility in mapping the positions at which a protein is bound to DNA (Drew and Travers, 1985).

The sensitivity of DNase I to the width and accessibility of the minor groove has proved useful in investigations of the interaction between spatially distinct protein-bound sites in DNA (Schleif, 1992). Lambda repressor binds cooperatively to sites separated by five or six turns of the DNA helix (Hochschild and Ptashne, 1986). This interaction involves the formation of a DNA loop which produced a characteristic cleavage pattern when the protein-DNA complex was analysed by DNase I footprinting. Between the two lambda repressor binding sites, the DNA showed an alternating pattern of protection, then enhancement of DNase I-mediated cleavage, with a periodicity of half a turn of the helix. This pattern is believed to reflect an inability of DNase I to gain access via the minor groove to attack phosphodiester bonds inside the loop, together with an increased activity at positions on the outside of the loop due to an opening out of the minor groove. Looping of the DNA in the subsite I-II spacer region of the γδ *res* site in the resolvase-single *res* site complex was suggested on the basis of a similar result (Salvo and Grindley, 1988), (see Chapter 1).

However, the sensitivity of DNase I to DNA conformation does present some difficulties when using the enzyme to footprint a protein-DNA

complex. Because DNA sequence affects conformation, DNase I does not cleave all the phosphodiester bonds in protein-free DNA with equal efficiency. A lower rate of cleavage, particularly apparent at homopolymeric tracts of (dA).(dT), is believed to reflect conformational rigidity of the DNA (Travers, 1993). A failure to cleave some of the phosphodiester bonds in a DNA molecule makes it impossible to determine the effect of protein binding at all positions within a binding site.

The alkylating agent dimethyl sulphate (DMS) has been used to probe the interaction of resolvase with the *res* site. DMS preferentially methylates at the N-7 position of guanine in the major groove and at the N-3 position of adenine in the minor groove of DNA, potentially identifying bases protected by contact with or proximity of a bound protein (Sun and Singer, 1975; Siebenlist and Gilbert, 1980). Guanine residues within the 9 bp consensus sequence at the ends of the three subsites of *res*, and in the central regions of subsites II and III, were protected from methylation by bound resolvase (Sherratt *et al.*, 1984; Brown, 1986), (see Section 6.2 for further details).

Methylation of purines, and ethylation of phosphates prior to interaction of resolvase with the *res* site DNA, so-called interference experiments (Siebenlist and Gilbert, 1980), have provided information on important protein-DNA contacts. Methylations within the consensus sequence at each subsite of *res* inhibited γδ resolvase binding to that subsite, as did ethylation of certain phosphates in the same regions (Falvey and Grindley, 1987). However, only modifications within subsite I inhibited *in vitro* resolution: methylation of guanines in the consensus sequence and adenines in the crossover site region. It was suggested that weaker binding of resolvase due to modification at a single position within the accessory subsites of *res*, although readily detected in the binding assay, could still allow the formation of a transient recombination intermediate and therefore have little effect on resolution. This interpretation is consistent with the apparent formation of a synaptic intermediate trapping three negative supercoils during resolution of a plasmid containing an intact *res* site and an isolated subsite I in direct repeat orientation (Bednarz *et al.*, 1990), (see Section 3.5).

Prior to the experiments described in this Chapter, there was no information on the interaction between resolvase and the *res* site DNA in the synaptic complex. However, protein-DNA complexes formed during

the *in vitro* Mu DNA transposition reaction have been investigated by footprinting techniques. DNase I and methylation protection footprinting revealed the MuA protein to be stably bound to only three of the six binding sites at the paired Mu DNA ends (Kuo *et al.*, 1991; Lavoie *et al.*, 1991; Mizuuchi *et al.*, 1991). Glutaraldehyde-crosslinked synaptic complexes formed by the FLP recombinase and a linear DNA fragment containing direct repeats of the FRT site, isolated by non-denaturing polyacrylamide gel electrophoresis, were footprinted using DNase I (Amin *et al.*, 1990). Only the two FLP binding sites flanking the core sequence were protected in these putative synaptic intermediates.

The rationale behind the choice of footprinting reagents used to probe the synaptic complex is discussed in Section 6.2. However, as an initial 'coarse' footprinting experiment, the effect of synapsis on cleavage at several restriction endonuclease sites within *res* was investigated. Although this technique only reports on the protection of a very limited region of DNA, this specificity is an advantage in some respects. The limited number of different species resulting from digestion can be analysed directly as protein-DNA complexes by agarose gel electrophoresis, in one case revealing differential protection of the material migrating as intramolecular substrate synaptic complex.

Results and discussion.

6.1 The effect of synapsis on restriction endonuclease cleavage at sites within *res*.

*Ssp*I, *Dra*III, and *Rsa*I cleave the DNA within the *res* site, as shown in Figure 6.1. Standard glutaraldehyde-crosslinked pMA21 synapsis reactions (as described in Section 2.15c) were digested with each of these restriction endonucleases. In order to determine any differential effect of the formation of substrate and product synaptic complexes on the ability of these restriction endonucleases to cleave at their recognition sites within *res*, synapsis reactions were incubated in the presence and absence of Mg^{2+}. Control reactions from which resolvase was omitted revealed the extent of digestion in the absence of complex formation. Figure 6.2 shows the results of agarose gel electrophoresis.

In this experiment, treatment of reactions with SDS prior to electro-

phoresis, resulting in the dissociation of protein-DNA complexes, reveals any partial restriction fragments indicative of a failure to cut within one or both *res* sites. The presence of such partial restriction fragments *only* in the reactions containing resolvase shows that resolvase binding (or a resolvase-induced distortion of the DNA) protected the site(s) in question from restriction endonuclease cleavage. When SDS treatment prior to gel electrophoresis is omitted, partial restriction fragments arising from failure to cut within the *res* site should migrate as a previously characterised crosslinked protein-DNA complex (provided all the material in the form of complex at the time of exposure to the restriction endonuclease remains as complex during electrophoresis). This will be synaptic complex if protection from restriction endonuclease cleavage occurred in the synapse, or single *res* site complex if protection occurred with resolvase bound to an unsynapsed *res* site. Any protection due to the crosslinked single *res* site complex should be readily apparent as the complex will migrate to a position in the gel slightly retarded with respect to the appropriate partial restriction fragment.

*Ssp*I cuts pMA21 at three locations (Figure 6.1), once within each copy of *res* subsite I (immediately 5' to the crossover site at -4 on both strands to give blunt ends), and once outside *res* in the 2616 bp domain of the plasmid. Complete *Ssp*I digestion of pMA21 produces linear DNA fragments of 2311 bp, 2259 bp, and 357 bp.

When resolvase was omitted from the crosslinked reaction , *Ssp*I digestion was virtually complete (Figure 6.2a, lanes 1 and 10). In contrast, in the presence of resolvase and following SDS treatment immediately prior to electrophoresis, a number of partial restriction fragments were also present (lane 11): 4927 bp (full length linear pMA21; suggests that both *res* sites were protected), 4570 bp linear (only the bottom *res* site was protected[1]), and 2668 bp linear (only the top *res* site was protected). When incubation of pMA21 with resolvase was in the presence of 10 mM Mg^{2+}, the *Ssp*I partial restriction fragments identified above were reduced in amount; 2616 bp linear and 2311 bp supercoiled species appeared, an indication of protection at both *res* sites in the product catenane (Figure 6.2a, lane 12).

---

[1] Reference to the 'bottom' or 'top' *res* site identifies the sites as reproduced in the map of pMA21 shown in Figure 6.1.

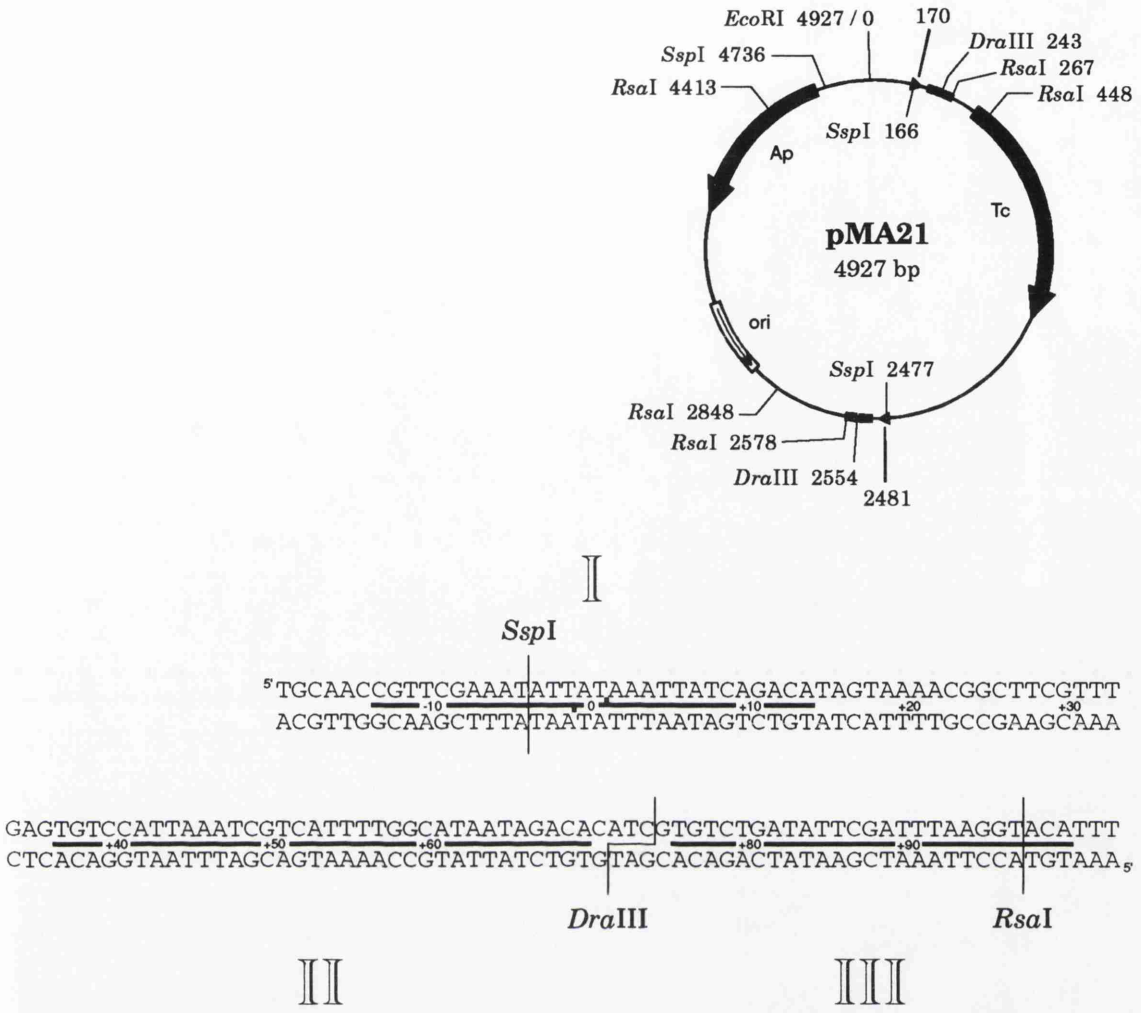

Figure 6.1 Selected restriction endonuclease sites within the *res* DNA sequence. The subsites (resolvase binding sites) are marked. The positions of phosphodiester bonds are numbered relative to the centre of the crossover site (designated zero).
Above is a map of pMA21 with the sites for *Ssp*I, *Dra*III, and *Rsa*I shown; *Ssp*I and *Rsa*I cleave at sites in the plasmid vector (pBR322) as well as within the *res* sites. Site locations are relative to the centre of the *Eco*RI site of pBR322 (designated zero) and are in base pairs. See the text for further details.

The *Ssp*I partial restriction fragments revealed by SDS treatment were present as cleaved synaptic complexes when SDS was omitted, migrating as five discrete bands between the positions of nicked and supercoiled pMA21 (Figure 6.2a, lanes 2 and 3). These intramolecular synaptic complexes were characterised by a second dimension of gel electro-

phoresis after in-gel treatment of the excised bands with SDS to free the component DNA fragments (Figure 6.2b). The bands, numbered 1 to 5 in Figure 6.2, are proposed to represent:

1. Relaxed 'full-size' α-form produced by *Ssp*I cleavage in the vector DNA only, yielding a 4927 bp restriction fragment upon dissociation.
2. a) Relaxed 'small' α-form resulting from *Ssp*I cleavage within the top *res* site as well as in the vector DNA; giving a 4570 bp restriction fragment upon dissociation.
   b) Migrating to the same position in the first dimension of electrophoresis, the 'full-size' χ-form resulting from *Ssp*I cleavage within the bottom *res* site as well as in the vector DNA. This complex yields 2668 bp and 2259 bp restriction fragments upon dissociation.
3. The 'small' χ-form produced by complete *Ssp*I digestion of synapsed pMA21, yielding 2311 and 2259 bp restriction fragments upon dissociation. These DNA fragments are too close in size to be resolved as separate bands following a second dimension of electrophoresis (Figure 6.2b).
4. The supercoiled 'full-size' α-form produced by *Ssp*I cleavage in the vector DNA only, giving a 4927 bp restriction fragment upon dissociation.
5. The supercoiled 'small' α-form produced by *Ssp*I cleavage within the top *res* site as well as in the vector DNA, giving a 4570 bp restriction fragment upon dissociation.

The *Ssp*I sites within *res* were not protected from cleavage in all of the crosslinked synapsed pMA21 molecules; cleaved synaptic complexes resulting from protection at both *res* sites (1 and 4), at the top *res* site only (2b), or at the bottom *res* site only (2a and 5) were evident, as was completely digested synaptic complex (3). Thus, the crosslinked synaptic complex could remain intact despite restriction endonuclease cleavage within subsite I of either or both *res* sites. It is not known whether the two copies of subsite I were synapsed in these crosslinked complexes, or whether the synapse involved the accessory subsites alone. From an estimation of the relative fluorescence after ethidium bromide staining, it appeared that about 40% of the total amount of synaptic complex was completely digested, about 40% was protected from *Ssp*I cleavage at a single *res* site, and about 20% was protected at both *res* sites. The significance of this differential protection is unknown, although one can speculate on the existence of several populations of synaptic complex

differing in structural details such that their susceptibility to restriction endonuclease cleavage is altered. In the presence of Mg^{2+}, *Ssp*I-cleaved forms of the product synaptic complex co-migrated with the aforementioned substrate synaptic complexes (data from second dimension of electrophoresis not shown).

*Rsa*I cuts pMA21 at five locations (Figure 6.1), once within each copy of *res* subsite III (3 bp in from the right end at +97 on both strands), and at three positions outside *res*. Complete *Rsa*I digestion of pMA21 produces linear DNA fragments of 2130 bp, 1565 bp, 781 bp, 270 bp, and 181 bp. When resolvase was omitted from the crosslinked reaction, *Rsa*I digestion was virtually complete (Figure 6.2a, lanes 4 and 13). In the presence of resolvase and following SDS treatment, partial restriction fragments of 2400 bp and 962 bp were apparent (lane 14). These DNA fragments reflect protection of the *Rsa*I sites within the bottom and top *res* sites, respectively. When incubation of pMA21 with resolvase was in the presence of Mg^{2+}, the substrate partial restriction fragments identified above were reduced in amount; 2311 bp and 1051 bp linear DNA fragments appeared, an indication of protection at both *res* sites in the product catenane (lane 15).

A single band representing χ-form of the synaptic complex was visible when the SDS treatment was omitted after reaction in the absence or presence of Mg^{2+}, suggesting protection of both *res* sites from *Rsa*I cleavage in substrate and product synaptic complexes that exhibit an identical gel mobility (Figure 6.2a, lanes 5 and 6). A second dimension of electrophoresis after in-gel SDS treatment showed this to be the case, with only the partial DNA restriction fragments identified above being released from the dissociated χ-form (data not shown). Thus, both *res* sites were protected from *Rsa*I cleavage in all the crosslinked substrate and product synaptic complex isolated. Furthermore, the absence of any free partial restriction fragments (above the background level seen in the absence of resolvase) indicated that all of the crosslinked synaptic complex present at the time of restriction endonuclease treatment remained intact during the subsequent electrophoresis. This is consistent with the apparent stability of the crosslinked pMA21 synaptic complex during two-dimensional agarose gel electrophoresis (see Section 3.2).

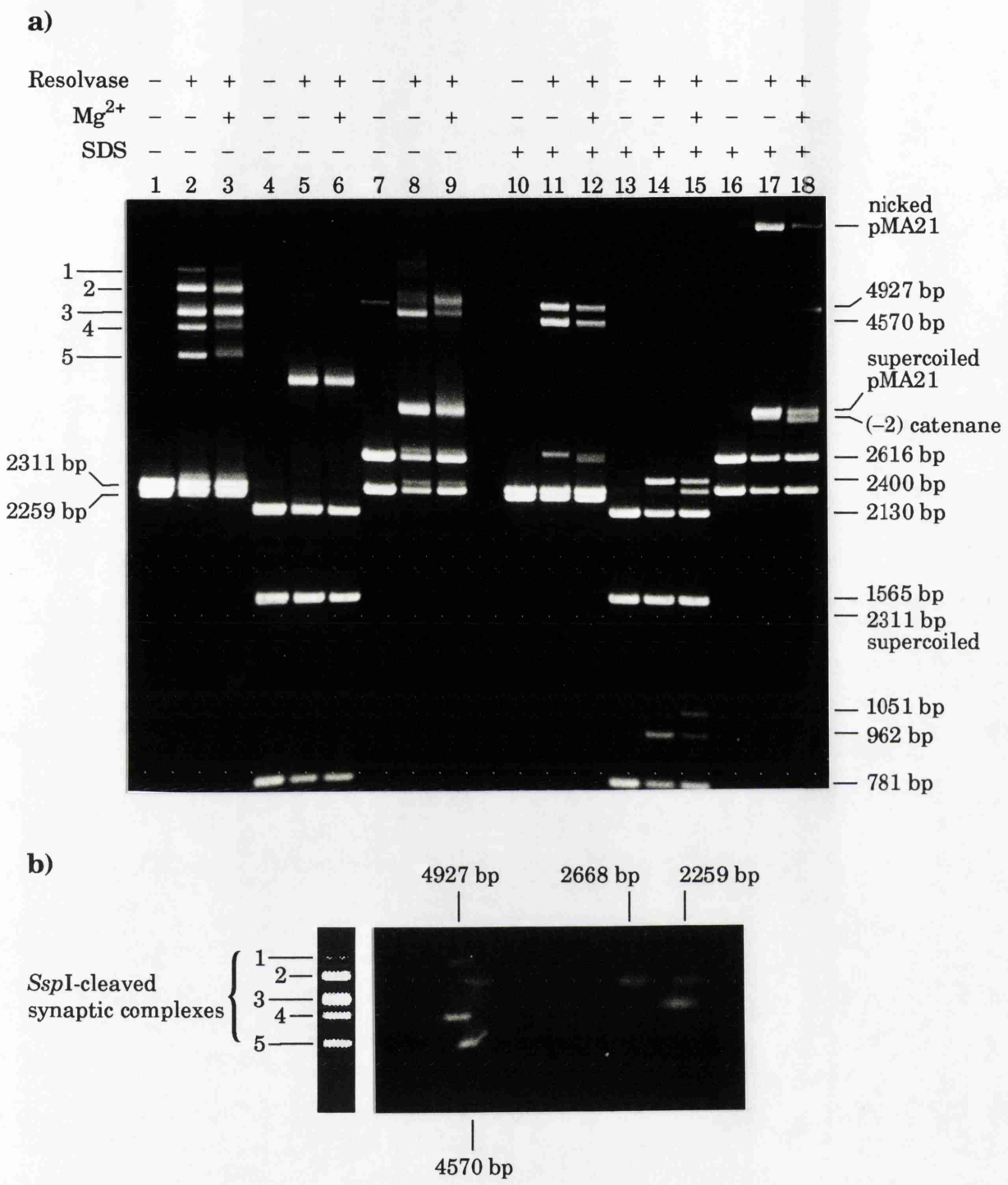

Figure 6.2 Agarose gel electrophoresis of glutaraldehyde-crosslinked pMA21 synapsis reactions: restriction endonuclease cleavage within the *res* site.

a) pMA21 reactions were digested with *Ssp*I (lanes 1-3 and 10-12), *Rsa*I (lanes 4-6 and 13-15), or *Dra*III (lanes 7-9 and 16-18) after crosslinking. Fragments smaller than 781 bp have been cropped from the gel photograph. Five bands representing *Ssp*I-cleaved synaptic complexes are numbered 1 to 5.

b) The five bands representing *Ssp*I-cleaved synaptic complexes were cut from lane 2 of the above gel. After in-gel treatment with SDS, the DNA restriction fragments forming these complexes were fractionated by a second dimension of electrophoresis, from left to right as shown (see Section 2.9g). See the text for further details.

Buffer C +/– Mg^{2+}; 0.05% glutaraldehyde; 1.2% agarose gel in both dimensions.

*Dra*III cuts pMA21 at two locations, in the centre of the subsite II-III spacer region of each *res* site (at +71 on the bottom strand and at +74 on the top strand as represented in Figure 6.1, leaving 3' overhangs of three nucleotides). Thus, complete *Dra*III digestion of pMA21 produces linear DNA fragments of 2616 bp, and 2311 bp (see Figure 6.1). SDS treatment of a *Dra*III-digested synapsis reaction revealed that about 50% of the input substrate was protected from cleavage at both sites, leaving supercoiled or nicked pMA21, while the remainder was completely digested (Figure 6.2a, lane 17). The similar yield of supercoiled substrate and (–2) catenane obtained when Mg^{2+} was included in the reaction (lane 18) is consistent with the relative yield of the χ-forms of the substrate and product synaptic complex generally observed under the same conditions (see Section 3.8). This suggests that the observed protection from *Dra*III cleavage was largely if not entirely due to synapsis. However, because the uncut supercoiled synaptic complex has the same gel mobility as supercoiled substrate with resolvase bound to unsynapsed *res* sites (see Section 3.2), it is not possible to determine unequivocally whether protection from *Dra*III cleavage is confined to the crosslinked synaptic complex.

In addition to the uncut retarded complex, a number of slower-migrating complexes were also apparent following *Dra*III digestion (Figure 6.2a, lane 8). The major band, in terms of the amount of DNA present, was shown to represent synaptic complex nicked in one domain (data not shown). In the presence of Mg^{2+}, the yield of this species was reduced, while a species migrating at a lower rate, apparently cut at a single site, increased in amount (lane 9). It is not known whether the nicking or cleavage was due to the restriction endonuclease or resolvase, although nicked synaptic complex relaxed in both domains probably resulted from synapsis of the small amount of nicked pMA21 present in the supercoiled DNA preparation.

There was some evidence of protection from *Rsa*I cleavage in the cross-linked single *res* site complex in the form of a very faint band retarded with respect to the 2400 bp partial restriction fragment (Figure 6.2a, lane 5). However, this was minimal compared to the protection conferred by the crosslinked synaptic complex. Indeed, *Rsa*I cleavage in subsite III of *res* appeared to destroy the crosslinked single *res* site complex, as the yield of complex retarded with respect to the restriction fragments containing the bulk of each cleaved *res* site (the 2130 bp and 781 bp DNA

fragments) was very low. This contrasts with the readily detected single *res* site complex retarded with respect to the 2259 bp *Ssp*I fragment (lane 2), and the 2616 bp and 2311 bp *Dra*III fragments (lane 8). Therefore, the crosslinked single *res* site complex, although susceptible to restriction endonuclease cleavage within the *res* site, was not dissociated by *Ssp*I or *Dra*III cleavage.

It is not known whether the single *res* site complex is stabilised by crosslinking of an interaction of resolvase dimers bound at different subsites of *res* (see Section 3.10). If this were the case, then the ability of such a complex to survive *Dra*III cleavage suggests that crosslinking of an interaction between resolvase bound at subsites I and II may be sufficient to maintain the complex. But, since *Dra*III cuts pMA21 within the *res* sites only, the possibility that the complexes retarded with respect to the fragments of complete digestion represent the remnants of completely digested synaptic complex cannot be ruled out. If this were the case, then the complexes would be in the form of a DNA loop with the ends of the restriction fragment joined by dint of subsites I and II of one *res* site remaining crosslinked to subsite III of the other *res* site. However, one might expect such a looped molecule to be more retarded with respect to its linear variant in a 1.2% agarose gel. Nevertheless, the survival of a single *res* site complex that has lost the whole of subsite III due to *Dra*III cleavage is seemingly at odds with the destruction of the same complex by *Rsa*I cleavage that results in the loss of only 3 bp from the end of subsite III.

In conclusion, sites for *Dra*III and *Rsa*I located within the *res* site (in the subsite II-III spacer region and within subsite III, respectively) were protected from restriction endonuclease cleavage predominantly in the crosslinked synaptic complex. The data suggested that both *res* sites were protected in virtually all of the crosslinked synaptic complex isolated. In contrast, although protection at an *Ssp*I site located within subsite I of *res* was confined to the synaptic complex, the protection was less clear-cut. Only about 20% of the total amount of synaptic complex isolated was protected from *Ssp*I cleavage in both *res* sites, while half the remainder was protected at a single *res* site and the other half was completely digested. Even when completely digested by *Ssp*I, the crosslinked synaptic complex remained intact. The relative distribution of crosslinked synaptic complex into different populations with respect to protection at the *Ssp*I site within subsite I of *res* was very similar when the experiment

was repeated (data not shown). However, it is not known whether these different populations reflect structural differences in the synaptic complexes.

The behaviour of the product synaptic complex was indistinguishable from that of the substrate synaptic complex when treated with any one of the three restriction endonucleases. The unequivocal protection at *Dra*III and *Rsa*I sites within *res* when crosslinked in a synaptic complex is further evidence of the importance of the accessory subsite interactions in resolvase-mediated synapsis.

In addition to the observed protection from cleavage within the *res* site DNA sequence by *Ssp*I, *Dra*III, and *Rsa*I, there was also some evidence of a resolvase-dependent interference with *Hin*dIII cleavage at the unique site 43 bp from the right end of subsite III in pMA21 (as shown in Figure 3.16). This resulted in the formation of substrate intramolecular synaptic complex nicked in one domain, presumably by the action of *Hin*dIII, the amount of which gradually increased during a time-course at 37°C to reach a maximum (representing about 5-10% of input substrate) 5 minutes after addition of resolvase, followed by a substantial decrease in yield at the 10 minute time-point (data not shown). Restriction endonucleases have been shown to cleave DNA in a non-concerted fashion, and substrate cleaved in a single strand is the major product of *Hin*dIII digestion in the presence of ethidium bromide (Halford, 1983; Österlund *et al.*, 1982). Thus, the behaviour of this resolvase-dependent effect was quite different from the behaviour of the substrate synaptic complex as assayed by restriction endonuclease cleavage after crosslinking a synapsis reaction at various times after addition of resolvase (see Section 3.9). Again, this suggests the existence of intramolecular synaptic complexes differing in structure.

6.2 Probing the synaptic complex with DNA footprinting reagents.

Choice of the footprinting reagents for the investigation of the interaction of resolvase with DNA in the synaptic complex was influenced by previously published analyses of resolvase binding to linear DNA molecules containing a single *res* site. Binding of Tn*3* resolvase to the Tn*3* *res* site was investigated by methylation protection footprinting

(Sherratt *et al.*, 1984; Brown, 1986), and by DNase I protection footprinting (Symington, 1982; Kitts *et al.*, 1983). In addition, there were DNase I protection footprinting data for γδ resolvase binding to a linear DNA fragment containing the γδ *res* site (Grindley *et al.*, 1982; Salvo and Grindley, 1988). Together, these data represented a valuable resource allowing direct comparison of footprints in order to determine any features unique to synapsis. Therefore, it was decided to utilise methylation protection footprinting, primarily to determine the occupancy of the subsites of *res* in the synaptic complex. In addition, DNase I protection footprinting was used to report on any distortion of the DNA, expected in a wrapped nucleoprotein structure such as that proposed for the synaptic complex formed by resolvase.

The decision to use a protein crosslinking reagent at some stage during footprinting of the synaptic complex was made on account of the demonstrated instability of the complex in the absence of crosslinking reagent and the failure to isolate intramolecular synaptic complex in quantitative yield. An analysis of the whole reaction may represent footprints of various species, and there was no means of isolating the species of interest without the stability conferred by protein crosslinking. In the future, there exists the possibility of using pMA2350 in an analysis of the whole synapsis reaction after treatment with a footprinting reagent. Although the synaptic complex formed by pMA2350 appeared very unstable in the standard synapsis assay, this substrate was resolved efficiently (see Section 3.4). Because the *res* sites are only 219 bp apart, the small DNA loop formed upon synapsis may be inaccessible to DNase I on the inside while exhibiting increased susceptibility to minor groove attack on the outside of the loop, resulting in a distinctive alternating pattern of DNase I protection and enhancement (see the introduction to this Chapter). The appearance of such a pattern would report on whether the yield of synapsed pMA2350 was relatively high when a non-crosslinked reaction was treated with DNase I.

Having decided to isolate the crosslinked synaptic complex at some point in the footprinting procedure, a number of alternatives were considered as to the stage at which to isolate complex. Treatment of the whole synapsis reaction with the footprinting reagent prior to crosslinking could turn into an interference as well as a protection experiment if the synaptic complex was not stable under the conditions used. The possibility of treating the gel-isolated synaptic complex with the footprinting

reagent was not pursued because of the demonstrated inability to get the crosslinked synaptic complex out of an agarose gel intact (see Section 3.1). Treatment of complex with the footprinting reagent in the agarose gel was considered difficult to control and problematic in view of the experience with in-gel ligation (see Section 4.1).

The alternative of treating the whole synapsis reaction with the footprinting reagent after crosslinking was chosen. However, subsequent isolation of the crosslinked synaptic complex demanded restriction endonuclease cleavage, preferably in both domains to generate a single χ-form from all of the intramolecular synaptic complex present. By judicious selection of the restriction endonucleases used, this approach allowed separate analysis of the substrate and product synaptic complexes isolated in the presence of Mg^{2+} (see Section 3.8). The requirement to stop DNase I digestion or dimethyl sulphate (DMS) methylation of the DNA after a short incubation prohibited the subsequent treatment with restriction endonuclease. Methods for stopping the reaction of the footprinting reagents (chelation of Mg^{2+} and phenol extraction, or harsh chemical reduction) either produce conditions which do not support restriction endonuclease digestion, or destroy the crosslinked synaptic complex before it can be isolated by agarose gel electrophoresis.

Thus, it was decided to footprint crosslinked synaptic complex after restriction endonuclease treatment to generate the χ-form, then separate it from free substrate and other footprinted complexes of potential interest by agarose gel electrophoresis. Commencing electrophoresis immediately after incubation with the footprinting reagent served as a means of stopping the reaction. Elution of the bands of interest, excised from the agarose gel, was by centrifugation through Miracloth (see Section 2.10), as it was no longer necessary for the complexes to remain intact at that stage. DNA was purified by phenol extraction and ethanol precipitation.

In a novel approach, radioactive labelling of the DNA was carried out after footprinting and isolation of the species of interest. The alternatives of starting with radiolabelled supercoiled substrate DNA, or of labelling the synapsis reaction after restriction endonuclease digestion but before footprinting, were eschewed in favour of an approach that reduced the number of experimental procedures involving radioactive material.

Because the χ-form comprised two restriction endonuclease DNA fragments with four 3' ends that potentially could be radiolabelled in a filling-in reaction using [α-^{32}P]dNTP and Klenow polymerase, one might envisage the need for additional restriction endonuclease digestion and isolation of a radiolabelled fragment of interest by a second gel electrophoresis step. However, careful selection of the DNA substrate and the restriction endonucleases used prior to footprinting produced a χ-form with three blunt ends and a single 5' overhang, allowing 3' end-label to be added to either the top or bottom strand of a DNA fragment containing the footprinted *res* site[2].

The plasmid used in these experiments, pMS12, is shown in Figure 6.3; both DNA strands forming the top *res* site (as depicted) were analysed in the substrate synaptic complex, while top and bottom strand footprints originated from different recombinant *res* sites in the product synaptic complex. Digestion with *Bam*HI and *Hin*cII produced discrete bands representing substrate and product χ-form that, when subsequently used as the DNA substrates in end-labelling reactions, were labelled at the 3' end of the top strand, 164 nucleotides from the site of resolvase-mediated cleavage in a 799 nucleotide substrate DNA or a 1711 nucleotide product DNA. Similarly, digestion with *Hin*dIII and *Hin*cII generated χ-forms that were labelled at the 3' end of the bottom strand, 150 nucleotides from the resolvase cleavage site in a 590 nucleotide substrate DNA or a 2143 nucleotide product DNA. The labelled fragments are depicted in Figure 6.3, and the experimental details are described in Section 2.16.

In addition to the χ-forms of the substrate and product synaptic complex, a number of other species were isolated from the agarose gel and labelled. The appropriate protein-free substrate and product restriction endonuclease DNA fragments were taken from the same reactions as the isolated χ-forms, as was the single *res* site complex retarded in the gel with respect to the free substrate. As well as the protein-free controls taken from the footprinted synapsis reactions, the same substrate DNA fragment was isolated from a minus-resolvase reaction.

Methylation of the DNA was achieved by addition of 1% dimethyl sulphate (DMS) to a standard glutaraldehyde-crosslinked pMS12 synapsis reaction after the incubation for restriction endonuclease digestion. After 3 minutes at room temperature, gel loading buffer was added and

[2] Top and bottom strands of the *res* site DNA are as depicted in Figure 6.1.

electrophoresis began shortly thereafter. Treatment with piperidine to cleave the DNA strand at the phosphodiester bond on the 3' side of methylated guanine residues was carried out after the end-labelling reaction (Section 2.16a). DNA was fractionated in an 8% polyacrylamide/7 M urea gel under denaturing conditions, and labelled DNA molecules were detected by autoradiography (see Sections 2.17-2.19).

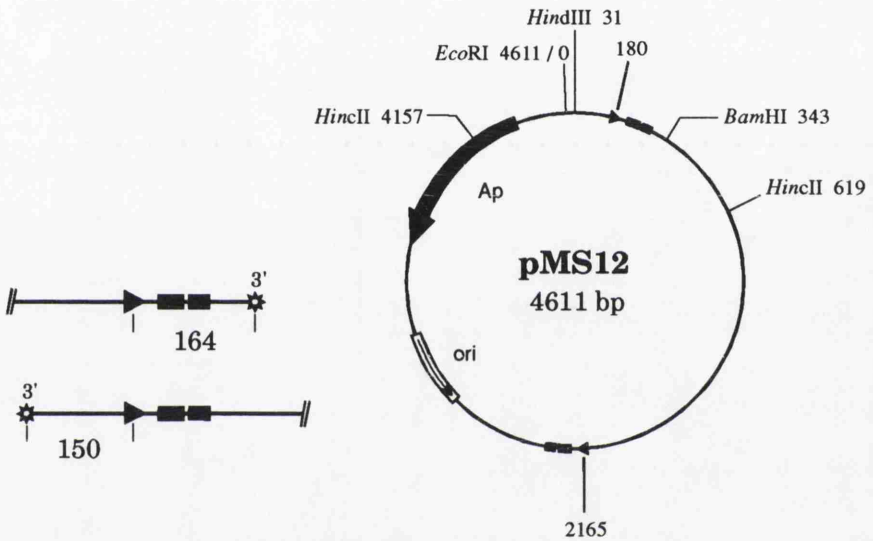

Figure 6.3 Map of pMS12 showing *res* sites and the restriction endonuclease sites utilised in the footprinting analysis (W.M. Stark, personal communication). Site locations are relative to the centre of the *Eco*RI site of pBR322 (designated zero) and are in base pairs.
The single-stranded DNA fragments labelled at their 3' ends by filling in at the *Bam*HI site (top strand) or the *Hin*dIII site (bottom strand) are shown. The distance between the 3' end and the site of resolvase-mediated strand cleavage during recombination is given (in nucleotides). See the text for further details.

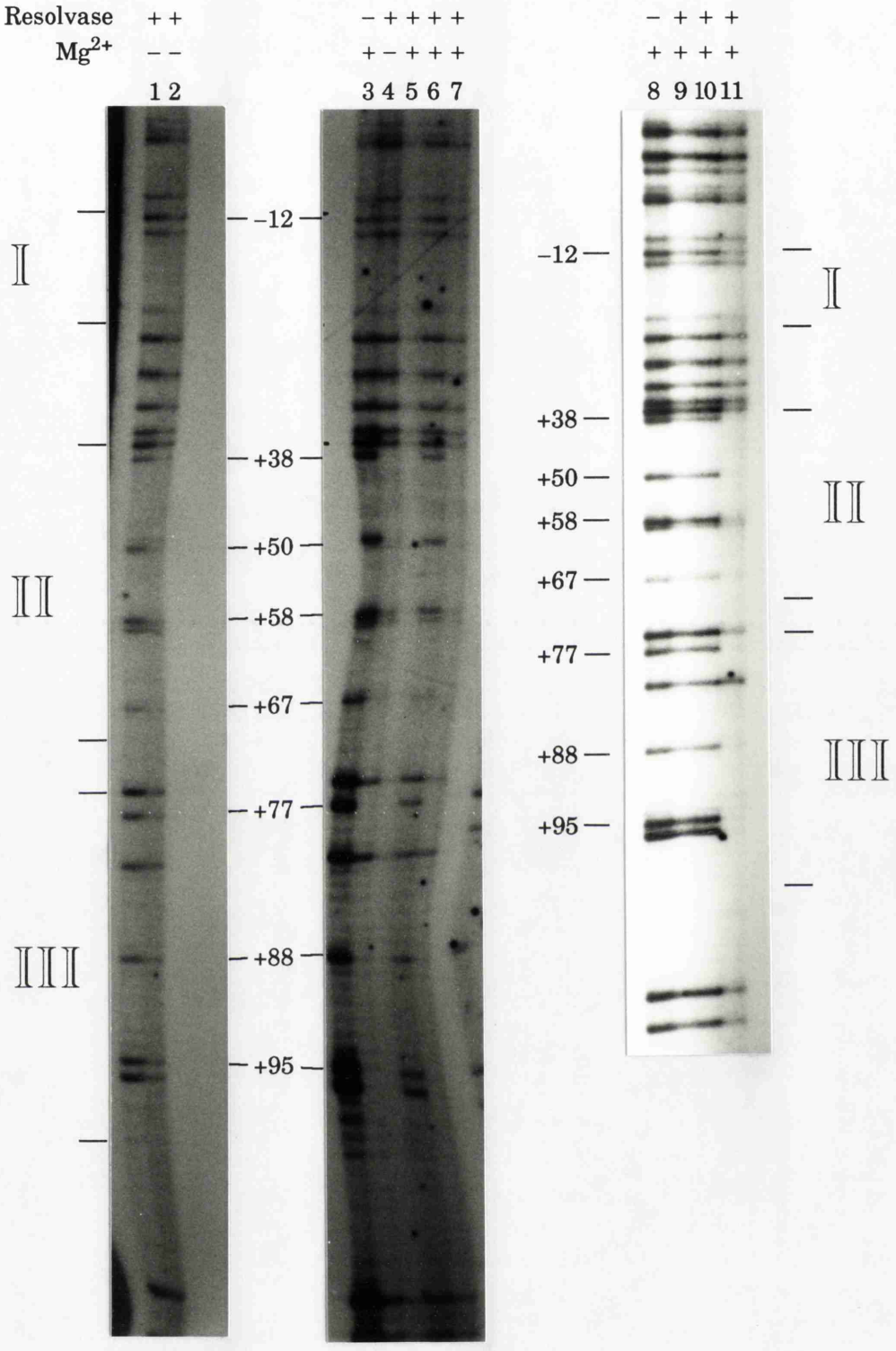

Figure 6.4 Methylation protection footprinting of the top strand of the *res* site in the χ-forms of the substrate and product synaptic complexes and in the single *res* site complex.

DNA fragments are identified by the phosphodiester bond cleaved on the 3' side of methylated guanine residues according to the numbering system introduced in Figure 6.1 (the centre of the crossover site is designated zero). The following species were eluted from the agarose gel: protein-free substrate DNA (lanes 1, 3, 8, and 9), the retarded single *res* site complex (lane 2), substrate χ-form (lanes 4 and 5), protein-free product DNA (lanes 6 and 10), product χ-form (lanes 7 and 11).

Buffer C +/– Mg^{2+}; 0.05% glutaraldehyde; 1% DMS; 1.2% agarose gel; 8% polyacrylamide/7 M urea gel.

Figure 6.4 reproduces an autoradiograph showing the results of methylation protection footprinting of the top strand of DNA in the region of the *res* site, while Figure 6.5 presents the data for the bottom strand. The pattern of DNA cleavage fragments obtained from the isolated χ-form of the intramolecular substrate synaptic complex (resulting from synapsis in the absence and in the presence of Mg^{2+}), the product χ-form, and the single *res* site complex were compared with the pattern obtained from the protein-free DNA isolated from the synapsis reaction and DNA isolated from a minus-resolvase reaction. The fragments present after cleavage of the DNA at phosphodiester bonds on the 3' side of methylated guanine residues are identified by the numbering system introduced in Figure 6.1. Guanine residues methylated in the protein-free DNA, but protected from methylation in the substrate and product χ-form of the synaptic complex are marked on the *res* site DNA sequence shown in Figure 6.6.

Cursory inspection of the autoradiographs reproduced in Figures 6.4 and 6.5 reveals a major problem encountered in all the footprinting experiments conducted: an inability to balance the samples, in terms of radioactive signal, at the time of loading on the sequencing gel. A high but variable proportion (estimated to be over 90%) of the counts per second (cps) incorporated after end-labelling of the DNA was in the form of a species that was fast-migrating during electrophoresis, making it impossible to judge the relative cps incorporated into the DNA fragments of interest. This may have been due to labelling of a contaminant arising from the agarose during elution of the DNA from the gel. However, thorough extraction and precipitation of the DNA before and after the end-labelling reaction failed to cure this pervasive problem, hence the poorly balanced lanes in the autoradiographs reproduced in this Chapter.

The interpretation of the methylation footprinting data is confined to protection at guanine residues as the different samples were not balanced sufficiently to judge weak enhancements occurring in the synaptic complex. Comparing the methylation protection footprints obtained from the χ-forms of the substrate and product synaptic complexes (the former after reaction in the absence or in the presence of Mg^{2+}) reveals a very similar pattern on both strands of DNA, in terms of the guanine residues protected by bound resolvase and the degree of protection conferred (Figure 6.4, lanes 4, 5, 7, and 11; Figure 6.5, lanes 2, 3, and 5). The resolvase-bound single *res* site fragment, isolated from the agarose gel as a retarded crosslinked complex, was generally only weakly protected at

the same positions in the top strand of DNA (the signal from the bottom strand was too weak to interpret), (Figure 6.4, lane 2). This may reflect incomplete occupancy of the *res* site in a random fashion. Thus, the question of which subsites resolvase is bound to when crosslinked in a stable complex with a single *res* site remains unanswered. It may be that various permutations of subsite occupancy within a single *res* site can form a stable complex when resolvase is crosslinked (see Section 3.10). DNA species that co-migrated with SDS-treated substrate or product DNA fragments during agarose gel electrophoresis of the crosslinked synapsis reaction produced a methylation cleavage pattern identical to the substrate fragment isolated from a minus-resolvase reaction (Figure 6.4, lanes 8, 9, and 10).

The protection of the *res* site DNA from methylation in the synaptic complex (Figure 6.6) can be compared with the protection observed following binding of resolvase to a linear DNA fragment containing a single *res* site (Sherratt *et al.*, 1984; Brown, 1986). Within subsite I, although there was partial protection of the guanine residue at –12 in the top strand and at –10 and +12 in the bottom strand of the synaptic complex, the same positions were more clearly protected from methylation in the linear single *res* footprint. Likewise, the G at +11 on the top strand was only protected in the linear single *res* footprint. This raises the question of whether the bands representing χ-forms of the substrate and product synaptic complexes are heterogeneous in terms of resolvase-DNA interactions at subsite I of *res*. The ability of resolvase to synapse two copies of the isolated accessory subsites in a crosslinkable complex was demonstrated in Section 3.5. Furthermore, the finding that *Ssp*I cleaved the DNA within subsite I in a large proportion of the synapsed pMA21 molecules without destroying the complex also suggested that the DNA was more accessible in that region (Section 6.1).

The methylation footprints for the remainder of the *res* site were very similar in the synaptic complex and when resolvase was bound to a small linear DNA fragment containing a single *res* site. The protection from methylation at a number of guanine residues in the bottom strand within subsites II and III (at +68, +78, and +86; see Figure 6.6) was more thorough in the synaptic complex. Thus, the accessory subsites appeared to be fully occupied in all the material migrating as the χ-form of the synaptic complex in the agarose gel, while some doubt remains regarding the occupancy and synapsis of subsite I.

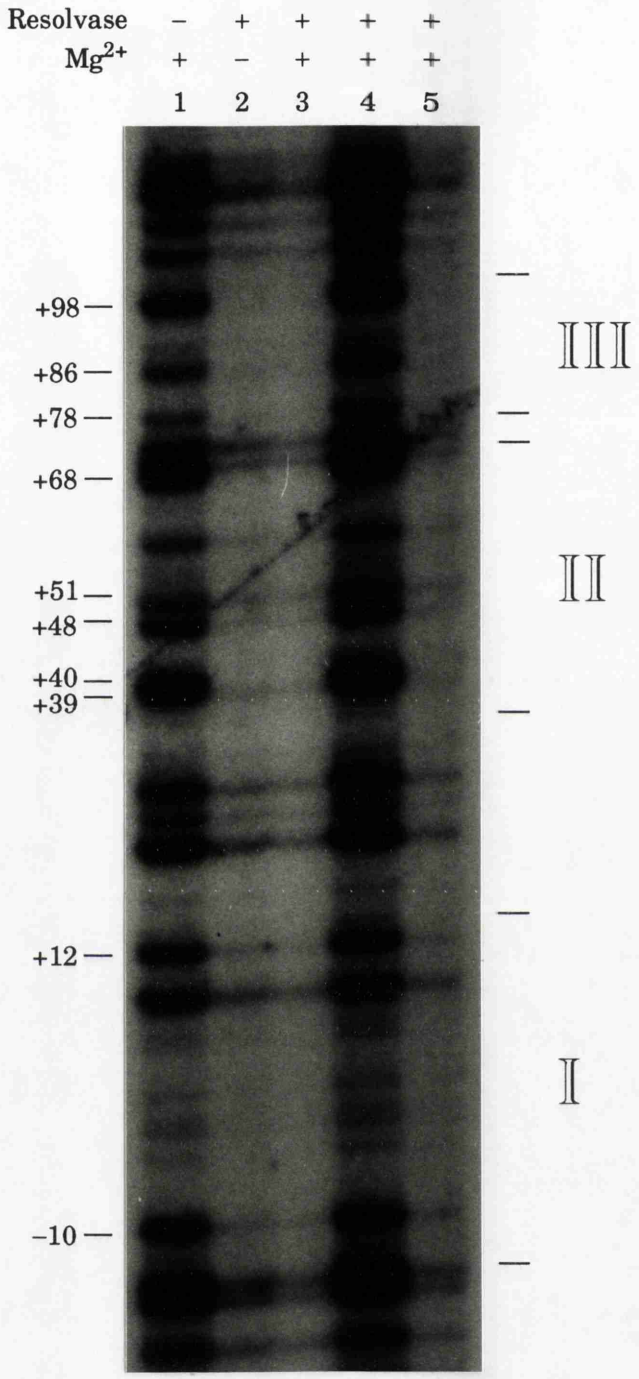

Figure 6.5 Methylation protection footprinting of the bottom strand of the *res* site in the χ-forms of the substrate and product synaptic complexes.

DNA fragments are identified by the phosphodiester bond cleaved on the 3' side of methylated guanine residues according to the numbering system introduced in Figure 6.1 (the centre of the crossover site is designated zero). The following species were eluted from the agarose gel: protein-free substrate DNA (lane 1), substrate χ-form (lanes 2 and 3), protein-free product DNA (lane 4), product χ-form (lane 5).

Buffer C +/– Mg^{2+}; 0.05% glutaraldehyde; 1% DMS; 1.2% agarose gel; 8% polyacrylamide/7 M urea gel.

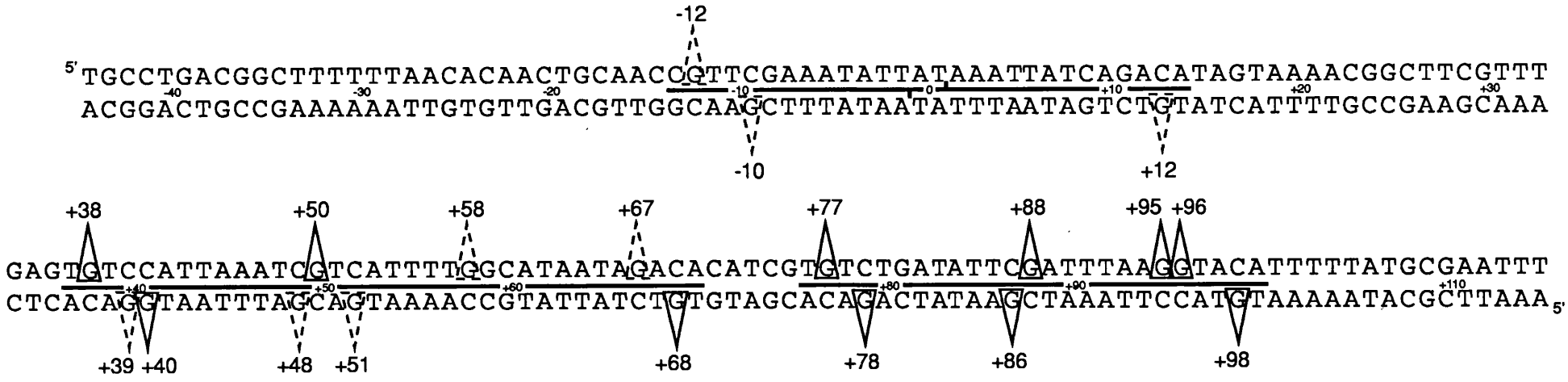

Figure 6.6 Guanine residues protected from methylation in the χ-form of the crosslinked intramolecular substrate synaptic complex are identified in the *res* site DNA sequence. Protected G residues, enclosed by solid or dashed triangles (the latter denoting weak protection), are identified by the 3' phosphodiester bond cleaved when the G is methylated. Numbering of the sequence is relative to the centre of the crossover site of *res*. The pattern on both DNA strands was identical in the χ-form of the product synaptic complex. The same G residues in the top DNA strand were affected in a footprint of the single *res* site complex isolated from the same reaction, but the protection was uniformly weak. See the text for further details.

Protection from methylation in the synaptic complex only of the guanine residues similarly protected when resolvase was bound to a linear fragment containing a single *res* site indicates that the synaptic complex trapped by glutaraldehyde crosslinking was not stabilised by additional resolvase interacting non-specifically with the DNA.

In order to obtain more information on the structure of the synaptic complex, DNase I protection footprinting was attempted. The procedure for generating the χ-form of the synaptic complex was as outlined for methylation protection footprinting. After incubation of standard glutaraldehyde-crosslinked pMS12 synapsis reactions with restriction enzyme to generate the χ-form, reactions were incubated with various concentrations of DNase I for 3 minutes at room temperature. DNase I cleavage was halted by addition of 20 mM EDTA and the samples underwent electrophoresis to isolate the various species of interest. Elution of DNA, ^{32}P end-labelling, and electrophoresis under denaturing conditions were as described (see Section 2.16b).

In addition to the aforementioned inability to balance samples in terms of cps incorporated into the DNA, further difficulties arose during the DNase I protection footprinting experiments. A failure to obtain efficient cleavage of the DNA under the standard synapsis reaction conditions necessitated the use of high concentrations of DNase I (between 1.0 and 2.0 μg/ml), and the omission of the sodium borohydride reduction step. There was some evidence of DNase I digestion degrading the DNA sufficiently to create alternative sites that could be labelled in Klenow polymerase end-labelling reactions. Thus, the *Hin*cII χ-form DNA fragment that was blunt at both ends was radiolabelled on occasion.

Figure 6.7 reproduces an autoradiograph of the top strand DNase I cleavage patterns obtained from the χ-form of the crosslinked intramolecular substrate synaptic complex (lane 3), and substrate DNA isolated from a minus-resolvase reaction (lane 4). Differences in the susceptibility of the *res* site DNA to DNase I attack in the synaptic complex are detailed in Figure 6.8. Attempts to generate a bottom strand footprint did not produce interpretable data. Noteworthy points from analysis of the DNase I protection footprint of the top strand of *res* in the synaptic complex, and comparison with data published on the footprint produced by resolvase binding to a linear DNA fragment containing a single *res* site, are outlined overleaf.

- Protection from DNase I cleavage **within subsite I** of *res* in the synaptic complex was very similar to that reported following binding of resolvase to a single *res* site on a linear DNA, with protection evident at –11 and +12 (Figure 6.8), (Symington, 1982; Kitts *et al.*, 1983). However, an enhancement of cleavage reported by Symington (1982) at –10 was not seen in the synaptic complex. Furthermore, significant enhancements at +4 and +13 in the synaptic complex were not evident in the footprint produced by Tn*3* resolvase bound to a linear *res* fragment, although the +13 enhancement was seen in the analogous γδ resolvase footprint (Grindley *et al.*, 1982). Enhanced DNase I activity at a number of positions outside subsite I (between –40 and –30; see Figure 6.8) in the synaptic complex may reflect a distortion of the DNA as it exits the nucleoprotein core.
- The enhanced DNase I cleavage in the **subsite I-II spacer region** at +29 was seen in both the linear single *res* footprint and the synaptic complex, but the additional enhancements at +30 and +31 appear to be unique to the synaptic complex (Figure 6.8). The enhancement at +29 was also noted when γδ resolvase was bound to a single *res* site, and was attributed to looping of the subsite I-II spacer DNA in the wrapped single *res* site complex (the 'resolvosome'), (Grindley *et al.*, 1982; Salvo and Grindley, 1988). The effect was best demonstrated when the size of the spacer was increased by insertion of one or two turns of the helix, whereupon alternating DNase I enhancement/ protection with a periodicity of about 5 bp was seen (Salvo and Grindley, 1988).
- **Within subsite II**, protection around +38 was seen in the synaptic complex and with resolvase bound to a linear DNA fragment containing the *res* site (Symington, 1982; Kitts *et al.*, 1983). The strong protection at +50 was unique to the synaptic complex formed by Tn*3* resolvase, but there was a minor protection at the corresponding position following γδ resolvase binding to a linear γδ *res* site (Grindley *et al.*, 1982).
- Protection at +72 in the **subsite II-III spacer region** was seen in both the synaptic complex and in the linear single *res* complex formed by Tn*3* resolvase, but the pronounced enhancement at +71 in the synapse was reported only for the γδ resolvase complex with a single *res* site (Grindley *et al.*, 1982).

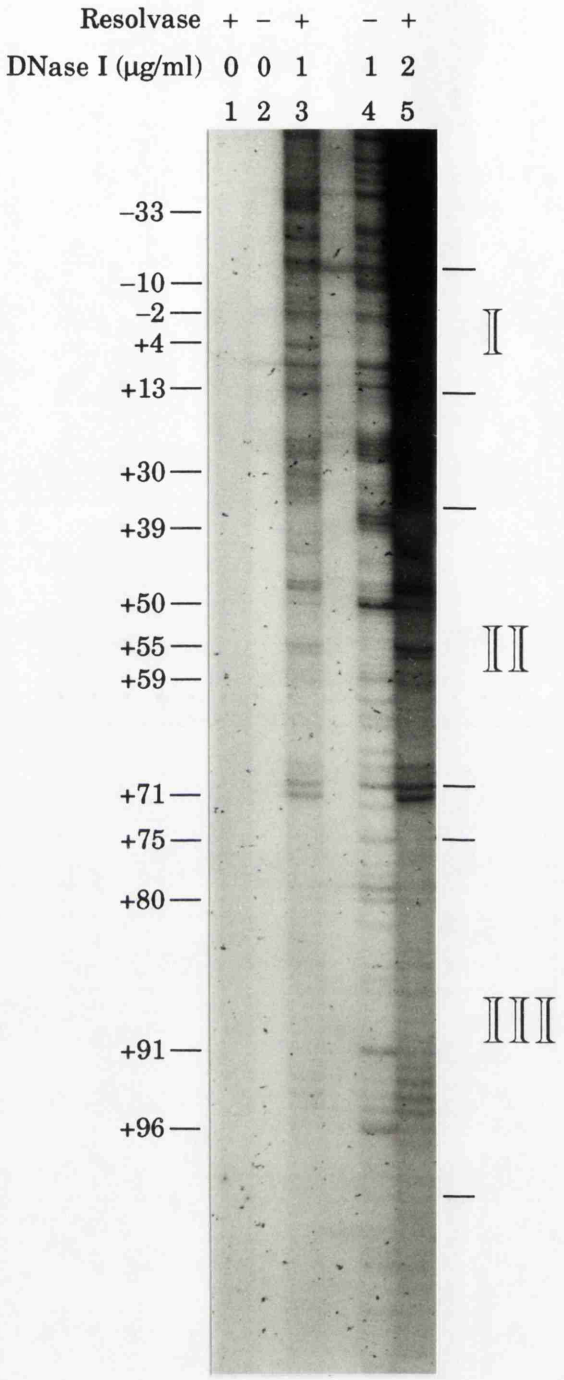

Figure 6.7 DNase I protection footprinting of the top strand of the *res* site in the χ-form of the crosslinked substrate synaptic complex.
DNA fragments are labelled by the phosphodiester bond cleaved according to the numbering system introduced in Figure 6.1 (the centre of the crossover site is designated zero). DNase I cleavage fragments were identified by comparison with co-electrophoresed samples cleaved at methylated guanine residues (not shown). When 3' end-labelled, the fragments detected following piperidine cleavage at methylated guanines or cleavage by DNase I at the same position are identical, both retaining a 5' phosphate group. The following species were eluted from the agarose gel: protein-free substrate DNA (lanes 2 and 4), substrate χ-form (lanes 1, 3 and 5).

Buffer C +/– Mg^{2+}; 0.05% glutaraldehyde; 1.2% agarose gel; 8% polyacrylamide/7 M urea gel.

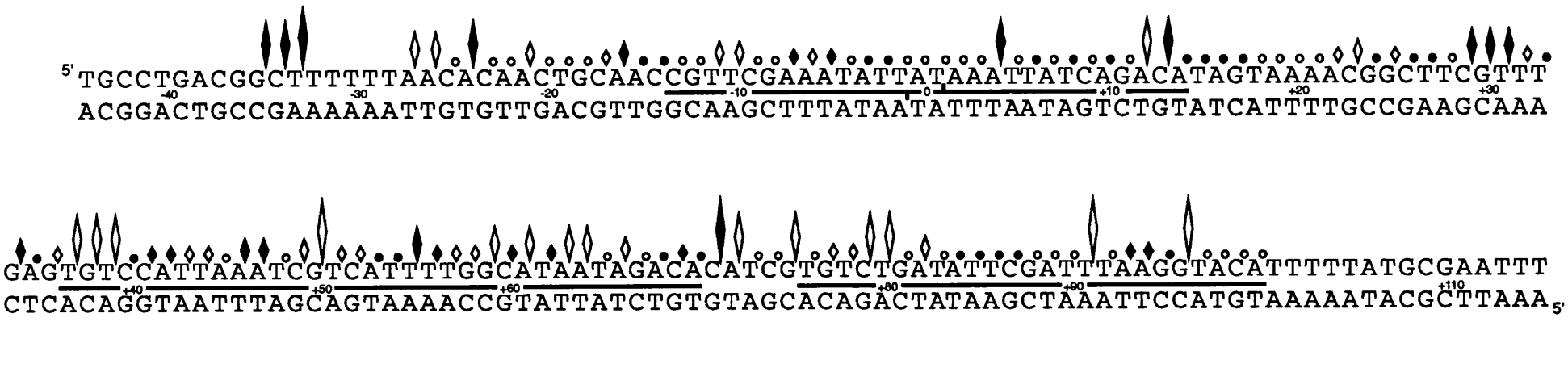

Figure 6.8 DNase I cleavage of the top strand of the *res* site in the χ-form of the crosslinked intramolecular substrate synaptic complex is compared with cleavage in the absence of resolvase. The cleavage pattern for the bottom DNA strand was not determined. Numbering of the sequence is relative to the centre of the crossover site of *res*. See the text for further details.

- ◊ protection in the complex
- ♦ enhancement in the complex (the bigger the symbol, the more pronounced the effect)
- o resistance, +/– resolvase
- • cleavage, +/– resolvase

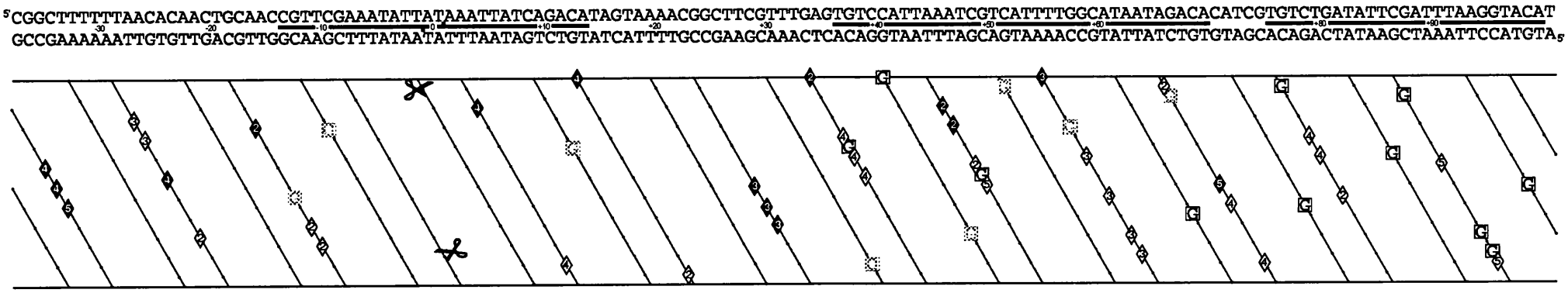

Figure 6.9 Planar representation of the DNA helix in the region of the *res* site, showing guanine residues protected from methylation and phosphodiester bonds protected from DNase I cleavage or exhibiting enhanced DNase I cleavage in the synaptic complex. A helical repeat of 10.5 bp is assumed. Black dots represent the phosphate groups of the sugar-phosphate backbone. The data are taken from Figures 6.6 and 6.8; only the more pronounced DNase I protection/enhancement positions are indicated. Guanine residues protected from methylation are positioned on the sugar-phosphate backbone for clarity, although the site of methylation (N-7) is in the major groove.

- protected from methylation in the synaptic complex
  - (a grey symbol indicates only partial protection)
- protected from DNase I cleavage in the synaptic complex
- enhancement of DNase I cleavage in the synaptic complex
  - the number inside the symbol indicates the degree of protection/enhancement (5 is maximal)
- resolvase-mediated cleavage at the crossover site

- **Within subsite III**, the pattern of protected positions was very similar in the synaptic complex and in the complex formed by either Tn*3* or γδ resolvase binding to a linear DNA fragment containing the cognate *res* site.

The data from methylation and DNase I protection footprinting of the χ-form of the crosslinked synaptic complex are shown on a planar representation of the DNA helix in Figure 6.9. However, the assumption of a uniform helical repeat of 10.5 bp per turn is unlikely to represent an accurate modelling of the DNA in the synapse (see Figure 1.6).

In the future, it may be wise to concentrate efforts to investigate resolvase-DNA interactions in the synaptic complex on an approach involving isolation of complex in a polyacrylamide gel. The complex could be formed by intramolecular synapsis in a supercoiled plasmid followed by restriction endonuclease digestion to generate a χ-form sufficiently small to migrate into a polyacrylamide gel. Alternatively, the possibility of intermolecular synapsis of small linear DNA molecules containing the *res* site should be investigated. In either case, evidence to date suggests that a protein crosslinking reagent will be required to stabilise the synapse (see Chapter 3). However, use of small linear DNA fragments radiolabelled from the outset and isolation of complex in a poly-acrylamide gel is an approach more in line with the established procedure for footprinting of single-site protein-DNA complexes. That said, I believe the labelling strategy used was inherently sound, and that the major difficulties were due to the isolation of complexes from agarose gels. Methylation protection footprinting provided satisfactory data apart from the aforementioned difficulties imposed by the high level of background radioactivity incorporated into what was believed to be a contaminant. In the final instance, the fragility of the synaptic complex formed by Tn*3* resolvase under the experimental conditions necessitated the use of some rather indirect and sometimes complex methods of analysis in order to obtain the data presented in this thesis.

Bibliography

Abdel-Meguid, S.S., Grindley, N.D.F., Templeton, N.S., and Steitz, T.A. (1984). Cleavage of the site-specific recombination protein γδ resolvase: the smaller of the two fragments binds DNA specifically. Proc. Natl. Acad. Sci. USA, **81**, 2001-2005.

Abdella, P.M., Smith, P.K., and Royer, G.P. (1979). A new cleavable reagent for cross-linking and reversible immobilisation of proteins. Biochem. Biophys. Res. Commun., **87**, 734-742.

Adrian, M., ten Heggeler-Bordier, B., Wahli, W., Stasiak, A.Z., Stasiak, A., and Dubochet, J. (1990). Direct visualization of supercoiled DNA molecules in solution. EMBO J., **9**, 4551-4554.

Amin, A.A., Beatty, L.G., and Sadowski, P.D. (1990). Synaptic intermediates promoted by the FLP recombinase. J. Mol. Biol., **214**, 55-72.

Ansari, A.Z., Chael, M.L., and O'Halloran, T.V. (1992). Allosteric underwinding of DNA is a critical step in positive control of transcription by Hg-MerR. Nature, **355**, 87-89.

Avila, P., Ackroyd, A.J., and Halford, S.E. (1990). DNA binding by mutants of Tn*21* resolvase with DNA recognition functions from Tn*3* resolvase. J. Mol. Biol., **216**, 645-655.

Baker, T.A., Mizuuchi, M., Savilahti, H., and Mizuuchi, K. (1993). Division of labour among monomers within the Mu transposase tetramer. Cell, **74**, 723-733.

Bednarz, A.L. (1989) Dissection of the Tn*3* resolution site. Ph.D. Thesis. University of Glasgow.

Bednarz, A.L., Boocock, M.R., and Sherratt, D.J. (1990). Determinants of correct *res* site alignment in site-specific recombination by Tn*3* resolvase. Genes Dev., **4**, 2366-2375.

Benjamin, H.W., Matzuk, M.M., Krasnow, M.A., and Cozzarelli, N.R. (1985). Recombination site selection by Tn*3* resolvase: topological tests of a tracking mechanism. Cell, **40**, 147-158.

Benjamin, H.W., and Cozzarelli, N.R. (1986). DNA-directed synapsis in recombination: slithering and random collision of sites. *In* Proceedings of the Robert A. Welch Foundation Conferences on Chemical Research, (Welch Foundation, Houston), pp. 107-126.

Benjamin, H.W., and Cozzarelli, N.R. (1988). Isolation and characterisation of the Tn*3* resolvase synaptic intermediate. EMBO J., **7**, 1897-1905.

Benjamin, H.W., and Cozzarelli, N.R. (1990). Geometric arrangements of Tn*3* resolvase sites. J. Biol. Chem., **265**, 6441-6447.

Birnboim, H.C., and Doly, J. (1979). A rapid alkaline extraction procedure for screening recombinant plasmid DNA. Nucleic Acids Res., **7**, 1513-1523.

Blake, D.G. (1993) Binding of Tn*3* resolvase to its resolution site. Ph.D. Thesis. University of Glasgow.

Blakely, G., Colloms, S., May, G., Burke, M., and Sherratt, D. (1991). *Escherichia coli* XerC recombinase is required for chromosomal segregation at cell division. N. Biologist, **3**, 789-798.

Bliska, J.B., Benjamin, H.W., and Cozzarelli, N.R. (1991). Mechanism of Tn*3* resolvase recombination *in vivo*. J. Biol. Chem., **266**, 2041-2047.

Boles, T.C., White, J.H., and Cozzarelli, N.R. (1990). Structure of plectonemically supercoiled DNA. J. Mol. Biol., **213**, 931-951.

Boocock, M.R., Brown, J.L., and Sherratt, D.J. (1986). Structural and catalytic properties of specific complexes between Tn*3* resolvase and the recombination site *res*. Biochem. Soc. Transac., **14**, 214-216.

Boocock, M.R., Brown, J.L., and Sherratt, D.J. (1987). Topological specificity in Tn*3* resolvase catalysis. *In* DNA Replication and Recombination, T.J. Kelly and R. McMacken, Eds. (Alan R. Liss, New York), pp. 703-718.

Bradford, M.M. (1976). A rapid and sensitive method for the quantitation of microgram quantities of protein utilising the principle of protein-dye binding. Anal. Biochem., **72**, 248-254.

Brown, J.L. (1986) Properties and action of Tn*3* resolvase. Ph.D. Thesis. University of Glasgow.

Calladine, C.R., Collis, C.M., Drew, H.R., and Mott, M.R. (1991). A study of electrophoretic mobility of DNA in agarose and polyacrylamide gels. J. Mol. Biol., **221**, 981-1005.

Carey, J. (1991). Gel retardation. *In* Protein-DNA Interactions, R.T. Sauer, Ed. (Academic Press), pp. 103-117.

Castell, S.E., Jordan, S.L., and Halford, S.E. (1986). Site-specific recombination and topoisomerisation by Tn*21* resolvase: role of metal ions. Nucleic Acids Res., **14**, 7213-7226.

Cox, M.M. (1989). DNA inversion in the 2μm plasmid of *Saccharomyces cerevisiae*. *In* Mobile DNA, D.E. Berg and M. Howe, Eds. (American Society for Microbiology, Washington, D.C.), pp. 661-670.

Cozzarelli, N.R., Boles, T.C., and White, J.H. (1990). Primer on the topology and geometry of DNA supercoiling. *In* DNA Topology and its Biological Effects, N.R. Cozzarelli and J.C. Wang, Eds. (Cold Spring Harbor, New York: Cold Spring Harbor Laboratory Press), pp. 139-184.

Craig, N.L. (1988). The mechanism of conservative site-specific recombination. Annu. Rev. Genet., **22**, 77-105.

Drew, H.R., and Travers, A.A. (1985). DNA bending and its relation to nucleosome positioning. J. Mol. Biol., **186**, 1-18.

Dröge, P., Hatfull, G.F., Grindley, N.D.F., and Cozzarelli, N.R. (1990). The two functional domains of γδ resolvase act on the same recombination site: implications for the mechanism of strand exchange. Proc. Natl. Acad. Sci. USA, **87**, 5336-5340.

Falvey, E., and Grindley, N.D.F. (1987). Contacts between γδ resolvase and the γδ *res* site. EMBO J., **6**, 815-821.

Falvey, E., Hatfull, G.F., and Grindley, N.D.F. (1988). Uncoupling of the recombination and topoisomerase activities of the γδ resolvase by a mutation at the crossover point. Nature, **332**, 861-863.

Fuchs, R., and Blakesley, R. (1983). Guide to the use of type II restriction endonucleases. Methods Enzymol., **100**, 3-38.

Galas, D.J., and Schmitz, A. (1978). DNAase footprinting: a simple method for the detection of protein-DNA binding specificity. Nucleic Acids Res., **5**, 3157-3170.

Gellert, M. (1992). Molecular analysis of V(D)J recombination. Annu. Rev. Genet., **26**, 425-446.

Glasgow, A.C., Hughes, K.T., and Simon, M.I. (1989). Bacterial DNA inversion systems. *In* Mobile DNA, D.E. Berg and M. Howe, Eds. (American Society for Microbiology, Washington, D.C.), pp. 637-660.

Graham, K.S., and Dervan, P.B. (1990). Structural motif of the DNA binding domain of γδ resolvase characterised by affinity cleaving. J. Biol Chem., **265**, 16534-16540.

Grindley, N.D.F., Lauth, M.R., Wells, R.G., Wityk, R.J., Salvo, J.J., and Reed, R.R. (1982). Transposon-mediated site-specific recombination: identification of three binding sites for resolvase at the *res* sites of γδ and Tn*3*. Cell, **30**, 19-27.

Grindley, N.D.F. (1993). Analysis of a nucleoprotein complex: the synaptosome of γδ resolvase. Science, **262**, 738-740.

Grindley, N.D.F. (1994). Resolvase-mediated site-specific recombination. In preparation.

Halford, S.E. (1983). How does *Eco*RI cleave its recognition site on DNA? Trends Biochem. Sci., **8**, 455-460.

Hames, B.D. (1990). One-dimensional polyacrylamide gel electrophoresis. *In* Gel Electrophoresis of Proteins: a practical approach, B.D. Hames and D. Rickwood, Eds. (IRL Press, Oxford), pp. 1-147.

Hamilton, D.L., and Abremski, K. (1984). Site-specific recombination by the bacteriophage P1 *lox*-Cre system. Cre-mediated synapsis of two *lox* sites. J. Mol. Biol., **178**, 481-486.

Han, K.-K., Richard, C., and Delacourte, A. (1984). Chemical cross-links of proteins by using bifunctional reagents. Int. J. Biochem., **16**, 129-145.

Hanahan, D. (1987). Mechanisms of DNA transformation. *In Escherichia coli* and *Salmonella typhimurium*: Cellular and Molecular Biology, F.C. Neidhardt, J.L. Ingraham, K.B. Low, B. Magasanik, M. Schaechter, and H.E. Umbarger, Eds. (American Society for Microbiology, Washington, D.C.), pp. 1177-1183.

Harrison, S.C., and Aggarwal, A.K. (1990). DNA recognition by proteins with the helix-turn-helix motif. Annu. Rev. Biochem., **59**, 933-969.

Hatfull, G.F., and Grindley, N.D.F. (1986). Analysis of γδ resolvase mutants *in vitro*: evidence for an interaction between serine-10 of resolvase and site I of *res*. Proc. Natl. Acad. Sci. USA, **83**, 5429-5433.

Hatfull, G.F., Noble, S.M., and Grindley, N.D.F. (1987). The γδ resolvase induces an unusual DNA structure at the recombinational crossover point. Cell, **49**, 103-110.

Hatfull, G.F., and Grindley, N.D.F. (1988). Resolvases and DNA-invertases: a family of enzymes active in site-specific recombination. *In* Genetic Recombination, R. Kucherlapati and G.R. Smith, Eds. (American Society for Microbiology, Washington, D.C.), pp. 357-396.

Hatfull, G.F., Salvo, J.J., Falvey, E.E., Rimphanitchayakit, V., and Grindley, N.D.F. (1988). Site-specific recombination by the γδ resolvase. Symp. Soc. Gen. Microbiol., **43**, 149-181.

Heery, D.M., Gannon, F., and Powell, R. (1990). A simple method for subcloning DNA fragments from gel slices. Trends Genet., **6**, 173.

Heichman, K.A., and Johnson, R.C. (1990). The Hin invertasome: protein-mediated joining of distant recombination sites at the enhancer. Science, **249**, 511-517.

Hochschild, A., and Ptashne, M. (1986). Cooperative binding of λ repressors to sites separated by integral turns of the DNA helix. Cell, **44**, 681-687.

Hughes, R.E., Hatfull, G.F., Rice, P.A., Steitz, T.A., and Grindley, N.D.F. (1990). Cooperativity mutants of the γδ resolvase identify an essential interdimer interaction. Cell, **63**, 1331-1338.

Hughes, R.E., Rice, P.A., Steitz, T.A., and Grindley, N.D.F. (1993). Protein-protein interactions directing resolvase site-specific recombination: a structure-function analysis. EMBO J., **12**, 1447-1458.

Jaenicke, R., and Rudolph, R. (1989). Folding proteins. *In* Protein Structure: a practical approach, T.E. Creighton, Ed. (IRL Press, Oxford), pp. 191-223.

Johnson, R.C. (1991). Mechanism of site-specific DNA inversion in bacteria. Curr. Opin. Genet. Dev., **1**, 404-411.

Kanaar, R., Klippel, A., Shekhtman, E., Dungan, J.M., Kahmann, R., and Cozzarelli, N.R. (1990). Processive recombination by the phage Mu Gin system: implications for the mechanisms of DNA strand exchange, DNA site alignment, and enhancer action. Cell, **62**, 353-366.

Kim, S., Moitoso de Vargas, L., Nunes-Düby, S.E., and Landy, A. (1990). Mapping of a higher order protein-DNA complex: two kinds of long-range interactions in λ *att*L. Cell, **63**, 773-781.

Kim, S., and Landy, A. (1992). Lambda Int protein bridges between higher order complexes at two distant chromosomal loci *att*L and *att*R. Science, **256**, 198-203.

Kitts, P.A., Symington, L.S., Dyson, P., and Sherratt, D.J. (1983). Transposon-encoded site-specific recombination: nature of the Tn*3* DNA sequences which constitute the recombination site *res*. EMBO J., **2**, 1055-1060.

Klippel, A., Mertens, G., Patschinsky, T., and Kahmann, R. (1988). The DNA invertase Gin of phage Mu: formation of a covalent complex with DNA via a phosphoserine at amino acid position 9. EMBO J., **7**, 1229-1237.

Klippel, A., Kanaar, R., Kahmann, R., and Cozzarelli, N.R. (1993). Analysis of strand exchange and DNA binding of enhancer-independent Gin recombinase mutants. EMBO J., **12**, 1047-1057.

Kovacic, R.T., and Wang, J.C. (1979). Rapid mapping of restriction sites of a DNA: restriction of DNA in agarose gel and two dimensional analysis of end-labeled DNA. Plasmid, **2**, 394-402.

Krämer, H., Niemöller, M., Amouyal, M., Revet, B., von Wilcken-Bergmann, B., and Müller-Hill, B. (1987). *lac* repressor forms loops with linear DNA carrying two suitably spaced *lac* operators. EMBO J., **6**, 1481-1491.

Krasnow, M.A., and Cozzarelli, N.R. (1983). Site-specific relaxation and recombination by the Tn*3* resolvase: recognition of the DNA path between oriented *res* sites. Cell, **32**, 1313-1324.

Kuo, C.-F., Zou, A., Jayaram, M., Getzoff, E., and Harshey, R. (1991). DNA-protein complexes during attachment-site synapsis in Mu DNA transposition. EMBO J., **10**, 1585-1591.

Laemmli, U.K. (1970). Cleavage of structural proteins during the assembly of the head of bacteriophage T4. Nature, **227**, 680.

Landy, A. (1989). Dynamic, structural, and regulatory aspects of λ site-specific recombination. Annu. Rev. Biochem., **58**, 913-949.

Lane, D., Prentki, P., and Chandler, M. (1992). Use of gel retardation to analyse protein-nucleic acid interactions. Microbiol. Rev., **56**, 509-528.

Lavoie, B.D., Chan, B.S., Allison, R.G., and Chaconas, G. (1991). Structural aspects of a higher order nucleoprotein complex: induction of an altered DNA structure at the Mu-host junction of the Mu Type 1 transpososome. EMBO J., **10**, 3051-3059.

Lim, H.M., and Simon, M.I. (1992). The role of negative supercoiling in Hin-mediated site-specific recombination. J. Biol. Chem., **267**, 11176-11182.

Liu, T., Liu, D., DeRose, E.F., and Mullen, G.P. (1993). Studies of the dimerization and domain structure of γδ resolvase. J. Biol. Chem., **258**, 16309-16315.

Lomant, A.J., and Fairbanks, G. (1976). Chemical probes of extended biological structures: synthesis and properties of the cleavable protein cross-linking reagent [^{35}S]dithiobis(succinimidyl propionate). J. Mol. Biol., **104**, 243-261.

Matthews, K.S. (1992). DNA looping. Microbiol. Rev., **56**, 123-136.

Maxwell, A., and Gellert, M. (1986). Mechanistic aspects of DNA topoisomerases. *In* Advances in Protein Chemistry, C.B. Anfinsen, J.T. Edsall, and F.M. Richards, Eds. (Academic Press, Orlando, FL), pp. 69-107.

Mazzarelli, J.M., Ermácora, M.R., Fox, R.O., and Grindley, N.D.F. (1993). Mapping interactions between the catalytic domain of resolvase and its DNA substrate using cysteine-coupled EDTA-iron. Biochemistry, **32**, 2979-2986.

Merril, C.R. (1990). Silver staining of proteins and DNA. Nature, **343**, 779-780.

Mizuuchi, M., Baker, T.A., and Mizuuchi, K. (1991). DNase protection analysis of the stable synaptic complexes involved in Mu transposition. Proc. Natl. Acad. Sci. USA, **88**, 9031-9035.

Mizuuchi, M., Baker, T.A., and Mizuuchi, K. (1992). Assembly of the active form of the transposase-Mu DNA complex: a critical control point in Mu transposition. Cell, **70**, 303-311.

Mizuuchi, K. (1992). Transpositional recombination: mechanistic insights from studies of Mu and other elements. Annu. Rev. Biochem., **61**, 1011-1051.

Nash, H.A. (1990). Bending and supercoiling of DNA at the attachment site of bacteriophage λ. Trends Biochem. Sci., **15**, 222-227.

Newman, B.J., and Grindley, N.D.F. (1984). Mutants of the γδ resolvase: a genetic analysis of the recombination function. Cell, **38**, 463-469.

Österlund, M., Luthman, H., Nilsson, S.V., and Magnusson, G. (1982). Ethidium-bromide-inhibited restriction endonucleases cleave one strand of circular DNA. Gene, **20**, 121-125.

Parker, C.N., and Halford, S.E. (1991). Dynamics of long-range interactions on DNA: the speed of synapsis during site-specific recombination by resolvase. Cell, **66**, 781-791.

Reed, R.R. (1981). Transposon-mediated site-specific recombination: a defined *in vitro* system. Cell, **25**, 713-719.

Reed, R.R., and Grindley, N.D.F. (1981). Transposon-mediated site-specific recombination *in vitro*: DNA cleavage and protein-DNA linkage at the recombination site. Cell, **25**, 721-728.

Reed, R.R., Shibuya, G.I., and Steitz, J.A. (1982). Nucleotide sequence of γδ resolvase gene and demonstration that its gene product acts as a repressor of transcription. Nature, **300**, 381-383.

Reed, R.R. (1983). The resolvase protein of the transposon γδ. Methods Enzymol., **100**, 191-196.

Reed, R.R., and Moser, C.D. (1984). Resolvase-mediated recombination intermediates contain a serine residue covalently linked to DNA. Cold Spring Harb. Symp. Quant. Biol., **49**, 245-249.

Rice, P.A., and Steitz, T.A. (1994). A model for the synaptic complex formed by γδ resolvase suggested by the packing of subunits within the crystal. In preparation.

Richardson, S.M.H., Boles, T.C., and Cozzarelli, N.R. (1988). The helical repeat of underwound DNA in solution. Nucleic Acids Res., **16**, 6607-6616.

Rimphanitchayakit, V., Hatfull, G.F., and Grindley, N.D.F. (1989). The 43 residue DNA-binding domain of gamma-delta resolvase binds adjacent major and minor grooves of DNA. Nucleic Acids Res., **17**, 1035-1050.

Rimphanitchayakit, V., and Grindley, N.D.F. (1990). Saturation mutagenesis of the DNA site bound by the small carboxy-terminal domain of γδ resolvase. EMBO J., **9**, 719-725.

Sadowski, P. (1986). Site-specific recombinases: changing partners and doing the twist. J. Bacteriol., **165**, 341-347.

Saldanha, R., Flanagan, P., and Fennewald, M. (1987). Recombination by resolvase is inhibited by *lac* repressor simultaneously binding operators between *res* sites. J. Mol. Biol., **196**, 505-516.

Salvo, J.J., and Grindley, N.D.F. (1988). The γδ resolvase bends the *res* site into a recombinogenic complex. EMBO J., **7**, 3609-3616.

Sambrook, J., Fritsch, E.F., and Maniatis, T. (1989). Molecular cloning: a laboratory manual. (Cold Spring Harbor Laboratory Press, New York).

Sammons, D.W., Adams, L.D., and Nishizawa, E.E. (1981). Ultrasensitive silver-based color staining of polypeptides in polyacrylamide gels. Electrophoresis, **2**, 135.

Sanderson, M.R., Freemont, P.S., Rice, P.A., Goldman, A., Hatfull, G.F., Grindley, N.D.F., and Steitz, T.A. (1990). The crystal structure of the catalytic domain of the site-specific recombination enzyme γδ resolvase at 2.7 Å resolution. Cell, **63**, 1323-1329.

Satchwell, S.C., Drew, H.R., and Travers, A.A. (1986). Sequence periodicities in chicken nucleosome core DNA. J. Mol. Biol., **191**, 659-675.

Schleif, R. (1992). DNA looping. Annu. Rev. Biochem., **61**, 199-223.

Schoenle, E.J., Adams, L.D., and Sammons, D.W. (1984). Insulin-induced rapid decrease of a major protein in fat cell plasma membranes. J. Biol. Chem., **259**, 12112.

Segall, A.M., and Nash, H.A. (1993). Synaptic intermediates in bacteriophage lambda site-specific recombination: integrase can align pairs of attachment sites. EMBO J., **12**, 4567-4576.

Sherratt, D., Dyson, P., Boocock, M., Brown, L., Summers, D., Stewart, G., and Chan, P. (1984). Site-specific recombination in transposition and plasmid stability. Cold Spring Harb. Symp. Quant. Biol., **49**, 227-233.

Sherratt, D. (1989). Tn*3* and related transposable elements: site-specific recombination and transposition. *In* Mobile DNA, D.E. Berg and M. Howe, Eds. (American Society for Microbiology, Washington, D.C.), pp. 163-184.

Siebenlist, U., and Gilbert, W. (1980). Contacts between *Escherichia coli* RNA polymerase and an early promoter of phage T7. Proc. Natl. Acad. Sci. USA, **77**, 122-126.

Stark, W.M., Boocock, M.R., and Sherratt, D.J. (1989a). Site-specific recombination by Tn*3* resolvase. Trends Genet., **5**, 304-309.

Stark, W.M., Sherratt, D.J., and Boocock, M.R. (1989b). Site-specific recombination by Tn*3* resolvase: topological changes in the forward and reverse reactions. Cell, **58**, 779-790.

Stark, W.M., Grindley, N.D.F., Hatfull, G.F., and Boocock, M.R. (1991). Resolvase-catalysed reactions between *res* sites differing in the central dinucleotide of subsite I. EMBO J., **10**, 3541-3548.

Stark, W.M., Boocock, M.R., and Sherratt, D.J. (1992). Catalysis by site-specific recombinases. Trends Genet., **8**, 432-439.

Stark, W.M., and Boocock, M.R. (1994). The linkage change of a knotting reaction catalysed by Tn*3* resolvase. Submitted to J. Mol. Biol.

Suck, D., Lahm, A., and Oefner, C. (1988). Structure refined to 2 Å of a nicked DNA octanucleotide complex with DNase I. Nature, **332**, 464-468.

Sun, L., and Singer, B. (1975). The specificity of different classes of ethylating agents towards various sites of HeLa cell DNA *in vitro* and *in vivo*. Biochemistry, **14**, 1795-1802.

Surette, M.G., Buch, S.J., and Chaconas, G. (1987). Transpososomes: stable protein-DNA complexes involved in the *in vitro* transposition of bacteriophage Mu DNA. Cell, **49**, 253-262.

Sutcliffe, J.G. (1978). Complete nucleotide sequence of the *Escherichia coli* plasmid pBR322. Cold Spring Harb. Symp. Quant. Biol., **43**, 77-90.

Symington, L.S. (1982) Transposon-encoded site-specific recombination. Ph.D. Thesis. University of Glasgow.

Tolan, Lambert, Boileau, Fanning, Kenny, Vassos, and Traut (1980). Radioiodination of microgram quantities of ribosomal proteins from polyacrylamide gels. Anal. Biochem., **103**, 101-109.

Travers, A.A. (1993). DNA-protein interactions. (Chapman & Hall, London).

van de Putte, P., and Goosen, N. (1992). DNA inversions in phages and bacteria. Trends Genet., **8**, 457-462.

van der Ploeg, L.H.T., Gottesdiener, K., and Lee, M.G.-S. (1992). Antigenic variation in African trypanosomes. Trends Genet., **8**, 452-457.

Wang, J.C., Peck, L.J., and Becherer, K. (1984). DNA supercoiling and its effects on DNA structure and function. Cold Spring Harb. Symp. Quant. Biol., **49**, 85-91.

Wasserman, S.A., and Cozzarelli, N.R. (1985). Determination of the stereostructure of the product of Tn*3* resolvase by a general method. Proc. Natl. Acad. Sci. USA, **82**, 1079-1083.

Wasserman, S.A., Dungan, J.M., and Cozzarelli, N.R. (1985). Discovery of a predicted DNA knot substantiates a model for site-specific recombination. Science, **229**, 171-174.

Wells, R.G., and Grindley, N.D.F. (1984). Analysis of the γδ *res* site: sites required for site-specific recombination and gene expression. J. Mol. Biol., **179**, 667-687.

West, S.C. (1992). Enzymes and molecular mechanisms of genetic recombination. Annu. Rev. Biochem., **61**, 603-640.

Yamada, H., Imoto, T., Fujita, K., Okazaki, K., and Motomura, M. (1981). Selective modification of aspartic acid-101 in lysozyme by carbodiimide reaction. Biochemistry, **20**, 4836-4842.

Yanisch-Perron, C., Vieira, J., and Messing, J. (1985). Improved M13 phage cloning vectors and host strains: nucleotide sequences of the M13mp18 and pUC19 vectors. Gene, **33**, 103-119.